Molecular Genetic Analysis of Familial Exudative Vitreoretinopathy in Indian Patients

THESIS

Submitted in partial fulfillment

of the requirements for the degree of

DOCTOR OF PHILOSOPHY

by

GANESWARA RAO MUSADA

Under the Supervision of

Dr. INDERJEET KAUR

BIRLA INSTITUTE OF TECHNOLOGY AND SCIENCE

PILANI (RAJASTHAN) INDIA

2015

BIRLA INSTITUTE OF TECHNOLOGY AND SCIENCE

PILANI (RAJASTHAN)

CERTIFICATE

This is to certify that the thesis entitled **"Molecular Genetic Analysis of Familial Exudative Vitreoretinopathy in Indian patients"** which is submitted by **Ganeswara Rao Musada**, ID No. **2008PHXF034P**, for award of Ph.D. degree of the institute, embodies original work done by him under my supervision.

Date:

Supervisor

Dr. Inderjeet Kaur

Scientist

Kallam Anji Reddy-

Molecular Genetics Lab

L.V. Prasad Eye Institute

Hyderabad – 500034

BIRLA INSTITUTE OF TECHNOLOGY AND SCIENCE

PILANI (RAJASTHAN)

CERTIFICATE

This is to certify that the thesis entitled **"Molecular Genetic Analysis of Familial Exudative Vitreoretinopathy in Indian patients"** which is submitted by **Ganeswara Rao Musada**, ID No. **2008PHXF034P**, for award of Ph.D. degree of the institute, embodies my original work.

Date:

Musada Ganeswara Rao

ID No. 2008PHXF034P

Kallam Anji Reddy-

Molecular Genetics Lab

L. V. Prasad Eye Institute

Hyderabad – 500034

Dedicated to

My family

and

Dr. Inderjeet Kaur

ACKNOWLEDGEMENTS

My sincere and heartfelt thanks to my mentor **Dr. Inderjeet Kaur** for the guidance and care provided to me during my graduation period at L V Prasad Eye Institute. I can strongly say that without her support I would not have achieved this. While this may be true in case of every graduate student, her inspiring words in few vulnerable moments of my life helped me to breathe once again and to overcome the obstacles during the journey of my PhD. With a deep sense of gratitude, I thank my guide for her valuable suggestions during bench work and thesis writing.

I am extremely grateful to **Dr. Subhadra Jalali**, Associate Director, Consultant, LVPEI, for clinically evaluating all the study patients, providing patient samples and clinical details. Her thirst for knowledge and hard work, and her way of treating people always inspired me and I am feeling proud to have worked with her. Madam, no doubt your joyful laugh is the oxygen not only for your patients but also for your students.

My heartfelt thanks to **Dr. Subhabrata Chakrabarti,** Associate Director of Research, LVPEI for his valuable suggestions during my thesis writing and for his support throughout my graduation period.

I extend my heartfelt gratitude to **Prof. D. Balasubramanian**, Director of Research, LVPEI for his unconditional support throughout my stay at LVPEI.

My sincere thanks to **Dr. Chitra Kannabiran, Dr. Indumathi Mariappan** and other faculty members for their valuable suggestions, excellent advices and constant encouragement.

I would like to specially thank **Dr. G. N. Rao**, Chairman, LVPEI for allowing me to work in this prestigious organization and for providing a well disciplined and organized environment.

I thank **Prof. S. K. Verma, Dr. Hemant R. Jadhav, Dr. Navin Singh, Dr. Palash Mandal** and nucleus members of Research and Consultancy division, BITS, Pilani for their official support and for guiding through various procedures and regulations of BITS.

I also thank the Doctoral Advisory Committee (DAC) members, Prof. Suman Kapur, Prof. Vidya Rajesh, Dr. Jayati Ray Dutta and Dr. Naga Mohan Kommu for putting their valuable time and effort to review the draft thesis and for providing me valuable suggestions.

I specially thank **Savitri Maddileti** for helping me to get through the difficult times and for all the support and care provided by her.

I thank my seniors **Saritha Katta, Nageswara Rao Kollu, Subhash Gaddipati, Hardeep Pal Singh, Kalyana Chakravarthi, Guru Prasad Manderwad, Surya Ponnam** and **Venu Talla** and my friends **Hameed, Sonika, Shahna, Rachana Shukla, Pulla Rao, Praveen K Balne, Meha, Almas, Sushma, Nishika Vasundhara Vahini, Vinay, Nanda Siva Shankar** and **Praveen Joseph** for their constant support and affection. I have learnt about life as well as science from you all.

My special thanks to the other staff members **Banu S, Sudhakar Kothapalli, Elena, Jai Ganesh, Moddin Pasha, Vijay, Hema** and **Mehar** for their help at various stages of my graduation.

I greatly acknowledge Hyderabad Eye Research Foundation for providing me the fellowship, which made my studies possible.

I am thankful to all the patients and their family members for their consent to participate in the project.

It would be meaningless if I forget the support received from my parents, brother and my wife. Without their help and support it would have been impossible for me to reach this stage. I thank my family wholeheartedly for their support and encouragement.

Ganeswara Rao Musada

Familial exudative vitreoretinopathy (FEVR) is a rare, inherited, bilateral eye disorder characterized largely by the avascular peripheral retina that leads to retinal ischemia and further progresses to retinal neovascularization, subretinal exudation and hemorrhages, partial or total retinal detachments and complete blindness. Mutations in genes involved in the formation of a ligand-receptor complex in Norrin-β catenin signaling pathway were linked with the disease pathogenesis in large FEVR families. The functional characterization of this signaling pathway was later identified to play a crucial role in FEVR.

Genetic heterogeneity is the hallmark of FEVR and mutations in five candidate genes (*NDP, FZD4, LRP5, TSPAN12* and *ZNF408*) have been reported to be linked with autosomal dominant, autosomal recessive and X-linked forms of this disease in different ethnic groups. The knock out animal models of these candidate genes provided further evidence to their role in the development of retinal angiogenesis and ocular features similar to FEVR. The implication of these candidate genes in FEVR has been well documented across different ethnicities. But despite a higher prevalence in the Indian context, there is only one report on *FZD4* gene in a relatively smaller cohort. Thus, the present study was undertaken to assess the overall contributions of the *NDP, FZD4, TSPAN12* and *ZNF408* genes and to assess their mutation spectrum in a large cohort of unrelated and clinically well characterized FEVR patients (n=110) from India. Furthermore, an attempt was made to establish a genotype-phenotype correlation.

The screenings of *NDP, FZD4, TSPAN12* and *ZNF408* genes led to identification of 22 potentially pathogenic mutations in 26.3% (29/110) of the FEVR probands in the coding regions, of which, 16 were novel. These included 14 missense changes, 5 small base pair deletions, a single base pair insertion, a non sense mutation and a nonstop change. None of these mutations were observed across the unrelated and ethnically matched normal subjects (n=110). Of the four candidate genes screened, mutations in the *NDP*, *FZD4* and *TSPAN12* were observed in 9.0%, 8.1% and 5.4% of the FEVR probands, respectively. The *ZNF408* mutations were involved in 3.6% of patients. The frequencies of FEVR patients identified with mutations in the corresponding candidate genes in the present study were comparable to those observed in the Chinese and Japanese

populations. No mutations were observed in 73.7% of the FEVR probands in the coding region. Additionally, novel changes in the untranslated regions and intronic variations were identified in 7.2% (8/110) of all probands. Further functional studies are required to understand their potential effect on the protein function and disease pathogenesis.

In the present study, majority of the coding region mutations segregated in the affected family members of the probands. The mutations in *FZD4* and *ZNF408* genes were linked with autosomal dominant inheritance while those in *TSPAN12* exhibited both autosomal dominant and autosomal recessive inheritance. The *NDP* gene mutations exhibited an X-linked mode of inheritance. Incomplete penetrance and variable expressivity leading to variable clinical course among the probands and affected family members harboring the same nucleotide change were also noted in these candidate genes. All the patients harboring mutations exhibited typical clinical features of the FEVR in terms of clinical presentation and severity that precluded any genotype phenotype correlation.

In conclusion, the present study provided information on the relative contributions of *NDP, FZD4, TSPAN12* and *ZNF408* genes, and further expanded the mutation spectrum of these genes in FEVR patients. It also validated the involvement of *ZNF408* (a relatively new gene) mutations in FEVR development. To the best of my knowledge and belief, this is the first study from India reporting mutations in these genes in a large cohort of patients that would be valuable for genetic counseling and provide means for predictive testing prior to the development of severe visual complications in FEVR. However, incomplete penetrance exhibited by the mutant alleles would make prenatal diagnosis of this disease very challenging.

LIST OF FIGURES

A	Adenine
A°	Angstrom units
AA	Amino acid
AD	Autosomal dominant
AR	Autosomal recessive
APC	Adenomatous polyposis coli
bp	Base pair
C	Cytosine
cDNA	Complementary deoxy ribonucleic acid
CF	Counting fingers
CTCK	C-terminal cysteine knot
BRB	Blood retina barrier
CK	Casein kinase
Cln	Claudin
CRA	Central retinal artery
CRD	Cysteine rich domain
CRV	Central retinal vein
dup	Duplication
DKK	Dickkopf
DMSO	Dimethyl sulphoxide
dNTPs	Deoxy nucleotide triphosphates
DVL	Dishevelled
DIX	Disheveled and axin
EDTA	Ethylene diamine tetra-acetic acid
ELM	External limiting membrane
ENU	N-ethyl-N-nitrosourea
FGF	Fibroblast growth factor
Fli1	Friend leukemia integration 1
FZD4	Frizzled-4
G	Guanine
GCL	Ganglion cell layer
GFP	Green fluorescent protein
GSK	Glycogen synthase kinase
HA	Hyaloid artery
HIF	Hypoxia inducible factor
HSF	Human splicing finder
Ins	Insertion
ILM	Inner limiting membrane
FEVR	Familial exudative vitreoretinopathy
NDP	Norrie disease pseudoglioma
INL	Inner nuclear layer
IPL	Inner plexiform layer
IRES	Internal ribosome entry site
KB	Kilo base pair
KO	Knock out

NFL	Nerve fiber layer
LEF	Lymphoid enhancer factor
LRP5	Low density lipoprotein receptor related protein 5
µg	Microgram
µl	Microlitre
µM	Micromolar
MIM	Mendelian inheritance in man
mM	Millimolar
nm	Nanometer
ND	Norrie disease
OA	Ophthalmic artery
OD	Optical density
OPL	Outer plexiform layer
OPPG	Osteoporosis pseudoglioma
P	Postnatal day
PAGE	Polyacrylamide gel electrophoresis
PBS	Phosphate buffer saline
PCA	Posterior ciliary arteries
PDGF	Platelet derived growth factor
PCR	Polymerase chain reaction
PFV	Persistent fetal vasculature
PHPV	Persistent hyperplastic primary vitreous
PM	Pupillary membrane
RD	Retinal detachment
REC	Retinal endothelial cells
RFLP	Restriction fragment length polymorphism
RGC	Retinal ganglion cells
ROP	Retinopathy of prematurity
RPE	Retinal pigment epithelium
RPM	Revolutions per minute
SDS	Sodium dodecyl sulphate
SIFT	Sorting intolerance from tolerance
SNP	Single nucleotide polymorphism
STF	Super top flash
T	Thymine
TAE	Tris acetate EDTA
TCF	T-cell factor
Tris	2-amino-2-(hydroxymethyl)propane-1,3-diol
TSPAN12	Tetraspanin-12
TVL	Tunica vasculosa lentis
VEGF	Vascular endothelial growth factor
WG	Weeks of gestation
WT	Wild type
ZNF408	Zinc finger protein-408

1.1 Introduction

Familial exudative vitreoretinopathy (FEVR) is a rare, inherited, vasoproliferative disorder of the retina (Gow *et al.*, 1971; Tasman *et al.*, 1981). In 1969, Criswick and Schepens first described this condition in six different families and termed it as familial exudative vitreo retinopathy (Criswick *et al.*, 1969). They reported autosomal dominant inheritance pattern of the condition and accordingly it was termed as dominant exudative vitreo retinopathy. Though, initially the disease was believed to be a familial disorder, in later descriptions of FEVR, sporadic cases were also reported (Miyakubo *et al.*, 1984; Shastry *et al.*, 1997). This disease is primarily characterized by failure in the development of peripheral retinal vasculature (Canny *et al.*, 1976; Laqua, 1980). Avascularized peripheral retina, especially, the temporal retina is the typical diagnostic feature in FEVR patients (Ebert *et al.*, 1993; Benson, 1995). In most of the patients, this feature would remain as asymptomatic without any further progression (Ebert *et al.*, 1993; Benson, 1995). Sometimes, even the patients are unaware of the condition throughout their life. The common clinical findings that have been described for the mild forms of the disease include vitreoretinal adhesions, arteriovenous anastomosis, super numerous vascular branching, dilated and tortuous retinal vessels at the peripheral retina (Miyakubo *et al.*, 1984). In some patients, the primary pathological feature could lead to retinal ischemia, neovascularization, formation of subretinal, intraretinal hemorrhages and exudates (Benson, 1995; Pendergast *et al.*, 1998). These secondary clinical features further progress to the development of fibrovascular epiretinal membranes, tractional macular ectopia, falciform retinal folds and total retinal detachment that lead to complete blindness (Van Nouhuys, 1981; Benson, 1995).

FEVR has been reported across all the ethnic groups worldwide but being a very rare disorder, its incidence and prevalence have not yet been documented. The disease exhibits a high degree of variability in its phenotype and also in its clinical course (Benson, 1995). Such variability has been observed even between the two eyes of a same patient and also across different affected members from the same families (Toomes *et al.*, 2004b). The course of the disease can vary tremendously from a non progressive or slowly progressive form to a rapidly progressive form with a total retinal detachment (Benson, 1995). The underlying reason for its variable expression and clinical course is yet unclear. While FEVR has been reported across all the age groups, retinal detachment and complete loss of vision has been observed during the first two decades of life in the severely affected patients (Benson, 1995). In milder forms, the disease may either progress to advanced stages or may be quiescent over the entire life of a patient (Benson, 1995).

Three major classifications have been proposed to describe the clinical course and severity of the disease. Based on severity, Gow and Oliver (1971) classified the disease into three stages. Later, Miyakubo *et al*., (1984) described a grading system and categorized the affected eyes of the patients under 5 different types based on their retinal vascular pattern (Miyakubo *et al.*, 1984). The third classification described by Pendergast and Trese (1998) grouped the affected eyes of the patients into five different stages according to the severity of the disease and type and extent of the retinal detachment. Currently, this is the most widely accepted classification for its implications in the surgical treatment of FEVR.

FEVR is a genetically heterogeneous disease and exhibits X-linked (MIM # 305390), autosomal dominant (MIM # 133780) and autosomal recessive (MIM # 601813) modes of inheritance, of which the autosomal dominant form is most widely reported. So far, one X-linked and five autosomal dominant loci have been mapped in this disease (Chen *et al.*, 1993; Robitaille *et al.*, 2002; Toomes *et al.*, 2004a; Nikopoulos *et al.*, 2010a;

Collin *et al.*, 2013). These loci were designated from *EVR1* to *EVR6*, of which the *EVR3* is yet to be characterized for mutations (Downey *et al.*, 2001).

EVR1 (Exudative vitreo retinopathy 1) was the first locus mapped on chromosome 11q13-q23 (Li *et al.*, 1992). In a refined genetic analysis at this locus, two small nucleotide base pair deletions were identified in the *FZD4* gene (MIM # 604579) in two multi generation FEVR families from Europe (Robitaille *et al.*, 2002). Further studies confirmed the presence of truncating changes and missense mutations in this gene accounting for 3.5 to 40 % of the FEVR patients from different ethnic backgrounds (Kondo *et al.*, 2003; Toomes *et al.*, 2004b; Boonstra *et al.*, 2009; Nikopoulos *et al.*, 2010b; Yang *et al.*, 2012b). This gene encodes for a 537 amino acid containing Frizzled-4 protein, which acts as a receptor in Norrin/β-catenin signaling pathway (Xu *et al.*, 2004).

Subsequently, the second FEVR locus, *EVR2* was mapped on the X chromosome at Xp11.4 (Fullwood *et al.*, 1993). The underlying gene was identified as *NDP* (Norrie disease pseudoglioma; MIM # 300658) (Chen *et al.*, 1993). Mutations in this gene have been linked to Norrie disease (ND), an allelic form of the FEVR. Norrie disease is a rare, X-linked recessive disorder characterized by neurodevelopmental abnormalities, sensorineural deafness and congenital blindness (Berger *et al.*, 1992b). The *NDP* gene encodes for a 133 amino acid containing secreted protein, Norrin. This protein is secreted by the retinal muller glial cells and binds specifically to the FZD4 receptor expressed on the vascular endothelial cells of the retina (Ye *et al.*, 2010). Thus, Norrin acts as a ligand and induces the canonical β-catenin signaling that is responsible for normal retinal vascularization (Ye *et al.*, 2010).

Later, a study on a large Scottish family Downey *et al*., (2001) identified the third locus in FEVR on chromosome 11p12-11p13. This locus spanned a 14 centi Morgan (cM) region flanked by the markers GATA34E08 and D11S4102 (Downey *et al.*, 2001).

Following this study, there were no other reports on the association of FEVR with this locus.

The fourth *EVR4* locus was mapped on chromosome 11q13 at 10 cM centromeric to the *FZD4* gene. The *LRP5* gene (Low density lipoprotein receptor related protein 5; MIM # 603506) was identified as a candidate at this locus (Toomes *et al.*, 2004a). Mutations in this gene have been reported from different ethnic groups that accounted for 10 to 25% of FEVR patients (Jiao *et al.*, 2004; Toomes *et al.*, 2004a; Qin *et al.*, 2005; Nikopoulos *et al.*, 2010b). In addition, the loss of function mutations in this gene were also reported to be responsible for osteoporosis pseudoglioma syndrome (OPPG; MIM # 259770) (Gong *et al.*, 2001). It is characterized by low bone mass and occasional blindness. The *LRP5* gene encodes for a 1615 amino acid containing single-pass transmembrane protein. It forms a functional receptor complex with the FZD4 receptor and binds to the ligand Norrin for inducing the canonical β-catenin signaling in the retina (Ye *et al.*, 2010; Ke *et al.*, 2013).

Nikopoulos *et al*., (2010) identified *TSPAN12* (Tetraspanin-12; MIM # 613138) as the fourth candidate gene in FEVR. By using genome wide SNP analysis and next generation sequencing, they reported two missense mutations in the *TSPAN12* gene in the affected family members of two autosomal dominant FEVR families (Nikopoulos *et al.*, 2010a). Subsequent studies reported different *TSPAN12* mutations in 4 to 10% of all FEVR patients from different ethnic groups (Poulter *et al.*, 2010; Kondo *et al.*, 2011; Yang *et al.*, 2011; Poulter *et al.*, 2012). A study by Poulter *et al*., (2012) found patients with homozygous mutations in this gene to have a severe phenotype compared to mild or normal phenotype in those with heterozygous mutations, suggesting an autosomal recessive inheritance pattern of this disease. The *TSPAN12* gene encodes for a 305 amino acid containing four-pass transmembrane protein. This protein acts as a component of the FZD4-LRP5 receptor complex and augments the FZD4 multimerization, thereby enhancing the physiological levels of Norrin/ β-catenin signaling (Junge *et al.*, 2009).

The proteins encoded by these four candidate genes are important components of the Norrin/β-catenin signaling pathway that plays a crucial role in the development of a pair of intraretinal capillary beds flanking the inner nuclear layer of the retina (Junge *et al.*, 2009; Ye *et al.*, 2009; Ye *et al.*, 2010). These intraretinal capillary beds arise by the process of angiogenesis from the superficial vascular plexes residing in the vitreous/inner surface of the retina (Ye *et al.*, 2010). The knock out mouse models of these candidate genes clearly demonstrated the absence of intraretinal capillary beds, defects in the development of superficial vascular plexes and delayed hyaloid vessel regression (Ohlmann *et al.*, 2004; Xu *et al.*, 2004; Luhmann *et al.*, 2005a; Junge *et al.*, 2009; Xia *et al.*, 2010). Together, these evidences suggested a major role of this pathway in FEVR development.

Recently, Collin *et al*., (2013) identified a disease associated locus on the short arm of the chromosome 11 (11p11.2) by performing a two point linkage analysis in the probands of two autosomal dominant Dutch FEVR families lacking mutations in the known candidate genes. Exome sequencing of the disease associated locus led to the identification of a missense mutation (H455Y) in a highly conserved region of Zinc finger protein-408 (*ZNF408*) gene. In both these families, H455Y mutation segregated across all the affected family members and was not observed in 220 ethnically matched normal controls. Further screening of this gene in 77 European and 55 Japanese FEVR patients led to identification of another novel missense mutation (S126N) in a Japanese FEVR patient (Collin *et al.*, 2013). This gene encoded a 720 amino acid protein and predicted to contain ten zinc finger DNA binding domains. Based on the presence of zinc finger domains, this protein was suggested to be a transcription factor (Collin *et al.*, 2013). The inhibition of expression of this gene using splicing and translation blocking morpholinos at embryonic stage in zebrafish animal model led to impaired ocular and trunk vascularization. However, the underlying molecular mechanism of its role in Norrin-β catenin signaling pathway is yet unknown. So far, the mutations reported in the five candidate genes together accounted for approximately 50% of the FEVR cases in

different cohorts (Nikopoulos *et al.*, 2010b; Collin *et al.*, 2013). This suggested the involvement of additional candidate genes and further genetic heterogeneity in FEVR.

The molecular genetics of FEVR has been well characterized in different ethnic groups. But, these studies have largely been limited to Caucasian, Chinese and Japanese patients. Other than a report by Nallathambi *et al*., (2006), that analyzed a small FEVR cohort for *FZD4* mutations, there are no reports on the mutation spectrum of these candidate genes in Indian FEVR patients (Nallathambi *et al.*, 2006). The biological implications of these candidate genes are better appreciated if they are universally replicated across diverse cohorts worldwide. Thus, the present study was undertaken to assess the underlying molecular genetic defects in these candidate genes in order to analyze their mutation spectrum and to understand their role in FEVR development among Indian patients.

1.2 Objectives of the study

The specific objectives of the study are

1. To assess the involvement and identification of mutation spectrum of *NDP, FZD4, TSPAN12* and *ZNF408* genes in a large cohort of Indian FEVR patients.
2. To perform a genotype-phenotype correlation in order to determine their association with the clinical phenotype.

2.1. Retina

2.1.1. Anatomy and Physiology

The human retina is the light sensitive innermost tunic of the eye. It transduces incoming light signals from the cornea and lens into nerve impulses and transmits to the visual cortex of the brain through the optic nerve. Retina originates from the optic nerve at posterior side and extends anteriorly until Ora-serrata. It is a complex structure composed of five types of neuronal cells (photoreceptor, horizontal, bipolar, amacrine, and ganglion cells), four types of glial cells (muller cells, astrocytes, microglia and oligodendrocytes) and retinal pigmentary epithelial cells. The neuronal cells are arranged into nine laminated layers of the neural retina with synaptic connections (figure 2.1) (Hildebrand *et al.*, 2010).

The inner most layer of the retina is the internal limiting membrane (ILM) and is in contact with the vitreous humor. This layer is composed of proximal ends of processes of muller cells. Muller cells extend vertically through the retina until the external limiting membrane (ELM) to provide structural support and growth factors for the neuronal cells. Nerve fiber layer (NFL) is next layer to ILM and is made up of axons of the ganglion cells. The cell bodies of the ganglion cells constitute the following ganglion cell layer. The long axons of the ganglion cells converge across the nerve fiber layer and carry the final electrical output of the retina to the optic nerve. The ganglion cell layer is followed the by inner plexiform layer and consists of synaptic junctions between the ganglion cell dendrites and axons of bipolar or amacrine cells. The cell bodies of bipolar, amacrine, horizontal and muller cells constitute the inner nuclear layer of the retina. Other than glial cells, the remaining cells present in this layer are secondary neurons. They play a role in transmitting the nerve impulses obtained from photoreceptors to ganglion cells. In addition to the neural signal transmission, the horizontal cells and amacrine cells also modulate the nerve impulses that aid in formation of a good contrast image. The next layer to the inner nuclear layer is the outer plexi form layer and it is made up of synaptic connections between dendrites of bipolar cells, processes of horizontal cells and axons of rods and cones (Hildebrand *et al.*, 2010).

The following three layers of the neural retina (outer nuclear layer, external limiting membrane and photoreceptor layer) are composed of photoreceptors namely rods and cones. Photoreceptors are the light sensitive cells which are responsible for transmission of light signals to nerve impulses (phototransduction). In human retina, the rods are abundant in number (~110 million) and are responsible for dim light vision. When compare to rods, cones are very less in number (~5 million) and play a role in bright light and color vision. Structurally, each photoreceptor contains an outer segment, inner segment (mitochondria and endoplasmic reticulum), nucleus, and an inner fiber similar to an axon. The nucleus of photoreceptor cells constitutes the outer nuclear layer of the retina. The distal ends of the processes of muller cells and inner segments of the photoreceptors encompass the next layer called as external limiting membrane. The outer segments of photoreceptors occupy the final neuronal layer of the retina (Hildebrand *et al.*, 2010).

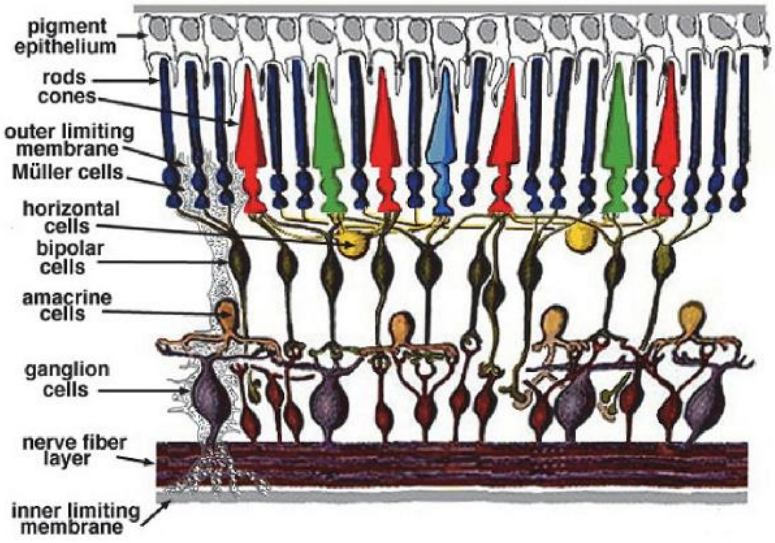

Figure 2.1: Schematic diagram of the retina showing major retinal cell types and neuronal cell inter connections (picture adapted from the source: http://webvision.med.utah.edu/book/part-i-foundations/simple-anatomy-of-the-retina/).

Other than the neural retina, a non neural layer of the retina termed retinal pigmentary epithelium (RPE) present adjacent to the photo receptor layer. It is the tenth layer of the retina and lies between the neuro sensory retina and Bruch's membrane. RPE is made up of a single layer of highly metabolically active hexagonal cells containing granules of melanin pigment. The space between the photoreceptor outer segments and RPE is filled with extracellular matrix proteins and is termed the subretinal space.

The RPE plays a vital role in the proper functioning of photoreceptors as they selectively transport nutrients, ions and metabolites from underlying choriocapillaries to the photoreceptor cells and it removes the end products of the photoreceptor metabolism. The photoreceptors regularly shed their outer segments that are damaged by free oxygen radicals generated under continuous light irradiation (Strauss, 2005). RPE cells phagocytose the discarded lipid membranes and desecrate the undigested cell debris towards the Bruch's membrane, which is later cleared by choroidal circulation. In addition, RPE cells also regenerate the photo pigment 11-cis retinol which is converted to transretinal during phototransduction process. The tight junctions between the RPE cells create a blood-retina barrier and prevent the free flow of molecules towards the neural retina from highly fenestrated choriocapillaris. Along with this, the melanin pigment present in RPE cells absorbs the scattering light and protects the other retinal cells against photo oxidative damage (Strauss, 2005; Hildebrand *et al.*, 2010) .

2.1.2. Blood supply to the Retina

The human retina is supplied with oxygen and nutrients by three different blood vascular circulations since its developmental stage to adult mature stage. They are hyaloid, choroid and retinal vasculature (Saint-Geniez *et al.*, 2004). During development, the retina is initially supplied with choroidal and hyaloid vasculatures to support outer and inner retina respectively. With maturation of the retina, the retinal vasculature replaces the hyaloid vasculature and supplies to the inner retina (Saint-Geniez *et al.*, 2004). The vasculature involved in these three different circulations is derived from retro bulbar vessels (Harris *et al.*, 2006).

2.1.2.1. Retro bulbar vessels

The blood supply to the different ocular tissues is carried out by the ophthalmic artery (OA) which emerges as a branch from internal carotid artery. While traveling anteriorly to the orbit, the OA subsequently branches into central retinal artery (CRA) and posterior ciliary arteries (PCA) and supplies to the retina and choroidal circulations respectively. The OA, CRA and PCA are combinely referred as the retro bulbar vessels (Harris *et al.*, 2006).

2.1.2.2. Choroidal vasculature and its development

Choroid is a vascular layer lying between the retina and outer fibrous layer termed as sclera. Sclera provides structural support and offers protection to the eyeball. From posterior to anterior side, the choroidal layer is further subdivided into three distinct sub layers: the Haller layer, the Sattler layer and the choriocapillaries. The Haller and Sattler layers comprise of large and medium sized blood vessels that are fed by posterior ciliary arteries (Hildebrand *et al.*, 2010). These blood vessels supply to the densest capillary network present in the inner layer of choriocapillaries. The choriocapillaries are made up of highly fenestrated endothelial cells and are separated from the RPE by Bruch's membrane. The fenestrations (800 A^0 in size) of these capillaries allow entry and exit of various molecules and provide oxygen and nutrients to the avascular RPE and photoreceptor layers through passive diffusion. (Saint-Geniez *et al.*, 2004; Anand-Apte *et al.*, 2011).

In humans, the mesoderm around the developing retina (optic cup) differentiates approximately at 28 days of gestation and form endothelial cells adjacent to the RPE. These clusters of endothelial cells are precursors for the choriocapillaries. The endothelial cells begin to proliferate and form primitive choriocapillaries between fourth and fifth weeks of gestation (WG) (Saint-Geniez *et al.*, 2004; Anand-Apte *et al.*, 2011). By the beginning of sixth WG the melanization of RPE occurs and its derived growth factors such as vascular endothelial growth factor (VEGF) and fibroblast growth factor-9 (FGF-9) support the growth of choriocapillaries. These capillaries develop characteristic fenestrated phenotype along with the development of primitive vorticose veins from

each quadrant of the choroid in the following week. In ensuing weeks, the vascular network forms the connections with posterior ciliary arteries and becomes matured by the recruitment of mural cells. Even though, the major part of choroidal vasculature development is completed by 12 to 16 WG, the density of the network increases and vascular remodeling continues until the development of final mature vascular pattern by 8 months of gestation (Saint-Geniez *et al.*, 2004; Anand-Apte *et al.*, 2011).

2.1.2.3. Hyaloid vasculature and its development

Hyaloid vasculature is a transient circulation system that provides blood supply to the avascular lens and inner retina during embryonic development. This circulation is composed of the hyaloid artery (HA), vasa hyaloidea propria, tunica vasculosa lentis (TVL) and pupillary membrane (PM). In humans, this circulation develops in concert with the choroidal vascular system. During fourth week of gestation (WG), the hyaloid artery arises from primitive ophthalmic artery and enters into the optic cup through the center of nascent optic nerve (Saint-Geniez *et al.*, 2004; Anand-Apte *et al.*, 2011). After its entrance into the optic cup, numerous branches of HA develop traversely throughout the primary vitreous and are termed as the vasa hyaloidea propria. The anterior aspect of the HA grows into a dense capillary network over the posterior portion of developing lens in the fifth WG. This capillary network around the lens is called as TVL and drains its circulation into choroidal vasculature through annular vessel at the anterior border of the optic cup. As this system lacks veins, its venous drainage is accomplished through the choroidal veins. By the end of third month of gestation, the anterior portion of the TVL develops into pupillary membrane and connects to the long posterior ciliary arteries. At 9-12 weeks of gestation, the development of hyaloid vasculature will be completed and it coincides with the initiation of retinal vascular development. As the retinal vasculature develops, the hyaloid vasculature gradually regresses and entirely disappears by the ninth month of gestation to ensure transparency of the vitreous (Saint-Geniez *et al.*, 2004; Hildebrand *et al.*, 2010; Anand-Apte *et al.*, 2011).

2.1.2.4. Retinal vasculature

Other than the choroidal vasculature which nourishes the outer layers (RPE and photoreceptors) of the retina, the inner layers of the mature retina are supplied by retinal vasculature. This vasculature is derived from the CRA and contains four major arteries (superior, inferior temporal and nasal branches) to supply each quadrant of the retina (Harris *et al.*, 2006). The major arterial branches (superficial vascular plexes) developed from these arteries are distributed radially in the nerve fiber layer of the retina close to ILM. These arteries extend from the center of the retina to peripheral retina with the decreasing diameter of the blood vessels and dichotomous branching. The branches of these arteries further develop into a dense capillary network. Along with the horizontal branches, vertical sprouts are also developed from the superficial vascular plexes and give rise to two horizontal layers of deep and intermediate retinal plexes on outer and inner plexiform layers respectively (either side of inner nuclear layer) (figure 2.2) (Saint-Geniez *et al.*, 2004; Anand-Apte *et al.*, 2011). Unlike the hyaloid circulation, this system contains veins and they are dispersed along with arteries. After reaching the Ora serrata at periphery, the retinal arterioles are connected to the venous drainage system. After completion of retinal circulation the capillary blood is drained into central retinal vein (CRV) through collecting venules. The CRV passes across the center of the optic nerve and drains its circulation into ophthalmic vein (Saint-Geniez *et al.*, 2004; Anand-Apte *et al.*, 2011).

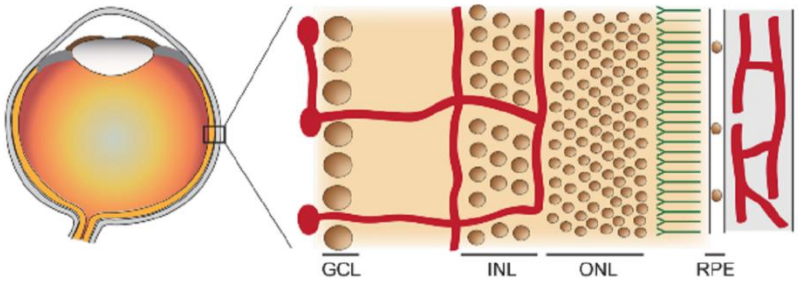

Figure 2.2: Anatomy of the retinal and choroidal vasculatures (red). Left: the human eye in cross-section; right: the retinal vasculature spans the Ganglion Cell Layer (GCL) and Inner Nuclear Layer (INL); the choroidal vasculature is immediately beyond (to the right of) the Retinal Pigmentary Epithelium (RPE). Picture adapted from Ye *et al*., (2010).

2.1.2.5. Development of retinal vasculature

Retinal vascular development is a complex process associated with the development of neuronal layers of the retina for fulfilling its metabolic needs. This process involves different bio-chemical signaling pathways, various angiogenic and anti-angiogenic factors and cellular interactions amongst the neuronal cells and endothelial cells of the developing retina (Saint-Geniez *et al.*, 2004; Anand-Apte *et al.*, 2011). The role and importance of these factors in normal retinal vascular development has come into light while studying the candidate genes for various retinal vascular diseases.

In humans, the retinal vascular development begins at the fourth month of gestational age (between 14-16 WG) when the spindle shaped mesenchymal precursor cells (haemangioblasts) enter into the nerve fiber layer from the posterior part of the hyaloid artery (Saint-Geniez *et al.*, 2004; Anand-Apte *et al.*, 2011). These precursor cells spread in a lobular fashion in each quadrant of the retina and later evolved into a vascular network of arteries and veins. The main branches of this vasculature (superficial vasculature or primary vasculature) lie in the NFL are formed by the process of vasculogenesis (McLeod *et al.*, 2006; Hasegawa *et al.*, 2008). In this process, the differentiated endothelial cells from mesenchymal precursor cells aggregate to form

blood vessels. The formation of primordial vasculature by coalescence of precursor cells is first observed near to the optic disc and later, extends centrifugally to the peripheral retina. A population of proliferating astrocytes that are migrated from the optic nerve head spread across the NFL and forms a template of cellular network to guide the growth of blood vessels in a radial fashion (Chan-Ling *et al.*, 2004; Saint-Geniez *et al.*, 2004). These astrocytes express platelet derived growth factor receptor-α (PDGFα) and they migrate in response to secretion of platelet derived growth factor-A (PDGFA) by the ganglion cells. By 21 WG, a mesh like capillary network is observed in the central retina and the precursor cells completely disappear from the developing retina. The later development of nasal and temporal capillary network of superficial vascular plexus and deep retinal vascular network is carried out by the process of angiogenesis. Angiogenesis is the process of formation of new blood vessels by budding or sprouting from the existing vessels (Saint-Geniez *et al.*, 2004; Hildebrand *et al.*, 2010; Anand-Apte *et al.*, 2011).

With the increasing metabolic activity in the developing ganglion cell layer of the retina, the astrocytes present at leading edge of the blood vessels experience hypoxia and in response they strongly express vascular endothelial growth factor (VEGF). VEGF is a well known stimulus for vascular endothelial cell survival, proliferation, migration and also responsible for the normal and pathological angiogenesis. The VEGF expression by astrocytes leads to the proliferation of blood vessels into the avascular retina which in turn, results in decrease of hypoxia and down regulation of VEGF in nearby astrocytes. As a result, an increased gradient of VEGF from central to peripheral retina is developed and it guides the growing blood vessels towards the retinal periphery. A similar VEGF gradient formed by the Muller cells during the development of photoreceptor cells guides the formation of deep retinal vascular plexus (Stone *et al.*, 1995). The endothelial tip cells present at the vascular fronts in both superficial and intra retinal networks express VEGF receptors (flk-1 or VEGFR2) and they develop cytoplasmic extensions (filopodia) to direct the growing blood vessels towards the increased VEGF gradient (Saint-Geniez *et al.*, 2004; Anand-Apte *et al.*, 2011).

The VEGF expression by astrocytes is mediated by a transcription factor hypoxia inducible factor-1 (HIF-1). Structurally, it is a heterodimeric protein containing α and β subunits. Under normoxic conditions, the oxygen dependent prolyl hyroxylase enzyme (Egl9) adds a hydroxyl group to a proline residues present in α subunit of HIF-1 (Gariano *et al.*, 2005). This reaction makes α subunit as the substrate for the ubiquitination reaction and further proteosomal degradation. Whereas, in hypoxic conditions the deactivation of Egl9 leads to stabilization of α subunit and formation of an active dimeric protein together with β subunit. After translocation into the nucleus, the HIF-1 binds to the downstream genes containing hypoxia responsive element and induces their expression. *VEGF* is one of such gene containing hypoxia responsive element and thereby its induced expression is observed under hypoxic conditions (Gariano, 2003; Saint-Geniez *et al.*, 2004).

The capillary network of superficial vascular plexes reaches the peripheral retina in some areas by 25 WG. Between 25 and 26 WG, new vessels sprout down from the superficial network and form deep network at the interface between inner nuclear and outer plexi form layers. The formation of deep retinal vascular network first occurs at the center of the retina and later expands towards the periphery. The nasal retina is completely vascularized at 36 WG, whereas the temporal vessels reach Ora serrata by approximately WG 40. Human term infants are thus born with fully developed retinal vessels with a regressed hyaloid vasculature (Stone *et al.*, 1995; Gariano *et al.*, 1996; Anand-Apte *et al.*, 2011).

2.2. Familial Exudative Vitreo Retinopathy

Familial Exudative Vitreo Retinopathy (FEVR) is a rare, bilateral, potentially blinding eye disorder caused by defects (mutations/variations) in genes that play a crucial role in development of the normal retinal vasculature. This disease was first identified as a separate entity from other morphologically similar retinal vascular disorders by Criswick and Schepens in 1969. They had described 6 patients from two different families with the ocular features; preretinal membranes, posterior vitreous detachments, retinal traction, heterotopia of the macula, neovascularization, peripheral subretinal exudates

and retinal detachments (Criswick *et al.*, 1969). The authors also suggested that vitreal abnormalities along with exudation could be responsible for the above mentioned ocular features and named the disease as FEVR. Initially, the disease was described as a familial disorder with a slowly progressive clinical course (Gow *et al.*, 1971).

In later descriptions of different FEVR families, failed development of peripheral retinal vasculature was observed predominantly at the temporal retina as the primary anomaly and this feature had been observed in majority of the patients (Canny *et al.*, 1976; Laqua, 1980). Fundus fluorescein angiograms of FEVR patients revealed abrupt termination of retinal capillaries and with fluorescein leakage at equator of the retina (Canny *et al.*, 1976; Laqua, 1980). In some patients, the avascularized peripheral retina progressed to secondary ocular complications such as abnormal vascular proliferation, hemorrhages, exudation, retinal traction owing to ectopic macula, subtotal and total retinal detachment. However, in majority of the patients for unknown reasons, the peripheral vascular non perfusion does not progress to secondary visual complications (Ober *et al.*, 1980; Benson, 1995). Avascularized peripheral retina by itself does not cause any visual complications and it may remain asymptomatic throughout the patient life or it may progress to mild or severe visual complications at any age point (Benson, 1995).

Though, initially, FEVR was believed as a slowly progressive disorder, the disease has a highly variable clinical course ranging from non-progressive/slowly progressive over the life time of a patient to rapidly progressive with severe visual impairment at infancy (Van Nouhuys, 1991; Benson, 1995). Similarly, in contrast to the initial belief that the disease was a familial disorder, Miyakubo *et al*., (1984) had observed 16 sporadic cases with previously described ocular features among 54 different FEVR patients (Miyakubo *et al.*, 1982). Since then, various studies have reported the disease in both familial and sporadic cases. The disease demonstrates incomplete gene penetrance and variable expressivity (Boonstra *et al.*, 2009; Nikopoulos *et al.*, 2010b).

2.2.1. Clinical features

2.2.1.1. Mildly affected eyes

Temporal zone of avascularized retina is the predominant feature and is the only manifestation in most of the mildly affected patients on fundus examination (Benson, 1995). However, in some cases the avascular zone may extend over different quadrants or the entire retina. Straightening, excessive branching, tortuosity of retinal vessels, micro aneurysms and arteriovenous shunts at peripheral retina are the additional features widely reported in mild disease conditions. The abrupt cessation of retinal capillaries and fluorescein leakage due to hyper permeability of the capillaries is better observed on fundus fluorescein angiography (Canny *et al.*, 1976; Ober *et al.*, 1980). The mildly affected patients are usually asymptomatic and show good visual acuity (Benson, 1995).

2.2.1.2. Moderately affected eyes

Neovascularization at the border of vascularized and avascularized retina, subretinal and intra retinal exudates and vitreo retinal adhesions are widely reported in moderately affected patients (Benson, 1995). The blood vessels involved in neovascularization are dilated and act as a source for retinal hemorrhages, formation of exudates and development of fibrovascular tissues in the retina. Fibrovascular lesions and surface elevated exudative lesions are usually observed at the temporal retina and are responsible for tractional and exudative (non rhegmatogenous) retinal detachments respectively. Vitreoretinal adhesions also lead to ectopic macula and tractional retinal detachment (Tasman *et al.*, 1981; Van Nouhuys, 1991). Retinal holes and horse shoe shaped retinal breaks are also commonly reported and are responsible for rhegmatogenous retinal detachments (Miyakubo *et al.*, 1984).

2.2.1.3. Severely affected eyes

In advanced or complicated phase of the disease, falciform retinal folds, radial retinal folds, preretinal membranes accompanied with or without massive subretinal exudates and partial or total retinal detachments are usually observed (Benson, 1995). The

falciform retinal folds extend from the optic disc to periphery of the retina and most commonly located towards the temporal or infero-temporal retina. Falciform retinal folds have been reported in 14% to 77% of the affected eyes of FEVR patients (Van Nouhuys, 1991; Benson, 1995; Ranchod *et al.*, 2011). In some cases, the folds continue from the optic disc to posterior part of the lens capsule. Rhegmatogenous retinal detachment is also a common complication along with tractional and exudative retinal detachment, and being reported in 9% to 26% of patients (Miyakubo *et al.*, 1984; Van Nouhuys an Nouhuys, 1991). Additionally, in some severely affected patients, anterior segment changes such as cataract formation, atrophy of the iris, band keratopathy, neovascular glaucoma and leukocoria are also observed (Miyakubo *et al.*, 1984; Benson, 1995).

2.2.2. Disease progression in different age groups

The rapid progression of the disease and severe visual complications are usually observed in first or second decade of the patient's life. Several infants have been reported with total blindness due to non rhegmatogenous retinal detachments within a few months after their birth (Benson, 1995). Tasman *et al*., (1981) described about rapid progression of the disease in a 6 year old patient whose vision deteriorated from 20/20 to counting fingers over a 4 week period because of retinal detachment accompanied with vitreoretinal adhesions (Tasman *et al.*, 1981). The clinical manifestations of the disease are usually stabilized after 20 years and show either non progression or slow progression in later life (Ober *et al.*, 1980; Benson, 1995). However, there are certain FEVR cases that reported with a slow progression in childhood and a rapid progression with severe visual impairment even after 20 years of age (Benson, 1995).

2.2.3. Classifications of FEVR

Three different classification systems were proposed by three individual groups of clinicians and characterized the fundus findings under different conditions of disease severity (Gow *et al.*, 1971; Miyakubo *et al.*, 1984; Pendergast *et al.*, 1998). These classification systems were proposed based on the clinician's observations in three different groups of FEVR patients from different geographic locations. Gow and Oliver

(1971) proposed the first classification and they categorized the FEVR patients under three different stages. In this classification, asymmetry of the disease between the two eyes of a same patient was not taken into account (Gow *et al.*, 1971). Later, Miyakubo *et al*., (1984) proposed a grading system to describe retinal vascular pattern under various intensities of fundus manifestations. They categorized the affected eyes into 5 distinct groups (table 2.1) mainly based on three parameters; avascular zone, neovascularization and vascular pattern in the peripheral vascularized retina. The main limitation of this classification system was it categorizes even the eyes with retinal detachment based on its vascular pattern in the peripheral retina (Miyakubo *et al*., 1984).

Table 2.1: Grades of affected eyes with FEVR and their corresponding clinical features according to Miyakubo's classification (Miyakubo *et al.*, 1984).

Grade	Corresponding clinical features
1	Avascular zone of the retina with < 2 disc diameter when measured from Ora-serrata
2	Avascular zone of the retina with > 2 disc diameter
3	V-shaped avascular zone of the retina and vitreo-retinal adhesion
4	Neovascularization and macular ectopia of the retina
5	Tractional and falciform retinal detachments and presence of solid cicatricial mass

The third classification was proposed by Pendergast and Trese in 1998. This system was a surgically oriented grading system and mainly focused on severe clinical manifestations of the disease (Pendergast *et al.*, 1998). This system had a similarity with International classification of Retinopathy of Prematurity and classified the affected eyes into five different stages according to severity of the disease and type and extent of retinal detachment. The stages described in this system also provides the information regarding the underlying mechanism for retinal detachment, and useful for guiding therapeutic interventions. The proponents of this system mainly considered tractional and exudative mechanisms responsible for retinal detachments in FEVR patients. The five stages of the disease and their prominent clinical features are described in the table 2.2.

Table 2.2: Different stages of FEVR and their corresponding clinical features according to Pendergast and Trese classification (Pendergast *et al.*, 1998).

Stages of FEVR	Corresponding clinical features	
1	Avascular retinal periphery	-
2A	Retinal neovascularization	Without exudate
2B		With exudate
3A	Extra macular retinal detachment	Without exudate
3B		With exudate
4A	Macular involving retinal detachment	Without exudate
4B		With exudate
5	Total retinal detachment	-

2.2.4. Diagnosis of FEVR

The diagnosis of FEVR is mainly based on the presence of any of the clinical features of the disease which have been described previously along with bilateral involvement and birth at full term (36-40 weeks of gestation) or preterm (before 36 weeks of gestation) with an inconsistent clinical course of retinopathy of prematurity. Family history of the disease would definitely support the diagnosis of FEVR along with autosomal dominant inheritance pattern observed in most of the FEVR patients (Benson, 1995).

During diagnosis, the fundus features of the patients are usually evaluated by indirect ophthalmoscope. In some patients, the subtle vascular abnormalities such as avascularized peripheral retina and hyper dilation of blood vessels are difficult to distinguish with the aid of indirect ophthalmoscope. In such ambiguous cases and suspected obligate carriers based on pedigree analysis, fundus fluorescein angiography is useful to detect even a mild avascularization and hyper dilation by fluorescein leakage (Ober *et al.*, 1980; Miyakubo *et al.*, 1984).

2.2.5. Differential diagnosis

2.2.5.1. Retinopathy of prematurity (ROP)

The disease condition that most closely resembles FEVR is the ROP. ROP is a disease developed in some of the premature infants with a low birth weight and short gestational age (Chen *et al.*, 2007). Oxygen supplementation and maternal health are the other risk factors of this disease. Because of premature birth, before completion of normal gestational age, these neonates are born with incomplete retinal vascularization similar to mild FEVR patients. The oxygen supplementation provided to prevent the respiratory distress in these neonates acts against oxygen sensitive vascular endothelial growth factor (VEGF) and prevents the growth of retinal blood vessels and vasoobliteration (pruning of capillaries at high oxygen concentrations) (Flynn *et al.*, 2006). Due to incomplete vascularization of peripheral retina, these neonates suffer ischemic conditions after shifting from high oxygen concentrations to normal room air. As a result, these neonates may develop neovascularization accompanied with retinal hemorrhages, fibrovascular proliferations and retinal detachments similar to moderately or severely affected FEVR patients (Benson, 1995; Flynn *et al.*, 2006). In general, lack of premature birth, lack of oxygen supplementation and normal birth weight are useful to rule out ROP during differential diagnosis of FEVR. However, the diagnosis of FEVR will be challenging in the presence of a history of premature birth and low birth weight. In these cases, the features that distinguish both the diseases are family history of the disease, presence of lipid exudates and slow progression observed in some cases of FEVR and clinical course of ROP (Ebert *et al.*, 1993; Benson, 1995; Shukla *et al.*, 2003). Inconsistent with FEVR, the clinical course of ROP follows a predictable time line. Usually, in ROP, the retinal neovascularization and retinal detachment occurs around 37 and 41 weeks of postmenstrual age respectively (Ranchod *et al.*, 2011). Additionally, in ROP patients, in absence of disease progression to severe stages, the peripheral retina becomes vascularized in subsequent weeks of growth; which is unlikely to be observed in FEVR patients.

2.2.5.2. Norrie disease (ND)

Norrie disease (ND) is an X chromosome linked (X-linked) disorder usually observed bilaterally in familial cases. The ocular features of ND include microphthalmia, retrolental masses of fibrovascular tissues (referred as pseudoglioma), vitreoretinal hemorrhages, total retinal detachment and bilateral leukocoria due to corneal opacifications (Benson, 1995). The ocular features of ND are usually observed at the time of birth or within a few months after birth. Retinal detachments and preretinal membranes are the common features in FEVR and ND. However, the corneal opacifications and microphthalmia that have been usually observed in ND are uncommon in FEVR (Tasman *et al.*, 1981; Benson, 1995; Shukla *et al.*, 2012). Additionally, one third of the ND cases have been reported with mental retardation and/or progressive hearing loss (Warburg, 1965). It has been reported that, ND is allelic with some cases of FEVR and the mutations in *NDP* gene are responsible for both ND and X-linked FEVR (Kondo *et al.*, 2007a).

2.2.5.3. Coats disease

The patients of Coats' disease show some of the ocular features similar to FEVR patients. In both the diseases, the commonly observed ocular features are dilated peripheral retinal capillaries (retinal telangiectasis), exudation and exudative retinal detachment (Benson, 1995; Shukla *et al.*, 2003). However, in coats' disease, a prominent capillary dilation and profuse exudation is observed compared to FEVR. Unilateral disease involvement, male predilection, vascularized peripheral retina and lack of family history are usually observed in Coats' disease in contrast to FEVR patients (Tasman *et al.*, 1981; Benson, 1995). Neovascularization and vitreoretinal traction is also very rare in Coats' disease which is often observed in moderately or severely affected FEVR patients (Benson, 1995).

2.2.5.4. Persistent hyperplastic primary vitreous (PHPV) or Persistent fetal vasculature (PFV)

The ocular features of PHPV include covering of vascularized tissue all over the lens or posterior part of the lens, centrally dragged ciliary process, persistence of hyaloid artery, intravitreal hemorrhages, retinal detachments and preretinal membranes (Benson, 1995). Preretinal membranes and retinal detachments are the common features observed in both FEVR and PHPV. However, unlike in FEVR, corneal opacifications, microphthalmia, remnants of hyaloid artery and leukocoria are often observed at the time of birth in PHPV (Tasman *et al.*, 1981; Shukla *et al.*, 2003). Inconsistent with FEVR, PHPV is usually observed in unilateral and sporadic cases (Benson, 1995).

2.2.6. Treatment

The treatment of FEVR mainly includes surgical procedures (Pendergast *et al.*, 1998). Peripheral laser ablation therapy is the widely used procedure for stage 2 FEVR patients with neovascularization. Scleral buckling is the treatment modality for the rhegmatogenous and non rhegmatogenous retinal detachments of FEVR patients with no vascular proliferation. In presence of aggressive proliferation with tractional retinal detachments, vitrectomy or vitrectomy along with scleral buckling are suggested to treat the disease (Pendergast *et al.*, 1998). Intravitreal injections of anti-VEGF antibodies are also useful to reduce the neovascularization and associated exudation in case of stage 2 disease (Tagami *et al.*, 2008). In a series of 15 eyes of 12 FEVR patients (mean age: 4.4±5 years) with stage 2 disease, Pendergast *et al*., (1997) reported improved visual acuity (median visual acuity 20/150) in all the eyes that underwent laser ablation therapy. In eight treated eyes, sub retinal exudates were resolved gradually and there was no progression of the disease up to 6 months follow-up. In the remaining seven eyes, the disease was progressed to further stages and required scleral buckling or vitrectomy surgeries to treat the disease. In 32 eyes of 24 FEVR patients (stage 3 and 4; mean age 3.3±4.7) which underwent retinal detachment surgeries (vitrectomy in 26 eyes and scleral buckling in 6 eyes) a mean improved visual acuity of 20/100 was reported (Pendergast *et al.*, 1998).

2.2.7. Pathogenesis

Ischemia resulting from an avascularized peripheral retina is the underlying cause of severe visual complications in FEVR patients. Hypoxic conditions lead to increased expression of VEGF-A, neovascularization accompanied with retinal hemorrhages, exudation and tractional retinal detachment (Luhmann *et al.*, 2005a). The reason for incomplete retinal vascularization along with a new signaling pathway that is crucial in developmental retinal angiogenesis came into light after the discovery of *NDP* and *FZD4* gene mutations in FEVR patients (Chen *et al.*, 1993; Robitaille *et al.*, 2002). Subsequently, Gong *et al*., (2001) observed the involvement of *LRP5* mutations in the development of a disease condition termed as osteoporosis pseudoglioma syndrome (OPPG) (Gong *et al.*, 2001). Along with the low bone mass phenotype, the ocular features observed in OPPG syndrome including congenital retinal folds, PFV and pseudoglioma were similar to ND and FEVR phenotype. A similar ocular phenotype observed in knock out mouse models of these genes (*NDP, FZD4 and LRP5*) added further support for the importance of these genes in retinal angiogenesis (Richter *et al.*, 1998; Xia *et al.*, 2008; Xia *et al.*, 2010). Based on this information, Xu *et al*., (2004), observed that Norrin, a secreted protein encoded by *NDP* gene, specifically binds to the FZD4 receptor and induces TCF/LCF transcription factor mediated gene expression in a manner similar to the canonical Wnt-β catenin signaling pathway. In the presence of a coreceptor- LRP5 encoded by the transfected *LRP5* gene, the Norrin-FZD4 signaling was significantly enhanced (Xu *et al.*, 2004). Later, Junge *et al*., (2009) had identified that another transmembrane protein Tetraspanin-12 (TSPAN12) was also a component of this pathway and it specifically induces Norrin-FZD4 signaling without having any effect on canonical Wnt-β catenin signaling mechanism (Junge *et al.*, 2009). In agreement with this finding, *TSPAN12* mutations were subsequently reported in some FEVR families (Nikopoulos *et al.*, 2010a; Poulter *et al.*, 2010).

2.2.7.1. Canonical Wnt-β catenin signaling

The Canonical Wnt-β catenin signaling pathway is one of the most extensively studied pathway in different organisms. This pathway is highly conserved across different species of invertebrates and vertebrates (Cadigan *et al.*, 1997; van Amerongen *et al.*, 2008) . In humans this signaling mechanism occurs in various tissues and plays a crucial role in embryonic development, homeostasis and cell differentiation (Logan *et al.*, 2004). As well as in various physiological processes, the role of this signaling mechanism is well established in different pathological processes including colon cancer, skin cancer, leukemia and Alzheimer's disease (Logan *et al.*, 2004; Lento *et al.*, 2013; Lim *et al.*, 2013).

Wnt proteins are secreted glycoproteins that act as ligands in this pathway. The name Wnt comes from a combination of gene '*wg*' responsible for Drosophila wingless phenotype and murine int-1 proto oncogene (Cadigan *et al.*, 1997). These are the first described Wnt proteins. There are nineteen Wnt genes in the human genome, of which the proteins encoded by *Wnt1, Wnt3A* and *Wnt 8* genes are known to be involved in the canonical Wnt signaling pathway (Cadigan *et al.*, 1997). After these proteins are secreted, they bind to the extracellular matrix and involved in paracrine signaling. These ligands specifically bind to their respective frizzled receptors and form a complex with LRP5/6 co-receptors (MacDonald *et al.*, 2012). In the absence of the Wnt ligands, the constitutively expressed cytoplasmic β-catenin molecules are recruited by a protein complex composed of a scaffold protein: Axin, tumor suppressor protein: adenomatous polyposis coli (APC) and serine or threonine kinases: glycogen synthase kinase - 3β (GSK-3β) and casein kinase-1 (CK1) (MacDonald *et al.*, 2012). Subsequently, kinases phosphorylate the serine and threonine residues of β-catenin (Ser45 is phosphorylated by CK1 and Ser33, 37 and Thr41 are phosphorylated by GSK-3β) and makes it as a substrate for ubiquitination and further degradation by 26S proteosomal complex (MacDonald *et al.*, 2012).

Conversely, in the presence of the Wnt ligands, the formed FZD receptor and LRP5/6 co-receptor complex recruits a cytoplasmic Dishevelled (Dvl) protein through the highly

conserved cytoplasmic PDZ (KTxxxW) domain of the FZD protein (Umbhauer *et al.*, 2000). The Dvl protein further recruits the axin molecule through the interaction between DIX (Disheveled and axin) domains present in both molecules (MacDonald *et al.*, 2012). Along with axin, the proteins involved in the β-catenin destruction complex (GSK-3β, CK1 and APC) are localized near the plasma membrane and phosphorylate the serine residues present in the cytoplasmic PPPSPxS motifs of LRP5/6 proteins (MacDonald *et al.*, 2012). The cytoplasmic domain of LRP5/6 protein contains five highly conserved PPPSPxS signature motifs and after their phosphorylation by GSK-3β and CK1 kinases, each motif individually recruits axin molecules and makes it unavailable for formation of the β-catenin destruction complex (MacDonald *et al.*, 2012) (Zeng *et al.*, 2005). As a result, the β-catenin molecules are stabilized and accumulate in the cytoplasm. After its accumulation in the cytoplasm they are translocated into the nucleus and physically displace a transcription factor inhibitor Groucho from TCF/LEF (T-cell factor/ lymphoid enhancer factor) transcription factors (Tam *et al.*, 2010). This displacement results in the activation of TCF/LEF transcription factors and promotes the expression of Wnt- β-catenin signaling target genes including *cMyc, cJun* and *Cyclin D1* etc., responsible for cell proliferation and migration (Tam *et al.*, 2010).

2.2.7.2. Norrin/ FZD4 signaling and its role in retinal vascular development and maintenance of its integrity

In Norrin/FZD4 signaling, Norrin acts as a ligand for induction of β-catenin stabilization and TCF/LEF mediated gene expression (Xu *et al.*, 2004). In the retina, Norrin is secreted by the muller glial cells, forms homodimers and binds to the extracellular matrix after its secretion (Ye *et al.*, 2009; Ke *et al.*, 2013). The high affinity between Norrin and extracellular matrix indicates the autocrine or paracrine activity of this ligand near the secreted region (Perez-Vilar *et al.*, 1997). Though, Norrin is structurally divergent from Wnt proteins, it specifically binds with extracellular cysteine rich domain (CRD) of FZD4 and does not detectably bind to the other nine FZD receptors expressed in humans (Smallwood *et al.*, 2007). In the retina, the FZD4 receptor, LRP5 co-receptor and TSPAN12 proteins are expressed by vascular endothelial cells and they form a ternary protein complex in response to binding of Norrin to the FZD4 receptor (Ye *et al.*,

2009). Structurally, Norrin is L- shaped structure with different binding surfaces for FZD4 and LRP5 proteins (Ke *et al.*, 2013). In the absence of Norrin, FZD4 does not interact with LRP5 (Ke *et al.*, 2013). In contrast, FZD4 physically interacts with TSPAN12 and colocalizes with it in the cell membrane (Knoblich *et al.*, 2013). TSPAN12 promotes multimerization of the FZD4 and thereby induces the signaling mechanism (Junge *et al.*, 2009). Induction of this signaling mechanism further leads to targeted gene expression responsible for vascular endothelial cell proliferation, migration and organized growth of retinal vasculature (figure 2.3).

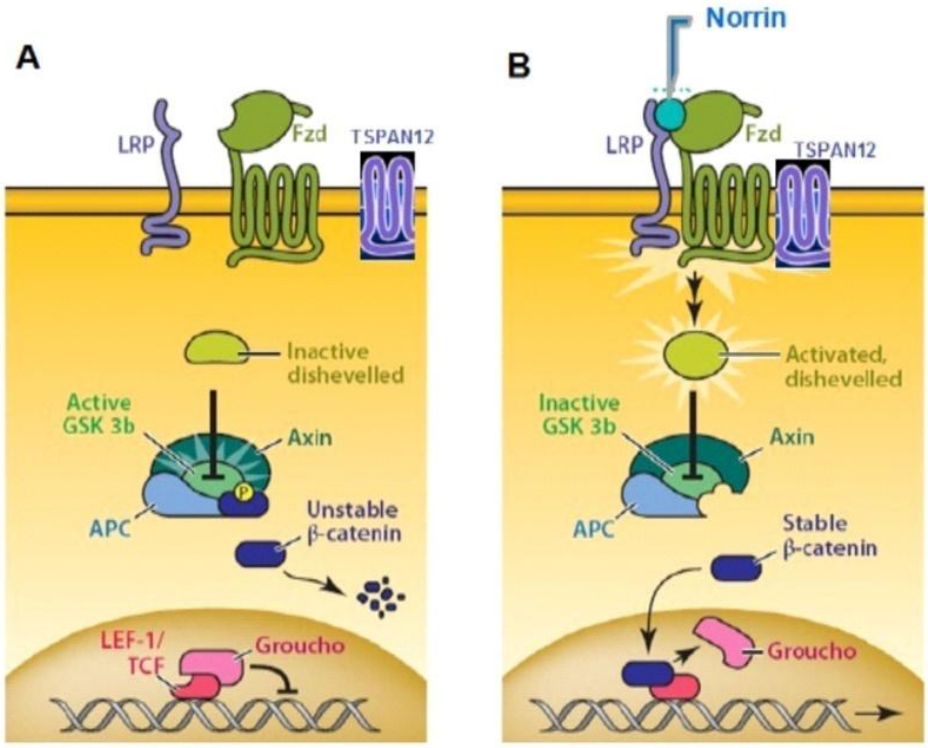

Figure 2.3: Norrin/FZD4 signaling. Figure A shows the phosphorylation of β-catenin molecule by a protein complex (β-catenin destruction complex; AXIN, APC and GSK3b) in absence of Norrin. The phosphorylated β-catenin is degraded by ubiquitination and proteosomal degradation pathway. Figure B shows in presence of Norrin ligand the Norrin/FZD4 signaling is activated and inhibits the β-catenin destruction complex through activation of dishevelled protein. As a result, the accumulated β-catenin in

cytoplasm is translocated into nucleus and activates the TCF/LEF transcription factor mediated gene expression. Figure adapted from Tam *et al*., 2010 (Tam *et al.*, 2010).

Consistent with the detected mutations in *NDP, FZD4, LRP5* and *TSPAN12* genes in FEVR patients and impaired development of retinal vasculature in knockout mouse models, the role of this signaling pathway in retinal vascular development is further evidenced by matrigel assays. In matrigel, the wild type retinal endothelial cells (REC) have shown proliferation, migration and formation of cord like structures (Ye *et al.*, 2009; Ye *et al.*, 2010). In contrast, the REC generated with any of mutated *NDP, FZD4* and *LRP5* genes have shown impaired network formation on matrigel.

In addition to the development of embryonic retinal vasculature, the role of Norrin/FZD4 signaling has also been implicated in the maintenance of vascular integrity in retina (Ye *et al.*, 2009; Ye *et al.*, 2010). The expression of the components of this signaling pathway in adult vasculature further supports its role in maintenance of vascular integrity. It seems this signaling pathway regulates the vascular integrity by two different mechanisms. The first mechanism suggested that it regulates the interactions between the vascular endothelial cells and mural cells (Luhmann *et al.*, 2005a; Wang *et al.*, 2012) based on the lower coverage of retinal vasculature with mural cells in *FZD4* and *NDP* KO mouse (*FZD4*$^{-/-}$ *and NDP*$^{-}$) during development and in adult vasculature (Luhmann *et al.*, 2005a; Wang *et al.*, 2012). Mural cells play an important role in maintaining homeostasis of vascular endothelial cells and in regulating vascular permeability through its contractile nature. The second mechanism suggested that Norrin/FZD4 signaling maintains the integrity of vasculature by regulating the expression of a vascular permeability marker 'Plvap' (plasma lemma vesicle associated protein) and a cell adhesion tight junction protein Claudin5 (*Cln5*). The retinal vasculature in KO mouse models of *NDP, FZD4, LRP5* and *TSPAN12* genes showed an increased expression of *Plvap* and a decreased expression of *Cln5* (Junge *et al.*, 2009; Schafer *et al.*, 2009; Chen *et al.*, 2012; Wang *et al.*, 2012). The varied expression of these proteins could be responsible for dilated retinal vessels and loss of the blood retina barrier in the transgenic mouse models and in FEVR and ND patients. In addition, the decreased interaction between vascular endothelial cells due to low expression of

Cln5 may also disrupt endothelial cell homeostasis, migration and vascular growth (Luhmann *et al.*, 2005a).

2.2.8. Mouse models with loss of function mutations (knockout) in *NDP, FZD4, LRP5* and *TSPAN12* genes

In an effort to understand the underlying mechanisms involved in retinal vascular development and the pathogenesis of FEVR, mouse models were developed with loss of function mutations in *NDP, FZD4, LRP5* and *TSPAN12* genes (Berger *et al.*, 1996; Rehm *et al.*, 2002; Xu *et al.*, 2004; Xia *et al.*, 2008; Junge *et al.*, 2009). Mouse models were found to be very useful to study different molecular events occurred during the development of retinal vasculature mainly because the entire growth of the retinal vasculature occurs after birth (Stahl *et al.*, 2010). The murine retinal vasculature and its morphology is highly comparable to humans (Fruttiger, 2007). In addition, the development of transgenic mouse models is technically and economically feasible compared to animal models of higher mammals.

2.2.8.1. Time course of retinal vascularization in mouse

The time course of retinal vascularization and hyaloid regression has been described for the C57BL/6J mouse strain. This strain has been widely used in development of transgenic mice with the above described gene knock outs.

Like humans, C57BL/6J mouse strains develop three different vascular beds in the retina (Fruttiger, 2007; Stahl *et al.*, 2010). The superficial vascular plexus at the top of the ganglion cell layer is developed during the first postnatal week. The growth of these blood vessels is initiated at the optic disc and reach the periphery of the retina at postnatal day 7 or 8 (P7/8). After P7, the superficial vascular plexus gives rise to vertical sprouts and develop deep and intermediate vascular plexus in the outer plexiform layer and inner plexi form layer of the retina respectively. The deep vascular plexus develops in the second postnatal week between P8 and P12. The development of intermediate plexus follows the development of deep plexus and occurs between P12 and P15. After

the development of the blood vessels, they further remodel and mature by the end of third postnatal week (Fruttiger, 2010).

2.2.8.2. The *Ndph* knockout mouse

The human *NDP* gene and the murine orthologue *Ndph* (Norrie disease pseudoglioma homologue) are highly conserved and consists 94% homology between their encoded amino acid (aa) sequences (Luhmann *et al.*, 2005a). In mouse the Norrin protein consists 131 aa whereas, in humans it consists 133 aa. A high *Ndph* gene expression was reported in retina, brain, inner ear, uterus and deciduae (Berger *et al.*, 1996; Ye *et al.*, 2011). In the retina, *Ndph* expression was observed in the muller glia (Ye *et al.*, 2009) while cerebellum, cortex, olfactory bulb and stem in brain showed a high expression of *Ndph* gene. Pituitary gland and Hippocampus of brain have shown low expression levels of *Ndph gene* (Luhmann *et al.*, 2008). In the cochlea of the inner ear, *Ndph* gene expression was limited to vasculature of the stria vascularis, capillary plexus between the organ of Corti and the spiral ganglion cells (Rehm *et al.*, 2002).

Similar to human *NDP*, mouse *Ndph* gene also consist three exons and is located on the X-chromosome. The exon 2 and 3 of *Ndph* gene partially contains the coding region for Norrin protein (Berger *et al.*, 1996). The *Ndph* knock out mouse was generated by a targeted replacement of the protein coding portion in exon 2 with a reverse oriented neomycin cassette in 3.5 days old blastocysts of C57BL/6 mouse (Berger *et al.*, 1996; Richter *et al.*, 1998). The initial phenotypic characterization of *Ndph*$^{-}$ male mice revealed a delayed and reduced outgrowth of the superficial capillary network towards the peripheral retina. The *Ndph*$^{-}$ mice showed a complete absence of deep retinal vasculature in inner plexi form layer (IPL) and outer plexi form layer (OPL) of retina compared to control mice (Luhmann *et al.*, 2005a). The vessels located in the ganglion cell layer (superficial vascular plexus) of *Ndph*$^{-}$ mice showed a high fenestrated phenotype (Richter *et al.*, 1998; Luhmann *et al.*, 2005a). At all the age groups, these knockout mice showed remnants of the hyaloid vessels in the vitreous (Richter *et al.*, 1998; Ohlmann *et al.*, 2004). By 3 weeks of age, the *Ndph*$^{-}$ mice developed retrolental membranes in the vitreous (Richter *et al.*, 1998). Dysmorphic retina with a prominent

disorganization of ganglion cell layer was the other conspicuous and commonly observed feature in these knockout mice (Richter *et al.*, 1998). Surprisingly, the heterozygous knockout (*Ndph*$^{+/-}$) females showed normal retinal vascular morphology and development as similar to wild type animals (Richter *et al.*, 1998; Luhmann *et al.*, 2005a). Similar to *Ndph*$^{+/-}$ mice, the heterozygous knockout mice of *Fzd4, Lrp5* and *Tspan12* genes also showed normal retinal vascular morphology and vascular development (Xu *et al.*, 2004; Xia *et al.*, 2008; Junge *et al.*, 2009).

The electroretinography (ERG) measurements conducted to investigate retinal function in *Ndph*$^{-}$ mice showed a severe defect in transducing the electrical signal by the inner nuclear layer of the retina. In *Ndph*$^{-}$ mice, a normal a-wave and severely reduced or negative b-wave was observed. In ERG, the a-wave represents the function of photoreceptors and b-wave represents the function of secondary neurons in the inner nuclear layer (Luhmann *et al.*, 2005a). In *Ndph*$^{-}$ mice retinas (P7), the reduced expression levels of a Muller cell specific glutamate (acts as a neurotransmitter in retina) transporter (Slc38a5; solute carrier family 38, member 5) was suggested to be responsible for a reduced b-wave in ERG (Schafer *et al.*, 2009). In consistent with *Ndph*$^{-}$ mice, a similar ERG patterns and reduced expression levels of glutamate transporters were observed in retina of *Fzd4*$^{-/-}$ and *Lrp5*$^{-/-}$ mice (Ye *et al.*, 2009; Xia *et al.*, 2010; Chen *et al.*, 2012). This information suggests the role of Norrin/Fzd4 signaling in Muller cell function along with normal retinal vascular development.

In addition to reduced levels of Slc38a5, a highly increased expression of vascular permeability marker 'Plvap' was also observed in the vasculature of *Ndph*$^{-}$ retina (Schafer *et al.*, 2009). Consistently, the increased 'Plvap' levels were also observed in *Fzd4*$^{-/-}$, *Lrp5*$^{-/-}$ and *Tspan12*$^{-/-}$ mice retina (P5 to P12) (Junge *et al.*, 2009; Paes *et al.*, 2011; Chen *et al.*, 2012; Wang *et al.*, 2012). The increased expression of Plvap was suggested to be responsible for leaky nature of retinal blood vessels, formation of retinal hemorrhages and loss of blood retina barrier (BRB) property (Schafer *et al.*, 2009).

In concordance with Norrie disease patients, the *Ndph*$^{-}$ mice have also exhibited a progressive hearing loss in addition to retinal vascular abnormalities (Rehm *et al.*,

2002). Initially, the hearing loss was observed at high frequencies of sound, later, it progressed to all frequencies of sound and the mice became profoundly deaf by 15 months of age. The primary defect that led to progressive hearing loss was observed as abnormal vasculature of the stria vascularis. In *Ndph*$^{-}$ mice, the development of cochlea was normal at P12. At 3 months of age, the vessels of stria vascularis became enlarged and their density was decreased progressively. The impaired function of stria vascularis, due to complete degeneration of its vasculature further led to loss of outer hair cells in the cochlea (Rehm *et al.*, 2002). A similar progressive hearing loss was also observed in *Fzd4*$^{-/-}$ mice (Wang *et al.*, 2001). In contrast to the developmental defect in the retina, the vessels of the inner ear developed normally during the initial life period of these knockout mice. But, the progressive pathological changes observed in adult life of *Ndph*$^{-}$ and *Fzd4*$^{-/-}$ mice led to profound deafness (Wang *et al.*, 2001; Rehm *et al.*, 2002). Thus, Norrin/Fzd4 signaling probably has variable effect on vasculature of eye and inner ear. It has a role in vascular development in the eye and maintains the vascular integrity in the inner ear.

In addition to previously described phenotypes, it was also reported that the complete loss of function of Norrin in *Ndph*$^{-/-}$ females led to infertility (Luhmann *et al.*, 2005b). In contrast, the heterozygous knockout females (*Ndph*$^{+/-}$) and hemizygous males (*Ndph*$^{y/-}$) maintained their fertility. In the *Ndph*$^{-/-}$ mice, after coitus, due to abnormal vascularization of the implants and the deciduae, the maternal reproductive tract (endometrium) failed to support fetal development. The remodeling of endometrium upon implantation of the embryo (decidualization) was impaired in the knockout mice and that led to embryonic lethality (Luhmann *et al.*, 2005b). In humans, the homozygous *NDP* mutations and infertility in females have not been reported so far.

2.2.8.3. The *Fzd4* knockout mouse

The human and murine *Frizzled-4* genes are highly homologous and share 96% sequence identity at the amino acid level. The *Fzd4* knockout mice were generated through a targeted replacement of the coding region of the *Fzd4* gene on chromosome 7 with a knock-in construct of β-galactosidase reporter after initiator methionine codon (Wang *et al.*, 2001). In these knock-out mice, the expression pattern of *Fzd4* gene was observed through X-gal staining. *Fzd4* gene expression was observed at a high amount in the embryo at mid gestation period and in the adult throughout the central nervous system, retinal vasculature, photoreceptors, inner ear, ovaries, vasculature of the heart, kidney and visceral organs (Kirikoshi *et al.*, 1999; Wang *et al.*, 2001; Descamps *et al.*, 2012).

In *Fzd4* homozygous knockout mice ($Fzd4^{-/-}$), low growth rate was observed compared to wild type littermates and *Fzd4* heterozygous knockout ($Fzd4^{+/-}$) mice. Nearly 50% of $Fzd4^{-/-}$ mice died during the first several months of postnatal life (Wang *et al.*, 2001). The homozygous knockout mice developed a light black or silver coat color in contrast to black or agouti coat color of their heterozygous knockout parents. In addition to coat color, $Fzd4^{-/-}$ mice showed hunch back appearance with an abnormal gait and esophageal dysfunction. The defects in esophagus were suggested to be responsible for retardation of growth in $Fzd4^{-/-}$ mice (Wang *et al.*, 2001).

Like *Ndph* knockout mice, the retina of $Fzd4^{-/-}$ mice have delayed growth of superficial retinal vascular plexus with complete absence of two intraretinal vascular beds (Xu *et al.*, 2004). Many of the blood vessels were dilated and highly fenestrated that might be due to increased expression of Plvap and lower levels of Claudin-5 protein (Wang *et al.*, 2012). The vitreous also showed remnants of hyaloid vessels and vitreal hemorrhages. However, in contrast to $Ndph^{-/-}$ mouse, no obvious disorganization or degeneration of retinal neurons were observed in $Fzd4^{-/-}$ mice retinas (Xu *et al.*, 2004).

In addition to the ocular phenotype, a progressive hearing loss was also observed in $Fzd4^{-/-}$ mice (Wang *et al.*, 2001). In contrast to $Fzd4^{-/-}$ mice, the FEVR patients with *FZD4* gene mutations were not reported with hearing loss. This phenotypic difference

might be due to heterozygosity of the *FZD4* gene mutations in FEVR patients. This information along with the normal phenotype in heterozygous *Fzd4* knockout (*Fzd4*$^{+/-}$) mice would therefore suggest that, the reduced dose of mutant protein might not induce auditory problems in contrast to ocular phenotype (Wang *et al.*, 2001).

Along with stria vascularis, progressive loss of vascular morphology was also observed in cerebellum of *Fzd4*$^{-/-}$ mice (Wang *et al.*, 2001). The changes in vascular morphology led to loss of blood brain barrier and formation of hemorrhages in the cerebellum that further leads to progressive loss of Purkinje cells and cerebellar degeneration (Wang *et al.*, 2012). Abnormal gait and wide stance observed in the *Fzd4*$^{-/-}$ mice had been suggested as a sign of the cerebellar degeneration (Wang *et al.*, 2001).

In addition to above described phenotypes, the *Fzd4*$^{-/-}$ female mice were also reported to be infertile similar to *Ndph*$^{-/-}$ female mice. The vascular development of corpora lutea was impaired in *Fzd4*$^{-/-}$ mice, which led to disorganization of cells in corpora luteum and thereby causing a failure in its development (Hsieh *et al.*, 2005), while the *Ndph*$^{-/-}$ mice were infertile due to impaired decidualization (Luhmann *et al.*, 2005b).

2.2.8.4. The *Lrp5* knockout and r18 mice

Mouse *Lrp5* is a 23 exon containing gene that shares 95% sequence identity with human LRP5 at amino acid level. The expression of *Lrp5* is almost ubiquitous in mouse tissues (Kato *et al.*, 2002). This gene encodes for a 1614 amino acid protein containing an extracellular domain with four LDLR domains and EGF like domains, a small transmembrane domain and an intracellular domain (Xia *et al.*, 2008).

Two different groups generated Lrp5 knockout mice for studying their phenotype (Kato *et al.*, 2002; Xia *et al.*, 2008; Xia *et al.*, 2010). The first *Lrp5* knockout mouse was generated through insertion of an IRES-*LacZ-Neomycin* cassette at codon position 373 in exon 6 (Kato *et al.*, 2002). This insertion led to formation of a truncated Lrp5 protein. The heterozygous *Lrp5*$^{+/-}$ mice generated through this approach were phenotypically normal. The homozygous *Lrp5*$^{-/-}$ mice were viable and fertile, but had a higher mortality rate presumably due to frequent bone fractures (Kato *et al.*, 2002). The *Lrp5*$^{-/-}$ mice

showed persistence of the hyaloid vessels even after post natal day 12. In wild type and *Lrp5*$^{+/-}$ mice, the regression of hyaloid vessels was initiated at P3 and usually completed by P12. In *Lrp5*$^{-/-}$ mice, it was observed that the macrophage mediated apoptosis was low compared to WT mice and it was responsible for persistence of hyaloid vessels (Kato *et al.*, 2002).

Xia *et al*., (2008) had reported another *Lrp5* knockout mouse with a similar ocular phenotype of *Ndph*$^{-}$ and *Fzd4*$^{-/-}$ mice. During their experiments of induced mutagenesis in mice with ENU (N-ethyl-N-nitrosourea), they had observed an ocular phenotype similar to FEVR in a group of mice. This group of mice was referred to as *Lrp5*^{r18} mice (Xia *et al.*, 2008). The whole genome linkage analysis and sequencing of DNA samples of these mice led to identification of a frame shift mutation at 1576 codon position of Lrp5 protein. This frame shift mutation replaces the C-terminal 39 aa of Lrp5 protein with 20 new aa residues and resulting in premature termination at codon 1596 position. This mutation was predicted to be responsible for loss of three PPPS/TP signature motifs out of five PPPS/TP motifs observed in C-terminal intracellular domain of wild type protein (Xia *et al.*, 2008). These signature motifs had been reported to be involved in transducing the signal to downstream messengers after binding of the Lrp5 with the ligand.

The hetero and homozygous r18 mice were viable and fertile. At 3 weeks of age, the homozygous *Lrp5* $^{r18/\ r18}$ mice developed blood vessels in ganglion cell layer and inner plexi form layer of the retina. But, compared to *Lrp5* $^{+/\ r18}$ and WT mice, the *Lrp5* $^{r18/\ r18}$ mice completely lost the blood vessels in the outer plexiform layer of the retina. In addition, the observed blood vessels of *Lrp5* $^{r18/\ r18}$ mice were leaky and lacking small capillaries, and lumen of the blood vessels in the inner plexi form layer of the retina (Xia *et al.*, 2008).

In addition to ocular phenotype, decreased bone mass was the other commonly observed phenotype in *Lrp5*$^{-/-}$ mice. In homozygous knockout mice, a severely decreased bone mass was observed compared to less extent of bone loss in heterozygous knockout mice (Kato *et al.*, 2002). In these mice, a decreased proliferation

of osteoblasts was observed postnatally and it was responsible for lower bone mass. Since, this phenotype was also observed in heterozygotes, it was proposed to be developed by dominant effect of the mutation (Kato *et al.*, 2002). A less vascular density was observed in forebrain tissues of *Lrp5* $^{-/-}$ mice compared to WT mice at 8 days of age (Chen *et al.*, 2012). The effect of *Lrp5* knockout on auditory system was not reported in these studies.

2.2.8.5. The *TSPAN12* knockout mouse

The murine *Tspan12* is located on the chromosome 6 and contains 9 exons (Junge *et al.*, 2009). The Tspan12 protein of mouse contains 305 amino acid residues and shares 98% sequence identity with human TSPAN12. The predicted topology of this protein contains four transmembrane domains, two extracellular loops, and an intracellular loop with intracellularly localized N and C terminals. The *Tspan12* knockout mouse was generated by a targeted replacement of 136 base pairs (bp) at 3' side of exon3 in addition to 97 bp in the following intron with IRES-*LacZ* cassette (Junge *et al.*, 2009). Thus, the targeted deletion resulted in loss of major portion of the first transmembrane domain including initiator methionine. Insitu hybridization and *LacZ* staining revealed *Tspan12* gene expression in neonatal retinal, meningeal vasculature, smooth muscle cells and neonatal intestine (Junge *et al.*, 2009).

The homozygous *Tspan12*$^{-/-}$ mice were viable and fertile. They showed similar ocular phenotype to the *Ndph, Fzd4* and *Lrp5* ko mice with delayed growth of superficial vascular plexus and complete loss of vasculature in inner and outer plexi form layers in retina (Junge *et al.*, 2009). Delayed regression of hyaloid vessels, micro aneurisms and vitreal hemorrhages were also observed in *Tspan12*$^{-/-}$ mice retina. In addition, vessel enlargement in stria vascularis was also observed. However, the interactions of this gene with *Ndph* and *Lrp5* genes resulted in moderate ocular phenotype in transheterozygous condition (*NDP*$^{+/-}$ and *Tspan12*$^{+/}$, *Lrp5*$^{+/-}$ and *Tspan12*$^{+/}$) (Junge *et al.*, 2009).

2.2.9. Genetics of FEVR

Since the first description of FEVR, the disease has been identified as an inherited disorder with a possible genetic involvement in disease pathogenesis. Gow and Oliver (1971) reported an autosomal dominant (ad) inheritance pattern for the first time in a large Caucasian family with FEVR (Gow *et al.*, 1971). Later, in various descriptions, autosomal dominant mode of inheritance had been reported in different families and termed the disease as autosomal dominant exudative vitreoretinopathy (Gitter *et al.*, 1978; Ober *et al.*, 1980; Feldman *et al.*, 1983). Chen *et al*., (1993) had first observed the X-linked inheritance pattern and identified a *NDP* gene mutation segregating with the disease in a FEVR family (Chen *et al.*, 1993). However, in majority of the FEVR families, autosomal dominant mode had been reported, very few families were observed with autosomal recessive inheritance pattern associated with mutations in *LRP5* and *TSPAN12* genes (Jiao *et al.*, 2004; Downey *et al.*, 2006; Poulter *et al.*, 2012).

2.2.9.1. Candidate loci/genes for FEVR

Six chromosomal loci (exudative vitreo retinopathy [EVR] - 1 to 6) and their associated candidate genes except in EVR3 loci have so far been implicated in FEVR pathogenesis (Chen *et al.*, 1993; Downey *et al.*, 2001; Robitaille *et al.*, 2002; Toomes *et al.*, 2004c; Nikopoulos *et al.*, 2010a; Collin *et al.*, 2013). The identified candidate genes in the corresponding EVR loci are represented in the table 2.3.

Table 2.3: Known loci and candidate genes for FEVR (Collin *et al.*, 2013)

EVR locus (OMIM)	Candidate gene (Gene code)	Chromosomal position
EVR1 (133780)	Frizzled-4 (*FZD4*)	11q14.2
EVR2 (305390)	Norrie Disease Pseudoglioma (*NDP*)	Xp11.13
EVR3 (605750)	Unknown	11p13-p12
EVR4 (601813)	Low density lipoprotein receptor related protein (*LRP5*)	11q13.2
EVR5 (613310)	Tetraspanin-12 (*TSPAN12*)	7q31.31
EVR6	Zinc finger protein 408 (*ZNF408*)	11p11.2

2.2.9.2. Identification of *Frizzled-4 (FZD4)* gene in EVR 1 locus

The first genetic locus (EVR1; OMIM #133780) associated with FEVR was mapped on long arm of chromosome 11 (11q) by Li *et al*., in 1992. By multipoint genetic linkage analysis in two different FEVR families, they identified an autosomal dominant (ad) disease associated locus between the microsatellite markers *D11S533* and *D11S35* at 11q13-q23 position (Li *et al.*, 1992). Kondo *et al*., (2001) had further delineated the associated disease locus to a 200 kilo base pair (Kb) region at 11q14 position by haplotype analysis in six different ad FEVR families (Kondo *et al.*, 2001). Through positional cloning experiments, Robitaille *et al*., (2002) further refined the disease locus and identified a 6 bp and 2 bp deletions in *FZD4* gene in the affected family members of two different FEVR families (Robitaille *et al.*, 2002).

2.2.9.3. Frizzled receptors

In human genome, there are ten different genes encode for 10 different Frizzled proteins (Schulte, 2010). They named based on their order of discovery from *FZD1* to *FZD10*. The name of the receptors 'Frizzled' is derived from a phenotype of *Drosophila melanogaster,* in which the receptor was first identified. Two different Frizzled proteins (*Dfz1* and *Dfz2*) are expressed in Drosophila. The *Dfz1* mutant shows irregularly arranged and tightly curled hairs on thorax, wings and feet. During the observation of this phenotype, Calvin Bridges *et al*., (1944) named it as 'Frizzled'. The International Union of Pharmacology classified these ten receptors as a subfamily under G-protein coupled receptor family of proteins (Schulte, 2010). These proteins are usually acted as receptors for conventional and non conventional Wnt ligands and induce canonical and/or non canonical Wnt signaling pathways.

2.2.9.4. *FZD4* gene expression

In humans, a high expression of *FZD4* mRNA was observed in adult heart, skeletal muscle, ovary and fetal kidney. A moderate amount of expression was observed in adult liver, kidney, pancreas, spleen and fetal lung. A very low expression was identified in placenta, adult lung, prostate, testis, colon, fetal brain and liver (Kirikoshi *et al.*, 1999).

2.2.9.5. FZD4 gene and protein structure

FZD4 gene consist 2 exons and encodes for a single transcript contains 7392 nucleotides. The open reading frame of this transcript codes for a 537 amino acid (aa) containing FZD4 protein. Compared to remaining paralogues, FZD4 contains a high sequence homology with human FZD9 (51.6%) and FZD10 (51.2%) proteins (Schulte, 2010). After expression, FZD4 dimerises in the endoplasmic reticulum and expressed as a plasma membrane protein (Kaykas *et al.*, 2004; Ke *et al.*, 2013). Structurally, FZD4 contain an N-terminal extracellular region, seven transmembrane helical domains, three extracellular loops, three intracellular loops and a short C-terminal cytoplasmic region (figure 2.4). The N-terminal extracellular region contains a signal peptide a (36 aa),

cysteine rich domain (CRD: 122 aa) and a linker region (64 aa) that connects CRD domain to the first transmembrane domain (Kirikoshi *et al.*, 1999).

The CRD domain of FZD4 is responsible for ligand (Norrin) binding. By *invitro* binding assays, it has been proved that, the CRD domain is sufficient for ligand binding (Smallwood *et al.*, 2007). This domain contains ten invariable cysteines that are highly conserved across all FZD orthologues and paralogues. These cysteine residues are predicted to form five disulfide bridges (45 ↔ 106, 53 ↔ 99, 90 ↔ 128, 117 ↔ 158 and 121 ↔ 145) and which are thought to be crucial for maintenance of its structure. The three dimensional model of FZD4-CRD has been developed based on the CRD crystal structure of mouse FZD8 (Smallwood *et al.*, 2007). The CRD domains of both of these proteins contain a 39% sequence identity including ten invariable cysteines.

In addition to CRD, two other highly conserved motifs in FZD4 protein are located in the C-terminal cytoplasmic tail. The KTxxxW motif is located immediately after the seventh transmembrane domain at 499 to 504 amino acid positions and it plays a crucial role in binding to the PDZ (Postsynaptic density 95, discs large, zona occludens-1) domain of Dishevelled protein (Kirikoshi *et al.*, 1999; Schulte, 2010). The second, highly conserved PDZ binding motif contains the sequence ‘ETVV’ and located at 535 to 537 amino acid positions of the FZD4 protein (Schulte, 2010). Structurally, the cytoplasmic tail is a flexible structure with a small α-helix and facilitates proper binding of dishevelled protein (Lemma *et al.*, 2013).

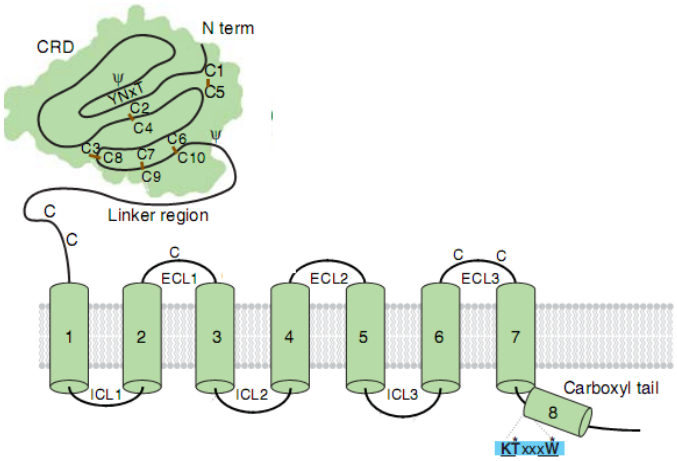

Figure 2.4: Illustration of the FZD4 protein structure with predicted extracellular cysteine rich domain (CRD), seven transmembrane, three extracellular, three intracellular and C-terminal domain. KTxxxW motif is the binding site for PDZ domain of Dishevelled protein. ECL: extra cellular loop; ICL: intra cellular loop. Picture adapted and modified from MacDonald and He, 2012 (MacDonald *et al.*, 2012).

2.2.9.6. FZD4 protein function

Based on the observed phenotypes in homozygous *Fzd4* knockout mouse models, the role of FZD4 protein is mainly implicated in developmental retinal angiogenesis, maintenance of vascular integrity in cerebellum, inner ear and in formation of corpus luteum vasculature (Wang *et al.*, 2001; Xu *et al.*, 2004; Wang *et al.*, 2012). However, in humans, the *FZD4* gene mutations are reported in some of the FEVR and ROP patients with retinal vascular abnormalities. Except one patient, remaining all of the patients have been reported with heterozygous *FZD4* mutations. Other than the ocular phenotype, no other gross abnormalities have been reported in these patients. The R417Q mutation, in homozygous condition has been reported in a female patient with severe FEVR (Kondo *et al.*, 2007b). However, no other abnormalities were reported in this patient with until the age of 20 years. Thus, in humans, FZD4 seems to play a major role in retinal vascular development and its haploinsufficiency due to heterozygous mutations is sufficient to cause FEVR (Jia *et al.*, 2010).

2.2.9.7. Reported mutations of *FZD4* gene in FEVR patients

Till date twelve different groups have reported 46 different *FZD4* mutations in FEVR patients from different ethnic backgrounds (http://www.hgmd.cf.ac.uk/ac/gene.php?gene=FZD4). The detected mutations include 29 missense, 7 nonsense, and one insertion and 9 deletions (table 2.4). So far, no splice site mutations have been reported in *FZD4* gene. These mutations are spread all over the gene without clustering at any specific hotspot. However, a higher number of mutations have been detected in the CRD, transmembrane domain 7 and C-terminal tail of the protein suggesting the important role for these regions in the protein function. The frequency of FEVR patients with *FZD4* mutations ranges from 3.5% to 40% in these reports (Kondo *et al.*, 2003; Toomes *et al.*, 2004b; Boonstra *et al.*, 2009; Yang *et al.*, 2012b). Though, majority of these mutations were found to be segregating with disease phenotype, they demonstrate variable expressivity and variable age of onset among the different affected family members. In addition, none of these studies could establish a genotype-phenotype correlation in these patients.

Excluding one mutation, remaining mutations identified in *FZD4* gene have been reported in heterozygous condition. Kondo *et al*., (2007) have reported R417Q mutation in homozygous condition in a female patient with severe FEVR at five months of age (Kondo *et al.*, 2007b). Both the parents were carrying the mutation in heterozygous condition and presented with a mild disease phenotype. In addition to a homozygous mutation in *FZD4* gene, Kondo's group also reported compound heterozygous *FZD4* mutations and a *FZD4* mutation along with an *LRP5* mutation in two different Japanese FEVR families. In family harboring compound heterozygous change, the severely affected proband was found to have H69Y and G488D heterozygous mutations on different chromosomes (Kondo *et al.*, 2003). He received G488D mutant allele from his mildly affected mother and H69Y mutant allele from his unaffected father. However, in several other studies H69Y mutation was reported in both familial and sporadic cases and predicted to be pathogenic. (Omoto *et al.*, 2004). The proband having two mutant alleles developed bilateral retinal detachments at one year of age. A case of digenic m

utations in a family has also been reported where, a mutation R417Q was observed *in FZD4* gene along with a mutation R444C *in LRP5 gene*. In this family both the mutations segregated with the disease phenotype and were suggested to be present on same chromosome. The authors had reported a severe ocular phenotype in this family compared to another FEVR patient with R417Q mutation alone (Kondo *et al.*, 2003) .

Table 2.4: List of *FZD4* mutations reported in FEVR patients

Exon	DNA change	Amino acid change	Occurrence in patients	Occurrence in control alleles	Reference
1	c.118G>C	E40Q	1/16	0/200	(Nikopoulos *et al.*, 2010b)
	c.134G>A	C45Y	1/5	0/400	(Zhang *et al.*, 2011)
2	c.173A>G	Y58C	1/5	0/400	(Zhang *et al*., 2011)
	c.313A>G	M105V	1/24	0/300	(Kondo *et al*., 2003)
			2/48	0/200	(Jia *et al*., 2011)
			2/49	NA	(Yang *et al.*, 2012b)
	c.314T>C	M105T	1/40	0/200	(Toomes *et al*., 2004)
	c.316 T>C	C106G	1/68	0/396	(Robitaille *et al.*, 2011)
	c.341 T>C	I114T	1/3	0/296	(Robitaille *et al.*, 2009)
	c.469A>G	M157V	1/40	0/200	(Toomes *et al*., 2004)
	c.470T>A	M157K	2/68	0/396	(Robitaille *et al*., 2011)
	c.538G>A	E180K	1/48	0/200	(Jia *et al*., 2011)
	c.611G>A	C204Y	1/16	0/200	Nikopoulos *et al*., 2010b)
	c.612T>C	C204R	1/53	0/200	(Nallathambi *et al.*, 2006)
			1/5	0/400	(Zhang *et al*., 2011)
	c.631T>C	Y211H	1/49	0/192	(Yang *et al*., 2012)
	c.668T>A	M223K	1/20	0/80	(Boonstra *et al*., 2009)
	c.710C>G	T237R	1/48	0/200	(Jia *et al*., 2011)
	c.757C>T	R253C	1/48	0/200	(Jia *et al*., 2011)
	c.983T>C	F328S	1/48	0/200	(Jia *et al*., 2011)
	c.1005G>C	W335C	1/56	0/300	(Qin *et al*., 2005)
	c.1015G>A	A339T	1/48	0/200	(Jia *et al*., 2011)
	c.1026A>G	M342V	1	0/120	(Yoshida *et al.*, 2004)
			1/56	0/300	(Qin *et al*., 2005)
	c.1250G>A	R417Q	2/24	0/300	(Kondo *et al*., 2003)
	c.1333A>C	T445P	1/20	0/80	(Boonstra *et al*., 2009)
	c.1408G>A	D470N	2/48	0/200	(Jia *et al*., 2011)
	c.1463G>A	G488D	1/24	0/300	(Kondo *et al*., 2003)
	c.1463G>T	G488V	1/68	0/396	(Robitaille *et al*., 2011)
	c.1474G>C	G492R	½	NA	(Muller *et al.*, 2008)
	c1490C>T	S497F	1/40	0/200	(Toomes *et al*., 2004)
	c.1573G>C	G525R	1/16	0/200	(Nikopoulos *et al*., 2010b)

DELETIONS					
1	c.39-49del CCCGGGGGCG	P14fsX57	1/48	0/200	(Jia *et al*., 2011)
	c.244_251del8	F82fsX135	1/53	0/200	(Nallathambi *et al*., 2006)
2	c.633delC	Y211fsX	1/68	0/396	(Robitaille *et al*., 2011)
	c.957delG	W319fsX323	1/40	0/200	(Toomes *et al*., 2004)
	c.1282-1285delGACA	D428SfsX2	1/68	0/396	(Robitaille *et al*., 2011)
			1/16	0/200	(Nikopoulos *et al*., 2010b)
			1/49	0/192	(Yang *et al*., 2012)
	c.1286-1290del	K429RfsX28	1	NA	(Muller *et al*., 2008)
	c.1479-1484GTGGAT	M493-W494del	2/5	0/306	(Robitaille *et al*., 2002)
			1/3	0/296	(Robitaille *et al*., 2009)
	c.1498delA	T500fsX512	1/40	0/200	(Toomes *et al*., 2004)
	c.1501-1502delCT	L501fsX533	2/5	0/306	(Robitaille *et al*., 2002)
			1/40	0/200	(Toomes *et al*., 2004)
2	**Insertions**				
	c.1508-1509insG	T503fsX31	1/68	0/306	(Robitaille *et al*., 2011)
	Nonsense mutations				
	c.678G>A	W226X	1/5	0/400	(Zhang *et al.*, 2011)
	c.856G>T	E286X	1/16	0/200	(Nikopoulos *et al*., 2010b)
	c.957G>A	W319X	1/24	0/300	(Kondo *et al*., 2003)
			5/20	0/80	(Boonstra *et al*., 2009)
	c.1472C>A	S491X	1/48	0/200	(Jia *et al*., 2011)
	c.1482G>A	W494X	1/49	0/192	(Yang *et al*., 2012)
	c.1448G>A	W496X	1/20	0/80	(Boonstra *et al*., 2009)
			1/48	0/200	(Jia *et al*., 2011)
			1/5	0/400	(Zhang *et al.*, 2011)
	c.1513C>T	Q505X	1/40	0/200	(Toomes *et al*., 2004)
			1/49	0/192	(Yang *et al*., 2012)

cDNA positions and amino acid positions have been obtained by following the reference sequences NM_012193.2 and NP_036325.2 respectively. cDNA position +1 corresponding to the A of the ATG translation initiation codon. IVS: intervening sequence (intron).

2.2.9.8. Functional characterization of *FZD4* mutations

The effect of different *FZD4* mutations either on ligand (Norrin) binding or induction of canonical-β catenin signaling had been tested by three independent groups (Xu *et al.*, 2004; Qin *et al.*, 2008; Zhang *et al.*, 2011). By employing, cell surface binding assays and STF (Super Top Flash) cell line, Xu *et al*., (2004) had tested the ligand binding and canonical-β catenin signaling inducing ability of the M105V, M157V and M493-W494del mutants of FZD4 protein. Through immunoblotting experiments by employing FZD4 antibodies, the expression levels of M105V, M157V mutant proteins were found to be similar to WT proteins, while expression of the M493-W494del mutant protein reduced by several fold. In cell surface binding assays, when Norrin fusion protein was employed with alkaline phosphotase (Norrin-myc-AP) as a probe, the recognition efficiency of the membrane localized three mutant FZD4 proteins by Norrin was comparable to the WT protein. However, severe defect in induction of LCF/TCF transcription factor mediated gene expression in STF cell line were seen (Xu *et al.*, 2004). In a 3 dimensional homology model of human FZD4-CRD, the authors had observed the near proximity of M105V and M157V mutations with partially exposed side chains of methionine towards the solvent. Based on this data, the authors have suggested this region of CRD might control the signal transduction either by contacting FZD4 membrane associated domain and/or the Lrp5 co receptor. The possible loss of protein fold in case of M493-W494del mutation was suggested to be responsible for its low signaling activity (Xu *et al.*, 2004).

Qin *et al*., (2008) had tested the effect of H69Y, M105V, R417Q and W319X mutants of *FZD4* on Norrin/FZD4 signaling. It was observed that the W319X nonsense mutation reduced the signaling activity up to 99% compared to WT protein while remaining missense mutations decreased the signaling activity in the order of H69Y (9%)>M105V (33%)>R417Q (48%). The binding ability of these mutant proteins to the Norrin decreased in the order of W319X > M105V > H69Y >R417Q compared to WT protein. The additive effect of R417Q mutation in *FZD4* gene and R444C mutation in *LRP5* gene as reported previously in a FEVR family reduced the signaling activity up to 77% when compared to a 48% decrease observed in R417Q mutation alone (Qin *et al.*, 2008). In addition to *invitro* assays, Kang Zhang *et al*., (2010) had employed Xenopus embryos

for testing the effect of five different mutations (C45Y, Y58C, C204R, W226X and W496X) of FZD4. In *invivo* assays these mutant proteins failed to induce the Norrin/FZD4 signaling.

In contrast to these studies, Kaykas *et al*., (2004) had reported the dominant negative effect of L501fsX533 mutation of *FZD4* gene. When they co-transfected 293T cells with L501fsX533 mutant and WT *FZD4* gene constructs, the mutant protein oligomerized with WT protein and retained in the endoplasmic reticulum. As a result, the membrane localization of FZD4 protein was not observed and Norrin dependent signaling was severely impaired (Kaykas *et al.*, 2004).

A study by Lemma *et al*., (2013), observed that the resulted 32 amino acid sequence after frame shift in case of L501fsX533 mutation led to formation of helix-loop-helix structure in C-terminal tail of FZD4 protein. The wild type protein had the C-terminal tail as a flexible structure with a single helix (Lemma *et al.*, 2013). The altered conformation of the C-terminal tail due to altered amino acid sequence in mutant protein was seen to interact with membrane of endoplasmic reticulum and retained in the endoplasmic reticulum. In addition to dominant negative effect of L501fsX533 mutation, these studies also observed the dimerization of FZD4 in endoplasmic reticulum and their localization in cell membrane as dimers (Kaykas *et al.*, 2004; Lemma *et al.*, 2013).

2.2.9.10. Identification of Norrie Disease Pseudoglioma (*NDP*) gene in EVR 2 locus

In various descriptions of FEVR patients, the X- linked inheritance pattern of the disease was observed in some of the FEVR families besides the widely observed autosomal dominant inheritance pattern. Dudgeon *et al*., (1979) reported an X-linked inheritance pattern in a five generation family with four affected males in the fourth generation and three affected males in the fifth generation (Dudgeon, 1979). In a subsequent study, seven affected males and five obligate carrier females of this family were genotyped for 20 DNA markers and identified a strong association of disease phenotype with the markers DXS7 (LOD score: 2.11) and DXS228 (LOD score: 1.81) on X-chromosome at positions Xp11.4-Xp11.3 and Xq21.31 respectively (Fullwood *et al.*, 1993). Since, the Xp11.4 was a known locus for Norrie disease pseudoglioma (*NDP*) gene; the different

mutations of this gene were suggested to be responsible for the development of Norrie disease and FEVR. Later, mutation screening of this gene was undertaken for the affected and unaffected males of this family through direct DNA sequencing. The sequencing data revealed a p.Leu124Phe mutation in the *NDP* gene in the affected family members (Chen *et al.*, 1993). The highly conserved nature of the mutated amino acid and the absence of mutation in 100 normal individuals further suggested the pathogenic nature of this mutation. The involvement of *NDP* gene in FEVR development was further supported by the identification of different mutations of this gene in FEVR patients from different ethnic backgrounds(Dickinson *et al.*, 2006; Drenser *et al.*, 2006; Kondo *et al.*, 2007a; Wu *et al.*, 2007; Boonstra *et al.*, 2009; Yang *et al.*, 2012a).

2.2.9.11. *NDP* gene expression

In humans, *NDP* gene expression was observed through RNA *in situ* hybridization experiments, in outer, inner nuclear layers and ganglion cell layers of the retina (Berger *et al.*, 1992a). Other than the retina *NDP* expression was observed only in human placenta (Luhmann *et al.*, 2005b). In mouse and rabbit, *NDP* expression had also been reported in cerebellum, hippocampus, neocortex and olfactory bulb of the brain (Hartzer *et al.*, 1999; Luhmann *et al.*, 2008). In addition, its expression was also observed in the inner ear of chick and mouse, uterus and deciduae of mouse (Rehm *et al.*, 2002; Luhmann *et al.*, 2005b; Ye *et al.*, 2011).

2.2.9.12. *NDP* gene and protein structure

NDP gene is located on the short arm of X-chromosome at Xp11.4 position. It spans a genomic region of 28 kb and contains 3 exons. The open reading frame is located in a part of exon 2 and exon 3. The exon1, initial part of exon 2 codes for the 5' untranslated region and the 3' end of exon 3 encodes the 3' untranslated region of the mRNA. This gene encodes for a 1.8 kb RNA transcript which further translates into 133 amino acid containing Norrin protein.

Norrin is a secreted protein, with a 24 amino acid N-terminal signal sequence and a 109 amino acid containing C-terminal cysteine knot motif (CTCK) (Perez-Vilar *et al.*, 1997).

The CTCK motif contains 11 highly conserved cysteine residues. The four intracellular disulfide bridges generated by eight cysteine residues are essential for maintenance of CTCK structure. The remaining three cysteine residues are involved in Norrin homodimer formation through intermolecular disulfide bridge formation (Ke *et al.*, 2013). While Norrin does not show strong sequence homology with any other proteins, the hydrophobic residues and spacing between the cysteine residues resemble the C-termini of secretory mucins and von Willebrand factor (Meitinger *et al.*, 1993). At physiologic pH, this protein contains a positive charge (pI=10.3). The high number of basic amino acid residues (out of 133 amino acids, 26 residues are basic [R, H and K]) present in Norrin are predicted to play a role in binding with the receptor and/or extracellular matrix through ionic interactions (Perez-Vilar *et al.*, 1997; Smallwood *et al.*, 2007).

The crystal structure of the Norrin has been solved with a resolution of 2.4 A° (figure 2.5) (Ke *et al.*, 2013). In this structure, Norrin is presented as a homodimer and contains two different symmetric surfaces for binding with FZD4 dimer and LRP5 proteins (figure 2.6). Each monomeric subunit of the Norrin is made up of three pairs of anti parallel β-hairpins and the connecting loops. At the center of the each monomeric structure, a ring shaped structure is formed by two disulfide bridges between the cysteine residues C65-C126 and C69-C128. The third disulfide bond generated between the cysteine residues C39 and C96 passes through the above described ring and forms a cysteine knot structure (Ke *et al.*, 2013). On one side of the cysteine knot four β-pleated sheets (β1- β4) are present and they form two anti parallel β-hairpin structures. The fourth disulfide bond is located between the two loops that are connected β1- β2 and β3-β4 sheets. The fourth disulfide bridge formed between the C55 and C110 residues provides additional strength to maintain the cysteine knot structure. On the other side of the cysteine knot, the third β-hairpin structure is formed by β2 and β3 strands. Two such Norrin monomers interact with each other through formation of three disulfide bridges between the cysteine residues C93-C95, C95-C93 and C131-C131 and form a homodimer. The interface between the two monomers is further stabilized by intermolecular hydrogen bonding between the side chains of amino

acid residues present in the β2 sheet of one monomer to β2 and β4 of other monomer (Ke *et al.*, 2013).

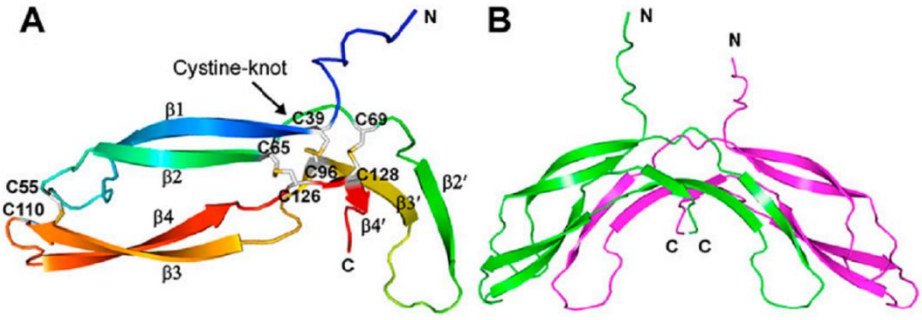

Figure 2.5: Crystal structure of human Norrin protein. (A) The structure of the Norrin monomer is represented in ribbon view with four intramolecular disulfide bonds (C39–C96, C65–C126, C69–C128, and C55–C110) and three β hairpin loops (B) Norrin homo dimer; the represented disulfide bridge is formed between C131-C131 amino acid residues. The remaining two disulfide bridges involved in dimer formation is not shown here. Picture adapted from Jiyuan Ke *et al*., 2013 (Ke *et al.*, 2013).

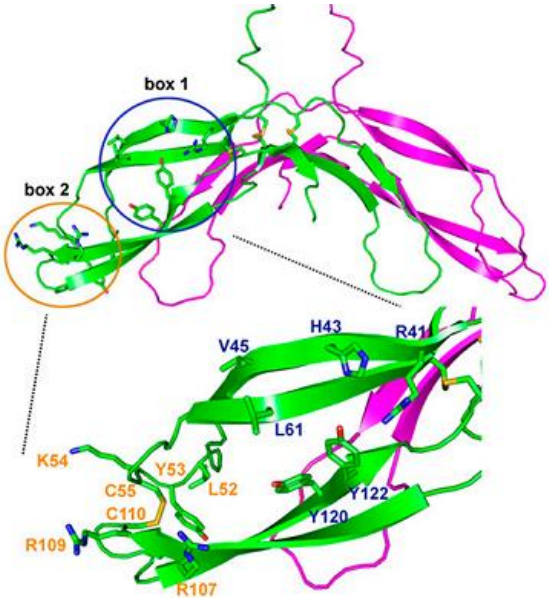

Figure 2.6: FZD4 and LRP5 binding sites of Norrin. Blue color and orange color circles represent the surfaces of FZD4 and LRP5 binding sites on Norrin monomer

respectively. The amino acids of Norrin involved in FZD4 and LRP5 binding are represented in blue and orange color respectively (zoom view). Figure adapted from Jiyuan Ke *et al*., 2013 (Ke *et al.*, 2013).

2.2.9.13. NDP protein function

In humans, the function of Norrin has been mainly implicated in retinal vascular development. Some of the Norrie disease patients also develop progressive hearing loss and various forms of mental retardation (Schuback *et al.*, 1995; Yamada *et al.*, 2001; Kondo *et al.*, 2007a). These additional phenotypes observed in Norrie disease patients suggest the role of Norrin in ear and brain function. The vascular abnormalities observed in inner ear and cerebellum of *NDP*$^{y/-}$ mice further supports its role in maintenance of vasculature in those corresponding organs (Rehm *et al.*, 2002; Luhmann *et al.*, 2008). However, only some of the Norrie disease patients with truncation mutations and the mutations in highly conserved residues that are involved in cysteine knot formation have been reported with these additional phenotypes along with the retinal vascular abnormalities (Wu *et al.*, 2007). In addition to the above described phenotypes, the homozygous knockout mice of *NDP* gene (*NDP*$^{-/-}$) have also shown infertility due to improper decidualization (Luhmann *et al.*, 2005b). However, in humans, so far there are no reports regarding the association of *NDP* gene mutations with infertility. Furthermore, the homozygous *NDP* mutations have also not been reported in female patients.

Other than vascular development and vasculature maintenance, the role of Norrin has also been implicated in maintenance of Retinal Ganglion Cells (RGC) and protection against vascular damage caused by high oxygen levels (Lin *et al.*, 2009; Ohlmann *et al.*, 2010; Seitz *et al.*, 2010). A progressive loss of RGC and disorganization of RGC layer has been widely observed in *NDP*$^{y/-}$ mice (Berger *et al.*, 1996). This phenotype has not been reported in *FZD4*$^{-/-}$, *LRP5*$^{-/-}$ and *TSPAN12*$^{-/-}$ mice (Wang *et al.*, 2001; Xia *et al.*, 2008; Junge *et al.*, 2009; Xia *et al.*, 2010). Though, the RGC cells lie near to the almost normally developed superficial vascular plexus, the loss of these cells in *NDP*$^{y/-}$ mice suggest the role of Norrin in maintenance of RGC cells. In transgenic mice, over

expression of Norrin led to increased number of RGC in the retina (Ohlmann *et al.*, 2005). Moreover, the RGC degeneration either in *NDP*$^{y/-}$ mice or induced by NMDA (N-methyl-D-aspartate) is rescued by the ectopic Norrin (Seitz *et al.*, 2010). This protective role of Norrin on RGC is mainly mediated by the induced expression neuroprotective growth factors including fibroblast growth factor-2, brain derived neurotrophic factor, and lens epithelium derived growth factor and ciliary neurotrophic factor by muller cells of the retina (Seitz *et al.*, 2010). The transgenic mice with over expression of Norrin had decreased loss of capillaries (vaso-obliteration) compared to wild type littermates following exposure to high oxygen levels (Ohlmann *et al.*, 2010; Tokunaga *et al.*, 2013). However, in these transgenic mice the anatomical regrowth of vasculature is significantly increased with reduced pathological neovascularization (Ohlmann *et al.*, 2010; Tokunaga *et al.*, 2013).

2.2.9.14. Reported mutations of *NDP* gene in FEVR patients

To date, 144 different mutations have been reported in *NDP* gene including 85 point mutations, 19 small deletions, 7 splice site variations, 8 small insertions, 19 gross deletions, 1 gross insertion and 3 indel mutations (http://www.hgmd.cf.ac.uk/ac/gene.php?gene=NDP). These mutations are spread throughout the gene. Of the 133 codon positions of Norrin, mutations have been observed in more than 70 different codon positions. However, the majority of mutations are reported for the Norrie disease patients.

So far, 14 missense and one 3' UTR variation have been reported in 25 male FEVR patients (probands) (table 2.5). Of the 25 reported FEVR cases, only eight were familial and the rest were sporadic cases (Shastry *et al.*, 1997; Kondo *et al.*, 2007a; Wu *et al.*, 2007; Pelcastre *et al.*, 2010). Majority of the missense mutations identified in FEVR patients (R41K, H42R, K54N, K58N, C110G, R121Q, R121L and R121W) were also reported in patients of Norrie disease and showed variable ocular phenotype and disease progression. The I18K, L61I, L103V, R115L, Y120C and L124F mutations were only reported in FEVR patients. Interestingly, excluding one mutation (I18K), remaining missense mutations were located either on FZD4 or LRP5 binding surfaces. In these

reports, the frequency of FEVR patients with *NDP* mutations ranged from 6 to 10% (Dickinson *et al.*, 2006; Drenser *et al.*, 2006; Kondo *et al.*, 2007a; Wu *et al.*, 2007; Boonstra *et al.*, 2009; Yang *et al.*, 2012a).

Table 2.5: List of *NDP* gene mutations reported in FEVR patients.

Exon	Nucleotide change	Amino acid change	Occurrence in patients	Occurrence in control alleles	Reference
2	c.53T>A	I18K	1/62	0/360	(Kondo *et al.*, 2007a)
	c.122G>A	R41K	1/5	0/54 [A]	(Shastry *et al.*, 1997)
	c.125A>G	H42R	2/5	0/54 [A]	(Shastry *et al.*, 1997)
			1/52	0/81 [A]	(Wu *et al.*, 2007)
			1/27	-	(Drenser *et al.*, 2006)
	c.162G>C	K54N	2/62	0/360	(Kondo *et al.*, 2007a)
			1/20	0/60 [A]	(Boonstra *et al.*, 2009)
	c.174G>T	K58N	1/5	0/54 [A]	(Shastry *et al.*, 1997)
3	c.181C>A	L61I	1/52	0/81 [A]	(Wu *et al*.,2007)
	c.307C>G	L103V	1/13	0/130 [A]	(Dickinson *et al*., 2006)
	c.328T>G	C110G	1/2	0/45 [A]	(Torrente *et al.*, 1997)
	c.344G>T	R115L	1/62	0/360	(Kondo *et al*.,2007)
	c.359A>G	Y120C	1/5	0/54 [A]	(Shastry *et al*.,1997)
	c.361C>T	R121W	1/52	0/81 [A]	(Wu *et al*.,2007)
			1	0/105 [A]	(Shastry, 1998)
			1/27	-	(Drenser *et al.*, 2006)
			1/2	-	(Pelcastre *et al*.,2010)
	c.362G>A	R121Q	1/3	0/75	(Riveiro-Alvarez *et al*.,2005)
			1/20	0/60 [A]	(Boonstra *et al*.,2009)
			1/2	-	(Pelcastre *et al*.,2010)
	c.362G>T	R121L	1/1	0/200	(Johnson *et al.*, 1996)
	c.370C>T	L124F	1/1	0/60	(Chen *et al.*, 1993)
3' UTR	c.*717T>C	-	1/52	0/81 [A]	(Wu *et al.*, 2007)

cDNA positions and amino acid positions have been obtained following the reference sequences NM_000266.3 and NP_000257.1 respectively. cDNA position +1 corresponding to the A of the ATG translation initiation codon. IVS: intervening sequence (intron); ND: Norrie disease; PFV: Persistent Fetal Vasculature; A: Number of alleles is estimated on the basis of equal distribution of control individuals between males and females as this is not specified in the original paper.

2.2.9.15. Functional characterization of *NDP* mutations

Four different groups have analyzed the effect of different *NDP* mutations on protein production, secretion efficiency and efficiency of mutant proteins in signal transduction using immunoblotting experiments in parallel with co-transfection signaling assays in STF cells (Xu *et al.*, 2004; Smallwood *et al.*, 2007; Qin *et al.*, 2008; Ke *et al.*, 2013). Xu *et al*., (2004) had analyzed the effect of 18 *NDP* mutations (L13R, R41K, R42R, K58N, V60E, L61P, A63D, R90P, S101F, K104Q, A105T, L108P, C110G, Y120C, R121Q, R121L, I123N and L124F) associated with FEVR or ROP. Except for L13R (signaling peptide mutation) mutant remaining mutant proteins were accumulated in the extracellular matrix comparable to wild type protein. All the mutants except K58N, had 20 to 80% of decreased signaling activity compared to wild type protein in STF cells (Xu *et al.*, 2004; Qin *et al.*, 2008).

Another study by Smallwood *et al*., (2007) tested various mutants of Norrin to explore the role of different amino acids in receptor binding and signaling activation. In this study, the replacement of cysteine residues (at 39, 65, 69, 96, 126 and 128 positions) that are predicted to be involved in CTCK domain formation with alanine residues led to severe impairment in receptor binding (FZD4-CRD) and signaling activation. When the additional cysteine residues (C55, C93, C95, C110 and C131) were replaced with alanine, a moderate reduction was observed in receptor binding and signaling activity. Further, when the basic amino acids were replaced with glutamate, a severe reduction (nearly 10 fold) in receptor binding with R41E and R64E mutant proteins was noted. Based on this information, the authors had suggested that the arginine residues at 41 and 64 codon positions were crucial for receptor binding (Smallwood *et al.*, 2007).

2.2.9.16. Identification of low density lipoprotein receptor related protein 5 (*LRP5*) gene in EVR 4 locus

Toomes *et al*., (2004) analyzed 25 polymorphic markers located on chromosome 11q12-11q14 in a large autosomal dominant FEVR family and identified EVR4 (OMIM # 601813) locus between the markers D11S1368 and D11S937 (Toomes *et al.*, 2004c). Though, nearly 250 genes have been located in this locus, the involvement of *LRP5* was speculated based on its role in OPPG syndrome and in canonical-β catenin signaling as a co-receptor for FZD4 receptor. *LRP5* gene was screened in a panel of 32 FEVR patients and six *LRP5* mutations were identified (Toomes *et al.*, 2004a).

2.2.9.17. *LRP5* gene expression

The expression of *LRP5* gene has been detected in variety of human tissues including bone, liver, heart, retina, skin and pancreas during various stages of development and in adult tissues (Kim *et al.*, 1998; Gong *et al.*, 2001; Koay *et al.*, 2005).

2.2.9.18. *LRP5* gene and protein structure

Human *LRP5* spans approximately 136 kb region on the long arm of chromosome 11 at position 11q13.4. The gene consists of 23 exons with flanking 5' and 3' UTR regions. The transcript of this gene contains 5,124 base pairs and encodes for a 1,615 amino acid protein.

The structure of LRP5 consists of a large extracellular domain, a single transmembrane domain and a cytoplasmic domain (figure 2.7). The extracellular domain contains a signal peptide followed by four tandem repeats of six bladed β-propeller domains (containing six YWDT motifs) separated by an epidermal growth factor (EGF) like repeat each, and three LDL receptor repeats (MacDonald *et al.*, 2012). Norrin and other Wnt ligands bind to the first two β-propeller regions (MacDonald *et al.*, 2012; Ke *et al.*, 2013). The Wnt antagonist protein dickkopf (DKK) initially has been proposed to bind to the third β-propeller, but later evidence suggested that, the DKK can bind to the any one of the β-propeller domains (Zhang *et al.*, 2004). The cytoplasmic domain plays a role in binding Axin (Axin 1) and inactivation of β-catenin destruction complex (MacDonald *et*

al., 2012). In cell membrane, before ligand induction, this protein does not interact with either FZD4 or TSPAN12 protein. In presence of a ligand, LRP5 acts as a coreceptor for FZD4 receptor and induce the β-catenin signaling activity (Ke *et al.*, 2013).

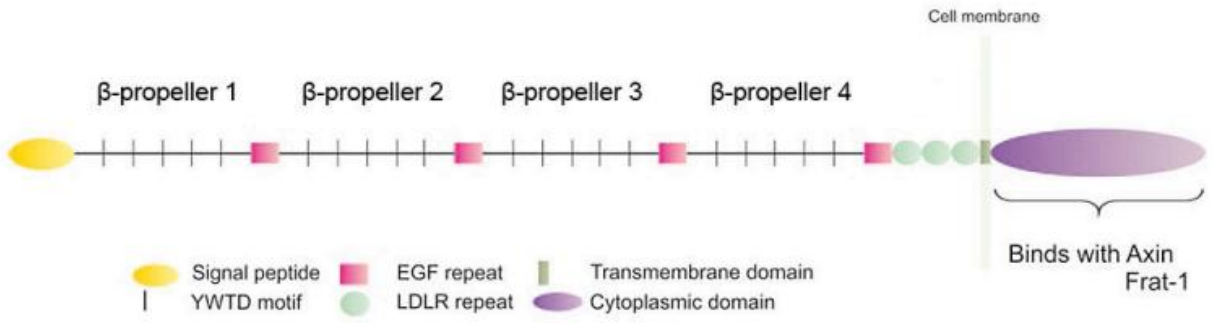

Figure 2.7: Illustration of LRP5 protein showing extracellular and intracellular domains (Figure adapted and modified from Balemans and Van Hul., 2007) (Balemans *et al.*, 2007)

2.2.9.19. LRP5 protein function

The function of LRP5 is mainly implicated in human retinal vascularization, bone mass development and glucose induced insulin secretion in pancreatic islet cells (Figueroa *et al.*, 2000; Gong *et al.*, 2001). By inducing the Norrin/β-catenin signaling in vascular endothelial cells, this protein plays a role in retinal vascular development (Xu *et al.*, 2004). In case of osteoblasts, LRP5 induces the osteoblast proliferation through other Wnt protein interaction and regulates the bone mass (Gong *et al.*, 2001; Kato *et al.*, 2002).

2.2.9.20. Reported mutations of *LRP5* gene in FEVR patients

Overall, 30 different *LRP5* mutations have been reported in 28 different FEVR families (12 familial and 16 sporadic) with varied ethnic backgrounds (table 2.6). These mutations including 23 missense, 3 small base pair deletions, an insertion, a nonsense mutation and 2 splice site variations. Interestingly all these mutations are located in the extracellular domain of LRP5. It indicates that the impaired interaction with ligand is mainly responsible for development of ocular phenotype in FEVR patients. Of these 28 FEVR families with *LRP5* mutations, autosomal recessive inheritance pattern has been observed in four families (Jiao *et al.*, 2004; Downey *et al.*, 2006). Four families have shown compound heterozygous mutations and their inheritance pattern suggests autosomal recessive mode of inheritance (Qin *et al.*, 2005; Nikopoulos *et al.*, 2010b; Yang *et al.*, 2012b). In these reports, the frequency of FEVR patients with *LRP5* mutations ranged from 10% to 25% (Toomes *et al.*, 2004a; Qin *et al.*, 2005; Boonstra *et al.*, 2009; Nikopoulos *et al.*, 2010b; Yang *et al.*, 2012b).

Table 2.6: List of *LRP5* mutations reported in FEVR patients.

Exon	AD/ AR	cDNA change	Amino acid change	Occurrence in patients	Occurrence in control alleles	Reference
2	AD	c.433C>T	L145F	1/56	0/181	Qin *et al*., 2005
3	AD	c.518C>T	T173M	1/32	0/200	Toomes *et al*., 2004
6	AD	c.1321G>A	E441K	1/16	0/100	Nikopoulos *et al*., 2010b
	AD	c.1330G>A	R444C	1/56	0/181	Qin *et al*., 2005
7	AD	c.1532A>C	D511A	1/20	0/40	Boonstra *et al*., 2009
	AD	c.1564G>A	A522T	1/56	0/181	Qin *et al*., 2005
8	AR	c.1648G>A	G550R	1/1	0/60	Downey *et al*., 2006
	AR	c.1757G>A	R570Q	1/3	0/100	Jiao *et al*., 2004
10	AR	c.2302C>G	R752G	1/3	0/100	Jiao *et al*., 2004
11	AD	c.2392A>G	T798A	1/56	0/181	Qin *et al*., 2005
11	AD	c.2413C>T	R805W	1/20	0/40	Boonstra *et al*., 2009
15	AD	C.3361A>G	N1121D	1/56	0/181	Qin *et al*., 2005
				1/49	0/96	Yang *et al*., 2012
16	AD	c.3502T>C	Y1168H	1/32	0/200	Toomes *et al*., 2004

Exon	AD/ AR	cDNA change	Amino acid change	Occurrence in patients	Occurrence in control alleles	Reference
19	AD	c.4025G>A	R1342Q	1/49	0/96	Yang *et al*., 2012
	AD	c.4081T>G	C1361G	1/32	0/200	Toomes *et al*., 2004
	AD	c.4087G>A	D1363N	1/49	0/96	Yang *et al*., 2012
	AR	c.4147G>A	E1367K	1/3	0/100	Jiao *et al*., 2004
4	AD	c.891–892delTC	R298LfsX2	1/49	0/96	Yang *et al*., 2012
18	AD	c.3804delA	E1270RfsX169	1/32	0/200	Toomes *et al*., 2004
IVS21	AD	c.4488+2T>G	-	1/32	0/200	Toomes *et al*., 2004
IVS21	AD	c.4489-1G>A	-	1/16	0/100	Nikopoulos *et al*., 2010
13	AD	c.2978G>A	W993X	1/16	0/100	Nikopoulos *et al*., 2010
20	AD	c.4119-4120insC	K1374fsX175	1/32	0/200	Toomes *et al*., 2004
8 & 7	CH (AR)	c.1604C>T & c.1850T>G	T535M & p.F617C	1/56	0/181	Qin *et al*., 2005
9&4	CH (AR)	c.1828G>A & c.803_812del10bp	G610R & G269RfsX4	1/56	0/181	Qin *et al*., 2005
12	CH (AR)	c.2484C>G & c.2626G>A	Ile828Met & Gly876Ser	1/49	0/96	Yang *et al*., 2012
17 & 9	CH (AR)	c.3758G>T	C1253F &G610R	1/16	0/100	Nikopoulos *et al*., 2010

cDNA positions and amino acid positions have been obtained by following the reference sequences NM_002335.2 and NP_002326.2 respectively. cDNA position +1 corresponding to the A of the ATG translation initiation codon. AD: autosomal dominant; AR: autosomal recessive; IVS: intervening sequence (intron); CH: compound heterozygous.

2.2.9.21. Identification of *TSPAN12* gene in EVR5 locus

Nikopoulos *et al*., (2010) had identified two large autosomal dominant FEVR families without any variations in coding region of known FEVR candidate genes (*NDP, FZD4* and *LRP5*). After genotyping 6090 SNP markers in 23 affected and unaffected individuals from these two families, through genetic linkage analysis genomic regions on chromosome 7 suggestive for linkage 40.5 Mb (LOD score 2.34) and 16.7 Mb (LOD score 3.31) were identified (Nikopoulos *et al.*, 2010a). By using array based sequence capture and next generation sequencing techniques, they further screened the suspected genomic regions and identified 14 nucleotide changes in *PTCD1, ZAN* and *TSPAN12* genes. The p.Ala237Pro mutation observed in *TSPAN12* gene in both the families was highly conserved across different species. Furthermore, all the affected individuals shared a similar risk haplotype for the region containing *TSPAN12* gene. Further, the role of TSPAN12 in retinal vascular angiogenesis was known from knock out mouse models of *TSPAN12* gene through its involvement in Norrin/FZD4 signaling. Based on this information, they speculated that the p.A237P mutation could be the causative of FEVR in the described two studied families. To confirm the involvement of *TSPAN12* gene in FEVR, further screening of this gene was undertaken in nine different FEVR probands and p.G188R and p.A237P amino acid changes were identified in three different subjects (Nikopoulos *et al.*, 2010a). In a parallel study, Poulter *et al*., (2010) also identified seven different mutations in *TSPAN12* gene in a panel of 70 different FEVR probands (Poulter *et al.*, 2010).

2.2.9.22. *TSPAN12* gene and protein structure

In humans, *TSPAN12* gene is located on long arm of the 7 chromosome at 7q31 position. It contains 8 exons, of which exon 2 to 8 consists the protein coding region (Nikopoulos *et al.*, 2010a). Exon 1 and a part of exon8 encodes for the 5' and 3' untranslated regions of the *TSPAN12* mRNA respectively. This gene encodes for a 2796 base pair transcript, which is translated into a 305 amino acid protein. As the name indicates, this protein consists four transmembrane domains and is located in the cell membrane. This protein is classified under tetraspanin superfamily, which includes 33 different members in humans (Bailey *et al.*, 2011).

In all the protein members of tetraspanin super family, two features are highly conserved that are: four transmembrane domains with well conserved residues and a large extracellular loop with a Cys-Cys-Gly motif and two additional cysteine residues (Boucheix *et al.*, 2001). The different members of this protein family are known to be involved in formation of homodimers and heterodimers with the other membrane proteins. By interacting with the other proteins, the tetraspanins form membrane associated protein clusters called as tetraspanin webs or micro domains (Boucheix *et al.*, 2001).

Structurally, tetraspanin proteins contain four transmembrane domains connected by two extracellular loops and an intracellular loop. The extra cellular loop 1 (EC1) is usually small compared to extracellular loop 2 (EC2). The EC2 contains a constant region and a variable region (Hemler, 2005). The variable region consists less conserved residues between different tetraspanin proteins and is responsible for interacting with other membrane proteins. Both, N and C terminals of these proteins are located in the cytoplasm. The intracellular terminals of these protein members are usually plamitoylated and facilitate the interactions between different tetraspanin proteins (Hemler, 2005). In TSPAN12, EC1 contains 26 amino acid residues and EC2 contains 114 amino acid residues. The conserved cysteine residues located at the 9, 12 and 83 positions in the intracellular domains of TSPAN12 are suggested to be involved in palmitoylation.

2.2.9.23. TSPAN12 protein function

In humans, the role TSPAN12 is mainly implicated in retinal vasculature development (Nikopoulos *et al.*, 2010a; Poulter *et al.*, 2010). Either by promoting FZD4 receptor oligomerization or FZD4 and LRP5 interactions, TSPAN12 enhances vascular endothelial cell proliferation or migration through Norrin mediated FZD4 signaling (Junge *et al.*, 2009).

2.2.9.24. Reported mutations of *TSPAN12* gene in FEVR patients

A total of 18 different mutations of *TSPAN12* were reported in 24 FEVR families (15 familial and 9 sporadic cases) by four independent groups (table 2.7) (Nikopoulos *et al.*, 2010a; Poulter *et al.*, 2010; Kondo *et al.*, 2011; Yang *et al.*, 2011; Poulter *et al.*, 2012). In two families, autosomal recessive inheritance pattern was reported (Poulter *et al.*, 2012), while remaining all the families had autosomal dominant inheritance pattern. The reported mutations were scattered throughout the gene without clustering at any specific region. The frequency of FEVR patients with *TSPAN12* mutations in different reports ranged from 4% to 10% (Nikopoulos *et al*., 2010a; Poulter *et al*., 2010; Kondo *et al*., 2011; Yang *et al*., 2011).

Table 2.7: List of *TSPAN12* mutations reported in FEVR patients.

Exon	AD/AR	cDNA change	Amino acid change	Occurrence in patients	Occurrence in control alleles	Reference
3	AD	c.146C>T	T49M	1/49	0/360	Yang *et al*., 2011
				1/11	0/500	Poulter *et al*., 2012
	AD	c.154G>C	E52Q	1/90	0/380	Kondo *et al*., 2011
5	AD	c.302T>A	L101H	1/70	0/400	Poulter *et al*., 2010
	AD	c.313T>C	C105R	1/49	0/360	Yang et a., 2011
6	AR	c.413A>G	Y138C	1/11	0/500	Poulter *et al*., 2012
7	AD	c.562G>C	G188R	1/11	0/280	Nikopoulos *et al*., 2010
8	AD	c.629T>G	M210R	1/70	0/400	Poulter *et al*., 2010
	AR	c.668T>C	L223P	1/11	0/500	Poulter *et al*., 2012
	AD	c.709G>C	A237P	4/11	0/280	Nikopoulos *et al*., 2010
	AD	c.734T>C	L245P	1/90	0/380	Kondo *et al*., 2011
7	AD	c.601delC	L201FfsX14	1/49	0/360	Yang *et al*., 2011
3	AD	c.68T>G	L23X	1/70	0/400	Poulter *et al*., 2010
6	AD	c.419T>A	L140X	2/90	0/380	Kondo *et al*., 2011
				1/70	0/400	Poulter *et al*., 2010
4	AD	c.218_219ins GCTCTTT	F73LfsX118	1/70	0/400	Poulter *et al*., 2010
IVS2	AR	c.67-1G>C	L23GfsX66	1/11	0/500	Poulter *et al*., 2012
IVS4	AD	c.149+3A>G	L23GfsX88	1/70	0/400	Poulter *et al*., 2010
IVS4	AD	c.285+1G>A	R50DfsX12	1/11	0/500	Poulter *et al*., 2012
IVS5	AD	c.3611_3615delACCAG	P122SfsX125	1/70	0/400	Poulter *et al*., 2010

cDNA positions and amino acid positions have been obtained by following the reference sequences NM_012338.3 and NP_036470.1 respectively. cDNA position +1 corresponding to the A of the ATG translation initiation codon. AD: autosomal dominant; AR: autosomal recessive; IVS: intervening sequence (intron).

2.2.9.25. Identification and functional characterization of fifth candidate gene (*Zinc Finger Protein-408*) for FEVR

Collin *et al*., (2013) further analyzed a large autosomal dominant Dutch FEVR family for disease associated locus after excluding the mutations in all the known candidate genes of FEVR (*NDP, FZD4, LRP5 and TSPAN12*). Through genetic linkage analysis, another disease associated locus was identified on chromosome 11 between the polymorphic markers rs1403970 and rs1995496 (Collin *et al.*, 2013). The whole exome sequencing analysis of the disease associated locus led to the identification of a missense mutation in a highly conserved amino acid (p.His455Tyr) of a transcription factor zinc finger protein 408 (*ZNF408*). This mutation was found to be segregated among all the affected family members (11 members) and not observed in 220 ethnically matched control alleles. In further screening analysis, the same mutation was observed in another autosomal dominant FEVR family (Collin *et al.*, 2013). For confirmation of the disease associated locus, the two point LOD score was calculated using microsatellite marker data obtained from genome wide SNP analysis in 10 affected family members from both the FEVR families. A significant LOD score of 3.05 was observed for the disease associated marker D11S1395. A further screening of this gene in a panel of 77 European and 55 Japanese FEVR patients led to identification of another missense mutation (p.Ser126Asn) in a FEVR patient from Japan. This change was also not observed in ethnically matched 191 control individuals.

In an effort to understand the role of ZNF408 in human retinal vascular development, Collin *et al*., (2013) observed nearly 30 times higher expression of *ZNF408* in the adult human retina compared to heart, placenta and liver. Further, its expression was also observed to be very high in the human fetal eye (Collin *et al*., 2013).

In order to understand the effect of the identified missense mutations, *invitro* assays using COS-1 cells and *invivo* assays using Zebra fish were performed (Collin *et al*., 2013). The transfected COS-1 cells with WT and S126N mutant *ZNF408* constructs showed localization of the protein in the nucleus, while the cells transfected with H455Y mutant construct showed the localization of the protein in cytoplasm of the cell.

Furthermore, the oligomerization of H455Y mutant protein with WT protein was observed in the cytoplasm and suggesting dominant negative effect of the mutation.

The retinal vascularization in *fli1* (Friend leukemia integration 1) : eGFP (enhanced Green Fluorescent Protein) transgenic zebrafish was observed after knock down of *znf408* by blocking splice sites using morpholinos and translation blocking morpholinos (MO) (Collin *et al*., 2013). The *fli1*: eGFP transgenic zebra fish expresses the green fluorescent protein under the promoter control of early endothelial marker fli1 and allows the monitoring of blood vessel growth during embryonic development. When splice blocking MO were micro injected in the yolk of embryos at one to two cell stage, a dose dependent increase in aberrantly spliced *znf408* was observed compared to controls at 2 days of post fertilization. 10 nano gram (ng) injections of *znf408* MO were observed as lethal due to complete absence of blood vessels, while 6 ng of MO injections produced defects in development of intraocular ring vessel and their branches around the lens in 92% of the embryos (Collin *et al*., 2013).

In addition to retinal vascular defects, abnormal trunk vascularization was also observed in affected morphants (Collin *et al*., 2013). The same phenotype was also observed when they injected translation blocking MO. When wild type *znf408* RNA was co-injected along with *znf408* splice blocking MO, more than one half of embryos were appeared normal. However, the mutant (H455Y) *znf408* RNA injections did not rescue the phenotype (Collin *et al*., 2013).

ZNF408 is a transcription factor and belongs to the family of zinc finger transcription factors. The members of this protein family are regulatory proteins and involved in variety of cellular activities including embryonic development and cellular differentiation (Laity *et al.*, 2001). Based on the presence of number of zinc fingers, these family members are classified under different subclasses. Zinc fingers are the functional and independently folded domains and require one or more zinc ions for their stabilization. Zinc ions are ligated with a pair of cysteines and histidines in the hydrophobic core of these proteins, (Laity *et al.*, 2001). The cysteine and histidine residues are differentially involved in formation of the structure of different zinc finger proteins. However, the

classical Cys2His2 zinc fingers are most abundant and found in 2% of all human proteins (Lander *et al.*, 2001). These zinc fingers play a role in nucleic acid interaction and/or protein-protein interactions. In humans, the ZNF408 is a 720 amino acid containing protein and encoded by the *ZNF408* gene. This gene is located on short arm of the chromosome 11 at position 11p11.2. It contains 5 exons and encodes for a 2442 base pair transcript. Based on the conserved amino acid sequences, the human ZNF408 is predicted to consist of a tandem array of 10 zinc finger motifs (Collin *et al*., 2013). The high number of zinc finger motifs present in ZNF408 suggests for its involvement in a wide range of functions along with its high affinity interaction with DNA (Collin *et al*., 2013). Being a recently identified protein, the structure and functions of ZNF408 in humans and other animal models is not well characterized. The mechanism of involvement of this protein either in retinal vascular development or β-catenin signaling pathway is also not clear. Further studies are required to unravel the mechanism of involvement of ZNF408 in retinal vascular development. Identification of the transcriptional targets of ZNF408 could find new components underlying FEVR.

3.1. Study purpose and design

The present study was aimed at understanding the underlying molecular genetic defects and the spectrum of mutations in candidate genes causing Familial Exudative Vitreoretinopathy (FEVR) among Indian patients. Further, this study tried to establish a correlation between the genotype and clinical phenotype of the FEVR patients. A total of 225 subjects comprising FEVR patients (n=110) and unaffected normal controls (n=115) were recruited as per the inclusion and exclusion criteria provided in section 3.3 (below). The DNA samples of the patients were screened for variations in the following candidate genes: *NDP*, *FZD4*, *TSPAN12*, and *ZNF408*. The observed variations were then characterized for mutations/polymorphisms based on the segregation of the affected allele in the family members, its frequency in the normal controls along with its effect on the structure and putative function of the protein predicted by *Insilco* analysis.

3.2. Protocol for enrollment of patients and normal subjects

The study was conducted in compliance with the tenets of the Declaration of Helsinki and was approved by the Institutional Review Board (IRB) of the L. V. Prasad Eye Institute, Hyderabad, India. Study participants were recruited between January 2008 to December 2010 at Smt. Kanuri Santhamma Centre for Vitreo Retinal Diseases, L. V. Prasad Eye Institute. The patients were recruited by a senior ophthalmologist in the retina outpatient department after confirming the diagnoses of FEVR and a prior informed consent (annexure-1) was obtained from all the subjects. Subsequently, their family history along with other clinical information and pedigree were documented and blood sample was collected. Patients were classified into five stages of disease severity (Table 3.1). The diagnosis and staging of the disease was further confirmed by reviewing the fundus photographs of these patients by another ophthalmologist, who was masked to the initial recruitment.

3.3. Clinical criteria for enrollment of study participants:

3.3.1. Inclusion criteria for the patients

a. Patients of all age groups with full term birth history (36 – 40 weeks of gestational age), normal birth weight (2.7 – 4 Kilo grams), and bilateral eye involvement along with a confirmed diagnosis of FEVR.
b. FEVR was defined by the peripheral retinal avascularity along with straightening of arcades, tortuous supernumerary retinal blood vessels, intra-retinal and sub-retinal exudation, vitreous condensation, neovascularization, vitreous traction in the form of retinal folds and subtotal or total retinal detachment.

3.3.2. Exclusion criteria for patients

a. Patients with premature birth history (≤ 35 weeks of gestational age) and unilateral disease.
b. Patients with the evidence of intraocular tumor and infection along with mental retardation and hearing loss.
c. .Patients with known history of any retinal diseases other than FEVR.

3.3.3. Inclusion criteria for normal subject

a. Normal individuals ≥ 60 years of age.
b. Ethnically and geographically matched to the habitat of the patient.
c. Presenting without any history of retinal disorders based on a comprehensive ocular examination.

3.3.4. Exclusion criteria for normal subjects

c. Age <60 years.
d. Subjects with an ocular disease other than senile cataract.
e. Subjects with present or past family history of retinal disorders.

3.4. Classification of FEVR patients

All the patients were further classified into five different stages of disease severity independently by two retina specialists. This was based on the Pendergast and Trese system for classification (Pendergast and Trese., 1998) using the collected fundus photographs. The prominent clinical features that served as criteria for different stages of the disease are mentioned in table 3.1.

Table 3.1: Different stages and prominent clinical features observed in each stage of FEVR.

Stages of the disease	Prominent clinical features (Pendergast and Trese., 1998)	
Stage 1	Avascular peripheral retina and supernumerary retinal vessels with straightening of arcades	
Stage 2	Neovascularization at junction of avascular and vascular retina, hard exudates and mild vitreous hemorrhage	
Stage 3	Subtotal retinal detachment (RD) excluding fovea	
	3A	Exudative RD
	3B	Tractional RD
Stage 4	Subtotal retinal detachment involving fovea	
	4A	Exudative RD
	4B	Tractional RD
Stage 5	Total RD and/or total vitreous hemorrhage	

3.5. Clinical examination of study participants

All the study participants underwent a detailed eye examination by an experienced ophthalmologist. Patients of younger age (≤ 5 years), who had not cooperated for the routine examination, were examined under general anesthesia (Savoflorane). The clinical examination included slit lamp biomicroscopy, applanation tonometery, binocular indirect ophthalmoscopy and fundus imaging.

3.5.1. Slit lamp biomicroscopy

Slit lamp biomicroscopy is the preferred method to examine the anterior segment of the eye (cornea, anterior chamber, iris and lens). It facilitates the visualization of a section of the anterior segment under various magnifications. This apparatus consists of an illumination system (slit lamp), an optical system with objective lenses and eye pieces and a mechanical system for supporting and coordinating the above two systems. By employing multiple methods of illumination (direct illumination, indirect illumination, retro illumination and oscillation) eyes of the all subjects were examined for corneal clarity, presence of opacities, scars and lesions within the cornea, lens and anterior chamber. Non-cooperative infants were examined with a portable hand-held slit lamp (Carl Zeiss Meditec Inc. Dublin, CA, USA) under general anaesthesia. The standard bench-top slit lamp biomicroscope was used to evaluate the eyes of cooperating elderly patients.

3.5.2. Tonometry

Tonometry is the process of measuring the intraocular pressure (IOP) using a tonometer. In normal eyes, the IOP range between 10 mm Hg (Mercury) to 20 mm Hg. Applantion tonometery is the widely accepted method to measure the IOP. In this method, the IOP is determined by measuring the amount of pressure that must be applied by a tonometer probe to flatten a convex corneal surface. In the present study, the IOP of elder patients was measured using a Goldman applanation tonometer, which has been designed as a part of slit lamp biomicroscope. Because of the difficulty in maintaining the stable head posture of the children without any movements on slit lamp biomicroscope, Perkins hand held applanation tonometer (Haag-Streit, USA) was used to measure the IOP. When using these instruments, the cornea was anaesthetised with 0.5 % proparacaine eye drops prior to the examination.

3.5.3. Fundus examination

For all study patients, a thorough fundus examination was conducted using a binocular indirect ophthalmoscope, and high resolution fundus photographs were taken using a Carl Zeiss fundus camera (Carl Zeiss Meditec Inc. Dublin, CA, USA). Prior to the examination, patients' pupils were dilated by instilling a combination of mydriatic agents

to allow for a better view of the fundus. For this purpose, one or two drops of 0.6 % Tropicamide and 5% phenyl nephrine were used. After a complete dilatation of the pupils, the fundus was examined for the clarity of the ocular media; the size, shape and color of the optic disc; the macula; retinal breaks and holes.

3.5.3.1. Binocular Indirect Ophthalmoscopy (BIO)

BIO (Heine, Germany) is a self-illuminating head-borne instrument specifically used to examine the fundus of patients. It differs from a direct ophthalmoscope in that it employs a +20.00 dioptre condensing lens to focus a condensed beam of light on the object. This instrument provides an inverted, real and stereoscopic image of the fundus with 1.9X magnification. Compared to the direct ophthalmoscope, BIO provides a large field of view (approximately area equal to 30 degrees of ocular fundus) with high resolution and varying degrees of stereopsis. As a result, it permits a better view of the peripheral fundus, retinal blood vessels, ciliary nerves, optic disc and macular area. By using this instrument, all study patients were examined for the presence of peripheral retinal avascularity, exudation, haemorrhages, neovascularisation, vitreous traction and retinal detachment.

3.6. Blood sample and data collection

Around 2-4 mL of blood was collected from each subject by venipuncture and stored in EDTA (anti coagulant) coated sterile vacutainers (BD Biosciences, USA). In case of infants, 0.2-2 mL blood samples were collected by using a 24-gauge butter fly needle. In majority of the infants, blood samples were collected during examination under general anaesthesia. The obtained blood samples were immediately stored at -20° C and later proceeded for DNA extraction. A predesigned questionnaire was used to document the patient's clinical symptoms, birth details (gestational age, birth weight), age, geographic location, consanguinity and family history of the disease. Pedigrees of the patients were drawn and documented by using Cyrillic 2.1 software. The clinical details of the study patients were compiled in an excel sheet (MS office-2010) for further reference.

3.7. Molecular genetic analysis

3.7.1 Extraction of genomic DNA

Depending on volume of blood samples, genomic DNA extraction was carried out either by the Sigma-Aldrich Gen Elute^{TM} blood genomic DNA kit (Cat No # NA2010, Sigma-Aldrich, St Louis, USA) (refer to appendix II) or the standard phenol-chloroform extraction method (Sambrook *et al.*, 1989). The DNA extraction kit was only used in case of volumes of blood sample (0.2 - 0.5 mL).

3.7.1.1. Extraction of genomic DNA by phenol chloroform method

The standard phenol chloroform method (Sambrook *et al*., 1989) with a few modifications was used to extract the genomic DNA from 1-4 mL of blood. In this method, phenol and chloroform denature and precipitate the protein components of cell lysate so that they are isolated in an organic phase. Consequently, the nucleic acids remain in the aqueous phase and thus can be extracted separately. The step-wise procedure is as follows:

1. The frozen blood samples, stored at -20° C, were thawed to room temperature and transferred to 15 mL polypropylene centrifuge tubes using a sterile Pasteur pipette [Tarsons, India].

2. Two volumes (4 mL) of autoclaved 1X phosphate-buffered saline (PBS) were added to each blood sample and mixed gently by tilting the tube for proper lysis of the RBCs. After gentle mixing, tubes were centrifuged at 3000 revolutions per minute (rpm) for 15 min.

3. Following centrifugation, the tubes were carefully observed for the formation of a tight WBC pellet. Without disturbing the pellet the supernatant was removed with a Pasteur pipette and discarded.

4. For further removal of the RBC remnants, a second wash was given to the WBC pellet with equal volume of 1X PBS. This procedure was repeated until the pellet became clear without any RBC remnants.

5. 1.5 mL of extraction buffer was added to the pellet (refer to appendix III) and mixed gently with a Pasteur pipette until a clear cell lysate without WBC clumps was observed.

6. For complete digestion of nucleoproteins, 10 µl of Proteinase K (20 mg/mL; Bangalore Genei, India) was added to the above cell lysate and the mixture was incubated in a water bath at 37°C overnight.

7. After incubation, an equal volume of Tris-equilibrated phenol (refer to appendix III) was added to the cell lysate and mixed thoroughly by swirling.

8. The mixture was centrifuged at 3000 rpm for 10 min to separate the denatured protein containing organic phase and nucleic acids containing aqueous phase.

9. The upper aqueous phase was transferred to a fresh 15 mL Tarson tube using a Pasteur pipette without disturbing the interphase. Equal volume of phenol, chloroform and iso-amyl alcohol (Qualigens Fine Chemicals, India) in the ratio of 25:24:1 was added to the isolated aqueous phase, mixed thoroughly and centrifuged at 3000 rpm for 10 minutes.

10. The same process was carried out once again with equal volumes of chloroform and iso-amyl alcohol mixture (24:1) for further removal of protein contaminants and phenol left over in the aqueous phase.

11. Two volumes of chilled absolute ethanol [Qualigens Fine Chemicals, India] were added to the separated aqueous phase and gently swirled to spool out the DNA.

12. The spooled DNA was transferred to a 1.5 mL microfuge tube and washed twice with 1 mL of 70% ethanol to remove the salt remnants.

13. The DNA pellet was air dried and dissolved in an appropriate amount of sterile deionised water and incubated at 37° C overnight.

14. The stock DNA was stored at -20° C, and the fraction of DNA required for experimental use was diluted to 50ng/uL as a working solution and stored at 4^0C for future experiments.

3.7.2. Quantitation of DNA using UV Spectrophotometer

The concentration and purity of the DNA was estimated using an ultraviolet spectrophotometer (UV-1601, Shimadzu, Japan). The UV-spectrophotometer functions upon the principle described by Beer-Lambert's law, wherein, the absorbance of a particular wavelength of light is proportional to the concentration of the estimated sample. To estimate DNA concentration, 5 µl of stock DNA was diluted with 995 µl of sterile deionised water (200 fold dilution) in a 1.5 mL microfuge tube. After a gentle mixing, the suspension was transferred to a quartz cuvette and the absorbance was measured at 260 nm and 280 nm. The optical density (OD) values at 260 nm and 280 nm correspond to the concentration of the DNA and protein present in the sample, respectively. The purity of the DNA was checked using the ratio of OD_{260} / OD_{280}. A ratio of 1.8 was an indication of pure DNA, whereas a value above or below 1.8 was an indication of RNA or protein contamination, respectively. The concentration of the DNA was calculated by using the following formula:

DNA concentration (µg/mL) = value of the OD_{260} x 200 x 50

Where 200 is the dilution factor and 50 is the concentration of double stranded DNA in µg/mL at OD_{260} value of 1.

3.7.3. Amplification of coding regions and untranslated regions (UTR) of candidate genes by polymerase chain reaction (PCR)

3.7.3.1. Polymerase chain reaction (PCR)

The coding and UTR regions of the four candidate genes (*NDP, FZD4, TSPAN12* and *ZNF408*) were amplified using the gene specific primers (appendix I). All PCR reactions were set up with a reaction mixture of 25 µL in 0.2 mL tubes (PCR-02-C, Axygen, CA, USA) or in 96-well flat-top PCR plates (PCR-96-FLTC, Axygen, CA, USA). The amplification reactions were carried out using GeneAmp PCR system 9700 and Veriti™ 96 well thermal cyclers (both from Applied Biosystems, Inc. [ABI], Foster City, CA). The reagents used for PCR are listed in table 3.2. The thermal cycle parameters are indicated in table 3.3.

Table 3.2: Reagents used in PCR reaction

Reagents	Working Concentration	Volume (µL) for one reaction
Taq buffer B (10X)	1X	2.5
dNTPs mix (2 mM)	200 µM	2.5
$MgCl_2$ (1.5 mM)	150 µM	1.5
Forward primer	5 pico moles/µL	1
Reverse primer	5 pico moles/µL	1
Taq DNA polymerase (1U/µL)	1U	1
Genomic DNA	50-100 ng	1
Autoclaved Mille Q water		Adjusted to a reaction mixture of 25 µL

Table 3.3: Conditions for thermal cycling program

Step	Temperature (°C)	Time (minutes)	Number of cycles
Initial denaturation	94	5	1
Denaturation	94	0.45	35
Annealing	Provided in appendix I	0.30	
Extension	72	0.45	
Final extension	72	10	1
Final hold	4^0C		

3.7.4. Visualization of PCR products by agarose gel electrophoresis:

The amplified products were checked on a 2% agarose gel. The protocol for casting and running the gel was as follows:

1. The gel casting platform (Bangalore Genei, Bangalore, India) and the gel comb of required size were fixed in an appropriate configuration.

2. The required amount of agarose was weighed for preparing the desired percentage (2% w/v) of the gel and added to 1X TAE (Tris-acetate EDTA; pH 8) in a conical flask.

3. The gel solution was boiled in a microwave oven until all the granules of agarose were completely dissolved.

4. The flask was then cooled to around 50-60°C under running water. 1µg/mL of Ethidium bromide (stock: 10 mg/mL) was added to the agarose gel solution .

5. The flask was gently swirled for an even mixing of the ethidium bromide and the gel was poured into the casting tray.

6. The gel was allowed to solidify for 15-20 minutes and then the comb was removed gently from the solidified gel.

7. The gel was then immersed in 1X TAE buffer present in an electrophoresis tank. 5 µL of the sample was loaded into each well after mixing with 1 µL of 6X loading dye (40% w/v sucrose, 0.25% bromophenol blue and 0.25% xylene cyanol).

8. A negative control (PCR product without template DNA) was loaded to determine the DNA contamination during the PCR reaction. In parallel, around 100 nanograms of 100bp ladder (Fermentas, Hanover, MD) was run to determine the size and approximate concentration of the amplicons.

9. The gel was run at a constant voltage supply of 100V till the desired separation of the bands was observed.

10. The gel was then visualized under UV light and photographed for documentation using the gel doc system (Bio Rad, USA). The preparation of stock solutions for this procedure is given in the appendix IV.

3.7.5. Mutation screening by sequencing

The coding and untranslated (UTR) regions of candidate genes were screened for the detection of mutations/polymorphisms resequencing on an automated DNA sequencer (3130xl Genetic Analyzer, Applied Biosystems, USA). This instrument utilizes Sanger's dideoxy nucleotide chain termination method (Sanger *et al*., 1975) and capillary electrophoresis. They are analogs of deoxy nucleotide triphosphates (dNTPs), but differ in a hydroxyl group (OH) group on the third carbon of the ribose ring. Once incorporated ddNTPs cannot form a phosphodiester bond with the succeeding nucleotide. Thus, the amplifying DNA strand will be terminated whenever there is incorporation of a ddNTP. In automated DNA sequencing process, single-stranded targeted DNA region amplification is carried out using DNA polymerase, normal dNTPs along with the four different fluorescently labelled ddNTPs (ddATP, ddGTP, ddCTP and

ddTTP) and a single primer (either forward or reverse primer). After amplification, the newly formed single-stranded DNA chains, of variable lengths, are subjected to capillary electrophoresis. During electrophoresis, the nucleotide chains migrate according to their size and as each fragment of the DNA passes through a detector at the end of the capillary, individually labelled ddNTPs emit light of specific wave lengths upon exposure to a laser beam. The emitted light signal is converted to a digital signal by a charge coupled device (CCD) camera. This raw data is collected by the data collection software (version 3) and analyzed by the ABI prism DNA sequencing analysis software (version 5.5, Applied Biosystems, Foster city, CA). The resulting DNA sequence is obtained as a chromatogram. It contains a sequence with 4 different colored peaks representing the 4 nucleotides in a given DNA sequence. DNA sequencing involves the following steps:

3.7.5.1. Column purification of PCR products

PCR products were used as templates for further amplification of single-stranded targeted regions for automated sequencing. The unused primers and dNTPs present in the PCR product may interfere in the process of single-strand amplification and cause noise during sequencing. Hence, the PCR products were purified by using Nucleospin extract II columns (Macherey-Nagel, Germany) following the manufacturer's protocol (refer to appendix VI).

3.7.5.2. Sequencing PCR for single strand targeted region amplification

All the sequencing PCR reactions were carried out in 10 µL of reaction volume using BigDye® terminator cycle sequencing kit (version 3.1). The kit was provided with a ready-to-use reaction mix termed as Big Dye Terminator (BDT) containing a thermally stable DNA polymerase, four different dNTPs and four different ddNTPs labeled with different fluorophores. A single primer (either forward or reverse), at a concentration of 3.2 pm/µL, was used for setting-up the reaction. Amplification was carried out in Veriti™ 96 well thermal cycler (Applied Biosystems, Inc. [ABI], Foster City, CA). The thermal cycling conditions are described in table 3.4.

Table 3.4: Conditions for sequencing PCR thermal cycling program

Step	Temperature (°C)	Time (Sec)	Number of cycles
Initial denaturation	96	60	1
Denaturation	96	10	25-30
Annealing	50	6	
Extension	60	240	
Storage	4	A	1

3.7.5.3. DNA precipitation

To avoid noise caused by unused dye terminators, primers and salts, the sequencing PCR products were purified and precipitated as per the protocol suggested in the manual of the BigDye® terminator cycle sequencing kit (version 3.1) (refer to appendix VII).

3.7.5.4. Capillary electrophoresis

The precipitated DNA pellets were resuspended in 10 µL of 50% freshly prepared Hi-di formamide and denatured at 95° C for 5 minutes and immediately snap chilled on ice for 5 minutes. The plates were then sealed with septa, loaded on a plate tray and linked to the sequencing machine for electrophoresis. Prior to linking the plate, a sample sheet was prepared to define the sample names, instrument protocol, protocol for analysis and results group. The instrument protocol determined the settings required for the electrophoresis during the run (run module, run time, voltage and current settings), whereas, the analysis protocol defined the settings necessary for sequence detection and sequence processing after obtaining the raw data.

3.7.5.5. Data Interpretation

Upon completion of sequencing, the data obtained in the form of electropherograms (.ab1 files) were collected and analyzed by using the Chromas (version 2.33) software. To identify the mutations, the sequence data obtained was matched with the corresponding reference gene sequence retrieved from the NCBI (National center for biotechnology information) web site (http://www.ncbi.nlm.nih.gov/). The

electropherograms were manually checked for peaks with low base calling signal and mixed peaks, which may either represent heterozygous variations or artifacts. The sequence alterations identified during analysis were recorded. The genomic and cDNA position of variations were annotated by using the corresponding reference sequences obtained from the NCBI or Ensembl (http://www.ensembl.org/Homo_sapiens/Info/Index) data base. The amino acid alterations corresponding to the nucleotide changes were observed using the reference amino acid sequence of the protein. To confirm the novelty of the observed variation, the sequence variations reported in Ensembl, dbSNP (http://www.ncbi.nlm.nih.gov/snp) and human gene mutation database (http://www.hgmd.cf.ac. uk/ac/index.php) were reviewed. The variations in the corresponding candidate genes were assessed with respect to the observed clinical phenotype for establishing the genotype-phenotype correlation.

3.7.6. Segregation of the detected variations

The variations detected by sequencing were further assessed for co-segregation with the disease phenotype and its presence in the normal subjects. PCR-based restriction digestion was used to confirm the presence or absence of variations in the family members of patients and normal subjects. In the event that a suitable restriction enzyme was not available, those variations were confirmed by re sequencing, as described previously.

3.7.6.1. PCR-based Restriction digestion

This method exploits the ability of type II bacterial restriction enzymes (RE) to digest foreign dsDNA molecules through the detection of a specific nucleotide sequence. These restriction enzymes recognize a 4-8 bp length specific nucleotide sequence and cleave the DNA molecule within the recognition site or at a given site near to the recognition site. The identified sequence variations at a specific DNA region may create or abolish the recognition site for a restriction enzyme. When the specific RE is used to digest the PCR product containing such sequence variations, it produces fragments of different lengths than those observed for the normal PCR product. The restriction digestion of PCR products were carried out by following protocol provided by restriction enzyme manufacturer (refer to appendix VIII)**.**

3.7.6.1.1. Polyacrylamide gel electrophoresis (PAGE)

Similar to agarose gel electrophoresis, PAGE is also a method for resolving and visualizing DNA fragments of varying size. With PAGE, high resolution can be achieved even if the fragments differ by very few base pairs. Better sensitivity can also be achieved by using sensitive staining techniques. Using this method DNA molecules can be separated based on their size and conformation. During electrophoresis, the tiny sieve pores of the gel better permits small DNA molecules to move faster than comparatively larger molecules. Therefore, the different sized DNA fragments can be separated. For this method, gels are prepared with acrylamide (monomer) and a cross-linking agent bis-acrylamide (N, N-methylenebisacrylamide). The catalytic agent TEMED (N, N, N, N-tetramethylethylenediamide) in presence of ammonium per sulfate (free radical generating agent) enhances the polymerization reaction between acryl amide and bis-acrylamide monomers responsible for the formation of the gel. With increased concentration of acrylamide, the pore size of the gel becomes reduced and more conducive for separating small DNA fragments.

3.7.6.1.2. Protocol for polyacryl amide gel electrophoresis

1. PAGE was carried out by using Hoefer SE600X Chroma Standard Vertical electrophoresis unit (Amersham Biosciences, San Francisco, USA).

2. Glass plates (18 x16 cm) were cleaned with isopropanol, assembled with 1.5 mm thick spacers and fixed on the gel casting stand with the help of tightening screws.

3. A 40 mL of 10% polyacrylamide gel was prepared. The reagents and their concentrations used in gel preparation are mentioned in table 3.5. Preparation of stock reagents used for this procedure is given in appendix V.

Table 3.5: Reagents used in acrylamide gel preparation

Reagent	Volume in mL
30% acrylamide; 29% acrylamide + 1% N, N´- Methylenebisacrylamide	13.3
10X TBE buffer	4
10% APS	0.280
TEMED	0.014
Mille Q water	22.4
	40 mL (total volume)

4. The acrylamide solution was poured immediately between the glass plates and the comb (1.5mm thick) was inserted. The gel was allowed to completely polymerize for about 30-40 min.

5. After polymerization, the comb was carefully removed without disturbing the wells. The leftover unpolymerised acrylamide in the wells was removed by flushing with deionized water.

6. The glass plates were fixed to a cathode buffer tank (at the top) with the help of tightening screws and then placed in a lower anode buffer tank.

7. Upper and lower buffer tanks were filled with 1X TBE buffer until the electrode connecting wires were immersed in the buffer.

8. Restriction digested samples mixed with 2 µL of 6X loading buffer were loaded in the appropriate wells along with undigested sample (negative control) and 100 bp DNA ladder.

9. The electrophoretic run was carried out at 25 mA standard current for 3-4 hours.

10. After completion of the electrophoresis, the glass plates were disassembled from the electrophoretic unit and the gel was gently transferred into a tray containing deionized water and ethidium bromide (0.5 µg/mL final concentration).

11. The gel was left to stain for 10-15 min on shaker, and was subsequently visualized and photographed under UV transilluminator (BioRad ChemiDoc™ XRS gel documentation system).

3.7.7. Prediction of the effect of detected variations by *in silico* analysis

3.7.7.1. Effect of variations on splice signals

Splicing and removal of intronic regions is an essential process during the maturation of pre messenger RNA (mRNA) in eukaryotic cells. This process is carried out by a protein complex called the spliceosome. The conserved nucleotide sequences at the exon and intron boundaries and a 14 base pair branch point signal at the 3' end of the introns act as the signals to allow the spliceosome to distinguish the exons from the introns. Along with these, specific short nucleotide sequences present in the exonic and intronic regions act as binding sites for the ribo-nucleo proteins (RNPs) of the spliceosome complex. These nucleotide sequences provide the signals to either promote or suppress the splicing process and play a pivotal role in proper transcript formation. These

conserved sequences are called exon/intron splicing enhancers or silencers. Human splicing finder (HSF-version 2.4.1) is an online tool that predicts the effect of the nucleotide changes on the splice signals. It creates predictions using position weight matrices (PWM) and a database of conserved nucleotide sequences, which have been shown experimentally to play an important role in the process of splicing (Desmet *et al.*, 2009). This tool recognizes the splice sites, enhancer and suppressor sites in a mutated region and gives the consensus values to indicate the strength of the splice signal in the wild type and mutated sequence. Consensus values greater than 80 can be considered as an indication of a strong splice signal. All nucleotide changes identified in the present study were tested for creation of new splice signals and destruction of existing splice signals, by submitting the wild type and mutant nucleotide sequences to the HSF online tool (http://www.umd.be/HSF/). Based on the obtained consensus values and their difference between the wild type and mutated sequence, the effect of the variation on splice signals can be predicted.

3.7.7.2. Multiple sequence alignment

Amino acid conservation across different species may be an indication that the amino acid plays an important role in protein structure formation or protein function. In the present study, the degree of conservation of the amino acid residues found to have mutations was evaluated by multiple sequence alignment using Clustal W software (http://www.ebi.ac.uk/clustalw/) (Thompson *et al.*, 2002). For this technique, the orthologues of the particular protein sequence were retrieved from the NCBI protein database (http://www.ncbi.nlm.nih.gov/) and submitted to the software. The software aligned all the submitted sequences of the protein and generated a multiple alignment. By analyzing the alignment, the degree of conservation of the mutated amino acid residues across various species was determined.

3.7.7.3. SIFT (Sorting intolerance from tolerance)

SIFT is a tool used to predict the evolutionary tolerability of an amino acid alteration observed in a protein sequence (Kumar *et al.*, 2009). This program generates a multiple sequence alignment for the query sequence using the orthologues of the protein. Based on these results, it calculates the normalized probabilities for each submitted amino acid alteration and gives a score to implicate the effect of that substitution as either neutral or deleterious. Substitutions with scores less than 0.05 are considered to be deleterious or evolutionarily intolerable, and those with scores equal to or greater than 0.05 are taken as neutral. To calculate the SIFT scores of the detected amino acid alterations, the corresponding protein sequence was retrieved in FASTA format and submitted to the online program (http://blocks.fhcrc.org/sift/SIFT_seq_submit2.html) along with the altered amino acid and its position. Based on the given score the pathogenic nature of the detected mutation was predicted.

3.7.7.4. PolyPhen-2

PolyPhen (polymorphism phenotyping) is another tool used to predict the effect of non-synonymous amino acid alterations (Adzhubei *et al.*, 2010; Adzhubei *et al.*, 2013). This method predicts the effect of the substitution by synthesizing the following information regarding the corresponding protein: physicochemical properties of the wild type and altered amino acids, phylogenic conservation data and structural data available in the protein data bank (PDB). Based on the obtained score, it classifies the submitted amino acid alterations into benign, possibly damaging or probably damaging. By submitting the identified amino acid substitutions along with their positions to the online server (http://genetics.bwh.harvard.edu/pph2/) the impact of the alterations were predicted.

3.8. Statistical analysis for gene variants

For all identified nucleotide polymorphisms, the control individuals were tested for Hardy Weinberg equilibrium to assess the genotyping error. The risks conferred by different alleles and genotypes were assessed by calculating their frequencies by gene counting method along with the P values and odds ratios using a Chi-square test.

4. Results

The main objective of the present study was to screen genes *NDP, FZD4, TSPAN12* and *ZNF408* in a cohort of 110 FEVR probands and 115 control individuals in order to understand their involvement in FEVR pathogenesis. The study cohort included 67 male and 43 female probands. Of the 110 FEVR probands, 34 probands had family history of the disease with at least one affected family member diagnosed with FEVR other than the proband. The remaining 76 FEVR probands were found to be sporadic without any family history of the disease. For sporadic FEVR cases, we have screened the first degree relatives of the probands through indirect ophthalmoscope and confirmed the absence of classical clinical features of the disease. However, we cannot rule out the presence of mild retinal vascular defects in the unexamined family members of the sporadic FEVR probands.

The mean age of presentation at our hospital for the patients was 5.9 years±7.5 years (range 1 month to 50 years). Stage of the disease in the affected eyes and age of the patients during initial diagnosis of FEVR in L V Prasad Eye institute have been described in tables 4.1 and 4.2 respectively. Intriguingly, for 74 patients, the disease was observed within 24 months after the birth with partial or total retinal detachment in 137 eyes. Of the 220 eyes of 110 FEVR patients, 168 (76%) eyes were legally blind and had the visual acuity less than 20/200 meters. The L.V. Prasad eye institute, a tertiary eye care center is located in Andhra Pradesh hence, majority of the patients recruited in this study were belonged to south India.

Table 4.1: Number of eyes of patients (probands) with different stages of FEVR

Stages of FEVR	Number of eyes (percent)
1 (avascularized peripheral retina)	6/220 (2.7)
2 (avascularized peripheral retina with neo vascularization)	12/220 (5.4)
3 (subtotal retinal detachment excluding macula)	14/220 (6.3)
4A (subtotal retinal detachment including macula without exudation)	21/220 (9.5)
4B (subtotal retinal detachment including macula with exudation)	44/220 (20)
5 (total retinal detachment)	123/220 (55.9)

Table 4.2: Number of patients (probands) with different age at presentation for FEVR

Age at presentation for FEVR at L V Prasad Eye Institute	Number of patients (percent)
≤ 1 year	59 (53.6)
Between 1 to 10 years	31 (28.1)
Between 10 to 20 years	10 (9)
Between 20 to 30 years	5 (4.5)
Between 30 to 40 years	3 (2.7)
Between 40 to 50 years	2 (1.8)

4.1 Mutation screening

4.1.1 *NDP* gene analysis

The three exons including intron-exon boundaries, 5' and 3' untranslated regions (UTR) of *NDP* gene were screened. Five novel and five reported mutations of *NDP* gene were identified in probands of 12 different FEVR families (tables 4.3 and 4.4, figures 4.1 and 4.2). These changes included 4 deletions, 4 missense mutations, a nonsense mutation and a 3' UTR mutation (figure 4.1). These nucleotide changes were not observed in 115 control individuals. In addition to these mutations, a novel Single Nucleotide Polymorphism (SNP) and a reported SNP were identified in two different FEVR probands located in 3' and 5' UTR respectively (tables 4.3 and 4.4, figures 4.1 and 4.2). Of the twelve different probands identified with *NDP* mutations, seven probands had family history of disease and the remaining five were sporadic cases (figure 4.2). Nine of the probands were males and three were females (table 4.4). A 14 bp deletion in 5' UTR was observed in homozygous condition in a female patient with neovascularization in both eyes (figure 4.2; FEVR family 8; II: 3). A novel missense mutation His50Asp was observed in three different probands and their affected family members (figure 4.2; FEVR families 33, 72 and 139). All other mutations, however, were detected in one family each.

The observed mutations in *NDP* were scattered throughout the gene (figure 4.1). Among the ten different mutations, one mutation was located in exon 1, five mutations were located in exon 2 and four mutations were located in exon 3 (figure 4.1). All the observed coding region mutations in the present study were located in structurally and functionally important cysteine knot domain of Norrin protein.

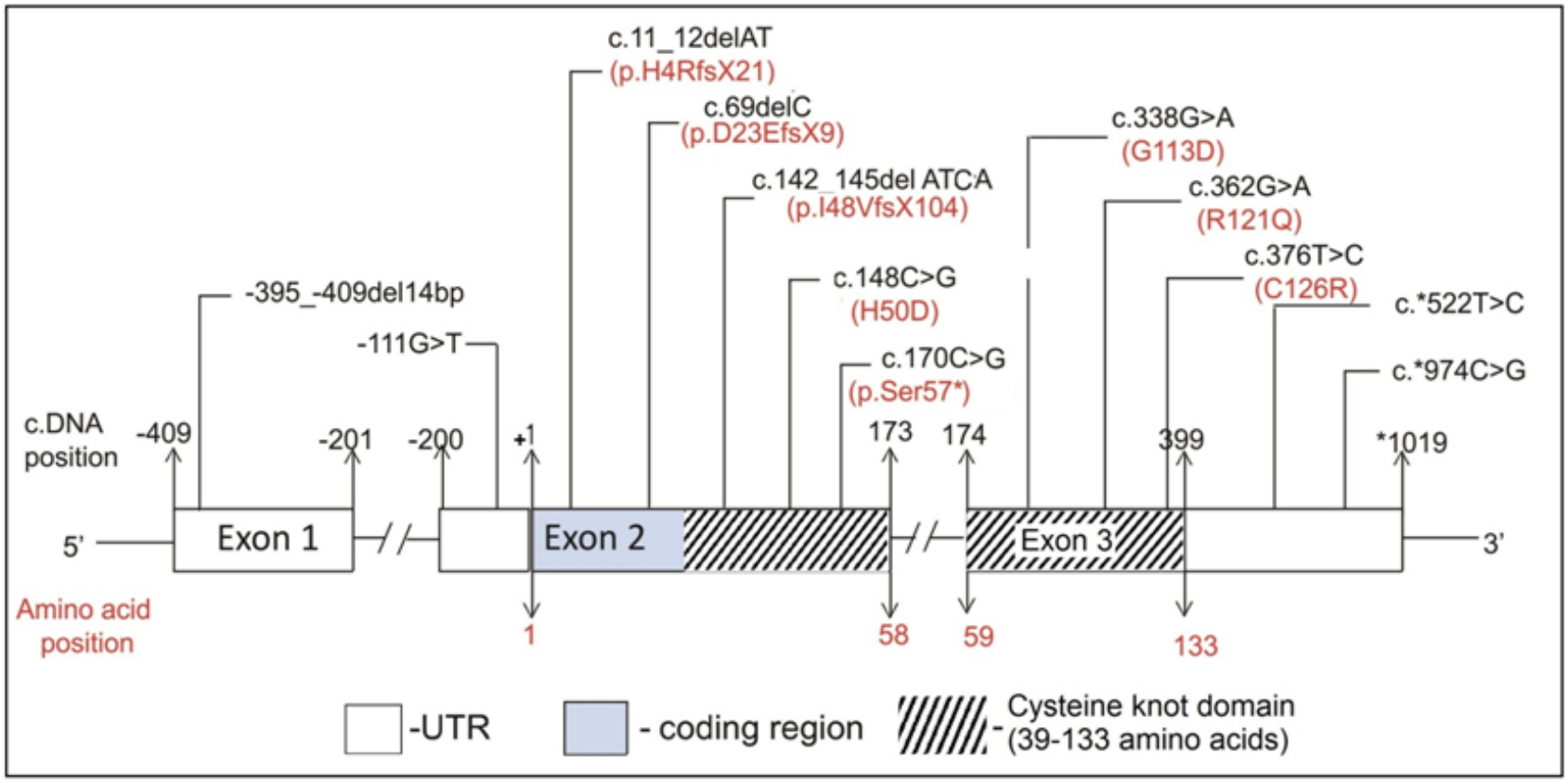

Figure 4.1: Schematic representation of the *NDP* gene with identified nucleotide changes in FEVR probands. +1 represents the transcription initiation site. cDNA positions and amino acid positions have been given by following the reference sequences NM_000266.3 and NP_000257.1 respectively.

Table 4.3: Nucleotide changes observed in the *NDP* gene in FEVR probands

Location in the *NDP* gene	cDNA position of the nucleotide change	Amino acid change	SIFT (score)	PolyPhen-2 (score)	Reported/ Novel	Study code of the proband	Number of probands with the nucleotide change [n=110] (frequency)	Number of controls with the nucleotide change [n=115] (frequency)
Exon 2	c.11_12delAT	His4Arg *fsX*21	-	-	Reported (Nikopoulos *et al.*, 2010b)	142 FEVR	1 (0.009)	0
	c.69delC	Asp23Glu *fsX*9	-	-	Novel	21 FEVR	1 (0.009)	0
	c.142_145del ATCA	Ile48Val *fsX*55	-	-	Novel	97 FEVR	1 (0.009)	0
	c.148C>G	His50Asp	Damaging (0.00)	Probably damaging (0.991)	Novel	33 FEVR 72 FEVR 139 FEVR	3 (0.027)	0
	c.170C>G	Ser57*	-	-	Reported (Berger *et al.*, 1992b)	108 FEVR	1 (0.009)	0

Location in the *NDP* gene	cDNA position of the nucleotide change	Amino acid change	SIFT (Score)	PolyPhen-2 (score)	Reported/ Novel	Study code of the proband	Number of probands with the nucleotide change [n=110] (frequency)	Number of controls with the nucleotide change [n=115] (frequency)
Exon 3	c.338G>A	Gly113Asp	Damaging (0.00)	Probably damaging (1.000)	Novel	85 FEVR	1 (0.009)	0
	c.362G>A	Arg121Gln	Damaging (0.01)	Probably damaging (0.998)	Reported (Boonstra *et al.*, 2009; Pelcastre *et al.*, 2010)	65 FEVR	1 (0.009)	0
	c.376T>C	Cys126Arg	Damaging (0.00)	Probably damaging (0.997)	Novel	94 FEVR	1 (0.009)	0
5' UTR	-395_-409del14bp	-	-	-	Reported (Dickinson *et al.*, 2006; Wu *et al.*, 2007)	8 FEVR	1 (0.009)	0
	-111G>T	-	-	-	Reported (rs45501198)	8 FEVR	1 (0.009)	0
3'UTR	c.*522T>C	-	-	-	Novel	75 FEVR	1 (0.009)	1 (0.008)
	c.*974C>G	-	-	-	Novel	98 FEVR	1 (0.009)	0

cDNA positions and amino acid positions have been given by following the reference sequences NM_000266.3 and NP_000257.1 respectively. '*' represents the stop codon.

Table 4.4: Clinical features of the FEVR probands identified with nucleotide changes in the *NDP* gene

Study code of the proband	cDNA position of the nucleotide change	Age at initial present-ation at LVPEI (Gender)	Stage of the disease/clinical features	Treatment	Outcome/ visual acuity in feet
142 FEVR	c.11_12delAT (2 bp deletion)	3 months (male)	OU:5 Bilateral nystagmus was observed. In the right eye retrolental membrane was seen. In the left eye closed funnel like retinal fold was observed with vessels from disc to lens	No	OU: No PL
21 FEVR	c.69delC (1 bp deletion)	4 months (male)	OD: 4B, OS: 5 Bilateral leukocoria was observed. In both eyes retinal fold was observed from posterior pole to periphery of the retina with vascularized gliotic tissue.	OD: LIO at 4 months of age	OD:PL OS:NO PL
97 FEVR	c.142_145del ATCA (4 bp deletion)	6 months (male)	OU:5 Poor vision was noted since birth. Bilateral leukocoria and total RD were observed with retrolental membranes in both eyes.	OU: Lensectomy at 6 months of age	OU: No PL
33 FEVR	c.148C>G (missense change)	6 years (male)	OU:4B Bilateral retinal folds were observed with dragged macula.	OU: Lensectomy at 6 years of age	OD: 20/400, OS: CF 1 meter
72 FEVR	c.148C>G (missense change)	5 years (female)	OD: 4B, OS:3B Poor vision and squint were noted at one year of age. Myopic astigmatism, macular dragging and retinal folds were observed in both eyes.	No	OD: 20/200, OS: 20/40
139 FEVR	c.148C>G (missense change)	5 months (male)	OD: 3B, OS: 5 In left eye leukocoria with dragged disc and macula was observed. In the right eye, avascular peripheral retina was observed with vitreous condensation.	OD:LIO at 13 years of age	OD:20/20, OS: No PL

108 FEVR	c.170C>G (nonsense change)	3 months (male)	OU:5 Leukocoria with total RD and retrolental membranes were observed in both eyes.	No	OU: No PL
85 FEVR	c.338G>A (missense change)	24 years (male)	OU:2B Avascular peripheral retina with vitreal condensation was observed bilaterally. Straightening of vessels and fluorescein leakage at temporal periphery of retina was also observed.	OU: LIO at 24 years of age	OU 20/30
65 FEVR	c.362G>A (missense change)	3 months (male)	OU: 5 Bilateral shallow anterior chambers and total RD with retrolental membranes were observed. In left eye corneal scarring with neovascular glaucoma was also observed.	No	OU: No PL
94 FEVR	c.376T>C (missense change)	3 months (male)	OU:5, Corneal scarring, total RD with retrolental membranes were observed bilaterally.	No	OU: No PL
8FEVR	-395_-409del14bp & -111G>T (deletion in 5' UTR & SNP)	12 years (female)	OU: 2 In both eyes avascularized peripheral retina was observed with neovascularization and retinal hemorrhages.	OU: LIO at 12 years of age	OU:2/20
75FEVR	c.*522T>C (3' UTR substitution)	2 years (female)	OU: 3 Avascularized peripheral retina with temporal falciform folds was observed in both eyes. Tortuous vessels were observed in both eyes with a macular hole in left eye.	OU: LIO at 3 years of age	OD:20/40 OS:20/400
98FEVR	c.*974C>G	5 months (female)	OU:5 Total RD was observed with vitreous traction in both eyes.	No	OU: No PL

RD: retinal detachment, OD: right eye, OS: left eye, OU: both eyes, LIO: Laser Indirect Ophthalmoscopy, PL: perception of light, CF: counting fingers.

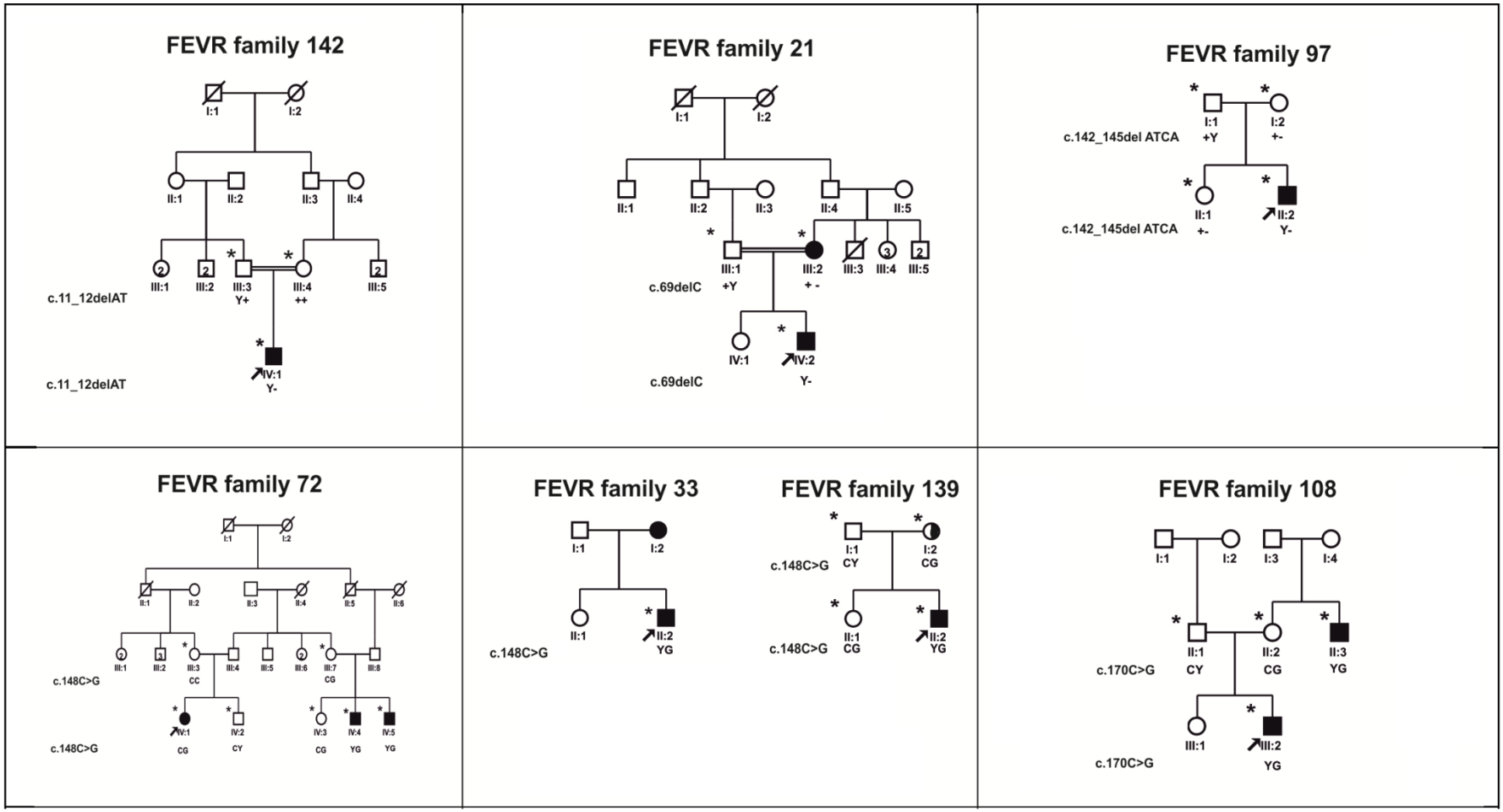
FEVR family 142
I:1
I:2
II:1
II:2
II:3
II:4
III:1
III:2
III:3
Y+
III:4
++
III:5
c.11_12delAT
IV:1
Y-
c.11_12delAT
FEVR family 21
I:1
I:2
II:1
II:2
II:3
II:4
II:5
III:1
+Y
c.69delC
III:2
+ -
III:3
III:4
III:5
IV:1
IV:2
Y-
c.69delC
FEVR family 97
c.142_145del ATCA
I:1
+Y
I:2
+-
II:1
+-
II:2
Y-
c.142_145del ATCA
FEVR family 72
I:1
I:2
II:1
II:2
II:3
II:4
II:5
II:6
III:1
III:2
III:3
CC
III:4
III:5
III:6
III:7
CG
III:8
c.148C>G
IV:1
CG
IV:2
CY
IV:3
CG
IV:4
YG
IV:5
YG
c.148C>G
FEVR family 33
I:1
I:2
II:1
II:2
YG
c.148C>G
FEVR family 139
c.148C>G
I:1
CY
I:2
CG
II:1
CG
II:2
YG
c.148C>G
FEVR family 108
I:1
I:2
I:3
I:4
II:1
CY
II:2
CG
II:3
YG
c.170C>G
III:1
III:2
YG
c.170C>G

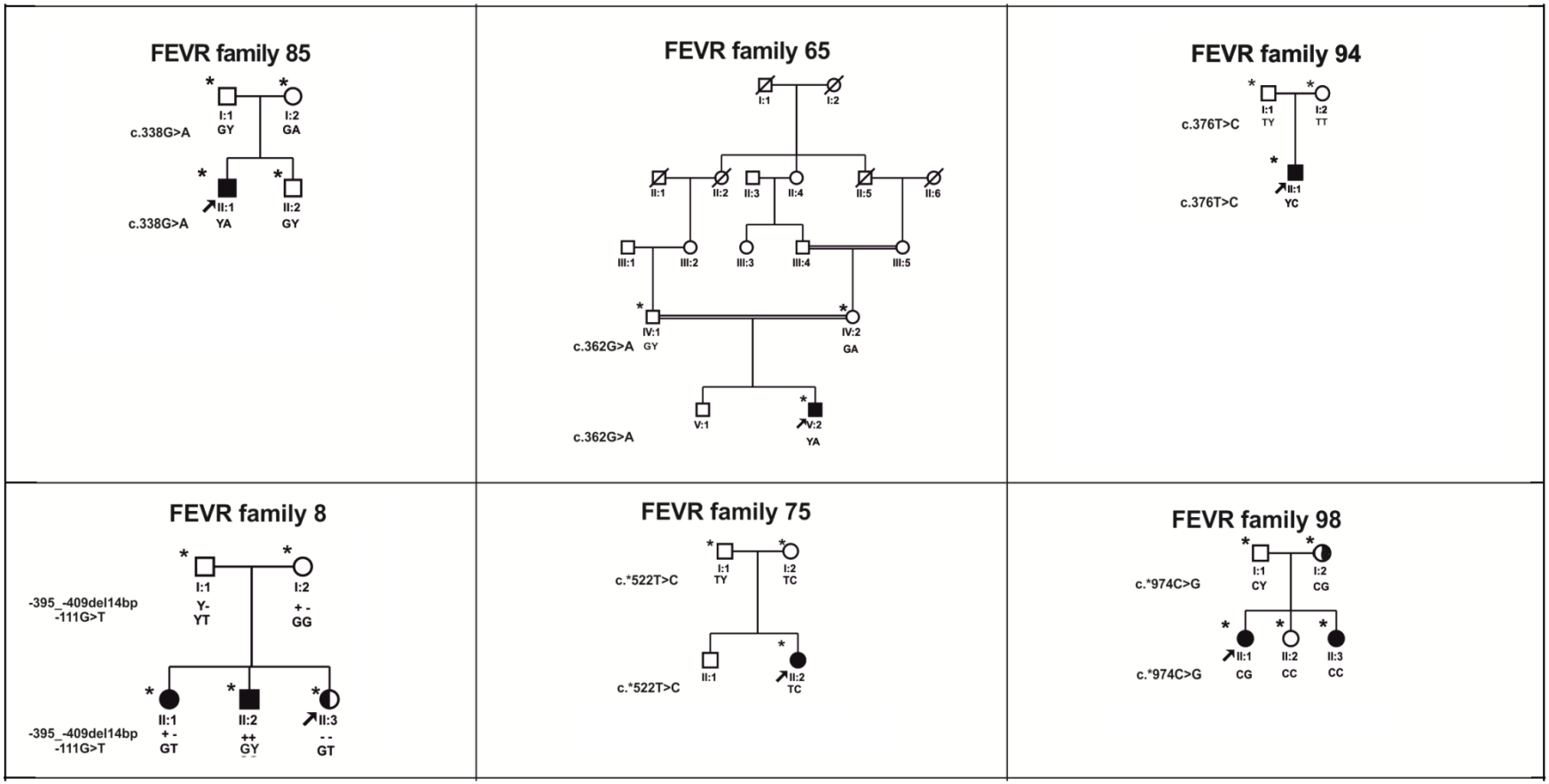

Figure 4.2: Pedigrees of the FEVR families identified with nucleotide changes in the *NDP* gene. Completely and partially shaded symbols represent severe stages and milder stages of the disease respectively. Open symbols represent unaffected individuals. Asterisk (*) over the pedigree symbols represent the individuals screened for nucleotide changes in the *NDP* gene. - indicates the presence of deletion and + indicates the wild type allele. The identified nucleotide change is represented left side of each pedigree.

4.1.1.1 Description of nucleotide changes observed in the coding region of the *NDP* gene

c.11_12delAT (His4Arg*fsX*21)

A previously reported 2 bp deletion (c.11_12delAT) was observed in hemizygous condition in the male proband (IV: 1) of a consanguineous FEVR family 142 (figure 4.2 and figure 4.3; A) (Nikopoulos *et al.*, 2010b). The deletion resulted in a frame shift at codon 4 and formation of a premature termination codon at position 24. The formed premature termination codon was located in the exon 2 and was followed by an intron. Therefore, it may lead to nonsense mediated mRNA decay (Hentze *et al.*, 1999). This nucleotide change was absent in both of the unaffected parents (III: 3 and III: 4) and therefore could be a *de novo* change (figure 4.2; FEVR family 142). This change was also not observed in 115 control individuals. The proband with this mutation developed total retinal detachment in both the eyes at the age of 1 year (table 4.4).

c.69delC (Asp23Glu*fsX*9)

A novel, hemizygous, single base pair (bp) deletion of nucleotide 'C' at cDNA position c.69 was observed in the proband (IV: 2) of a consanguineous FEVR family 21 (figure 4.2 and figure 4.3; C). This deletion was not observed in 115 control individuals. This deletion resulted in a frame shift at codon 23 and formation of a premature termination codon after 8 amino acid residues in exon 2. The formation of premature termination codon in exon 2, followed by an intron may lead to nonsense mediated mRNA decay (Hentze *et al.*, 1999). The proband with this deletion developed falciform retinal folds in both the eyes and became blind at four months of age (table 4.4). The mother of the proband (III: 2) was also harboring this deletion in heterozygous condition and exhibited exudative retinal detachment in the left eye and neovascularization in the right eye (figure 4.2; FEVR family 21 and figure 4.3; B). In the right eye, the disease was stable and showed visual acuity 20/50 meters without any medical intervention.

c.142_145delATCA (Ile48Val*fsX*55)

In an Index proband (II: 2) of 97 FEVR family, a novel, hemizygous 4 base pair deletion was observed at cDNA position c.142_145 (figure 4.2 and figure 4.3; E). The deletion led to frame shift at codon 48 and formation of a premature termination codon after the addition of 54 altered amino acids. The formed premature termination codon was located in exon 3 and was not followed by an intron. As a result, it may lead to formation of a truncated protein with 102 amino acid residues as compared to 133 amino acid containing wild type Norrin protein (Hentze *et al.*, 1999). The proband observed with this deletion developed bilateral leukocoria with total retinal detachment at the age of 6 months (table 4.4). The mother of the proband (I: 2) was also observed with this deletion in heterozygous condition but did not exhibit any clinical features of the disease under examination of indirect ophthalmoscope (figure 4.2; FEVR family 97 and figure 4.3; D). This deletion was not observed in 115 control individuals.

c.148C>G (His50Asp)

A novel substitution of cytosine to guanine at position c.148 was observed in three different FEVR probands (33, 72 and 139 FEVR families) (figure 4.2 and figure 4.3; F and G). This nucleotide change was not observed in 115 control individuals. This substitution resulted in the replacement of histidine with aspartic acid at amino acid position 50 in the Norrin protein. The three different probands and their affected family members with this substitution showed varied disease phenotypes at different age of onset (table 4.4). The proband (II: 2) of the FEVR family 139 (figure 4.2) developed severe ocular features at very young age (5 months) compared to the other two families with a total retinal detachment in the left eye and a partial retinal detachment in the right eye. This patient finally gained 20/20 best corrected visual acuity (BCVA) in the right eye after multiple sessions of laser treatment at 13 years of age. The mother of this patient (figure 4.2; FEVR family 139; I: 2) was a carrier for this nucleotide change and had avascularized peripheral retina in both eyes. In the male proband (II: 2) of FEVR family 33, bilateral subretinal detachments with dragged macula were observed at the first examination at 6 years of age. The mother of the proband (figure 4.2; FEVR family

33; I: 2), who also harbored this change exhibited subretinal detachment with dragged macula in the right eye and avascularized peripheral retina in the left eye. In FEVR family 72, the H50D change was observed in heterozygous condition in a female proband (figure 4.2; FEVR family 72; IV: 1). At the age of 5 years, the patient had bilateral subtotal retinal detachments accompanied with dragged macula in the right eye. The mutation was also observed in two of her cousin brothers (figure 4.2; FEVR family 72; IV: 4 and IV: 5) with bilateral retinal detachments. They also developed the ocular features in the first decade of their life.

c.170C>G (Ser57*)

S57X, a known mutation was observed in a proband (III: 2) of FEVR family 108 (figure 4.2 and figure 4.3; I) (Berger *et al.*, 1992b). The cytosine to guanine substitution at position of c.170 resulted in the formation of a stop codon instead of codon for serine residue. The formation of premature stop codon in exon 2, which was followed by an intron, may lead to nonsense mediated mRNA decay (Hentze *et al.*, 1999). The proband with this mutation had bilateral retrolental membranes and total retinal detachments at 3 months of age (table 4.4). This mutation was also detected in the mother (II: 2) and uncle (II: 3) of the proband in heterozygous and hemizygous conditions respectively (figure 4.2 and figure 4.3; H and I). The uncle of the proband was also blind since birth and exhibited shallow anterior chambers and total retinal detachments in both eyes at 25 years of age. Though, the mother of the proband, a carrier for this mutation, did not have any clinical features of the disease under ophthalmoscopic examination. This nucleotide change was not observed in 115 control individuals.

c.338G>A (Gly113Asp)

A novel change from guanine to adenine at position c.338 was observed in an index, male proband (II: 1) of FEVR family 85, (figure 4.2 and figure 4.3; K). This change was not identified in 115 control individuals. This substitution resulted in the replacement of a glycine residue with aspartic acid at 113 amino acid position of Norrin. The proband with this substitution showed a slow progression of the disease and developed bilateral neovascularization at the age of 24 years (table 4.4). Post laser treatment, the disease

was stabilized and the patient gained 20/30 BCVA in both the eyes. Though, the mother of the proband (figure 4.2; FEVR family 85; I: 2 and figure 4.3; J) also had this nucleotide change, she did not exhibit the clinical features of the disease under indirect ophthalmoscopic examination.

c.362G>A (Arg121Gln)

R121Q, a recurrent mutation observed in an index proband (V: 1) of a consanguineous FEVR family 65 (figure 4.2 and figure 4.3; M) (Boonstra *et al.*, 2009; Pelcastre *et al.*, 2010). The guanine to adenine substitution at position c.362 led to replacement of an arginine residue by glutamine at 121 amino acid position of Norrin. The proband with this mutation showed total retinal detachment in both the eyes at the age of 3 months (table 4.4). No clinical features pertaining to the disease were observed in the mother of the proband, despite of harboring the mutation in heterozygous condition (figure 4.2; FEVR family 65; IV: 2 and figure 4.3; L).

c.376T>C (Cys126Arg)

In an index proband (II: 1) of a FEVR family 94, a thymine to cytosine transition was observed at cDNA position of c.376 (figure 4.2 and figure 4.3; N). This substitution led to alteration of a highly conserved cysteine residue with arginine at amino acid position 126 of Norrin. This change was not observed in 115 control individuals. The proband showed bilateral leukocoria with total retinal detachments at 3 months of age (table 4.4). As this mutation was not observed in the unaffected parents of the proband (figure 4.2; FEVR family 94; I: 1 and I: 2), it was considered as a *de novo* mutation.

4.1.1.2 Description of nucleotide changes observed in the 5' and 3' UTR of the *NDP* gene

-395_-409del14bp and -111G>T

In the female proband (II: 3) of a FEVR family 8, a reported 14 base pair deletion (-395_-409del14bp) was observed along with a known SNP (rs45501198) in the 5' UTR of *NDP* (figure 4.2 and figure 4.3; O and T) (Dickinson *et al.*, 2006; Wu *et al.*, 2007). The

14 base pair deletion was observed in homozygous condition while -111G>T SNP was observed in heterozygous condition. These changes were not observed in 115 control individuals. MatInspector analysis predicted that, both these changes did not affect any transcription factor binding sites in the 5' UTR. The proband harboring these changes had avascularized peripheral retina along with neovascularization in both the eyes (table 4.4). At 12 years of age, both eyes of the proband underwent laser treatment and gained 20/20 feet visual acuity after 5 years of follow-up. Though, the male (II: 2) and female (II: 1) siblings of the proband were also severely affected, only the female sibling had both of the nucleotide changes in heterozygous condition (figure 4.2; FEVR family 8). Both of these changes were also observed in hemizygous condition in unaffected proband's father (figure 4.2; FEVR family 8; I:1, figure 4.3; P and S) while unaffected mother (I: 2) only had 14 bp deletion in heterozygous condition. The development of severe clinical features of the disease in absence of these changes in the male sibling (II: 2) of the proband suggested for the involvement of other candidate genes of FEVR in this family (figure 4.2; FEVR family 8). Interestingly, we have identified an adenine to guanine missense change at position c.1078 in *FZD4* gene (figure 4.6; FEVR family 8). This change resulted in the alteration of isoleucine by valine at amino acid position 360 of FZD4 protein (figure 4.7; F). The heterozygous form of this nucleotide change was observed in all the affected members of this family. However, the presence of all the three changes in phenotypically normal proband's father suggests either the less pathogenic nature or variable expressivity of these variations.

c.*522T>C

A novel, heterozygous nucleotide change from thymine to cytosine was observed in the 3' UTR at c.*522 position in the proband (II: 2) of FEVR family75 (figure 4.2 and figure 4.3; Q). The proband showed avascularized peripheral retina with neovascularization and retinal hemorrhages in both the eyes at 2 years of age (table 4.4). After laser, the disease was stable in both the eyes and exhibited 20/20 feet visual acuity at 6 years of follow-up examination. The observation of this change in a control individual along with phenotypically normal mother (figure 4.2; FEVR family 75; I: 2) of the proband suggests the less pathogenic nature of this variation.

c.*974C>G

A novel cytosine to guanine nucleotide change was observed in 3' UTR after 973 base pairs of stop codon in the female proband (II: 1) of FEVR family 98 (figure 4.2 and figure 4.3; R). This change was not observed in 115 control individuals. The proband exhibited bilateral tractional retinal detachments and completely lost her vision at five months of age (table 4.4). This substitution was also observed in mildly affected mother (II: 2) of the proband (figure 4.2; FEVR family 98). However, the development of severe clinical features of the disease in absence of this substitution in a female sibling (figure 4.2; FEVR family 98; II: 3) of the proband suggested for the involvement of other candidate genes of FEVR in this family.

4.1.1.3 *In silico* analysis of missense mutations observed in the *NDP* gene

Multiple sequence alignment was carried out using Clustal W software to determine the conservation of the wild type residues. The wild type amino acid residues located at the four identified missense mutations (H50D, G113D, R121Q and C126R) in the Norrin protein were highly conserved across the different species of vertebrates (figure 4.4). SIFT and PolyPhen-2 analysis predicted the deleterious effect of these mutations and suggested their pathogenic nature (table 4.3). In the crystal structure of the Norrin, these missense mutations were located in FZD4, LRP5 binding surfaces (H50D, G113D and R121Q) or central core of cysteine knot domain (C126R). These missense changes were predicted to have no significant effect either on potential splice sites or splicing regulatory elements through Human Splicing Finder (HSF) analysis.

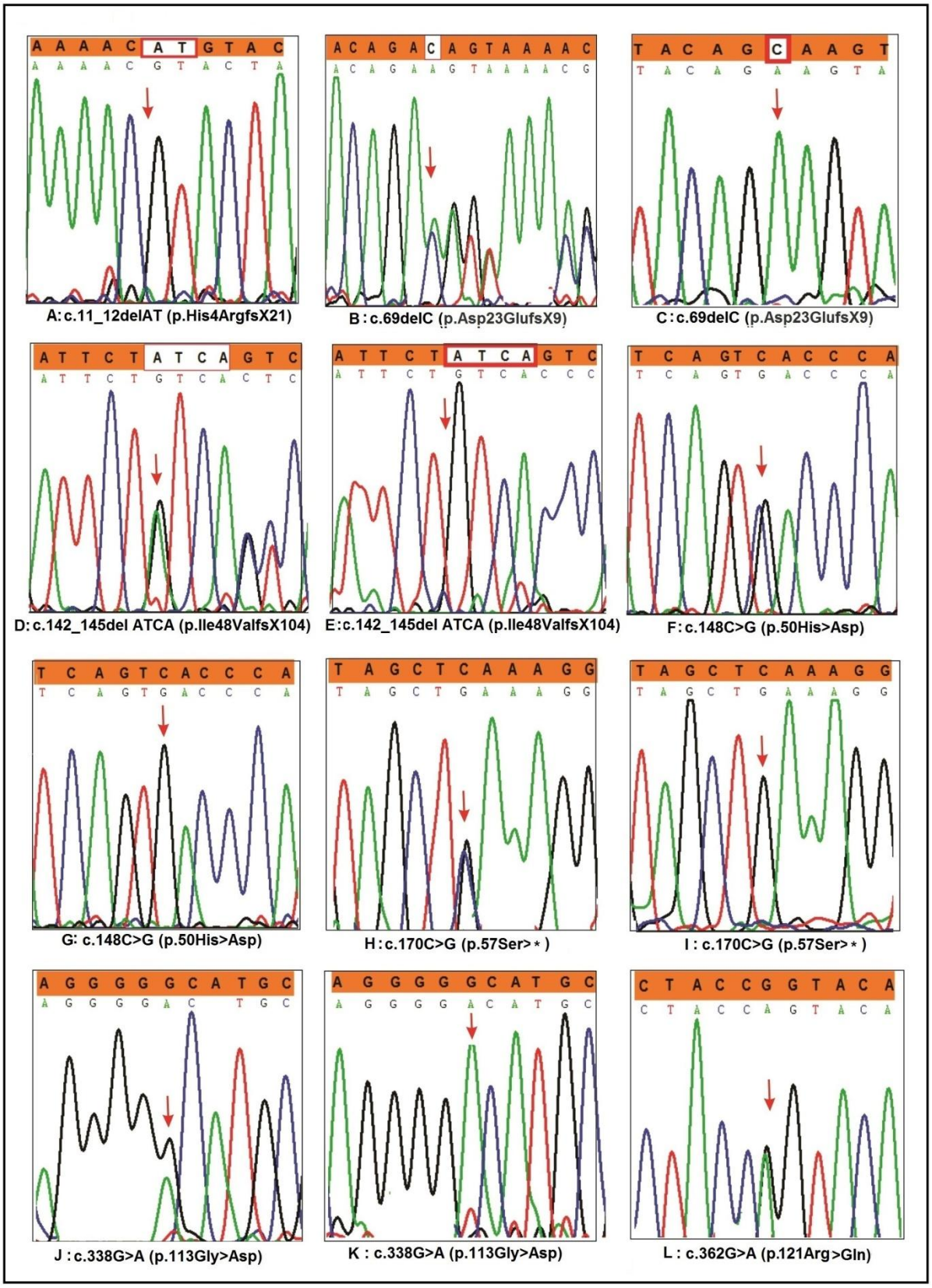
A: c.11_12delAT (p.His4ArgfsX21)
B : c.69delC (p.Asp23GlufsX9)
C : c.69delC (p.Asp23GlufsX9)
D: c.142_145del ATCA (p.Ile48ValfsX104)
E: c.142_145del ATCA (p.Ile48ValfsX104)
F: c.148C>G (p.50His>Asp)
G: c.148C>G (p.50His>Asp)
H : c.170C>G (p.57Ser>*)
I : c.170C>G (p.57Ser>*)
J : c.338G>A (p.113Gly>Asp)
K : c.338G>A (p.113Gly>Asp)
L : c.362G>A (p.121Arg>Gln)

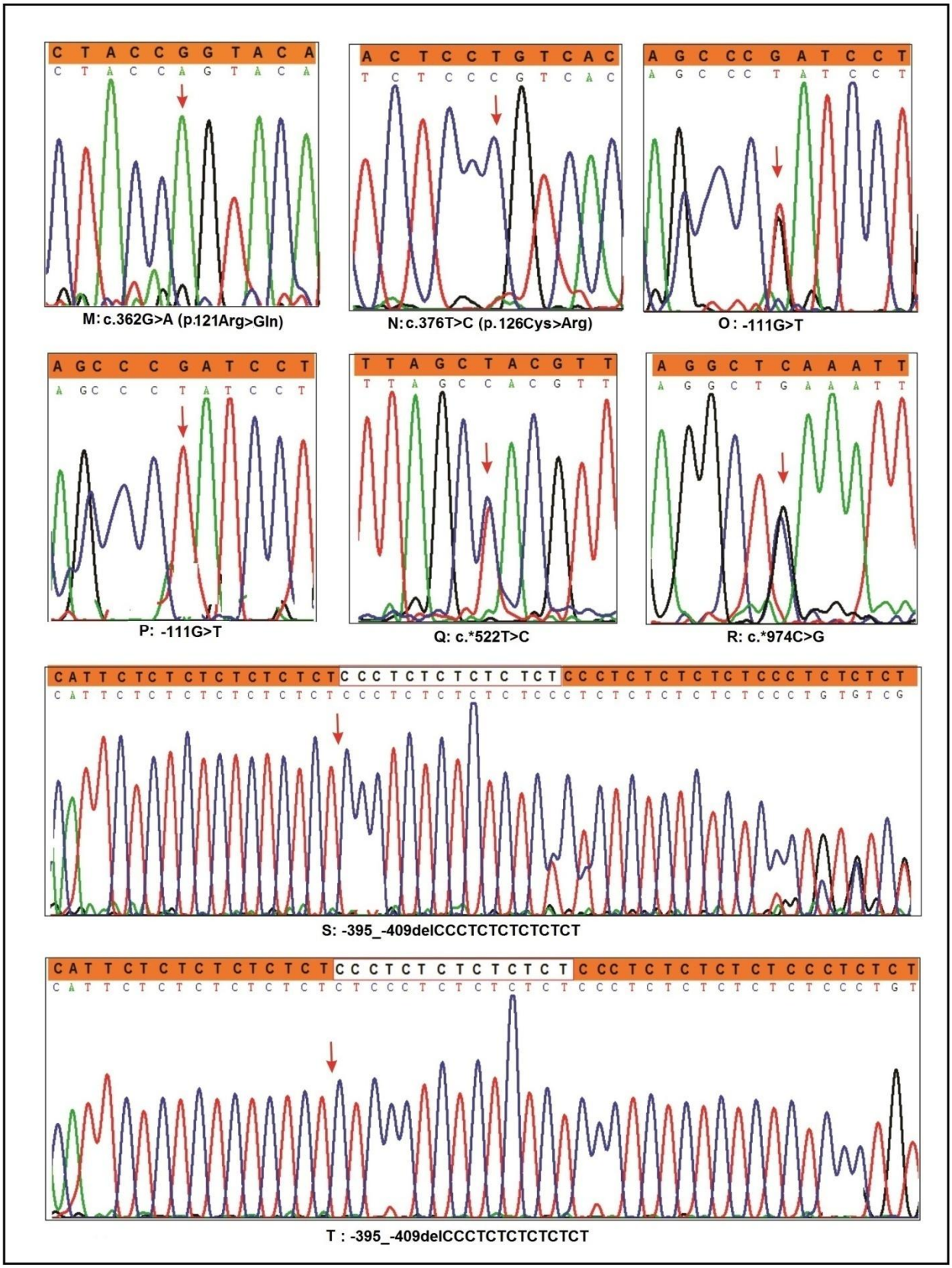
M: c.362G>A (p.121Arg>Gln)
N: c.376T>C (p.126Cys>Arg)
O : -111G>T
P: -111G>T
Q: c.*522T>C
R: c.*974C>G
S: -395_-409delCCCTCTCTCTCTCT
T : -395_-409delCCCTCTCTCTCTCT

Figure 4.3: Electropherograms representing the nucleotide changes identified in the *NDP* gene in FEVR patients. The sequence above the electropherogram in the shaded portion represents the wild type sequence. The arrow head indicates the site of nucleotide change. A) A hemizygous 2 base pair (AT) deletion at c.11_12 position resulted in a frame shift after codon position 4 B) A heterozygous single base pair deletion of nucleotide 'C' at c.69 position resulted in a frame shift after codon position 23. C) A hemizygous single base pair deletion of nucleotide 'C' at c.69 position resulted in a frame shift after codon position 23. D) A heterozygous 4 base pair (ATCA) deletion at c.142_145 position resulted in a frame shift after codon position 48. E) A hemizygous 4 base pair (ATCA) deletion at c.142_145 position resulted in a frame shift after codon position 48. F) A heterozygous substitution of CAC>GAC at c.148 position resulted in the His50Asp amino acid change. G) A hemizygous substitution of CAC>GAC at c.148 position resulted in the His50Asp amino acid change. H) A heterozygous substitution of TCA>TGA at c.170 position resulted in the Ser57stop mutation. I) A hemizygous substitution of TCA>TGA at c.170 position resulted in the Ser57stop mutation. J) A heterozygous substitution of GGC>GAC at c.338 position resulted in the Gly113Asp amino acid change. K) A hemizygous substitution of GGC>GAC at c.338 position resulted in the Gly113Asp amino acid change. L) A heterozygous substitution of CGG>CAG at c.362 position resulted in the Arg121Gln amino acid change. M) A hemizygous substitution of CCG>CAG at c.362 position resulted in the Arg121Gln amino acid change. N) A hemizygous substitution of TGT>CGT at c.376 position resulted in the Cys126Arg amino acid change. O) A heterozygous guanine to thymine change at c.-111 position in 5' UTR. P) A hemizygous guanine to thymine change at c.-111 position in 5' UTR. Q) A heterozygous thymine to cytosine substitution at c.*522 position in 3' UTR. R) A heterozygous cytosine to guanine substitution at c.*974 position in 3' UTR. S) A heterozygous 14 base pair deletion at -395_-409 position in 5' UTR. T) A hemizygous 14 base pair deletion (CCCTCTCTCTCTCT) at -395_-409 position in 5' UTR

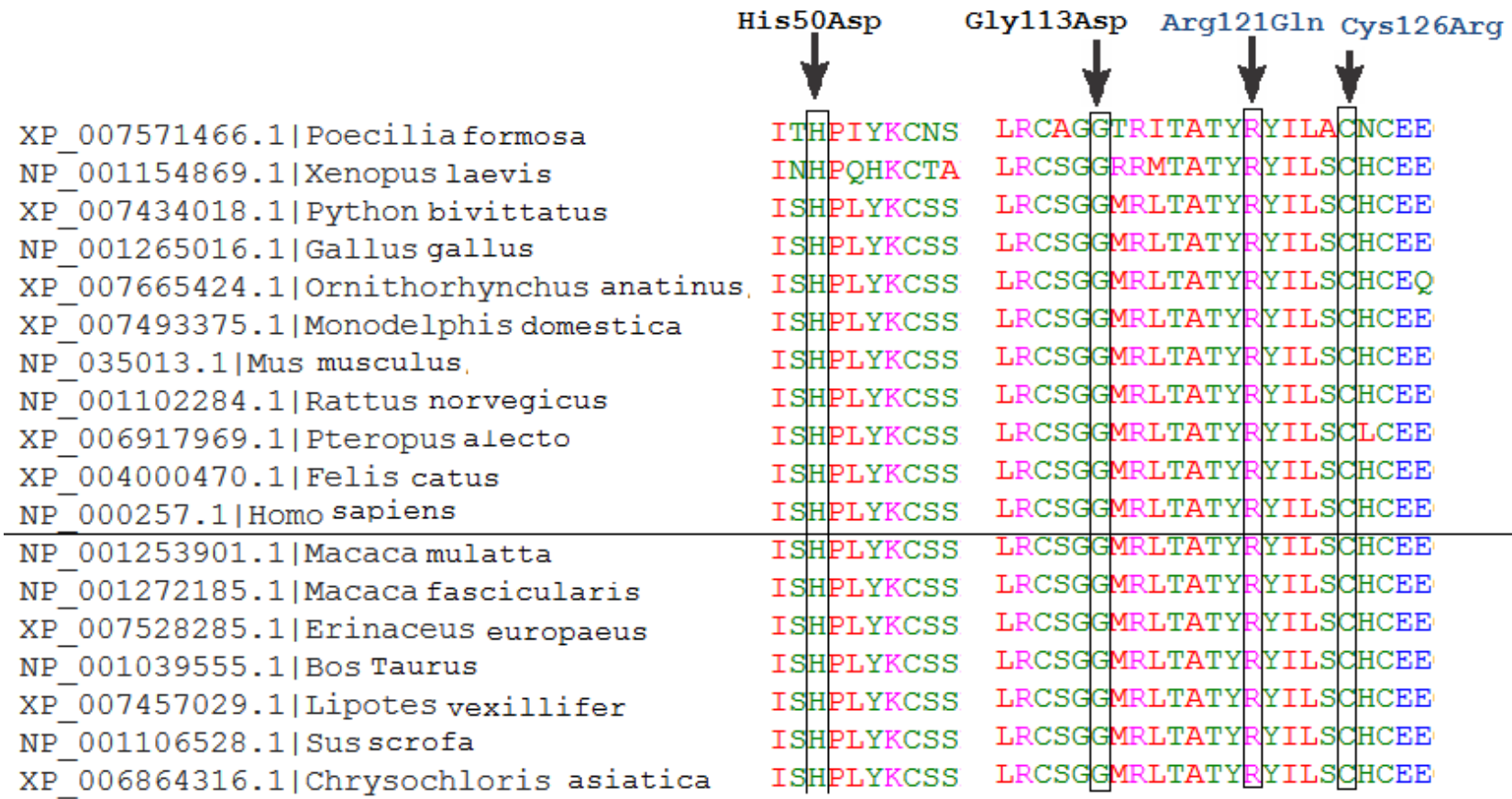

Figure 4.4: Multiple sequence alignment showing the conservation of wild type residues in respect to identified missense nucleotide changes in Norrin protein across various species. The human Norrin protein sequence is underlined. Accession numbers (NCBI) and name of the species are mentioned at the left side of the picture.

4.1.2 *FZD4* gene analysis

Screening of two exons including intron-exon boundaries of *FZD4* gene revealed ten different nucleotide changes in probands of fourteen different FEVR families (table 4.5 and 4.6, figures 4.5 and 4.6). These nucleotide changes included five missense changes, two small base pair deletions, a single base pair insertion, a non-stop change and a synonymous nucleotide change (tables 4.5 and 4.6, figure 4.5). Of these ten nucleotide changes, five changes were novel. All the nucleotide changes were observed in heterozygous state. Of the fourteen probands identified with *FZD4* nucleotide changes, five probands had family history of the disease while the remaining nine were sporadic cases (figure 4.6). Intriguingly, all the nucleotide changes were identified in second exon of *FZD4* gene.

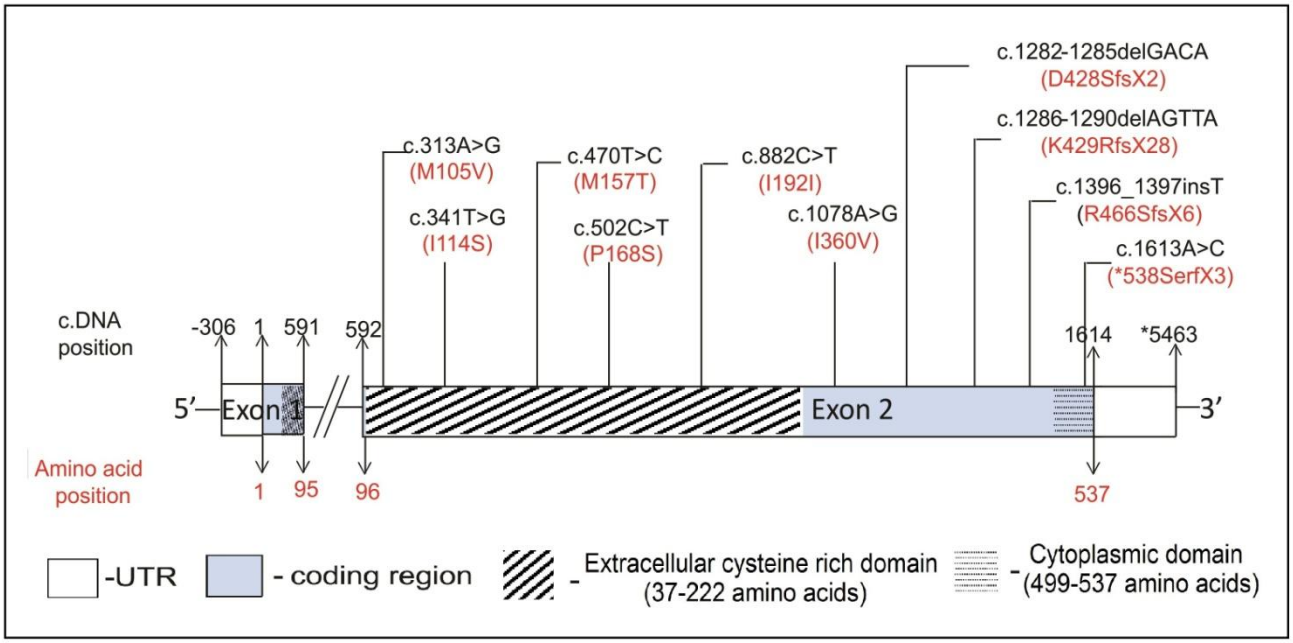

Figure 4.5: Schematic representation of the *FZD4* gene with identified nucleotide changes in FEVR probands. +1 represents the transcription initiation site. cDNA positions and amino acid positions have been given by following the reference sequences NM_012193.2 and NP_036325.2 respectively.

Table 4.5: Nucleotide changes observed in the *FZD4* gene in FEVR probands

Location in the *FZD4* gene	cDNA position of the nucleotide change	Amino acid change	SIFT (score)	PolyPhen-2 (score)	Reported/ Novel	Study code of the proband	Number of probands with the nucleotide change [n=110] (frequency)	Number of controls with the nucleotide change [n=115] (frequency)
Exon2	c.313A>G	Met105Val	Tolerated (0.95)	Possibly damaging (0.793)	Reported (Kondo *et al.*, 2003; Jia *et al.*, 2010; Yang *et al.*, 2012b)	35 FEVR 64 FEVR 134 FEVR	3 (0.027)	0
	c.341T>G	Ile114Ser	Damaging (0.01)	Probably damaging (0.996)	Novel	52 FEVR	1 (0.009)	0
	c.470T>C	Met157Thr	Tolerated (0.06)	Benign (0.256)	Novel	51 FEVR	1 (0.009)	0
	c.502 C>T	Pro168Ser	Tolerated (0.18)	Benign (0.146)	Reported (rs61735303)	116 FEVR	1 (0.009)	1 (0.086)
	c.882 C>T	Ile192Ile	-	-	Reported (rs201168680)	80 FEVR 122 FEVR 129 FEVR	3 (0.027)	3 (0.026)

Location in the *FZD4* gene	cDNA position of the nucleotide change	Amino acid change	SIFT (score)	PolyPhen-2 (score)	Reported/ Novel	Study code of the proband	Number of probands with the nucleotide change [n=110] (frequency)	Number of controls with the nucleotide change [n=115] (frequency)
Exon2	c.1078A>G	Ile360Val	Tolerated (0.26)	Possibly damaging (0.840)	Novel	8 FEVR	1 (0.009)	1 (0.086)
	c.1282-1285delGACA	Asp428Ser *fsX*2	-	-	Reported (Nikopoulos *et al.*, 2010b; Robitaille *et al.*, 2011; Yang *et al.*, 2012b)	89 FEVR	1 (0.009)	0
	c.1613A>C	*538Ser*fsX*3	-	-	Novel	89 FEVR	1 (0.009)	0
	c.1286-1290delAGTTA	Lys429Arg *fsX*28	-	-	Reported (Muller *et al.*, 2008)	61 FEVR 136 FEVR	2 (0.018)	0
	c.1396_1397insT	Arg466Ser *fsX*6	-	-	Novel	98 FEVR	1 (0.009)	0

cDNA positions and amino acid positions have been given by following the reference sequences NM_012193.2 and NP_036325.2 respectively. '*' represents the stop codon.

Table 4.6: Clinical features of the FEVR probands identified with nucleotide changes in the *FZD4* gene

Study code of the proband	cDNA position of nucleotide change	Age at initial present-ation at LVPEI (gender)	Stage of the disease/clinical features	Treatment	Outcome/ visual acuity in feet
35 FEVR	c.313A>G (missense change)	3 months (female)	OU: 4B Tractional RD with falciform retinal folds were observed in both the eyes at 3 months of age	No	OU: PL
64 FEVR	c.313A>G (missense change)	6 months (male)	OD: 3, OS: 5 Funnel shaped, total RD was observed in the left eye. In the right eye avascularized peripheral retina was observed with sub retinal hemorrhages and vitreous traction.	OD: LIO & BB	OD:20/40, OS: No PL
134 FEVR	c.313A>G (missense change)	2 years (male)	OD: 3, OS: 4B White reflex and photophobia were reported to be observed in the left eye after few months of birth. Neovascularization with sub retinal hemorrhages were observed in the right eye. Falciform retinal folds were observed in the left eye.	OD: LIO	OD: 20/170, OS: No PL
52 FEVR	c.341T>G (missense change)	8 months (female)	OU:4B Nystagmus, falciform retinal folds were observed bilaterally.	No	OU:PL
51 FEVR	c.470T>C (missense change)	35 years (female)	OD:5, OS:4A Gradual decrease in vision was reported to be observed in left and right eyes at 32 and 35 years of age respectively. Nystagmus was observed in the right eye. Total RD with dragging of the disc towards the temporal side was observed in both the eyes.	No	OD: CF 1M, OS: No PL
116 FEVR	c.502 C>T (SNP)	3 months (male)	OD:5 Bilateral fibro vascular proliferations and total RD was observed.	No	OU: No PL
80 FEVR	c.882 C>T (SNP)	10 years (male)	OU: 5 Sudden decrease in vision was reported at 10 years of age. Exudative total RD was observed bilaterally.	OD: Vitrectomy	OU: PL

122 FEVR	c.882 C>T (SNP)	3 months (female)	OD: 2, OS:5 Avascularized peripheral retina was observed with hemorrhages in the right eye. In the left eye falciform retinal fold was observed with total RD.	OD: LIO	OD: PL, OS: No PL
129 FEVR	c.882 C>T (SNP)	4 months (female)	OD: 4B, OS: 2 Disc dragging and vitreo retinal traction was observed along with fibro vascular proliferation in the right eye. In the left eye avascular temporal retina was observed with active neovascularization	OD: Vitrectomy, OS: LIO	OU: PL
8 FEVR	c.1078 A>G (missense change)	12 years (female)	OU: 2 Bilateral avascularized peripheral retina was observed with neovascularization and retinal hemorrhages.	OU:LIO at 12 years of age	OU:20/20
89 FEVR	c.1282-1285delGACA & c.1613A>C (4bp deletion & non-stop change)	9 years (female)	OD: 4A, OS: 5, Squint present in both the eyes. Sudden decrease in vision was reported in the left eye at 9 years of age. Total RD was observed in right eye at initial presentation. Funnel shaped RD was observed with dragged disc and fibrovascular proliferations at temporal side of the retina in the left eye.	OD: Vitrectomy, lensectomy	OD: PL, OS: NO PL
61 FEVR	c.1286-1290delAGTTA (5bp deletion)	10 years (male)	OD:5, OS: 4A Visual defects were reported to be observed at 6 years of age. Further decrease in vision was observed at 10 years of age. Total RD was observed in the right eye. Nonrhegmatogenous RD was observed with exudation in the left eye.	OD: Vitrectomy, Lensectomy, OS: BB	OD: No Pl, OS: 20/20
136 FEVR		2 years (female)	OD:4A, OS:5 Total rhegmatogenous RD with temporally dragged retina was observed in the left eye. In the right eye fibrovascular proliferation was observed along with avascular peripheral retina and retinal exudation.	OD: BB, OS: Lensectomy and vitrectomy	OD:20/30, OS: No PL
98 FEVR	c.1396_1397insT (1 bp insertion)	5 months (female)	OU:5 Total RD was observed with vitreous traction in both eyes.	No	OU: No PL

RD: retinal detachment, OD: right eye, OS: left eye, OU: both eyes, LIO: Laser Indirect Ophthalmoscopy, PL: perception of light, BB: belt buckle, CF: counting fingers.

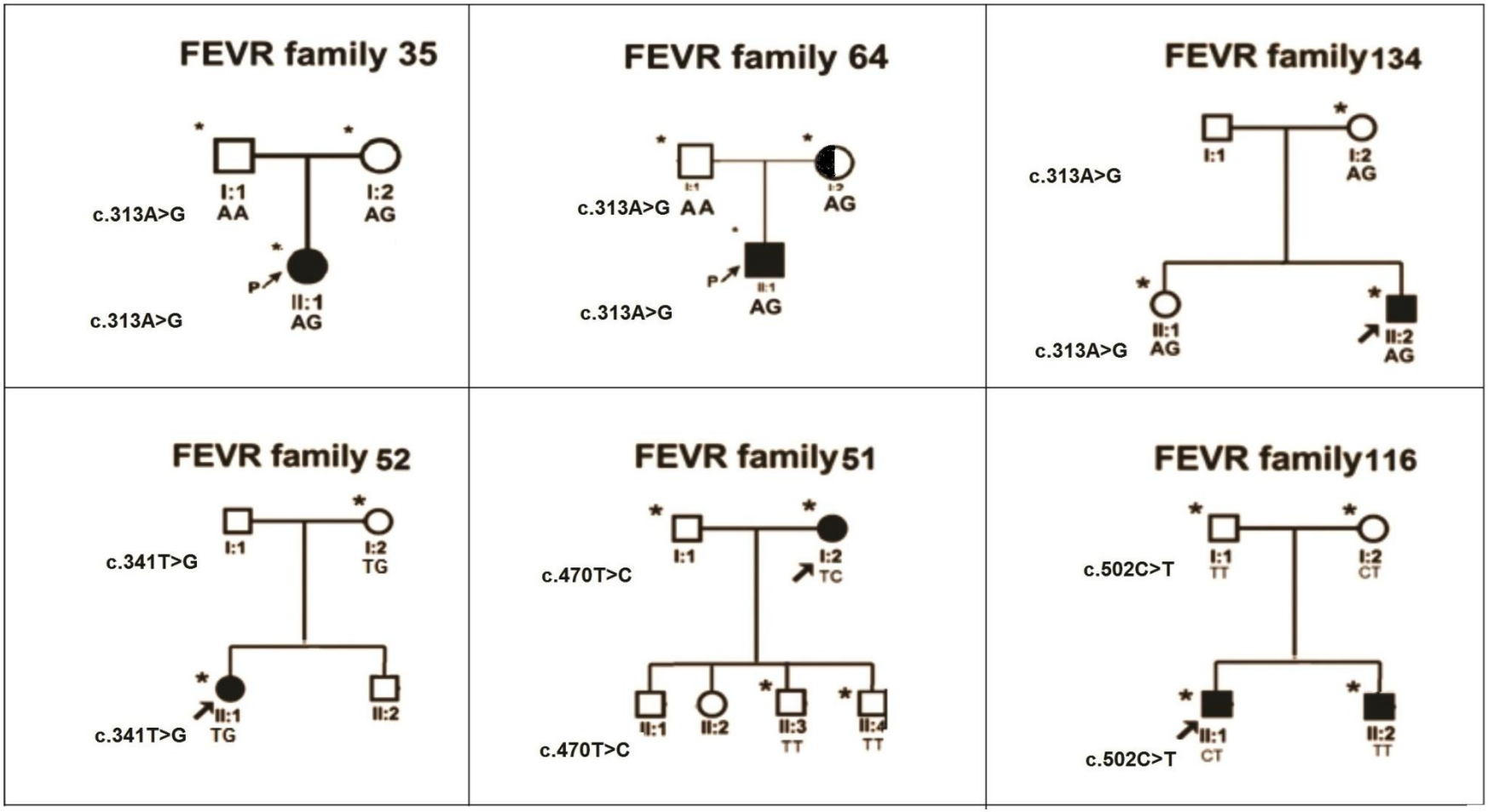
FEVR family 35
c.313A>G
I:1
AA
I:2
AG
P
II:1
AG
c.313A>G
FEVR family 64
c.313A>G AA
AG
P
AG
c.313A>G
FEVR family134
I:1
I:2
AG
c.313A>G
II:1
AG
II:2
AG
c.313A>G
FEVR family 52
c.341T>G
I:1
I:2
TG
II:1
TG
II:2
c.341T>G
FEVR family51
c.470T>C
I:1
I:2
TC
II:1
II:2
II:3
TT
II:4
TT
c.470T>C
FEVR family116
c.502C>T
I:1
TT
I:2
CT
II:1
CT
II:2
TT
c.502C>T

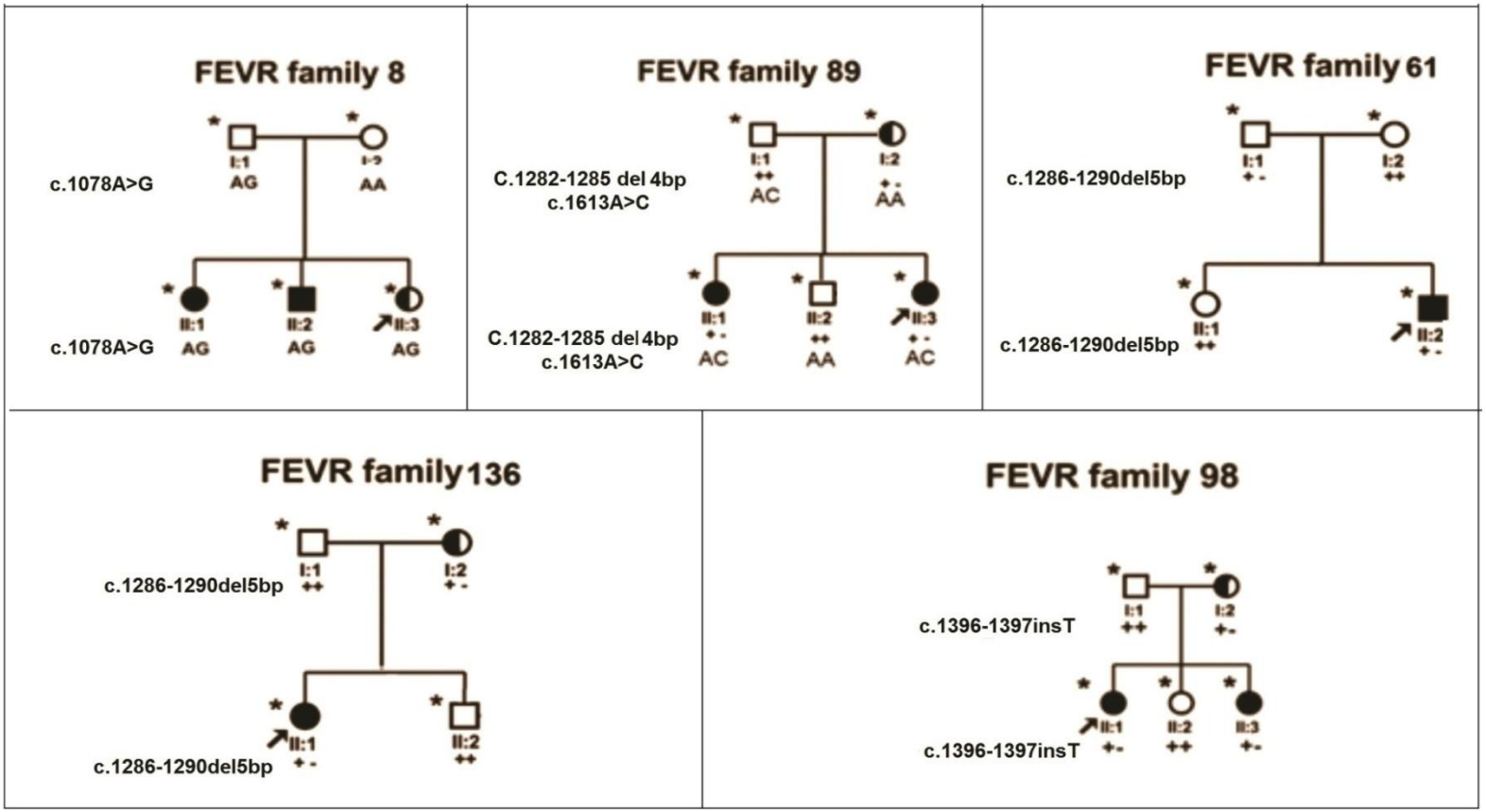

Figure 4.6: Pedigrees of the FEVR families with nucleotide changes in the *FZD4* gene. Completely and partially shaded symbols represent severe stages and milder stages of the disease respectively. Open symbols represent unaffected individuals. Asterisk (*) over the pedigree symbols represent the individuals screened for the nucleotide changes in FZD4 gene. - indicates the presence of deletion and + indicates the wild type allele. The identified nucleotide change is represented left side of each pedigree.

4.1.2.1 Description of nucleotide changes observed in the *FZD4* gene

c.313A>G (Met105Val)

A reported, adenine to guanine change was observed at cDNA position c.313 (figure 4.7; A) in the probands of three different FEVR families (35, 64 and 134) (Kondo *et al.*, 2003; Jia *et al.*, 2010; Yang *et al.*, 2012b). This change was not observed in 115 control individuals. This nucleotide change led to replacement of a methionine residue with valine at 105 amino acid position of FZD4 protein. All the three probands harboring this mutation had bilateral retinal falciform folds with subtotal or total tractional retinal detachments within few months after their birth (table 4.6). The mother of the proband-64 (figure 4.6; FEVR family 64; I: 2), who was also carrying the mutation was observed with peripheral retinal avascularization. However, in the other two FEVR families 35 and 134, proband's mothers (figure 4.6; FEVR family 35 and 134; I: 2) and a sibling (figure 4.6: FEVR family 134; II: 1) also shared similar mutation but did not exhibit the clinical features of disease under ophthalmoscopic examination. SIFT analysis predicted that this amino acid change was tolerated by the protein, whereas it was found to have a damaging affect on PolyPhen-2 analysis. HSF analysis suggested nonharmful effect of this substitution on splice sites and splicing regulatory elements.

c.341T>G (Ile114Ser)

A novel, thymine to guanine change was observed in an index proband (II: 2) of FEVR family 52 (figure 4.6 and figure 4.7; B). The variation resulted in the substitution of an isoleucine residue with serine at amino acid position 114 of FZD4 protein. The change was not observed in 115 control individuals. The proband with this mutation exhibited bilateral, exudative subtotal retinal detachments including macula when examined at 8 months of age (table 4.6). The proband mother (I: 2) also harbored this change but appeared normal under indirect ophthalmoscopic examination (figure 4.6; FEVR family 52; I: 2). On multiple sequence alignment, wild type isoleucine residue was found to be highly conserved across different species (figure 4.8). Further, SIFT and PolyPhen-2 analysis suggested the damaging effect of the substitution. HSF analysis predicted no

significant effect of this substitution either on splicing regulatory elements and potential splice sites.

c.470T>C (Met157Thr)

A novel, thymine to cytosine substitution was observed at position c.470 in the female proband (I: 2) of a FEVR family 51 (figure 4.6 and figure 4.7; C). This change was not observed in 115 control individuals. This mutation led to substitution of a methionine residue by a threonine at 157 amino acid position of FZD4 protein. The proband had total retinal detachment in the left eye and exudative subtotal retinal detachment including macula in the right eye (table 4.6). SIFT and PolyPhen-2 analysis predicted the nonharmful effect of the substitution. In HSF analysis, this substitution did not show significant effect on splice enhancer, suppressor and potential splice sites.

c.502 C>T (Pro168Ser)

A reported single nucleotide polymorphism c.502 C>T (rs61735303) was observed in the proband (II: 1) of a FEVR family 116 (figure 4.6 and figure 4.7; D). The cytosine to thymine substitution at position c.502 led to replacement of a proline residue with a serine at amino acid position 168 of FZD4 protein. The proband exhibited total retinal detachment in both the eyes at 3 months of age (table 4.6). In addition to the proband, the change was also observed in the unaffected mother (figure 4.6; FEVR family 116; I: 2) of the proband and two control individuals. In the severely affected brother of the proband ((figure 4.6; FEVR family 116; II: 2), the change was not observed indicating the involvement of other gene mutations in disease pathogenesis in this family. SIFT and PolyPhen-2 analysis indicated the nonharmful effect of the substitution on protein function. HSF analysis suggested no significant effect of the substitution on mRNA splicing.

c.882 C>T (Ile192Ile)

Another reported single nucleotide polymorphism c.576C>T (rs201168680) was observed in the probands of three different FEVR families (80, 122 and 129) (figure 4.7; E). The cytosine to thymine nucleotide change at position c.882 resulted in a synonymous Isoleucine residue change at amino acid position 192 of FZD4 protein. Out of 115 control individuals screened for this variation, the change was observed in three control individuals. The presence of the mutated allele with a similar allele frequency in both the patients (0.027) and control (0.026) individuals indicated the non-pathogenic nature of this substitution. HSF analysis indicated no significant effect of this substitution either on potential splice sites or splicing regulatory elements.

c.1078 A>G (Ile360Val)

A novel, adenine to guanine substitution at cDNA position c.1078 was observed in the female proband (II: 3) of a FEVR family 8 (figure 4.6 and figure 4.7; F). The change led to substitution of an isoleucine residue with valine at amino acid position 360 of FZD4 protein. The change was also observed in heterozygous condition in severely affected male (II: 2) and female (II: 1) siblings and unaffected father (I: 1) of the proband (figure 4.6; FEVR family 8). In addition to the family members of the proband, the change was observed in one control individual. In multiple sequence alignment, valine residue was observed instead of an isoleucine residue at 360 amino acid position of FZD4 protein in beetle (Tribolium *castaneum*) and sea urchin (Paracentrotus *lividus*) (figure 4.8). SIFT analysis predicted the substitution to be tolerated, whereas PolyPhen-2 analysis suggested it damaging on the protein function. In HSF analysis, this substitution did not show significant effect on splicing regulatory elements.

c.1282-1285delGACA (Asp428Ser*fsX*2) and c.1613A>C (*538SerfX3)

In the proband (II: 3) of FEVR family 89, a reported four base pair deletion at position c.1282-1285 was observed along with a heterozygous, non-stop change (c.1613A>C) in second exon of *FZD4* gene (figure 4.6 and figure 4.7; G and H) (Nikopoulos *et al.*, 2010b; Robitaille *et al.*, 2011; Yang *et al.*, 2012b). The four base pair deletion resulted

in a frame shift at codon position 428 and formation of a stop codon at codon position 429. This change may result in formation of truncated protein with 429 amino acid residues as compared to wild type FZD4 protein with 537 amino acid residues. The non-stop change, adenine to cytosine substitution at position c.1613 was resulted in the replacement of a stop codon (TAA) with a codon for the serine (TCA) residue at codon position 538 of the FZD4 mRNA. This change led to formation of a new stop codon at codon position 540 and formation of a mutant protein with 539 amino acid residues. Both these changes were not observed in 115 control individuals. The proband with these mutations exhibited bilateral falciform retinal folds with total retinal detachments at nine years of age (table 4.6). Along with the proband, both the mutations were also observed in heterozygous condition in a severely affected proband's sibling (figure 4.6; FEVR family 89; II: 1). In the proband and her sibling, the two mutations were located on different chromosomes and were inherited from both parents. The mother of the proband (I: 2) was harboring the four base pair deletion, whereas the father (I: 1) was carrying the non-stop change (figure 4.6; FEVR family 89). In presence of two mutated alleles a severe disease phenotype was observed in the proband and her sibling compared to the mother with avascularized peripheral retina and father with normal retinal phenotype.

c.1286-1290delAGTTA (Lys429Arg*fsX*28)

Another reported five base pair deletion at position c.1286-1290 was observed in probands of two different FEVR families 61 (II: 2) and 136 (II: 1) (figure 4.6 and figure 4.7; I) (Muller *et al.*, 2008). The deletion led to frame shift at codon position 429 and formation of a premature termination codon after addition of 27 altered amino acid residues. This change may lead to formation of truncated protein with a loss of 81 amino acid residues as compared to wild type protein. Both the probands with the deletion exhibited bilateral subtotal retinal detachment including macula or total retinal detachment in their early childhood (table 4.6). The mother (I: 2) of the proband 136 was carrying the deletion and exhibited peripheral retinal avascularization (figure 4.6; FEVR family 136). In family 61, however, the proband's father (I: 1) who had the

mutation did not develop any retinal vascular abnormalities (figure 4.6; FEVR family 61). This change was not observed in 115 control individuals.

c.1396_1397insT (Arg466Ser*fsX*6)

A novel, single base pair insertion of nucleotide 'C' was observed at position c.1396_1397 in the proband (II: 1) of a FEVR family 98 (figure 4.6 and figure 4.7; J). The insertion resulted in a frame shift at codon 466 and formation of premature termination codon after addition of five altered amino acid residues. It may leads to formation of a truncated protein shorter by 67 amino acid residues as compared to wild type protein. The insertion was also observed in the mother (I: 2) and a female sibling of the proband (II: 3) and segregated with the disease (figure 4.6; FEVR family 98). At five months of age, the proband developed bilateral falciform retinal folds with subtotal retinal detachments including macula (table 4.6). The sibling of the proband also exhibited subtotal retinal detachments in both the eyes at early childhood. The mother of the proband was observed with peripheral avascularized retina under indirect ophthalmoscope. This change was not observed in 115 control individuals.

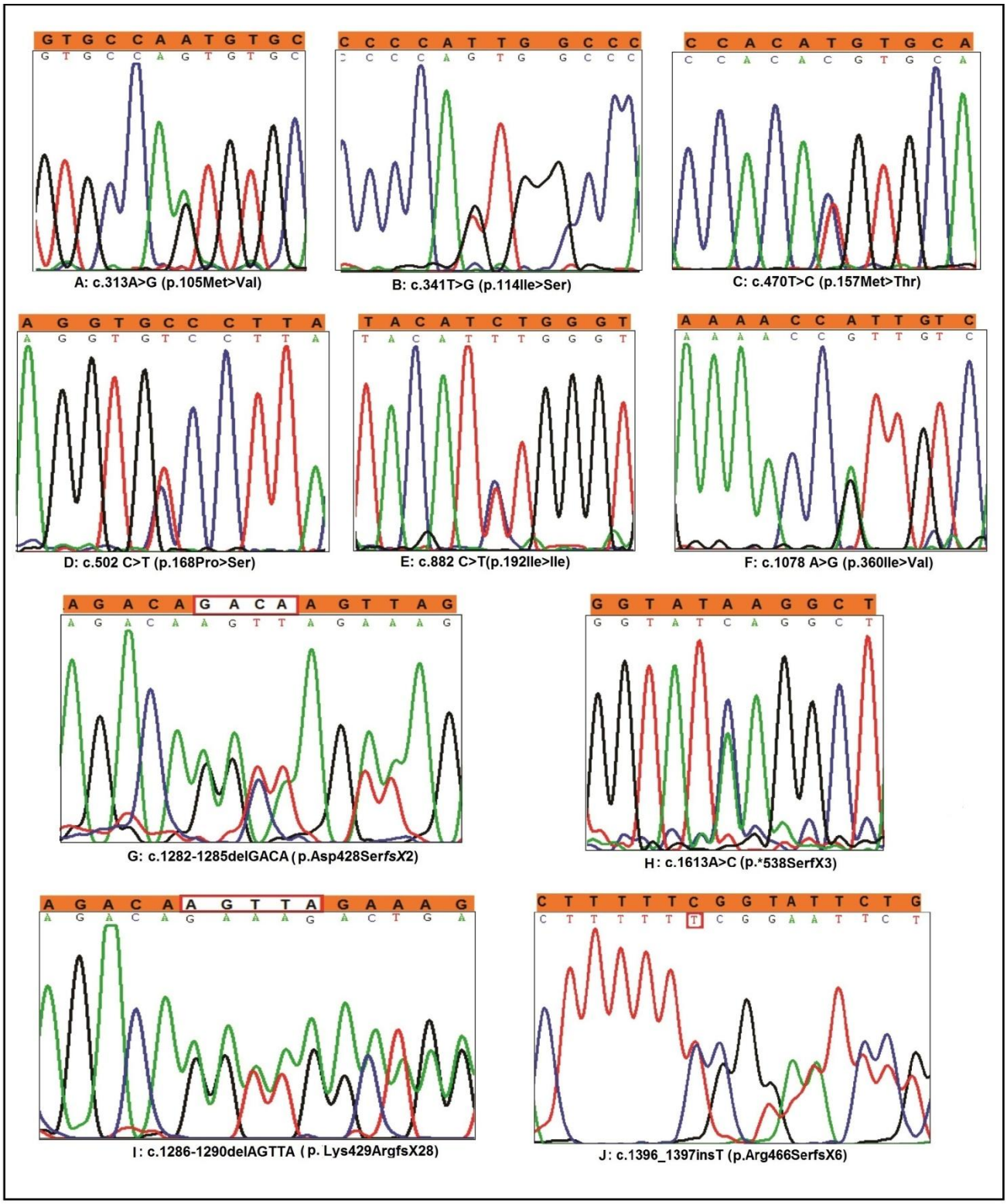
A: c.313A>G (p.105Met>Val)
B: c.341T>G (p.114Ile>Ser)
C: c.470T>C (p.157Met>Thr)
D: c.502 C>T (p.168Pro>Ser)
E: c.882 C>T(p.192Ile>Ile)
F: c.1078 A>G (p.360Ile>Val)
G: c.1282-1285delGACA (p.Asp428SerfsX2)
H: c.1613A>C (p.*538SerfX3)
I: c.1286-1290delAGTTA (p. Lys429ArgfsX28)
J: c.1396_1397insT (p.Arg466SerfsX6)

Figure 4.7: Electropherograms representing the identified nucleotide changes in the *FZD4* gene. The sequence above the electropherogram in the shaded portion represents the wild type sequence. The arrow head indicates the site of nucleotide change. A) A heterozygous substitution of ATG>GTG at c.313 position resulted in the Met105Val amino acid change. B) A heterozygous substitution of ATT>AGT at c.341 position resulted in the Ile114Ser amino acid change. C) A heterozygous substitution of ATG>ACG at c.470 position resulted in the Met157Thr amino acid change. D) A heterozygous substitution of CCC>TCC at c.502 position resulted in the Pro168Ser amino acid change. E) A heterozygous substitution of ATC>ATT at c.882 position resulted in a synonymous Ile192Ile amino acid change. F) A heterozygous substitution of ATT>GTT at c.1078 position resulted in the Ile360Val amino acid change. G) A heterozygous 4 base pair (GACA) deletion at c.1282_c.1285 position resulted in a frame shift after amino acid position 428. Deleted nucleotide bases have shown in white color box. H) A heterozygous substitution of TAA>TCA at c.1613 position resulted in the alteration of a stop codon into a codon corresponding to serine residue. I) A heterozygous 5 base pair (AGTTA) deletion at c.1286_1290 position resulted in a frame shift after amino acid position 429. Deleted nucleotide bases have shown in white color box. J) A heterozygous single base pair (T) insertion at c.1396_1397 position resulted in a frame shift after amino acid position 466. Inserted nucleotide has shown in red color box.

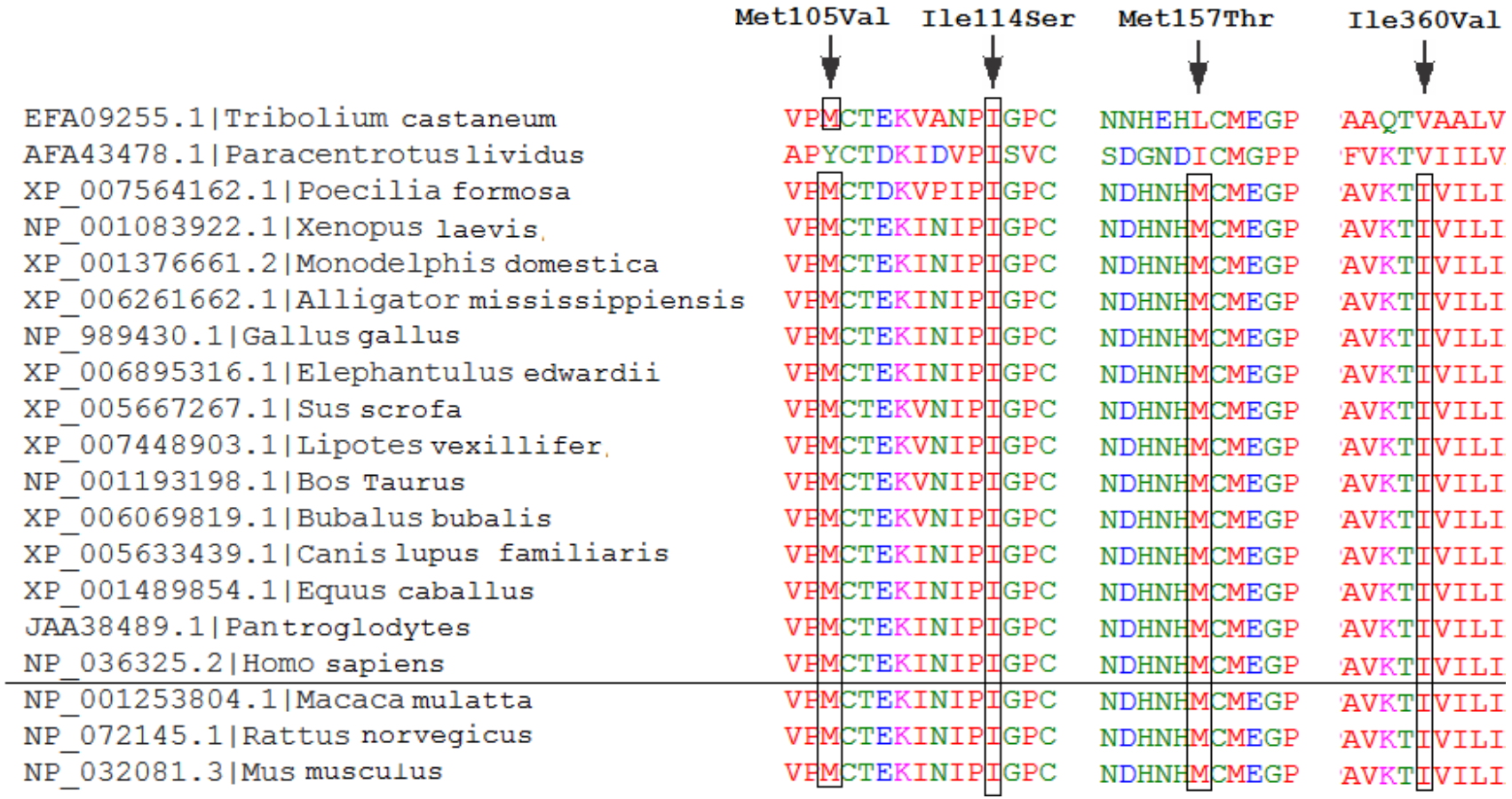

Figure 4.8: Multiple sequence alignment showing the conservation of wild type residues in respect to identified missense changes in FZD4 protein across various species. The human FZD4 protein sequence is underlined. Accession numbers (NCBI) and name of the species are mentioned at the left side of the picture.

4.1.3 *TSPAN12* gene analysis

Direct sequencing of entire coding region, intron-exon boundaries and UTR of *TSPAN12* gene revealed two novel (c.125T>C and c.479G>A) and one reported missense changes (c.334G>A) in six different FEVR families (tables 4.7 and 4.8, figures 4.9 and 4.10). These changes were located in exon 3, 5 and 7 of the *TSPAN12* gene (figure 4.9). Of the six families observed with the missense changes, five families had more than one affected family members (figure 4.10). These missense changes were not observed in 115 control individuals. In addition to missense changes, two novel changes in the intronic region, three nucleotide changes in the 3' UTR were also identified (figure 4.9). Intriguingly, a novel missense change c.479G>A (p.C160Y) was observed in four different FEVR families. In two of the consanguineous FEVR families, this missense change was observed in homozygous state in the probands and in heterozygous condition in their parents (figure 4.10; FEVR families 117 and 147). In addition to this missense change, the previously reported missense change c.334G>A (rs143445702) was also observed in homozygous state in the severely affected proband (figure 4.10; FEVR family 69). Other than these two missense changes, remaining all nucleotide changes were observed in heterozygous condition across all FEVR patients.

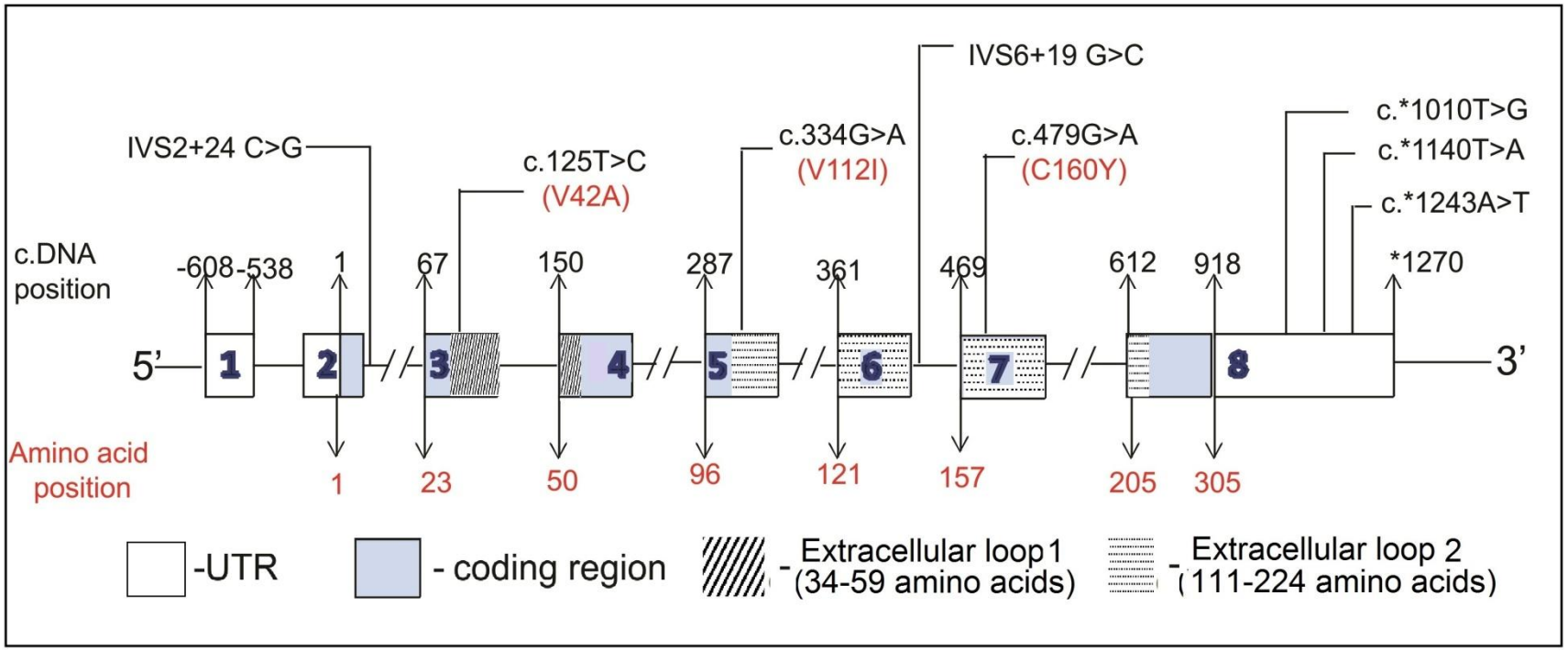

Figure 4.9: Schematic representation of the *TSPAN12* gene with identified nucleotide changes in FEVR probands. Exon numbers are indicated inside the boxes. +1 represents the transcription initiation site. cDNA positions and amino acid positions have been given by following the reference sequences NM_012338.3 and NP_036470.1 respectively.

Table 4.7: Nucleotide changes observed in *TSPAN12* gene in FEVR probands

Location in the *TSPAN12* gene	cDNA position of the nucleotide change	Amino acid change	SIFT (Score)	PolyPhen-2 (score)	Reported/ Novel	Study code of the proband	Number of probands with the nucleotide change [n=110] (frequency)	Number of controls with the nucleotide change [n=115] (frequency)
Exon3	c.125T>C	Val42Ala	Tolerated (0.14)	Benign (0.127)	Novel	140 FEVR	1 (0.009)	0
Exon5	c.334G>A	Val112Ile	Tolerated (1)	Possibly damaging (0.533)	Reported (rs143445702)	69 FEVR	1 (0.009)	0
Exon7	c.479G>A	Cys160Tyr	Damaging (0.00)	Probably damaging (1.000)	Novel	20 FEVR 78 FEVR 117 FEVR 147 FEVR	4 (0.03)	0
Exon 8 (3' UTR)	c.*1010T>G	-	-	-	Novel	95 FEVR	1 (0.009)	0
Exon 8 (3' UTR)	c.*1140T>A	-	-	-	Novel	102 FEVR	1 (0.009)	0
EXON8 (3'UTR)	c.*1243A>T	-	-	-	Reported (rs189221112)	-	10 (0.09)	17 (0.15)
Intron2	IVS2+24 C>G	-	-	-	Novel	64 FEVR	1 (0.009)	1 (0.008)
Intron6	IVS6+19 G>C	-	-	-	Novel	35 FEVR	1 (0.009)	0

cDNA positions and amino acid positions have been given by following the reference sequences NM_012338.3 and NP_036470.1 respectively. '*' represents the stop codon.

Table 4.8: Clinical features of the FEVR probands identified with nucleotide changes in the *TSPAN12* gene

Study code of the proband	cDNA position of nucleotide change	Age at initial present-ation at LVPEI (gender)	Stage of the disease/clinical features	Treatment	Outcome/ visual acuity in feet
140 FEVR	c.125T>C (missense change)	4 months (female)	OU: 5 Bilateral nystagmus along with attached retrolental membranes to the posterior capsule and funnel shaped retinal folds were observed	OU: lensectomy & vitrectomy	OU: PL
69 FEVR	c.334G>A (missense change)	24 years (male)	OU: 5 Defects in vision were reported to be present since birth. Bilateral nystagmus was observed. Falciform retinal fold was observed in the right eye. Total RD was observed in the left eye	OS: Vitrectomy & Lensectomy	OD: 20/400, OS: No PL
20 FEVR	c.479G>A (missense change)	10 years (female)	OU: 4B Bilateral squint was observed. Total RD was observed with dragged disc and epiretinal membranes in both the eyes.	No	OU: No PL
78 FEVR		16 years (female)	OD: 4A, OS:5 Decreased vision was reported to be observed since 2 years of age. In left eye total RD was observed. In right eye fibrovascular proliferations and epiretinal membranes were observed with exudative RD.	OD: BB, OS: evisceration	OD: 20/200
117FEVR		3 months (female)	OU: 5 Bilateral total RD was observed in an open funnel shape.	OD: vitrectomy & lensectomy	OU: No PL

147 FEVR	c.479G>A (missense change)	4 months (female)	OU: 5 Corneal oedema was observed in the left eye. Total RD was observed in both eyes and appeared like a closed funnel.	No	OU: No PL
95 FEVR	c.1010C>T (3' UTR change)	2 months (male)	OU: 5 Bilateral leukocoria was observed. Vitreous hemorrhage, total tractional RD and retinal fold were observed nasally in the right eye. Total closed funnel RD was observed in the left eye.	OD: Lensectomy & Vitrectomy	OD: 20/2700 OS: No PL
102 FEVR	c.*1140T>A (3' UTR change)	12 months (male)	OU: 5 Cataractous lens, neovascularization and closed funnel like RD were observed in the left eye. Total RD with epiretinal membrane was observed in the right eye.	No	OU: No PL
64 FEVR	IVS2+24 C>G (intronic change)	6 months (male)	OD: 3, OS: 5 Funnel shaped, total RD was observed in the left eye. In the right eye avascularized peripheral retina was observed with sub retinal hemorrhages and vitreous traction.	OD: LIO & BB	OD:20/40, OS: No PL
35 FEVR	IVS6+19 G>C (intronic change)	3 months (female)	OU: 4B Tractional RD with falciform retinal folds were observed in both the eyes at 3 months of age	No	OU: PL

RD: retinal detachment, OD: right eye, OS: left eye, OU: both eyes, LIO: Laser Indirect Ophthalmoscopy, PL: perception of light, BB: belt buckle, CF: counting fingers.

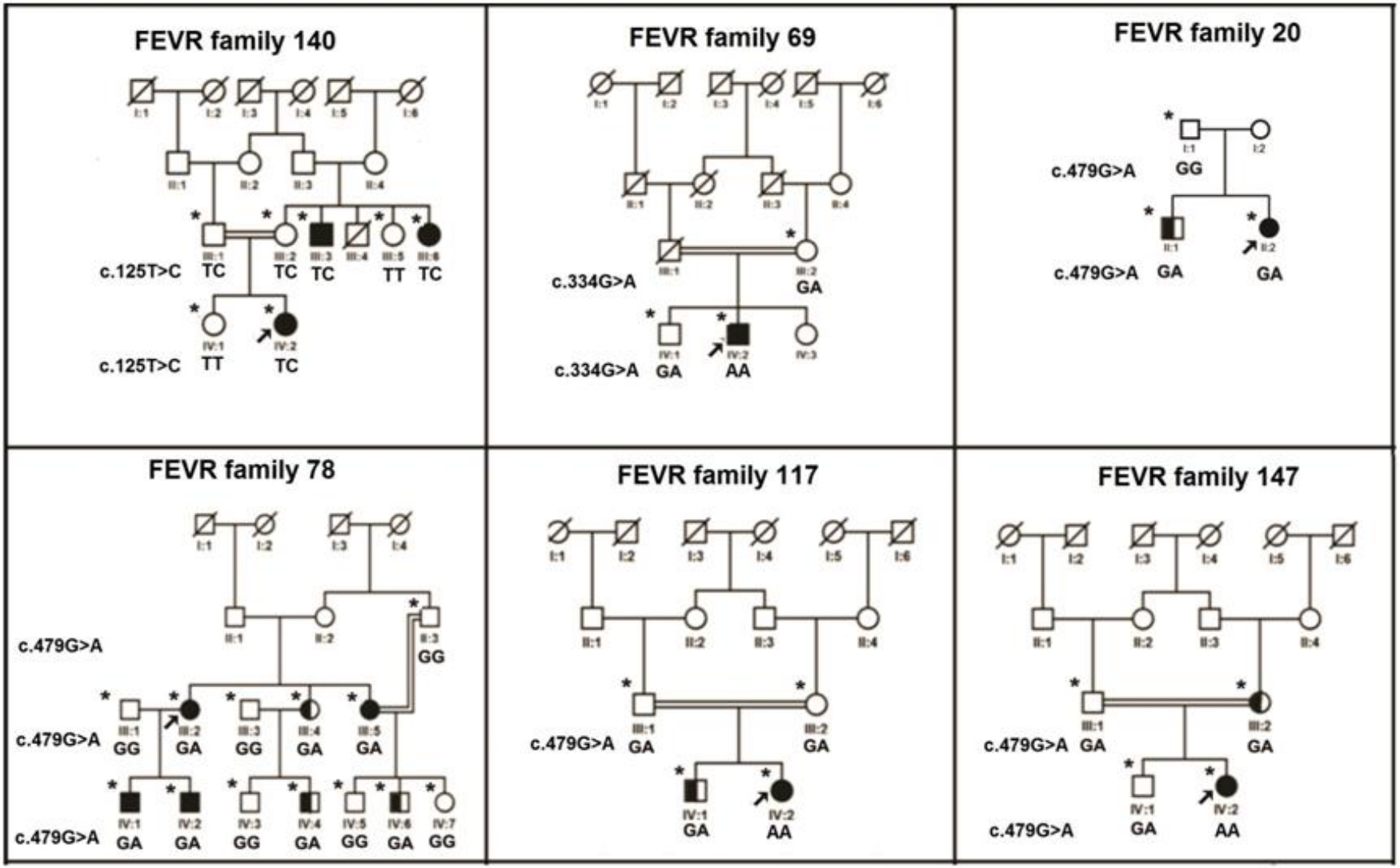
FEVR family 140
c.125T>C
TC
TC
TC
TT
TC
c.125T>C
TT
TC
FEVR family 69
c.334G>A
GA
c.334G>A
GA
AA
FEVR family 20
c.479G>A
GG
c.479G>A
GA
GA
FEVR family 78
c.479G>A
GG
c.479G>A
GG
GA
GA
GA
c.479G>A
GA
GA
GG
GA
GG
GA
GG
FEVR family 117
c.479G>A
GA
GA
GA
AA
FEVR family 147
c.479G>A
GA
GA
GA
AA
c.479G>A

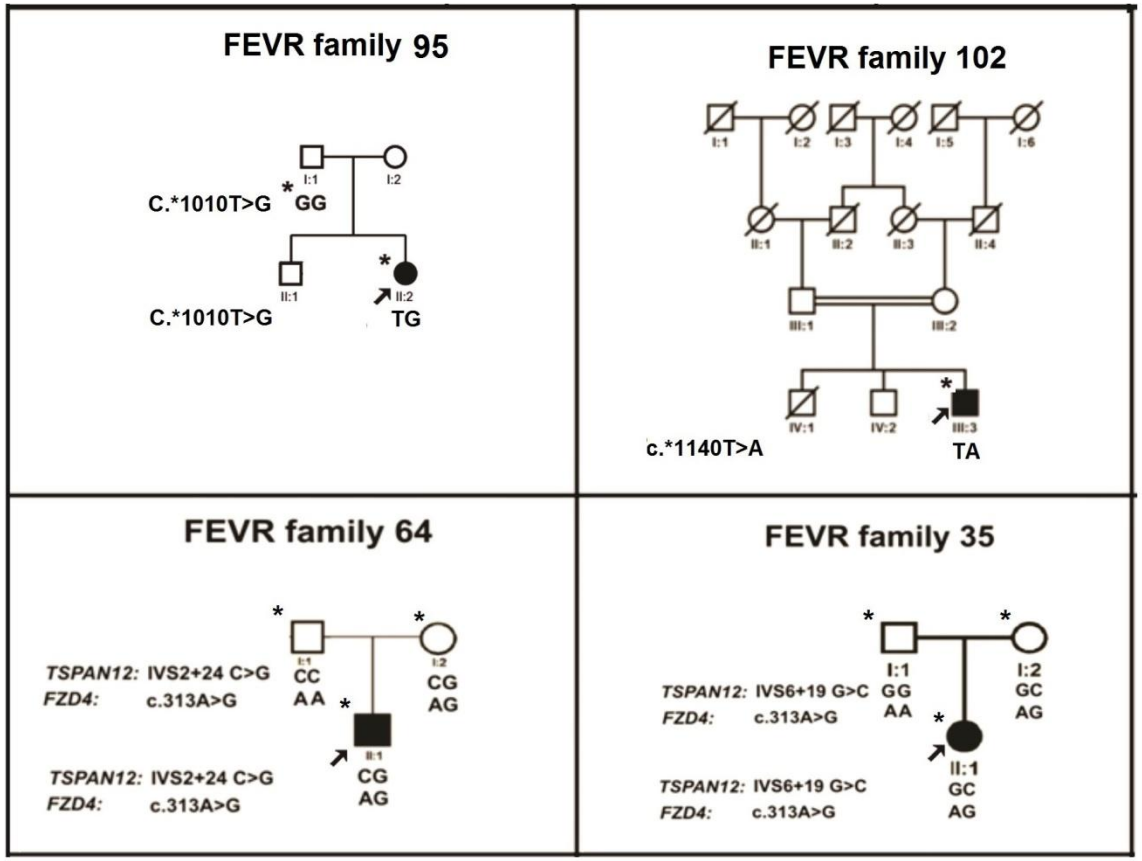

Figure 4.10: Pedigrees of the FEVR families with nucleotide changes in the *TSPAN12* gene. Completely and partially shaded symbols represent severe stages and milder stages of the disease respectively. Open symbols represent unaffected individuals. Asterisk (*) over the pedigree symbols represent the individuals screened for nucleotide changes in the TSPAN12 gene. The identified nucleotide change is represented at left side of each pedigree.

4.1.3.1 Description of nucleotide changes observed in the coding region of *TSPAN12* gene

c.125T>C (Val42Ala)

A novel, heterozygous change from thymine to cytosine at cDNA position c.125 was observed in the proband (IV: 2) of a consanguineous FEVR family 140 (figure 4.10 and figure 4.11; A). The change was not observed in 115 control individuals. This nucleotide substitution resulted in the replacement of a valine residue with alanine at amino acid position 42 of TSPAN12 protein. The proband developed bilateral total retinal detachments at 4 months of age and retained visual acuity of light perception after vitrectomy surgery in both the eyes at 6 months of age (table 4.8). The mutation was also observed in the unaffected parents (III: 1 and III: 2), severely affected maternal uncle (III: 3) and aunt (III: 6) of the proband (figure 4.10; FEVR family 140). The wild type amino acid residue located at the site of substitution was conserved across different species as evident on multiple sequence alignment (figure 4.12). However, SIFT and PolyPhen-2 scores predicted it to be a benign change. HSF analysis predicted no significant effect of this substitution on potential splice sites and splicing regulatory elements.

c.334G>A (Val112Ile)

The proband (IV: 2) of the FEVR family 69 was observed to have a previously reported SNP (rs143445702), a guanine to adenine substitution in homozygous form (figure 4.10; FEVR family 69 and figure 4.11; B). This nucleotide change resulted in the replacement of a wild type valine residue by an isoleucine residue. The change was not observed in 115 ethnically matched control individuals. The proband with this nucleotide change exhibited rhegmatogenous retinal detachment in the left eye and tractional retinal detachment in the right eye (table 4.8). The unaffected mother (III: 2) and brother (IV: 1) of the proband were also harboring this change in heterozygous state (figure 4.10; FEVR family 69) This change was previously reported in heterozygous condition in NHLBI (*National Heart, Lung and Blood Institute)* exome sequencing project with an allele frequency of 0.0004 in African-American population. SIFT analysis predicted this

change to be tolerated by the protein, while PolyPhen-2 analysis suggested it to be pathogenic. HSF analysis suggested nonharmful effect of this substitution on splice sites, splicing enhancer and suppressor elements.

c.479G>A (Cys160Tyr)

A novel guanine to adenine substitution at c.479 position was observed in the probands and affected family members of four different FEVR families (figure 4.10; FEVR families 20, 78, 117 and 147). This nucleotide substitution led to replacement of a highly conserved cysteine residue with a tyrosine residue at 160th amino acid position of TSPAN12 protein. In the probands of 117 (IV: 2) and 147 (IV: 2) FEVR families, the change was observed in homozygous condition, whereas in the probands of 20 (II: 2) and 78 (III: 2) FEVR families, the substitution was observed in heterozygous condition (figure 4.11; C and D). Two of these probands (117 and 147) exhibited bilateral total retinal detachments at less than 6 months of age (table 4.8). The probands of FEVR family 20 and 78 were observed with nonrhegmatogenous retinal detachments in both the eyes during their first examination in our hospital at 10 and 16 years of age respectively (table 4.8).

The FEVR families 117 and 147 showed autosomal recessive inheritance pattern of the disease. In homozygous state of the mutated allele, the probands exhibited severe disease phenotype compared to mild disease or normal phenotype in heterozygous family members (table 4.8). The brother (IV: 1) of the 117 FEVR proband and mother (III: 2) of the 147 FEVR proband was carrying the mutation in heterozygous condition and exhibited avascularized peripheral retina in both the eyes (figure 4.10; FEVR families 117 and 147). Though, the change was observed in heterozygous condition in the proband's fathers (III: 1) of these two families and brother (IV: 1) of the 147 proband, they were phenotypically normal under ophthalmoscopic examination (figure 4.10; FEVR families 117 and 147).

In contrast to previously described two families, in 20 and 78 FEVR families autosomal dominant inheritance pattern was observed. All the affected members of these families were observed with the nucleotide change in heterozygous condition (figure 4.11; C).

Though, the mutation was segregated with the disease phenotype in all the affected members of these two families, variable disease progression and ocular phenotypes were observed among different family members. In FEVR family 20, the brother (II: 1) of the proband was harboring the change and exhibited mild disease phenotype (figure 4.10; FEVR family 20). The father (I: 1) of the proband was phenotypically and genotypically normal, whereas the mother (I: 2) was unavailable for both ocular and genetic testing (figure 4.10; FEVR family 20). In 78 FEVR family, seven affected family members were observed with variable ocular phenotypes ranging from avascular peripheral retina and neovascularization to complete retinal detachments (figure 4.10; FEVR family 78). In multiple sequence alignment the wild type cysteine residue was highly conserved across different species (figure 4.12) and predicted to be pathogenic in SIFT and PolyPhen-2 analysis.

4.1.3.2 Description of nucleotide changes observed in the 3' untranslated region of *TSPAN12* gene

Two novel 3' UTR changes c.*1010T>G and c.*1140T>A were observed in two different sporadic cases of 95 and 102 FEVR families respectively (figure 4.10; FEVR families 95 and 102 and figure 4.11; E and F). The probands with these changes exhibited bilateral total retinal detachment within the first year after their birth (table 4.8). These variations were not observed in 115 control individuals. The parents of these two probands were phenotypically normal, whereas their genetic status was not known due to the unavailability of their DNA samples. Due to the location of these variations in noncoding region, we are unable to predict the effect of these variations. In addition to these two variations, a reported SNP c.*1243A>T (rs189221112) was observed in heterozygous state in ten FEVR probands and 17 control individuals (figure 4.11; G).

4.1.3.3 Description of nucleotide changes observed in the intronic region of *TSPAN12* gene

Two novel intronic changes IVS2+24 C>G and IVS6+19 G>C were observed in heterozygous condition in two different probands of FEVR families 64 and 35 respectively (figure 4.11; H and I). In addition to these intronic changes, M105V mutation of *FZD4* gene was also observed in these two probands (figure 4.10; FEVR families 64 and 35). In both the cases, the unaffected proband's mothers (I: 2) were also carrying the two changes in heterozygous condition (figure 4.10; FEVR families 64 and 35). The IVS6+19 G>C variation was not observed in 115 control individuals, whereas the IVS2+24 C>G change was observed in one control individual (table 4.7). In HSF analysis, these intronic variations did not show significant effect on splice enhancer, suppressor and potential splice sites. Based on this information we speculated that the M105V change was mainly responsible for development of ocular features in these probands. However, further functional studies are required to confirm the effect of these variations.

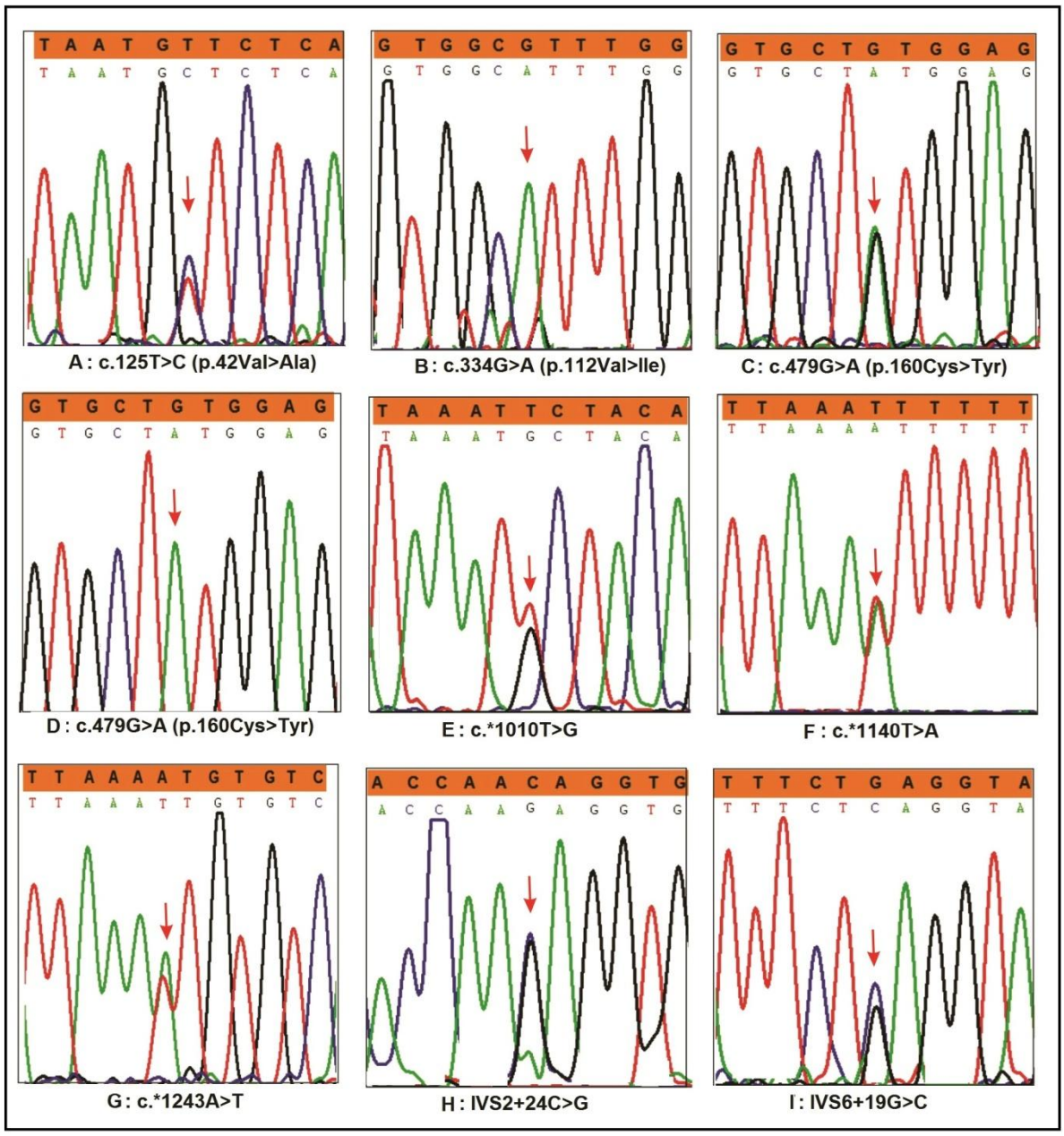

Figure 4.11: Electropherograms representing identified nucleotide changes in *TSPAN12* gene. The sequence above the electropherogram in the shaded portion represents the wild type sequence. The arrow head indicates the site of nucleotide change. A) A heterozygous substitution of GTT>GCT at c.125 position resulted in the Val42Ala amino acid change. B) A heterozygous substitution of GTT>ATT at c.334 position resulted in the Val112Ile amino acid change. C) A heterozygous substitution of

TGT>TAT at c.479 position resulted in the Cys160Tyr amino acid change. D) A homozygous substitution of TGT>TAT at c.479 position resulted in the Cys160Tyr amino acid change. E) A heterozygous thymine to guanine change after 1009 base pairs of stop codon in 3' UTR. F) A heterozygous thymine to adenine change at c.*1140 position in 3' UTR. G) A heterozygous adenine to thymine change at c.*1243 position in 3' UTR. H) A heterozygous cytosine to guanine change in the second intronic sequence after 23 base pairs of splice donor site. I) A heterozygous guanine to cytosine change in the sixth intronic sequence after 18 base pairs of splice donor site.

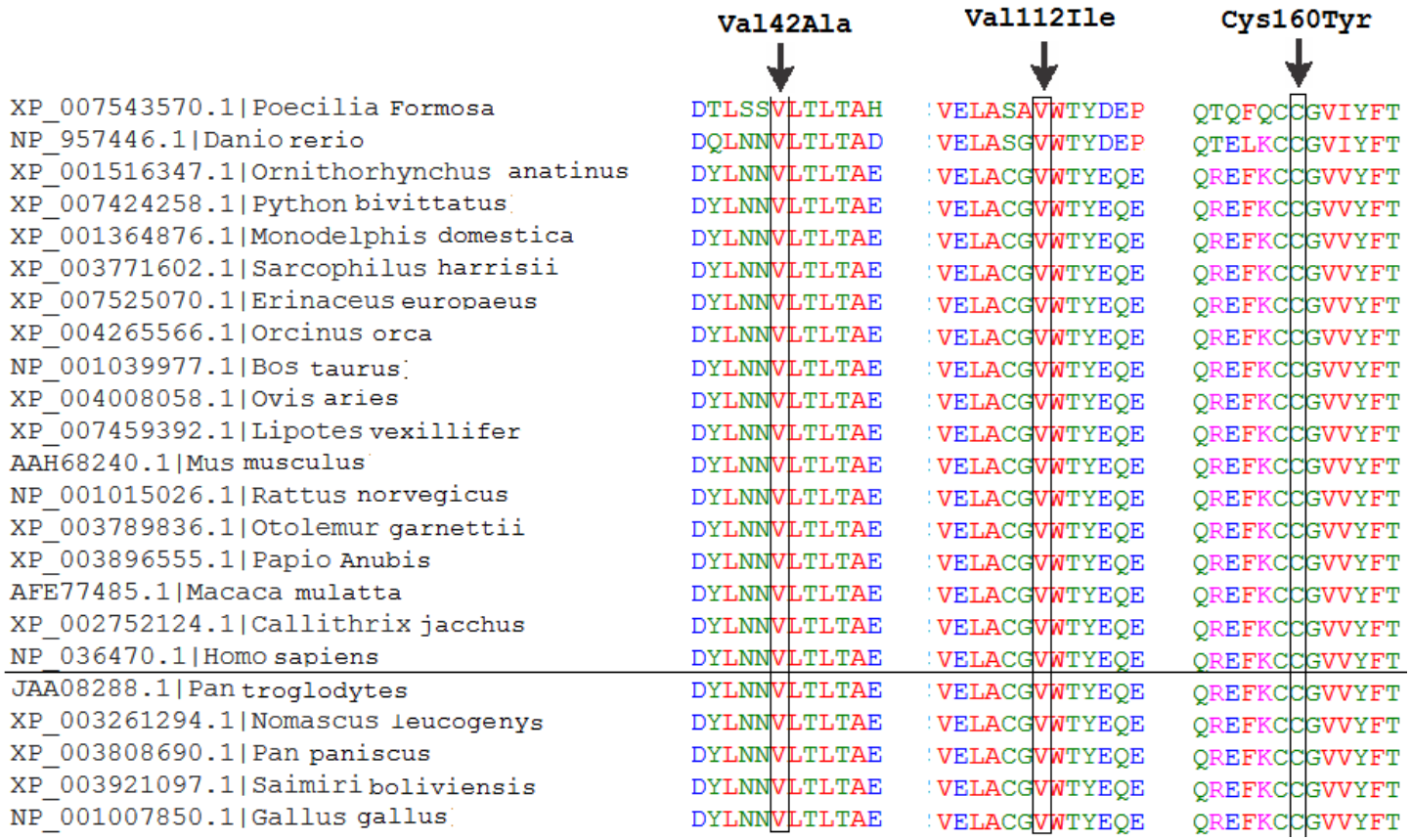

Figure 4.12: Multiple sequence alignment showing the conservation of wild type residues in respect to identified missense changes in TSPAN12 protein across various species. The human TSPAN12 protein sequence is underlined. Accession numbers (NCBI) and name of the species are mentioned at the left side of the picture.

4.1.4 *ZNF408* gene analysis

The five exons of *ZNF408* gene including intron-exon boundaries and UTR regions were screened. Eleven different nucleotide changes were observed, of which eight changes were novel (tables 4.9 and 4.10, figures 4.13 and 4.14). These changes included four missense changes, two synonymous substitutions, three polymorphisms and two 5' UTR nucleotide changes (table 4.9). The nucleotide changes were observed in all exons except third exon (figure 4.13). Some of the nucleotide changes including a missense change, one synonymous change and three polymorphisms were also observed in control individuals (table 4.9). Except for the two polymorphisms (figure 4.15; D and H), all the changes were observed in heterozygous condition across all the FEVR probands.

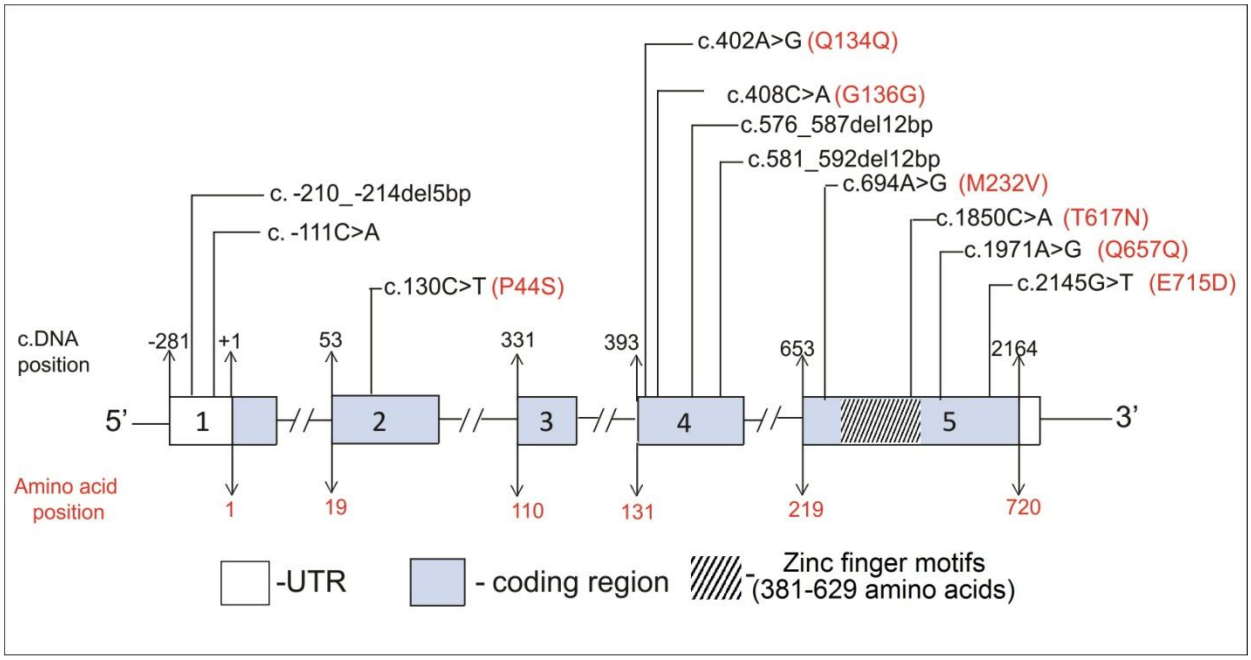

Figure 4.13: Schematic representation of *ZNF408* gene with identified nucleotide changes in FEVR probands. +1 represents the transcription initiation site. cDNA positions and amino acid positions have been given by following the reference sequences NM_024741.2 and NP_079017.1 respectively.

Table 4.9: Nucleotide changes observed in the *ZNF408* gene in FEVR probands

Location in the *ZNF408* gene	cDNA position of the nucleotide change	Amino acid change	SIFT (score)	PolyPhen-2 (score)	Reported/ Novel	Study code of the proband	Number of probands with the nucleotide change [n=110] (frequency)	Number of controls with the nucleotide change [n=115] (frequency)
Exon 2	c.130C>T	Pro44Ser	Damaging (0.01)	Benign (0.062)	Novel	95 FEVR	1 (0.009)	0.00
Exon 4	c.402A>G	Gln134Gln	-	-	Novel	70 FEVR	1 (0.009)	0.00
	c.408C>A	Gly136Gly	-	-	Novel	-	10 (0.09)	1 (0.008)
	c.576_587 del12bp	Val193_Glu196del	-	-	Reported (rs148055528)	-	3 (0.027)	15 (0.13)
	c.581_592 del12bp	Val194_Val197del	-	-	Reported (rs72461400)	-	32 (0.29)	26 (0.22)
Exon 5	c.694A>G	Met232Val	Tolerated (0.6)	Benign (0.00)	Novel	51 FEVR	1 (0.009)	0.00

Location in the *ZNF408* gene	cDNA position of the nucleotide change	Amino acid change	SIFT (score)	PolyPhen-2 (score)	Reported/ Novel	Study code of the proband	Number of probands with the nucleotide change [n=110] (frequency)	Number of controls with the nucleotide change [n=115] (frequency)
Exon5	c.1850C>A	Thr617Asn	Tolerated (0.23)	Probably damaging (0.966)	Novel	135 FEVR	1 (0.009)	1 (0.008)
	c.1971A>G	Gln657Gln	-	-	Reported (rs376536252)	43 FEVR	1 (0.009)	1 (0.008)
	c.2145G>T	Glu715Asp	Damaging (0.05)	Probably damaging (0.966)	Novel	82 FEVR	1 (0.009)	0.00
5' UTR	c. -210_-214del5bp	-	-	-	Novel	3 FEVR	1 (0.009)	0.00
	-111C>A	-	-	-	Novel	86 FEVR 114 FEVR	2 (0.018)	0.00

cDNA positions and amino acid positions have been given by following the reference sequences NM_024741.2 and NP_079017.1 respectively. '*' represents the stop codon.

Table 4.10: Clinical features of the FEVR probands identified with nucleotide changes in the *ZNF408* gene

Study code of the proband	cDNA position of nucleotide change	Age at initial present-ation at LVPEI (gender)	Stage of the disease/clinical features	Treatment	Outcome/ visual acuity in feet
95 FEVR	c.130C>T (missense change)	2 months	OU:5 Bilateral vitreous hemorrhage, closed funnel RD and leukocoria were observed.	OD: Lensectomy & Vitrectomy	OD: No PL OS: No PL
70 FEVR	c.402A>G (synonymo-us change)	1 year	OU: 5 White reflex in both eyes were noted since 3 months of age. Shallow anterior chamber, posterior synechiae, closed funnel RD and intraocular hemorrhage were observed in the right eye. Corneal scar, flat anterior chamber and closed funnel RD were observed in the left eye.	No	OU: No PL
51 FEVR	c.694A>G (missense change)	35 years	OD:4B, OS:5 Progressive visual loss noted since 3 years of age. Macular fold with subretinal exudates, avascular retina and vitreous condensation were observed in the right eye. Neovascularization and closed funnel RD were observed in the left eye.	No	OD: CF 1Meter OS: No PL
135 FEVR	c.1850C>A (missense change)	2 months	OU: 5 White reflex in both eyes noted since birth. Bilateral shallow anterior chambers with closed funnel RD were observed.	No	OU: No PL
43 FEVR	c.1971A>G (synonymo-us change)	8 months	OU: 5 White reflex in both eyes noted since birth. Closed funnel RD was observed in the right eye. Open funnel RD with avascular retina was observed in the left eye.	No	OU: No PL

82 FEVR	c.2145G>T (missense change)	1 year	OD: 5, OS: 4B White reflex and poor vision noted at 4 months of age. Flat anterior chamber and closed funnel RD was observed in the right eye. Radial retinal fold with subretinal exudates, vitreous condensation and avascular retina were observed in the left eye.	No	OD: No PL, OS: PL
3 FEVR	c. -210_-214del5bp (5' UTR change)	10 years	OD 4B; OS 4B Bilateral peripheral avascular retina, neovascularization and exudative RD were observed. In the right eye, peripheral retinal breaks were also observed.	OD: LIO & BB	OD: No PL OS: No PL
86 FEVR	-111C>A (5' UTR change)	3 years	OU: 5 Bilateral congenital leukocoria, nystagmus and closed funnel RD were observed.	No	OU: PL
114 FEVR		46 years	OD: 2A, OS: 5 Poor vision was noted since 3 years of age. Avascular retinal periphery, vitreous condensation and straightening of arcades were observed in the right eye. Phthisis bulbi with total RD were observed in the left eye	OD: LIO	OD: 20/20 OS: No PL

RD: retinal detachment, OD: right eye, OS: left eye, OU: both eyes, LIO: Laser Indirect Ophthalmoscopy, PL: perception of light, BB: belt buckle, CF: counting fingers.

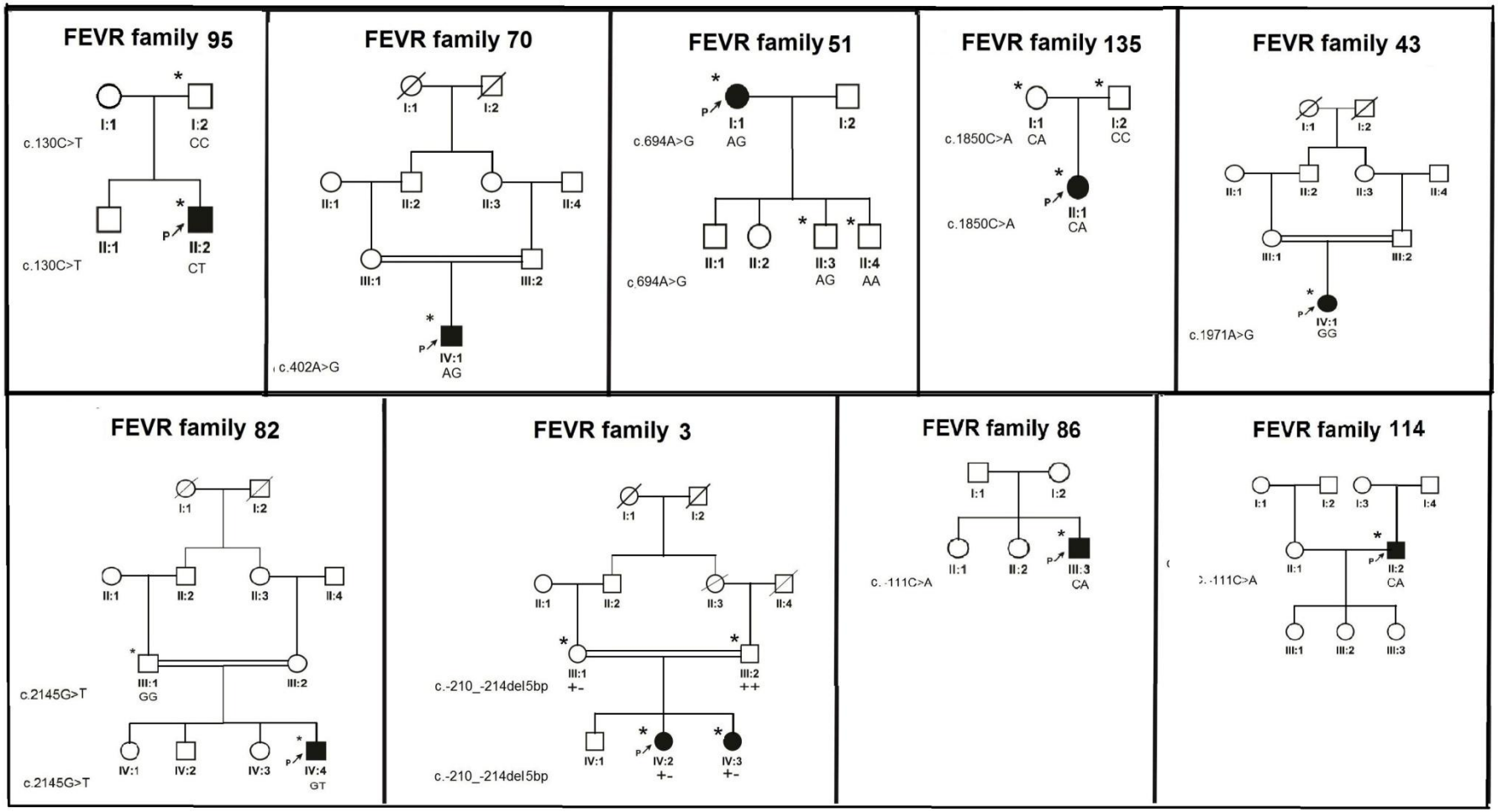

Figure 4.14: Pedigrees of the FEVR families with nucleotide changes in *ZNF408* gene. Completely shaded symbols represent severe stages of the disease. Open symbols represent unaffected individuals. Asterisk (*) over the pedigree symbols represent the individuals screened for nucleotide changes in *ZNF408* gene. - indicates the presence of deletion and + indicates the wild type allele. The identified nucleotide change is represented left side of each pedigree.

4.1.4.1 Description of nucleotide changes observed in the coding region of *ZNF408* gene

c.130C>T (Pro44Ser)

A novel, heterozygous, cytosine to thymine change was observed at position c.130 in a male, index proband (II: 2) of FEVR family 95 (figure 4.14 and figure 4.15; A). The substitution led to replacement of a proline residue with serine at amino acid position 44 of the ZNF408 protein. The proband had bilateral total retinal detachments with retrolental membranes at 2 months of age (table 4.10). The father of the proband (figure 4.14; FEVR family 95; I: 2) was found to be normal both phenotypically and genotypically while the unaffected proband's mother (figure 4.14; FEVR family 95; I: 1) remained unavailable for genetic analysis. This change was not observed in 115 control individuals. Multiple sequence alignment showed that the wild type proline residue was highly conserved across different species (figure 4.16). SIFT analysis predicted for the damaging effect of this substitution on the protein function. In contrast, PolyPhen-2 analysis suggested it to be of benign nature. HSF analysis suggested nonharmful effect of this substitution either on splice sites or splicing regulatory elements.

c.402A>G (Gln134Gln)

A novel, heterozygous adenine to guanine change was observed at position c.402 in an index, male proband (IV: 1) of consanguineous FEVR family 70 (figure 4.14 and figure 4.15; B). This nucleotide change resulted in the replacement of a codon CAA to CAG at amino acid position 134 of ZNF408 protein. Both the wild type and altered codon encoded for the same amino acid glutamine. The proband with this nucleotide change had bilateral total retinal detachment at 12 months of age (table 4.10). The mother and father (figure 4.14; FEVR family 70; III: 1 and III: 2) of the proband were phenotypically normal. This change was not observed in 115 control individuals. In HSF analysis, no significant effect of this substitution was observed in splice sites and splicing regulatory elements.

c.408C>A (Gly136Gly)

Another novel, heterozygous, synonymous variation c.408C>A (figure 4.15; C) resulted in the codon change GGC to GGA at 136 amino acid position of ZNF408 was observed in ten different FEVR probands. Both the wild type and altered codon encoded for the amino acid residue glycine. This nucleotide change was also observed in heterozygous condition, in one of the 115 control individuals screened for this variation (table 4.9). The probands with this nucleotide change exhibited subtotal or total retinal detachments in both the eyes. HSF analysis predicted that neither splice sites nor splicing regulatory elements were affected by this nucleotide change.

c.576_587del12bp (Val193_Glu196del)

A reported 12 base pair deletion (rs148055528) at cDNA position c.576_587 was observed in homozygous condition (figure 4.15; D) in the probands of three different FEVR families (24, 90 and 115). The deletion resulted in the removal of four amino acid residues from valine 193 to glutamic acid 196 of the ZNF408 protein. The deletion was also observed in homozygous condition in 15 of the 115 control individuals (table 4.9). The presence of this deletion in normal individuals suggested the non-pathogenic nature of this deletion.

c.581_592del12bp (Val194_Val197del)

Another known, heterozygous 12 base pair deletion (rs72461400) at position c.581_592 was observed in the probands of 32 different FEVR families (figure 4.15; E). The deletion was also observed in 26 control individuals (table 4.9). Similar to the previously described deletion, this variation also led to removal of four codons from amino acid position 194 to 197 of the open reading frame. The presence of this deletion with a similar frequency in both the patients (0.28) and control subjects (0.22) indicating the non-pathogenic nature of the deletion.

c.694A>G (Met232Val)

A novel, heterozygous, adenine to guanine substitution was observed at position c.694 in the severely affected female proband (I: 1) of a FEVR family 51 (figure 4.14 and figure 4.15; F). The substitution led to replacement of a methionine residue with a valine at 232 amino acid position of ZNF408 protein. The substitution was also identified in one unaffected son of the proband (figure 4.14; FEVR family 51; II: 3) but not observed in any of the 115 control individuals. In multiple sequence alignment, it was observed that the wild type methionine residue was less conserved across different species. The presence of valine residue was observed instead of methionine at 232 position of ZNF408 in different vertebrate species (figure 4.16). Both SIFT and PolyPhen-2 analysis predicted the mutation to be nonharmful on protein function. In addition to this mutation, Met157Thr mutation in *FZD4* gene was also observed in the proband. Though, both these mutations were predicted as non-pathogenic by SIFT and PolyPhen-2 analysis, the mild effect of these mutations synergistically might be responsible for development of ocular features in the proband.

c.1850C>A (Thr617Asn)

In an index, female proband (II: 1) of FEVR family 135, a novel cytosine to adenine substitution was observed in heterozygous condition at c.1850 position (figure 4.14 and figure 4.15; G). This nucleotide change resulted in the substitution of threonine residue by asparagine at 617 amino acid position of *ZNF408* protein. This change was also found in the unaffected mother of the proband (figure 4.14; FEVR family 135; I: 1) along with a control. Though, this change was located in a highly conserved region of the protein, the presence of alanine residue was observed instead of a threonine in bovine (Bos *taurus*) ZNF408. SIFT analysis predicted that this amino acid change was tolerated by the protein, whereas it was found to have a damaging affect on PolyPhen-2 analysis. HSF analysis suggested nonharmful effect of this substitution on potential splice sites and splicing regulatory elements.

c.1971A>G (Gln657Gln)

A known synonymous substitution c.1971A>G (rs376536252) was observed in homozygous condition in a female proband (IV: 1) of FEVR family 43 (figure 4.14 and figure 4.15; H). This variation led to replacement of a codon CAA into CAG at 657 amino acid position of ZNF408 protein. Both the wild type and mutated codons encoded for the amino acid residue glutamine. The proband with this nucleotide change had bilateral total retinal detachment at 8 months of age (table 4.10). Previously, this variation was reported in heterozygous condition in NHLBI exome sequencing project with an allele frequency 0.0001 in European-American population. In the present study, one control individual was observed with this change in heterozygous condition (table 4.9). HSF analysis predicted no significant effect of this substitution either on potential splice sites or splicing regulatory elements.

c.2145G>T (Glu715Asp)

At cDNA position c.2145, a novel guanine to thymine change was observed in heterozygous condition in an index proband (IV: 4) of FEVR family 82 (figure 4.14 and figure 4.15; I). This nucleotide change resulted in the replacement of a glutamic acid residue with aspartic acid at 715 position of ZNF408 protein. The proband exhibited total retinal detachment in the right eye and subtotal retinal detachment including macula in the left eye at one year of age (table 4.10). Both parents (figure 4.14; FEVR family 82; III: 1 and III: 2) of the proband were phenotypically normal with complete vascularization of the retina by ophthalmoscope. Both SIFT and PolyPhen-2 analysis indicated the damaging effect of the mutation on protein function. HSF analysis predicted nonharmful effect of this substitution on splice sites and splicing regulatory elements.

4.1.4.2 Description of nucleotide changes observed in the 5' untranslated region of *ZNF408* gene

c. -210_-214delGAATC

A novel, heterozygous 5 base pair deletion at position c. -210_-214 was observed in the proband (IV: 2) of a consanguineous FEVR family 3 (figure 4.14 and figure 4.15; J). The proband had total retinal detachment in both the eyes at 10 years of age (table 4.10). The deletion was also observed in heterozygous condition in a severely affected female sibling (figure 4.14; FEVR family 3; IV: 3) and unaffected mother (figure 4.14; FEVR family 3; III: 2) of the proband. The deletion was located 16 base pairs upstream from the transcription start site and not observed in 115 control individuals. MatInspector analysis found no transcription factor binding sites at this location.

c. -111C>A

A novel, cytosine to adenine change at position c.-111 was observed in heterozygous condition in two index probands of FEVR families 86 and 114 (figure 4.15; K). The proband (III:3) of FEVR family 86 (figure 4.14) had bilateral total retinal detachments at 3 years of age (table 4.10). The proband (II: 2) of FEVR family 114 (figure 4.14) was observed with a subtotal retinal detachment in the right eye and a complete retinal detachment in the left eye (table 4.10). This substitution was not found in 115 control individuals. MatInspector analysis predicted the disruption of a PAX6 transcription factor binding site by this substitution in the promoter region of *ZNF408* gene.

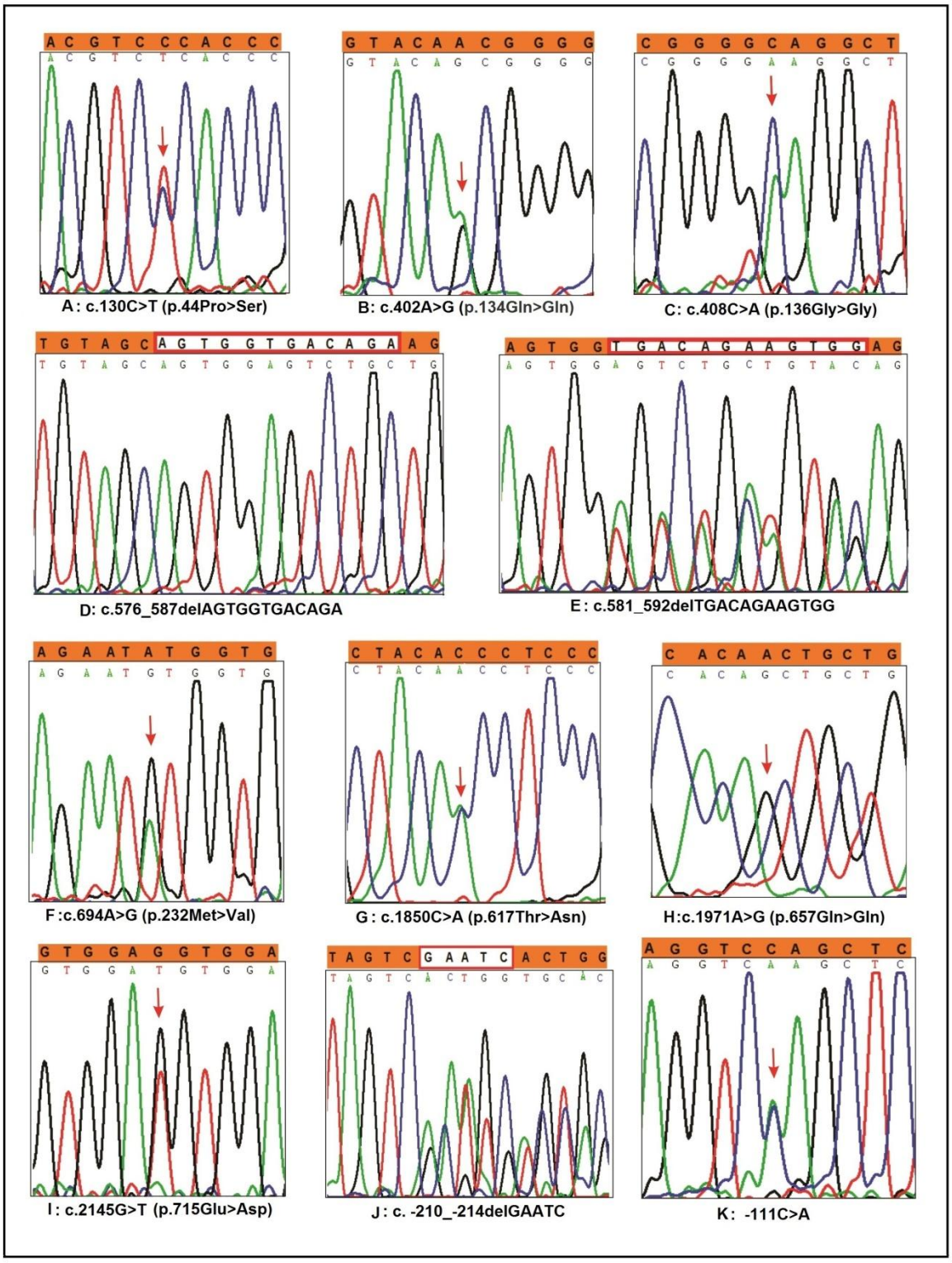
A : c.130C>T (p.44Pro>Ser)
B: c.402A>G (p.134Gln>Gln)
C: c.408C>A (p.136Gly>Gly)
D: c.576_587delAGTGGTGACAGA
E : c.581_592delTGACAGAAGTGG
F :c.694A>G (p.232Met>Val)
G : c.1850C>A (p.617Thr>Asn)
H:c.1971A>G (p.657Gln>Gln)
I : c.2145G>T (p.715Glu>Asp)
J : c. -210_-214delGAATC
K: -111C>A

Figure 4.15: Electropherograms representing identified nucleotide changes in the *ZNF408* gene in FEVR patients. The sequence above the electropherogram in the shaded portion represents the wild type sequence. The arrow head indicates the site of nucleotide change. A) A heterozygous substitution of CCA>TCA at c.130 position resulted in the Pro44Ser amino acid change. B) A heterozygous substitution of CAA>CAG at c.402 position resulted in a synonymous Gln134Gln amino acid change. C) A heterozygous substitution of GGC>GGA at c.408 position resulted in a synonymous Gly136Gly amino acid change. D) A homozygous 12 base pair deletion at c.576_587 position resulted in the removal of four amino acid residues from amino acid position 193 to 196 of ZNF408 protein. Deleted nucleotides have shown in white color box. E) A heterozygous 12 base pair deletion at c.581_592 position resulted in the removal of four amino acid residues from amino acid position 194 to 197 of ZNF408 protein. Deleted nucleotides have shown in white color box. F) A heterozygous substitution of ATG>GTG at c.694 position resulted in the Met232Val amino acid change. G) A heterozygous substitution of ACC>AAC at c.1850 position resulted in the Thr617Asn amino acid change. H) A homozygous substitution of CAA>CAG at c.1971 position resulted in the Gln657Gln amino acid change. I) A heterozygous substitution of GAG>GAT at c.2145 position resulted in the Glu715Asp amino acid change. J) A heterozygous 5 base pair (GAATC) deletion at c.-210_214 position in 5' UTR. Deleted nucleotides have shown in white color box. K) A heterozygous cytosine to adenine substitution identified at c.-111 position in 5' UTR.

Figure 4.16: Multiple sequence alignment showing the conservation of wild type residues in respect to identified missense changes in ZNF408 protein across various species. The human ZNF408 protein sequence is underlined. Accession numbers (NCBI) and name of the species are mentioned at the left side of the picture

4.2. Overall involvement of the candidate gene mutations in Indian FEVR patients

Of the four candidate genes screened (*NDP, FZD4, TSPAN12* and *ZNF408*), we identified the mutations in 26.3% of the FEVR probands. Compared to remaining candidate genes, *NDP* gene mutations were observed in a higher number of probands (9%). Next to the *NDP*, *FZD4* and *TSPAN12* gene mutations were involved in 8.1% and 5.4% of the FEVR probands respectively. *ZNF408* mutations were involved in a less number of FEVR probands (3.6%).

Familial exudative vitreoretinopathy (FEVR) is a rare, proliferative vascular disorder of the retina. Five genes (*NDP, FZD4, LRP5, TSPAN12* and *ZNF408*) have been identified as candidates for the disorder by linkage analysis in large FEVR families and targeted exome sequencing in FEVR patients (Chen *et al.*, 1993; Robitaille *et al.*, 2002; Toomes *et al.*, 2004a; Nikopoulos *et al.*, 2010a; Collin *et al.*, 2013). Interestingly, four of the five known candidate genes (*NDP, FZD4, LRP5* and *TSPAN12*) are involved in formation of ligand-receptor complex in Norrin-FZD4 signaling pathway and responsible for retinal angiogenesis (Junge *et al.*, 2009). The role of the recently identified *ZNF408* gene in Norrin-FZD4 signaling pathway is not yet understood. While the role of these genes in disease development has been well studied in Caucasian, Chinese and Japanese FEVR patients, till date, there is only a single report on mutation screening in *FZD4* gene from a relatively smaller south Indian FEVR cohort (n=53) (Nallathambi *et al.*, 2006). Therefore, the present study attempted to unravel the role of *NDP, FZD4, TSPAN12* and *ZNF408* genes in disease pathogenesis and their mutation spectrum in a large cohort of 110 Indian FEVR patients. The knowledge about the role of different candidate genes in disease development and their mutation spectrum would be helpful in genetic counseling and prenatal diagnosis of the disease respectively.

The screening of *NDP, FZD4, TSPAN12* and *ZNF408* candidate genes led to the identification of 22 potentially pathogenic mutations in 26.3% (29/110) of the FEVR probands in the coding region of these genes. In addition to these mutations, two novel synonymous changes, two small base pair deletions and a nucleotide substitution in the 5' UTR, four novel single nucleotide substitutions in the 3' UTR, 2 intronic changes and 8 reported polymorphisms were observed (table 5.1). The identified polymorphisms were observed with similar frequencies in both the probands and controls with no association to the disease phenotype (table 5.2). The clinical features of the patients identified with the nucleotide changes varied from avascularized peripheral retina with or without neovascularization, retinal hemorrhages and exudation to subtotal or total retinal detachments. Irrespective of the candidate gene involved, all the FEVR probands identified with the mutations/variations exhibited classical clinical features of the FEVR without any specific genotype-phenotype correlation. Similar to the previous reports on genetic analysis of the FEVR, the present study identified variable disease phenotype

among different FEVR probands and their family members even with the same mutation in the candidate genes (Toomes *et al.*, 2004b; Boonstra *et al.*, 2009; Nikopoulos *et al.*, 2010b). Notably, incomplete penetrance was also observed for some of the mutations identified in the present study as described in previous mutation reports on FEVR patients (Toomes *et al.*, 2004b; Boonstra *et al.*, 2009; Nikopoulos *et al.*, 2010b)

Table 5.1: Frequencies of the FEVR probands identified with different types of nucleotide changes in the present study

Types of nucleotide changes identified in the present study	Number of mutations/variations	Frequency of the FEVR probands (%)
Missense changes	15	20 (22/110)
Deletions	7	7.2 (8/110)
Insertions	1	0.9 (1/110)
Nonstop change	1	0.9 (1/110)
Intronic changes	2	0.9 (2/110)
Synonymous changes	2	0.9 (1/110)
UTR variations	5	5.4 (6/110)
Reported polymorphisms	8	38 (42/110)

Table 5.2: Frequencies of the reported polymorphisms observed in the present study in FEVR probands and control individuals

Gene (polymorphisms)	Genotype	Frequency (%) in FEVR probands	Frequency (%) in control individuals
NDP (rs45501198 G>T)	GT	0.9 (1/110)	0
FZD4 (rs61735303 C>T)	CT	0.9 (1/110)	0.8 (1/115)
FZD4 (rs201168680 C>T)	CT	2.7 (3/110)	2.6 (3/115)
TSPAN12 (rs41622 C>T)	CT	14.5 (16/110)	14.7 (17/115)
TSPAN12 (rs189221112 A>T)	AT	9 (10/110)	14.7 (17/115)
ZNF408 (rs148055528; c.576_587del12bp)	--	2.7 (3/110)	13 (15/115)
ZNF408 (rs72461400; c.581_592del12bp)	+-	29 (32/110)	22.6 (26/115)
ZNF408 (rs376536252; A>G)	GG	0.9 (1/110)	0.8 (1/115)

'-' represents the deleted allele and '+' indicates the wild type allele

The total frequency (26.3%) of the FEVR probands identified with the mutations in the coding region of *NDP*, *FZD4*, *TSPAN12* and *ZNF408* genes in the present study was comparable to the FEVR patients reported from Chinese and Japanese population (table 5.3). In Caucasian, Chinese and Japanese FEVR patients, the mutations in the known candidate genes accounted for less than 50% of the FEVR cases (table 5.3) (Kondo *et al.*, 2003; Toomes *et al.*, 2004a; Toomes *et al.*, 2004b; Qin *et al.*, 2005; Kondo *et al.*, 2007a; Boonstra *et al.*, 2009; Kondo *et al.*, 2011; Yang *et al.*, 2011; Yang *et al.*, 2012a; Yang *et al.*, 2012b; Collin *et al.*, 2013). This suggest for the involvement of other unidentified candidate genes in disease pathogenesis.

Table 5.3: Frequencies of FEVR patients with mutations in the coding region of known candidate genes from different ethnic groups

Ethnicity	Frequency (%) of the FEVR probands with mutations						
	NDP	***FZD4***	***TSPAN12***	***ZNF408***	***LRP5***	**Total**	**Reference**
Caucasian	5.7 (n=52)	17.5 (n=40)	10 (n=70)	2.5 (n=79)	18.7 (n=32)	55.4	(Toomes *et al.*, 2004a; Toomes *et al.*, 2004b; Wu *et al.*, 2007; Poulter *et al.*, 2010; Poulter *et al.*, 2012; Collin *et al.*, 2013)
Japanese	6.4 (n=62)	8.7 (n=80)	4.4 (n=90)	1.8 (n=55)	12.5 (n=56)	33.8	(Kondo *et al.*, 2003; Qin *et al.*, 2005; Kondo *et al.*, 2007a; Kondo *et al.*, 2011)
Chinese	0 (n=38)	12.2 (n=49)	6.12 (n=49)	NR	10 (n=49)	28.4	(Yang *et al.*, 2011; Yang *et al.*, 2012a; Yang *et al.*, 2012b)
Indian	9 (n=115)	8.1 (n=115)	5.4 (n=115)	3.6 (n=115)	NR	26.3	Present study

NR: No reports; 'n' represents number of probands analyzed in the study.

To the best of our knowledge, this is the first study from India on mutation screening in *NDP, FZD4, TSPAN12* and *ZNF408* genes in a large cohort of Indian FEVR patients. The present study provides an extensive baseline data on mutation spectrum for these genes in Indian patients in order to better understand their role in disease pathogenesis and for better diagnosis and prognosis.

5.1 *NDP* gene screening

The mutations in *NDP* gene were reported to be responsible for X-linked FEVR. *NDP* gene mutations had been reported in Caucasian and Japanese FEVR patients with a frequency ranges from 6% to 10% (Dickinson *et al.*, 2006; Drenser *et al.*, 2006; Kondo *et al.*, 2007a; Wu *et al.*, 2007; Boonstra *et al.*, 2009). In the present study, *NDP* gene mutations in the coding region were identified in 9% (10/110) of the FEVR patients, which was comparable to previous studies (table 5.4). Previously, 14 different missense mutations and a 3' UTR change had been reported in *NDP* gene in FEVR patients (table 2.5) (Shastry *et al.*, 1997; Dickinson *et al.*, 2006; Drenser *et al.*, 2006; Kondo *et al.*, 2007a; Wu *et al.*, 2007; Boonstra *et al.*, 2009; Pelcastre *et al.*, 2010). Intriguingly, majority of these missense mutations were located on surface of the Norrin crystal structure and regions of the gene crucial for either FZD4 (receptor) and LRP5 (co-receptor) binding or Norrin dimer interface (Ke *et al.*, 2013).

Table 5.4: Frequencies of FEVR patients with the *NDP* gene mutations reported in different ethnic groups

Reference	Ethnicity	Reported frequency of FEVR probands with *NDP* gene mutations	Type of mutations reported and their frequency (%)
Dickinson *et al*., 2006	Caucasian	7% (1/13)	Missense (7)
Drenser *et al*., 2006	Caucasian	7.5% (2/27)	Missense (7.5)
Wu *et al*., 2007	Caucasian	5.7% (3/52)	Missense (5.7)
Kondo *et al*., 2007	Japanese	6% (4/62)	Missense (6)
Boonstra *et al*., 2009	Caucasian	10% (2/20)	Missense (10)
Present study	Indian	9% (10/110)	Missense (5.4)
			Deletions (2.7)
			Nonsense (0.9)

The three deletions (p.His4Arg*fsX*21, p.Asp23Glu*fsX*9, p.Ile48Val*fsX*104) and S57X mutation identified in the present study were located in second exon of *NDP* gene in male probands of four unrelated FEVR families (figure 4.2). These mutations might result in either nonsense mediated mRNA decay or formation of truncated mutant proteins with a loss of 24 (p.Ile48Val*fsX*104) to 77.5% (p.His4Arg*fsX*21) of the wild type Norrin protein. All these probands exhibited classical clinical features of the FEVR such as falciform retinal folds, total retinal detachments and/or with avascularized peripheral retina and exudation (table 4.4). The typical clinical features of the Norrie disease such as microphthalmia, anterior segment dysplasia, mental retardation and hearing loss were not observed in these patients. However, following some of the recently published reports on FEVR, our study preferentially avoided trying to define and distinguish between Norrie disease and FEVR due to overlapping phenotypes and genotypes (Dickinson *et al.*, 2006; Wu *et al.*, 2007). The mothers of some of the probands of FEVR families 21, 97 and 108 (figure 4.2) were found heterozygous for the p.Asp23Glu*fsX*9, p.Ile48Val*fsX*104 deletions and S57X mutation; however, they had variable clinical expressions. The mother of the proband of FEVR family 21 exhibited variable disease phenotype (stage 4B in the left eye and stage 2 in the right eye) in both of her eyes while those of proband's mothers in FEVR families 97 and 108 were found phenotypically normal under indirect ophthalmoscope examination (figure 4.2). This variable expression of disease phenotype in these female family members could be explained by X-chromosome inactivation for the mutated allele. The other possibility could be the inability to detect very mild clinical features of the disease through ophthalmoscopic examination. However, further studies are required to confirm these possibilities.

The four missense mutations (H50D, G113D, R121Q and C126R) were found localized to highly conserved cysteine knot domain of the Norrin. Both SIFT and PolyPhen-2 analysis predicted these mutations as damaging to the protein function. The novel H50D mutation was observed in three probands of unrelated FEVR families and segregated with the disease phenotype in all the affected family members. However, severity of the disease varied between the probands and their affected family members. The paternal aunt (III: 7), cousin sister (IV: 3) of the proband of FEVR family 72 and

sister (I: 2) of the proband of FEVR family 139 (figure 4.2), who were heterozygous for this mutation, were found phenotypically normal on indirect ophthalmoscopic examination. The inactivation of X-chromosome harboring mutant allele might be responsible for normal phenotype in female members of these families. In the crystal structure of the Norrin, the wild type Histidine at amino acid position 50 was located on the surface crucial for receptor binding (figure 5.1) (Ke *et al.*, 2013). The positively charged amino acids present at this location might be involved in ionic interactions with the receptor protein (Ke *et al.*, 2013). Thus, the replacement of a positively charged histidine by an acidic (negative charge) aspartic acid could probably interfere in receptor binding, signaling induction and thereby responsible for disease development.

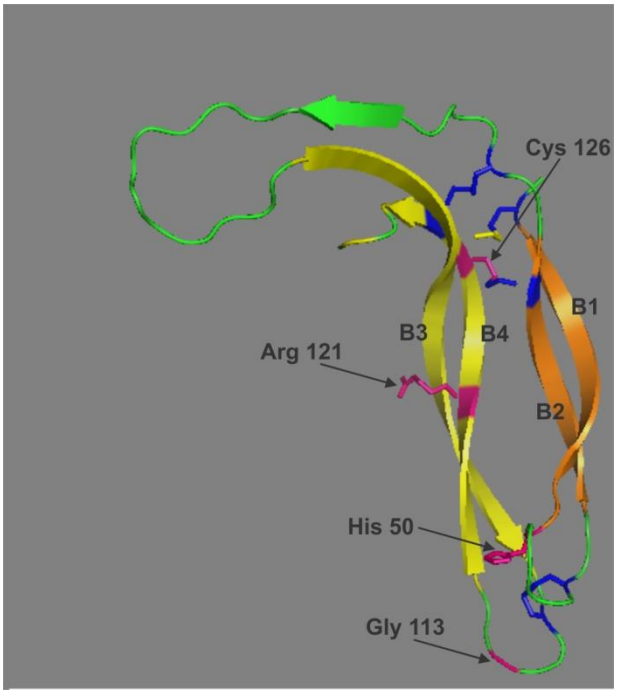

Figure 5.1: Ribbon view of the crystal structure of the Norrin protein showing wild type amino acid residues at the positions of H50D, G113D, R12Q and C126R mutations. The four disulfide bridges formed between C39–C96, C65–C126, C69–C128, and C55–C110 residues are represented in blue color. Wild type amino acid residues at the positions of H50D, G113D, R12Q and C126R mutations are represented in pink color. Structure of the protein (Protein data bank ID: 4MY2) is visualized using PyMOL tool (The PyMOL Molecular Graphics System, Version 1.2r3pre, Schrödinger, LLC).

The second novel missense mutation p.Gly113Asp was located on the surface of the protein and the site that plays a role in LRP5 binding (Ke *et al.*, 2013). The wild type glycine at 113 amino acid position is involved in the formation of a loop along with another glycine at 112 position of Norrin (figure 5.1). This loop joins the β3 and β4 pleated sheets of the Norrin. This loop is connected to another loop formed between β1 and β2 strands through a disulfide bridge between the cysteine residues at 55 and 110 positions of the Norrin (figure 5.1). The formation of this disulfide bridge is crucial for the maintenance of three dimensional conformation of the Norrin and formation of a surface for LRP5 binding (Ke *et al.*, 2013). The replacement of a flexible glycine by an aspartic acid residue with a bulky side chain in G113D mutation could interfere in disulfide bridge formation between C55-C110 and LRP5 binding. This could result in the impaired Norrin-FZD4 signaling that might be responsible for peripheral retinal avascularization in the proband. The importance of this region in Norrin-FZD4 signaling was further supported by the reported mutations at glycine-112 (G112E) and arginine-115 (R115L) positions of Norrin in Norrie disease and FEVR patients respectively (Allen *et al.*, 2006; Kondo *et al.*, 2007a).

C126R, another novel missense mutation was observed as a *de novo* mutation in an index FEVR proband of FEVR family 94. The cysteine at 126 amino acid position of Norrin is involved in formation of a disulfide bridge with another cysteine residue at 65 amino acid position (figure 5.1). This disulfide bridge is one of the four disulfide bridges that are essential for maintenance of Norrin structure (Ke *et al.*, 2013). The replacement of a cysteine with a bulky side chain containing arginine residue may be responsible for the loss of tertiary conformation of the cysteine knot domain of Norrin and thereby an impaired signaling mechanism. Gal *et al*., (1996) reported the replacement of cysteine 126 of the Norrin with a serine residue in a Norrie disease patient (Gal *et al.*, 1996). Likewise, Smallwood *et al*., (2007) reported the replacement of cysteine 126 with an alanine residue that severely impairs FZD4 binding and activation of Norrin-FZD4 signaling in Super Top Flash (STF) cells (Smallwood *et al.*, 2007). These observations further support the highly pathogenic nature of the C126R mutation.

The fourth missense mutation, R121Q was a recurrent mutation reported in different studies in FEVR and Norrie disease patients in Caucasian population (Boonstra *et al.*, 2009; Pelcastre *et al.*, 2010). Arginine at 121 codon position in Norrin is a hot spot for mutations and replacement of this residue was observed by glutamine or tryptophan or lysine in various studies (table 2.5). The arginine 121 locates to the surface of the protein as per the crystal structure of the Norrin, in the region crucial for FZD4 receptor binding (figure 5.1). As previously mentioned, the positively charged arginine might be involved in ionic interactions with the receptor. In STF cells, the reduced signaling activity of up to 50% in case of R121Q and R121W mutations suggest for an important role of arginine in the protein function and disease pathogenesis (Xu *et al.*, 2004; Qin *et al.*, 2008).

Other than the coding region mutations, a reported 14 bp deletion in the CT repeat region (-395_-409del14bp), a SNP (rs45501198) in the 5' UTR and two novel nucleotide changes in the 3' UTR were also observed in the probands of three unrelated FEVR families (8, 75 and 98). The 14 bp deletion in the 5' UTR has already been reported in Norrie disease and ROP patients (Talks *et al.*, 2001; Dickinson *et al.*, 2006). Kenyon *et al*., (1999) had shown that the deletion of CT repeat region leads to reduced expression of *NDP* mRNA in transiently transfected WeriB cell line (Kenyon *et al.*, 1999). In the present study, the father of the proband was hemizygous for this change but lacked clinical presentation of FEVR (figure 4.2; FEVR family 8; I: 1). The presence of this deletion in a normal individual has also been reported by Dickinson *et al*., (2006) thereby suggesting for minor or non pathogenic nature of this change (Dickinson *et al.*, 2006).

Two novel nucleotide changes c.*522T>C and c.*974C>G were identified in 3' UTR of *NDP* in probands of FEVR families 75 and 98 respectively. Previously, Wu *et al*., (2007) too had reported a 3' UTR variation (c.*717T>C) in a FEVR patient (Wu *et al.*, 2007). In the present study, the heterozygous c.*522T>C nucleotide change was observed in a female proband (II: 2) of FEVR family 75 along with her mother (I: 2) and in a control individual in (table 4.3 and figure 4.2). The presence of this variation in a control individual suggests it to be non pathogenic. The c.*974C>G change was not observed

in severely affected sibling of the proband of FEVR family 98 ruling out it to be a pathogenic change. (figure 4.2; FEVR family 98; II: 3). Since these variations do not seem to be pathogenic, the involvement of nucleotide changes in other candidate genes in disease pathogenesis for these FEVR families could not be ruled out.

5.2: *FZD4* gene screening

Screening of *FZD4* gene led to identification of 5 novel nucleotide changes that are likely to cause impaired vascular development in five unrelated FEVR probands. These variations include 3 missense changes (I114S, M157T and I360V), a single bp insertion (R466S*fsX*6) and a nonstop mutation (*538Serext*3). In addition to novel mutations, two reported small bp deletions (D428S*fsX*2 and K429R*fsX*28) and a missense mutation (M105V) were identified in five different FEVR families (table 4.5). In agreement with previous reports, the *FZD4* gene mutations identified in the present study were responsible for autosomal dominant FEVR (Kondo *et al.*, 2003; Toomes *et al.*, 2004b; Boonstra *et al.*, 2009; Nikopoulos *et al.*, 2010b).

The missense mutations M105V, I114S and M157T were located in the extracellular cysteine rich domain (CRD) of FZD4, which has experimentally been shown responsible for ligand binding during Norrin signal transduction (Xu *et al.*, 2004; Smallwood *et al.*, 2007; Ke *et al.*, 2013). Though, I114S and M157T substitutions have been identified for the first time in the present study, the other amino acid substitutions have been reported before at these codon positions. Robitaille *et al*., (2009) had reported I114T mutation in a familial FEVR case with a highly variable disease phenotype among the different family members with this mutation (Robitaille *et al.*, 2009). The isoleucine residue at 114 codon position of FZD4 was highly conserved across multiple vertebrate species (figure 4.8). Replacement of hydrophobic isoleucine with a hydrophilic serine residue at codon 114 as observed in the present study is predicted to have greater pathogenic effect compared to previously reported I114T by PolyPhen-2 analysis. These findings provide support for the possible role of I114S mutation in disease pathogenesis.

M157V and M157K mutations at codon 157 of FZD4 had earlier been reported in Caucasian population (Toomes *et al.*, 2004b; Robitaille *et al.*, 2011). M157V was reported in one FEVR family, with ocular phenotypes ranging from normal to complete retinal detachment among different family members harboring this mutation (Toomes *et al.*, 2004b). M157K mutation was also reported in two different FEVR patients with severe disease phenotype (Robitaille *et al.*, 2011). In contrast to previous studies, the present study found the replacement of methionine by threonine (M157T) at 157 codon

position. The methionine at this position was highly conserved and its replacement with valine in case of M157V mutation resulted in severe impairment of human Norrin induced FZD4 signaling in the STF cell line (Xu *et al.*, 2004). The methionine at 157 codon position precedes a cysteine (codon 158), which is involved in the formation of a disulfide bond crucial for structural maintenance of CRD (Dann *et al.*, 2001; Schulte, 2010). Based on this information, we speculate that the altered solvent interactions of hydrophilic threonine instead of hydrophobic methionine in M157T mutation may interfere with disulfide bridge formation by following cysteine. Thus, the structural alteration caused by this mutation may interfere with ligand interaction or homodimer formation and responsible for its pathogenicity.

The missense mutation M105V, a recurrent mutation has been reported in familial FEVR cases of Caucasian, Japanese and Chinese populations (Kondo *et al.*, 2003; Jia *et al.*, 2010; Yang *et al.*, 2012b). M105T, another mutation was observed at the same codon position in a familial, Caucasian FEVR patient (Toomes *et al.*, 2004b). Unlike previous studies that have reported the M105V mutation in familial FEVR cases, the present study identified the mutation in three index FEVR cases. Notably, like M157T mutation, the M105V mutation also precedes a cysteine residue (codon 106) that plays a crucial role in CRD structure formation via disulfide bridge formation with another cysteine at codon 45. Replacement of the highly conserved methionine at codon 105 with a valine residue led to severe impairment of FZD4 signaling in STF cell line when induced with ectopic Norrin (Xu *et al.*, 2004; Qin *et al.*, 2008). Furthermore, the 3D homology model of FZD4 CRD revealed the close proximity of the wild type residues in M105V and M157T mutations (Xu *et al*., 2004). The region of CRD comprising the M105V and M157T mutations was suggested to be crucial for both ligand binding and homodimer formation in previous studies (Dann *et al.*, 2001; Xu *et al.*, 2004; Smallwood *et al.*, 2007; Qin *et al.*, 2008). The data based on published evidences strongly suggests for the pathogenic nature of these missense mutations.

The novel I360V change was observed in a familial FEVR case (FEVR family 8) and it was located in the fourth transmembrane domain of the FZD4 protein. Previously, no variations had been reported in this domain in FEVR patients. The isoleucine residue at

codon position 360 of FZD4 was conserved across different species of vertebrates. However, the presence of valine was observed at this codon position in Beetle (Tribolium *castaneum*) and Sea urchin (Paracentrotus *lividus*) species indicating the non-pathogenic nature of this variation (figure 4.8). The presence of this change in phenotypically normal father of the proband (figure 4.6; FEVR family 8; I: 1) and even in a control subject further suggests for the non-pathogenic nature of this variation.

The frameshift mutations (R466S*fsX*6, D428SfsX2 and K429RfsX28) identified in this study were located in the second exon and predicted to result in the formation of a truncated protein with a loss of 13 (R466S*fsX*6) to 20 % (D428SfsX2) of the wild type FZD4 protein. Due to the presence of only two exons in the *FZD4* gene, the frameshift mutations observed in the second exon may result in the formation of truncated protein (Hentze *et al.*, 1999). The resulting truncated proteins are predicted to not have the conserved KTXXXW domain and PDZ binding motif that are required for its interaction with downstream regulator proteins and could fail to induce the signaling pathway.

The novel single bp insertion 1396_1397insT (R466SfsX6) identified in the present study was the second insertion mutation observed in the *FZD4* gene so far, and it segregated with the disease phenotype. The reported 5 bp deletion: c.1286-1290delAGTTA (K429RfsX28) was observed in two index FEVR cases with a severe disease phenotype. Similar to previous findings (Muller *et al.*, 2008), this mutation showed variable expressivity among different carriers of 61 and 136 FEVR families (figure 4.6). Another previously reported deletion c.1282-1285delGACA (D428SfsX2) in was observed in the proband of FEVR family 89 along with a nonstop (c.1613A>C) mutation in compound heterozygous condition (figure 4.6) (Nikopoulos *et al.*, 2010b; Robitaille *et al.*, 2011; Yang *et al.*, 2012b). Severe disease phenotypes were observed in two of the siblings having two mutant alleles that could have resulted from the synergistic effect of these changes. The parents of these siblings carrying a single copy of mutation were either normal or had avascularized peripheral retina. The nonstop mutation is identified for the first time in *FZD4* gene and it is predicted to result in addition of two extra amino acids to the C-terminal cytoplasmic domain of FZD4 protein. The C-terminal tail of the FZD4 has a flexible disordered structure in its wild type

condition (Lemma *et al.*, 2013). The addition of two extra amino acids may alter the conformation of the C-terminal tail either before or after ligand binding and thereby interfere in its binding to downstream regulator proteins. Previously, Kondo *et al*., had reported compound heterozygous mutations in *FZD4* gene in a FEVR family and suggested that this could be one of the possible reason for inter and intra familial variability of disease phenotype (Kondo *et al.*, 2003; Jia *et al.*, 2010).

The present study identified *FZD4* mutations in 8.1% (9/110) of the Indian FEVR patients. The results of the present study were comparable to previous mutation reports which showed 3.5% to 40% (table 5.5) of FEVR patients to harbor *FZD4* mutations in different populations. The frequency of patients with *FZD4* mutations in our cohort was relatively high when compared to a previous *FZD4* gene mutation report by Nallathambi *et al*., (2006) in Indian FEVR patients.

Table 5.5: Frequencies of FEVR patients with *FZD4* mutations reported in different ethnic groups

Reference	Ethnicity	Reported frequency of FEVR probands with *FZD4* gene mutations	Type of mutations reported and their frequency (%)
Kondo *et al*., 2003	Japanese	16.6% (4/24)	Missense (2) Nonsense (2)
Toomes *et al*., 2004	Caucasian	17.5% (7/40)	Missense (7.5) Deletions (7.5) Nonsense (2.5)
Qin *et al*., 2005	Japanese	3.5% (2/56)	Missense (3.5)
Nallathambi *et al*., 2006	Indians	5.6% (3/53)	Missense (3.7) Deletion (1.8)
Boonstra *et al*., 2009	Caucasian	40% (8/20)	Missense (10) Nonsense (30)
Nikopoulos *et al*., 2010	Caucasian	31% (5/16)	Missense (18.75) Deletion (6.25) Nonsense (6.25)
Jia *et al*., 2011	Chinese	23 (11/48)	Missense (18.7) Nonsense (4.1) Deletion (8)
Robitaille *et al*., 2011	Majority Caucasian	17.6% (12/68)	Missense (8.8) Deletion (4.4) Nonsense (3.9) Insertion (1.4)
Yang *et al*., 2012	Chinese	9.6% (5/52)	Missense (6.1) Deletion: (1) Nonsense (2)
Present study	Indian	8.1% (9/110)	Missense (4.5) Deletion (2.7) Insertion (0.9) Nonstop (0.9)

5.3 *TSPAN12* gene screening

The *TSPAN12* gene mutations have been reported in Caucasian, Chinese and Japanese FEVR patients and were responsible for autosomal dominant and autosomal recessive form of the disease (Nikopoulos *et al.*, 2010a; Poulter *et al.*, 2010; Kondo *et al.*, 2011; Yang *et al.*, 2011; Poulter *et al.*, 2012). The frequency of the FEVR patients with the *TSPAN12* gene mutations varied from 4% to 10% in different studies (Poulter *et al.*, 2010; Kondo *et al.*, 2011). The present study identified two novel and a reported missense changes in *TSPAN12* gene in 5.4% (6/110) of the FEVR probands. These missense changes were not observed in 115 control individuals. In addition to these mutations, two novel intronic changes, two novel 3' UTR variations and a reported SNP were also detected in 18% (20/110) of the FEVR probands (table 4.7).

Table 5.6: Frequencies of FEVR patients with *TSPAN12* mutations reported in different ethnic groups

Reference	Ethnicity	Reported frequency of FEVR probands with *NDP* gene mutations	Type of mutations reported and their frequency (%)
Poulter *et al*., 2010	Caucasian	10% (7/70)	Missense (2.8)
			Nonsense (2.8)
			Deletions (1.4)
			Insertions (1.4)
			Splice site (1.4)
Yang *et al*., 2011	Chinese	6% (3/49)	Missense (4)
			Deletions (1)
Kondo *et al*., 2011	Japanese	4% (4/90)	Missense (2.2)
			Nonsense (2.2)
Present study	Indian	5.4% (4/110)	Missense (5.4)

So far, 18 different mutations have been reported in *TSPAN12* gene in FEVR patients and were located in extracellular loops 1 and 2, transmembrane domains 3 and 4 and putative splice donor or acceptor sites (table 2.7). In the present study, the identified missense mutations were located in extracellular loop 1 (V42A), extracellular loop 2 (C160Y) and transmembrane domain 3 (V112I) of the TSPAN12 protein. The novel V42A mutation was observed in heterozygous state in the severely affected (stage 5 in both eyes) proband (IV: 2) and the severely affected family members of FEVR family

140 (figure 4.10 and table 4.8). However, the presence of this mutation in the unaffected parents of the proband and the predictions by SIFT and Polyphen-2 analysis suggested for the less pathogenic nature of this nucleotide change. The reported missense change V112I was observed in homozygous condition in a severely affected male proband (IV: 2) of the FEVR family 69 (figure 4.10 and table 4.8) suggesting for an autosomal recessive pattern of inheritance of the disease. The mother (III: 2) and brother (IV: 1) of the proband having heterozygous change, lacked any ocular manifestation of the disease (figure 4.10; FEVR family 69). The recessive inheritance pattern of the disease had previously been described in three *TSPAN12* mutations by Poulter *et al*., (2012). The patients homozygous for these mutations had severe ocular phenotype in comparison to those who had heterozygous changes with mild disease phenotype.

A novel missense mutation 'C160Y' was observed as the prevalent mutation (3.6% of the FEVR probands) in the present study cohort. This mutation was observed in the probands and their affected family members of four unrelated FEVR families. Two severely affected probands of the FEVR families (117 and 147) had homozygous C160Y mutation while the remaining probands of two FEVR families (20 and 78) and their affected family members had heterozygous mutation (figure 4.10). Compared to patients those having homozygous mutation, the patients with a single mutated copy (heterozygous) showed a slow progression of the disease or relatively less severe ocular phenotype, suggesting the recessive inheritance pattern of the disease and effect of allelic dosage on disease severity. Interestingly, previously described couple of FEVR patients with homozygous mutations in FEVR candidate genes too had severely reduced protein expression that was shown to be responsible for severity and rapid progression of the disease (Jiao *et al.*, 2004; Downey *et al.*, 2006). Later, Poulter *et al*., (2012) and Kondo *et al*., (2007) had also reported two different FEVR families with homozygous *TSPAN12* mutations and a FEVR family with homozygous mutation in *FZD4* gene respectively. All the probands with the respective homozygous mutation in these reported FEVR families, had a rapid progression of the disease and a severe ocular phenotype (Kondo *et al.*, 2007b; Poulter *et al.*, 2012).

The wild type cysteine as seen for C160Y mutation, was located at the second position in the highly conserved CCG signature motif of extracellular loop 2 (ECL2) of the TSPAN12 protein. This cysteine residue was predicted to be involved in formation of a disulfide bridge with another cysteine residue located at 181 position of TSPAN12. The formation of this disulfide bond was shown to be crucial for maintaining the structure of ECL2 (Kondo *et al.*, 2011). The ECL2 was suggested to be involved in protein-protein interactions with targeted proteins in the cell membrane (Boucheix *et al.*, 2001). Therefore, the disrupted structure of ECL2 due to C160Y mutation could probably interfere in TSPAN12 interaction with FZD4 protein and thereby affects the protein function and Norrin-FZD4 signaling. Furthermore, the highly conserved nature of cysteine residues in CCG motifs of all orthologues of TSPAN12 proteins (figure 4.12) and all tetraspanin protein family members along with the SIFT and PolyPhen-2 analysis suggested for the highly pathogenic nature of this mutation.

The novel heterozygous IVS2+24C>G and IVS6+19G>C intronic changes were observed in the probands of FEVR families 64 and 35 respectively (figure 4.10). Along with the proband (II: 1), the IVS2+24C>G change was also observed in the mildly affected proband's mother (figure 4.10; FEVR family 64; I: 2) and in one control individual in heterozygous state. Similarly, the heterozygous IVS6+19G>C change was also seen in the unaffected proband's mother (figure 4.10; FEVR family 35; I: 2), but was not identified in 115 control individuals. These variations were not predicted to have any significant effect on splice sites, branch points and enhancer or silencer motifs by HSF analysis. Intriguingly, these two intronic variations co-segregated with M105V change of *FZD4* in the probands and their mothers. As a result, the individual effect of the intronic variations could not be commented. However, the presence of M105V change alone in another severely affected proband (II: 2) of FEVR family 134 (figure 4.6) suggested this change to be mainly responsible for the development of ocular phenotype in the probands of these FEVR families. On the other hand, the identification of IVS2+24C>G change in a control individual further suggests the non pathogenic nature of the substitution.

Apart from coding region and intronic nucleotide changes, the present study identified two novel 3' UTR changes: c.*1010T>G and c.*1140T>A in two different index probands of FEVR families 95 and 102 respectively (figure 4.10). The asymptomatic parent DNA samples of these probands were unavailable for the segregation analysis of these nucleotide changes. These 3' UTR changes were not identified in 115 control individuals. Further studies are warranted to understand the effect of these 3' UTR changes on mRNA stability of *TSPAN12*. In addition to these novel 3' UTR changes, two reported SNPs: rs41622 and rs189221112 in 3' UTR were identified in FEVR probands with frequencies 14% (16/110) and 9% (10/110) respectively. The detection of these SNPs with higher frequencies (15%) in control individuals compared to probands suggested the non-pathogenic nature of these variations (table 5.2).

5.4. *ZNF408* gene screening

ZNF408 has been recently identified candidate gene for FEVR. The protein encoded by *ZNF408* gene was functionally shown to play a role in retinal vascular development in zebrafish animal model, however, only two missense mutations (H455Y and S126N) have been reported in the FEVR patients in the original study (Collin *et al*., 2013). In this context, we attempted to assess its role in disease development in Indian patients.

The screening of entire coding region and UTR of *ZNF408* gene has led to the identification of four novel heterozygous missense changes (P44S, M232V, T617N and E715D) in four unrelated FEVR probands (table 4.9). All the missense changes were observed in severely affected (stage 4 or 5) FEVR probands (table 4.10). Except T617N, remaining three missense changes were not observed in 115 control individuals. The T617N change was observed in one control individual out of 115 controls screened for this variation. SIFT analysis predicted the P44S and E715D mutations to have a harmful effect on the protein function, whereas M232V and T617N changes were predicted to be tolerated by the protein. In PolyPhen-2 analysis, the T617N and E715D mutations were predicted to be pathogenic, whereas P44S and M232V mutations were suggested to be non harmful for the protein function. The P44S, M232V and E715D mutations were not located in the functionally important domains of the protein. Whereas T617N change was located in tenth zinc finger domain of the

protein and therefore could interfere with DNA interaction. However, the presence of T617N change in the unaffected mother of the proband (figure 4.14; FEVR family 135; I: 1) and in a control individual suggested for a less or non pathogenic nature of this variation. In multiple sequence alignment, it was found that except M232V change, remaining missense changes were observed in moderately conserved amino acid positions of ZNF408 across different species (figure 4.16). Presence of valine instead of methionine at 232 amino acid position of ZNF408 in Wild boar Sus *scrofa*), Cow (Bos t*aurus*), Marmoset (Callithrix *jacchus*) and Star nosed mole (Chondylura *cristata*) indicated a less pathogenic nature of M232V mutation. Furthermore, the proband of FEVR family 51 with M232V misesence change also harbored a heterozygous M157T mutation in *FZD4* gene. The heterozygous M232V change was also observed in one of the two unaffected sons of the proband of FEVR family 51 (figure 4.14) however, they lack the M157T mutation of *FZD4.* The data thus suggested that M157T mutation was mainly responsible for the ocular phenotype in the proband. However, further structural and functional studies are required to understand the effect these missense changes on ZNF408 protein structure and function.

In addition to these missense changes, two novel synonymous substitutions (p.Gln134Gln and p.Gly136Gly) and three reported polymorphisms (rs148055528, rs72461400 and rs376536252) were also identified in the coding region of *ZNF408* gene. Out of 115 controls screened for these variations, Gln134Gln substitution was not observed in any of the control subjects, while Gly136Gly substitution was identified in one control. The three reported polymorphisms were observed with similar frequencies in both probands and controls and were not associated with disease phenotype (table 5.2). None of these coding region variations were predicted to have any significant effect on potential splice sites and splicing regulatory elements in HSF analysis.

In addition to the coding region variations, a novel 5 bp deletion (c.-210_-214del5bp) and a novel nucleotide substitution (-111C>A) were observed in the 5' UTR in three unrelated FEVR probands. Both these variations were not observed in 115 control individuals. The 5 bp deletion was observed in a familial FEVR case and segregated with the disease phenotype in a severely affected sibling of the proband. However, this

deletion was also observed in unaffected mother of the proband suggesting either incomplete penetrance of the variation or involvement of other candidate gene in the disease development. The present study identified *ZNF408* mutations in the coding region in 3.6% (4/110) of the unrelated Indian FEVR probands. Thus, the present study independently validates and confirms the potential role *ZNF408* gene in FEVR development.

In summary, the present study provided the mutation spectrum of four candidate genes (*NDP, FZD4, TSPAN12* and *ZNF408)* for the first time in a large cohort of Indian FEVR patients. The mutations in these candidate genes together accounted for 26.3% (29/110) of all the FEVR cases. Excluding the probands with mutations in the coding region of these candidate genes, 7.2% (8/110) of the probands were having novel intronic and UTR variations. These intronic and UTR changes were not identified in 115 control individuals. However, the remaining 66.5% of cases did not exhibit any involvement of these genes, which suggested for the role of other unidentified candidate loci/genes in FEVR pathogenesis. Majority of the mutations identified in the present study were novel mutations (16/29) and except for four mutations (H50D of *NDP*, M105V and K429R*fsX*28 of *FZD4*, C160Y of *TSPAN12*), remaining all the mutations identified in the present study were observed each in one proband suggesting allelic heterogeneity of the condition. In agreement with previous reports, phenotypic variability and incomplete penetrance was observed for some of the mutations in the present study. The identified compound heterozygous mutations of *FZD4* gene and identification of digenic variations in some FEVR families could provide the plausible reason for the observed phenotypic variability among different carriers in a FEVR family. However, further studies are warranted to explain the incomplete penetrance of the identified mutations and phenotypic variability.

1. The present study for the first time demonstrated the relative contributions of the *NDP, FZD4, TSPAN12* and *ZNF408* genes among Indian FEVR patients.

2. This study also provided a baseline data on the mutation spectrum of these candidate genes in Indian patients.

3. Majority of the mutations identified in the present study were non-recurrent that suggested allelic heterogeneity of the condition.

4. Similar to the previous reports, this study was unable to generate any specific genotype-phenotype correlations.

5. The compound heterozygous mutations and digenic variations identified in this study could be linked to the variable expressivity of the disease.

6. The lower mutation frequency of the candidate genes in this cohort indicated the involvement of other uncharacterized genes that may be involved in the disease pathogenesis.

To the best of my knowledge and belief, this is perhaps the first study to demonstrate the cumulative involvement of *NDP, FZD4, TSPAN12* and *ZNF408* genes in a large cohort of Indian FEVR patients. This study also validated the involvement of the recently identified *ZNF408* gene in FEVR pathogenesis, which was based only on two missense mutations in FEVR patients from the European and Japanese populations. The novel mutations identified in the present study further enlarged the mutation spectrum of the candidate genes in FEVR patients and would be valuable for genetic counseling and prenatal diagnosis.

Due to paucity of time and resources, the present study could not attempt to screen the *LRP5* gene and to identify the unknown genes, which may have a possible involvement in the disease pathogenesis. Similarly, specific functional assays, such as X inactivation etc. could not be performed to explain the underlying variable expressivity and incomplete penetrance of the disease.

1. The patients/ families who lacked mutations in the known candidate genes will be a potential resource for identifying unidentified candidate genes through high through put screening methods like next generation DNA sequencing.

2. Functional assessment of the coding region mutations and UTR variations in the present study would provide better insights on the effect of these nucleotide changes on protein trafficking and induction of the Norrin-FZD4 signaling pathway.

Adzhubei, I., Jordan, D.M., and Sunyaev, S.R. (2013). Predicting functional effect of human missense mutations using PolyPhen-2. Curr Protoc Hum Genet *Chapter 7*, Unit7. 20.

Adzhubei, I.A., Schmidt, S., Peshkin, L., Ramensky, V.E., Gerasimova, A., Bork, P., Kondrashov, A.S., and Sunyaev, S.R. (2010). A method and server for predicting damaging missense mutations. Nat Methods *7*, 248-249.

Allen, R.C., Russell, S.R., Streb, L.M., Alsheikheh, A., and Stone, E.M. (2006). Phenotypic heterogeneity associated with a novel mutation (Gly112Glu) in the Norrie disease protein. Eye (Lond) *20*, 234-241.

Anand-Apte, B., and Hollyfield, J.G. (2011). The Retina and its Disorders (Elsevier Science).

Bailey, R.L., Herbert, J.M., Khan, K., Heath, V.L., Bicknell, R., and Tomlinson, M.G. (2011). The emerging role of tetraspanin microdomains on endothelial cells. Biochem Soc Trans *39*, 1667-1673.

Balemans, W., and Van Hul, W. (2007). The genetics of low-density lipoprotein receptor-related protein 5 in bone: a story of extremes. Endocrinology *148*, 2622-2629.

Benson, W.E. (1995). Familial exudative vitreoretinopathy. Trans Am Ophthalmol Soc *93*, 473-521.

Berger, W., Meindl, A., van de Pol, T.J., Cremers, F.P., Ropers, H.H., Doerner, C., Monaco, A., Bergen, A.A., Lebo, R., Warburg, M. (1992a). Isolation of a candidate gene for Norrie disease by positional cloning. Nat Genet *1*, 199-203.

Berger, W., van de Pol, D., Bachner, D., Oerlemans, F., Winkens, H., Hameister, H., Wieringa, B., Hendriks, W., and Ropers, H.H. (1996). An animal model for Norrie disease (ND): gene targeting of the mouse ND gene. Hum Mol Genet *5*, 51-59.

Berger, W., van de Pol, D., Warburg, M., Gal, A., Bleeker-Wagemakers, L., de Silva, H., Meindl, A., Meitinger, T., Cremers, F., and Ropers, H.H. (1992b). Mutations in the candidate gene for Norrie disease. Hum Mol Genet *1*, 461-465.

Boonstra, F.N., Van Nouhuys, C.E., Schuil, J., de Wijs, I.J., van der Donk, K.P., Nikopoulos, K., Mukhopadhyay, A., Scheffer, H., Tilanus, M.A., Cremers, F.P.*, et al.* (2009). Clinical and molecular evaluation of probands and family members with familial exudative vitreoretinopathy. Invest Ophthalmol Vis Sci *50*, 4379-4385.

Boucheix, C., and Rubinstein, E. (2001). Tetraspanins. Cell Mol Life Sci *58*, 1189-1205.

Cadigan, K.M., and Nusse, R. (1997). Wnt signaling: a common theme in animal development. Genes Dev *11*, 3286-3305.

Canny, C.L., and Oliver, G.L. (1976). Fluorescein angiographic findings in familial exudative vitreoretinopathy. Arch Ophthalmol *94*, 1114-1120.

Chan-Ling, T., McLeod, D.S., Hughes, S., Baxter, L., Chu, Y., Hasegawa, T., and Lutty, G.A. (2004). Astrocyte-endothelial cell relationships during human retinal vascular development. Invest Ophthalmol Vis Sci *45*, 2020-2032.

Chen, J., and Smith, L.E. (2007). Retinopathy of prematurity. Angiogenesis *10*, 133-140.

Chen, J., Stahl, A., Krah, N.M., Seaward, M.R., Joyal, J.S., Juan, A.M., Hatton, C.J., Aderman, C.M., Dennison, R.J., Willett, K.L.*, et al.* (2012). Retinal expression of Wnt-pathway mediated genes in low-density lipoprotein receptor-related protein 5 (Lrp5) knockout mice. PLoS One *7*, e30203.

Chen, Z.Y., Battinelli, E.M., Fielder, A., Bundey, S., Sims, K., Breakefield, X.O., and Craig, I.W. (1993). A mutation in the Norrie disease gene (NDP) associated with X-linked familial exudative vitreoretinopathy. Nat Genet *5*, 180-183.

Collin, R.W., Nikopoulos, K., Dona, M., Gilissen, C., Hoischen, A., Boonstra, F.N., Poulter, J.A., Kondo, H., Berger, W., Toomes, C.*, et al.* (2013). ZNF408 is mutated in

familial exudative vitreoretinopathy and is crucial for the development of zebrafish retinal vasculature. Proc Natl Acad Sci U S A *110*, 9856-9861.

Criswick, V.G., and Schepens, C.L. (1969). Familial exudative vitreoretinopathy. Am J Ophthalmol *68*, 578-594.

Dann, C.E., Hsieh, J.C., Rattner, A., Sharma, D., Nathans, J., and Leahy, D.J. (2001). Insights into Wnt binding and signalling from the structures of two Frizzled cysteine-rich domains. Nature *412*, 86-90.

Descamps, B., Sewduth, R., Ferreira Tojais, N., Jaspard, B., Reynaud, A., Sohet, F., Lacolley, P., Allieres, C., Lamaziere, J.M., Moreau, C.*, et al.* (2012). Frizzled 4 regulates arterial network organization through noncanonical Wnt/planar cell polarity signaling. Circ Res *110*, 47-58.

Desmet, F.O., Hamroun, D., Lalande, M., Collod-Beroud, G., Claustres, M., and Beroud, C. (2009). Human Splicing Finder: an online bioinformatics tool to predict splicing signals. Nucleic Acids Res *37*, e67.

Dickinson, J.L., Sale, M.M., Passmore, A., FitzGerald, L.M., Wheatley, C.M., Burdon, K.P., Craig, J.E., Tengtrisorn, S., Carden, S.M., Maclean, H.*, et al.* (2006). Mutations in the NDP gene: contribution to Norrie disease, familial exudative vitreoretinopathy and retinopathy of prematurity. Clin Experiment Ophthalmol *34*, 682-688.

Downey, L.M., Bottomley, H.M., Sheridan, E., Ahmed, M., Gilmour, D.F., Inglehearn, C.F., Reddy, A., Agrawal, A., Bradbury, J., and Toomes, C. (2006). Reduced bone mineral density and hyaloid vasculature remnants in a consanguineous recessive FEVR family with a mutation in LRP5. Br J Ophthalmol *90*, 1163-1167.

Downey, L.M., Keen, T.J., Roberts, E., Mansfield, D.C., Bamashmus, M., and Inglehearn, C.F. (2001). A new locus for autosomal dominant familial exudative vitreoretinopathy maps to chromosome 11p12-13. Am J Hum Genet *68*, 778-781.

Drenser, K.A., Dailey, W., Capone, A., and Trese, M.T. (2006). Genetic evaluation to establish the diagnosis of X-linked familial exudative vitreoretinopathy. Ophthalmic Genet *27*, 75-78.

Dudgeon, J. (1979). Familial exudative vitreo-retinopathy. Trans Ophthalmol Soc U K *99*, 45-49.

Ebert, E.M., and Mukai, S. (1993). Familial exudative vitreoretinopathy. Int Ophthalmol Clin *33*, 237-247.

Feldman, E.L., Norris, J.L., and Cleasby, G.W. (1983). Autosomal dominant exudative vitreoretinopathy. Arch Ophthalmol *101*, 1532-1535.

Figueroa, D.J., Hess, J.F., Ky, B., Brown, S.D., Sandig, V., Hermanowski-Vosatka, A., Twells, R.C., Todd, J.A., and Austin, C.P. (2000). Expression of the type I diabetes-associated gene LRP5 in macrophages, vitamin A system cells, and the Islets of Langerhans suggests multiple potential roles in diabetes. J Histochem Cytochem *48*, 1357-1368.

Flynn, J.T., and Chan-Ling, T. (2006). Retinopathy of prematurity: two distinct mechanisms that underlie zone 1 and zone 2 disease. Am J Ophthalmol *142*, 46-59.

Fruttiger, M. (2007). Development of the retinal vasculature. Angiogenesis *10*, 77-88.

Fullwood, P., Jones, J., Bundey, S., Dudgeon, J., Fielder, A.R., and Kilpatrick, M.W. (1993). X linked exudative vitreoretinopathy: clinical features and genetic linkage analysis. Br J Ophthalmol *77*, 168-170.

Gal, A., Veske, A., Jojart, G., Grammatico, B., Huber, B., Gu, S., del Porto, G., and Senyi, K. (1996). Norrie-Warburg syndrome: two novel mutations in patients with classical clinical phenotype. Acta Ophthalmol Scand Suppl, 13-16.

Gariano, R.F. (2003). Cellular mechanisms in retinal vascular development. Prog Retin Eye Res *22*, 295-306.

Gariano, R.F., and Gardner, T.W. (2005). Retinal angiogenesis in development and disease. Nature *438*, 960-966.

Gariano, R.F., Kalina, R.E., and Hendrickson, A.E. (1996). Normal and pathological mechanisms in retinal vascular development. Surv Ophthalmol *40*, 481-490.

Gitter, K.A., Rothschild, H., Waltman, D.D., Scott, B., and Azar, P. (1978). Dominantly inherited peripheral retinal neovascularization. Arch Ophthalmol *96*, 1601-1605.

Gong, Y., Slee, R.B., Fukai, N., Rawadi, G., Roman-Roman, S., Reginato, A.M., Wang, H., Cundy, T., Glorieux, F.H., Lev, D.*, et al.* (2001). LDL receptor-related protein 5 (LRP5) affects bone accrual and eye development. Cell *107*, 513-523.

Gow, J., and Oliver, G.L. (1971). Familial exudative vitreoretinopathy. An expanded view. Arch Ophthalmol *86*, 150-155.

Harris, A., and Bingaman, D. (2006). Retinal and choroidal blood flow in health and disease (Elsevier/Mosby).

Hartzer, M.K., Cheng, M., Liu, X., and Shastry, B.S. (1999). Localization of the Norrie disease gene mRNA by in situ hybridization. Brain Res Bull *49*, 355-358.

Hasegawa, T., McLeod, D.S., Prow, T., Merges, C., Grebe, R., and Lutty, G.A. (2008). Vascular precursors in developing human retina. Invest Ophthalmol Vis Sci *49*, 2178-2192.

Hemler, M.E. (2005). Tetraspanin functions and associated microdomains. Nat Rev Mol Cell Biol *6*, 801-811.

Hentze, M.W., and Kulozik, A.E. (1999). A perfect message: RNA surveillance and nonsense-mediated decay. Cell *96*, 307-310.

Hildebrand, G.D., and Fielder, A.R. (2010). Pediatric Retina (Springer).

Hsieh, M., Boerboom, D., Shimada, M., Lo, Y., Parlow, A.F., Luhmann, U.F., Berger, W., and Richards, J.S. (2005). Mice null for Frizzled4 (Fzd4-/-) are infertile and exhibit impaired corpora lutea formation and function. Biol Reprod *73*, 1135-1146.

Jia, L.Y., Li, X.X., Yu, W.Z., Zeng, W.T., and Liang, C. (2010). Novel frizzled-4 gene mutations in chinese patients with familial exudative vitreoretinopathy. Arch Ophthalmol *128*, 1341-1349.

Jiao, X., Ventruto, V., Trese, M.T., Shastry, B.S., and Hejtmancik, J.F. (2004). Autosomal recessive familial exudative vitreoretinopathy is associated with mutations in LRP5. Am J Hum Genet *75*, 878-884.

Johnson, K., Mintz-Hittner, H.A., Conley, Y.P., and Ferrell, R.E. (1996). X-linked exudative vitreoretinopathy caused by an arginine to leucine substitution (R121L) in the Norrie disease protein. Clin Genet *50*, 113-115.

Junge, H.J., Yang, S., Burton, J.B., Paes, K., Shu, X., French, D.M., Costa, M., Rice, D.S., and Ye, W. (2009). TSPAN12 regulates retinal vascular development by promoting Norrin- but not Wnt-induced FZD4/beta-catenin signaling. Cell *139*, 299-311.

Kato, M., Patel, M.S., Levasseur, R., Lobov, I., Chang, B.H., Glass, D.A., 2nd, Hartmann, C., Li, L., Hwang, T.H., Brayton, C.F.*, et al.* (2002). Cbfa1-independent decrease in osteoblast proliferation, osteopenia, and persistent embryonic eye vascularization in mice deficient in Lrp5, a Wnt coreceptor. J Cell Biol *157*, 303-314.

Kaykas, A., Yang-Snyder, J., Heroux, M., Shah, K.V., Bouvier, M., and Moon, R.T. (2004). Mutant Frizzled 4 associated with vitreoretinopathy traps wild-type Frizzled in the endoplasmic reticulum by oligomerization. Nat Cell Biol *6*, 52-58.

Ke, J., Harikumar, K.G., Erice, C., Chen, C., Gu, X., Wang, L., Parker, N., Cheng, Z., Xu, W., Williams, B.O.*, et al.* (2013). Structure and function of Norrin in assembly and activation of a Frizzled 4-Lrp5/6 complex. Genes Dev *27*, 2305-2319.

Kenyon, J.R., and Craig, I.W. (1999). Analysis of the 5' regulatory region of the human Norrie's disease gene: evidence that a non-translated CT dinucleotide repeat in exon one has a role in controlling expression. Gene *227*, 181-188.

Kim, D.H., Inagaki, Y., Suzuki, T., Ioka, R.X., Yoshioka, S.Z., Magoori, K., Kang, M.J., Cho, Y., Nakano, A.Z., Liu, Q.*, et al.* (1998). A new low density lipoprotein receptor related protein, LRP5, is expressed in hepatocytes and adrenal cortex, and recognizes apolipoprotein E. J Biochem *124*, 1072-1076.

Kirikoshi, H., Sagara, N., Koike, J., Tanaka, K., Sekihara, H., Hirai, M., and Katoh, M. (1999). Molecular cloning and characterization of human Frizzled-4 on chromosome 11q14-q21. Biochem Biophys Res Commun *264*, 955-961.

Knoblich, K., Wang, H.X., Sharma, C., Fletcher, A.L., Turley, S.J., and Hemler, M.E. (2013). Tetraspanin TSPAN12 regulates tumor growth and metastasis and inhibits beta-catenin degradation. Cell Mol Life Sci.

Koay, M.A., and Brown, M.A. (2005). Genetic disorders of the LRP5-Wnt signalling pathway affecting the skeleton. Trends Mol Med *11*, 129-137.

Kondo, H., Hayashi, H., Oshima, K., Tahira, T., and Hayashi, K. (2003). Frizzled 4 gene (FZD4) mutations in patients with familial exudative vitreoretinopathy with variable expressivity. Br J Ophthalmol *87*, 1291-1295.

Kondo, H., Kusaka, S., Yoshinaga, A., Uchio, E., Tawara, A., Hayashi, K., and Tahira, T. (2011). Mutations in the TSPAN12 gene in Japanese patients with familial exudative vitreoretinopathy. Am J Ophthalmol *151*, 1095-1100 e1091.

Kondo, H., Ohno, K., Tahira, T., Hayashi, H., Oshima, K., and Hayashi, K. (2001). Delineation of the critical interval for the familial exudative vitreoretinopathy gene by linkage and haplotype analysis. Hum Genet *108*, 368-375.

Kondo, H., Qin, M., Kusaka, S., Tahira, T., Hasebe, H., Hayashi, H., Uchio, E., and Hayashi, K. (2007a). Novel mutations in Norrie disease gene in Japanese patients with

Norrie disease and familial exudative vitreoretinopathy. Invest Ophthalmol Vis Sci *48*, 1276-1282.

Kondo, H., Qin, M., Tahira, T., Uchio, E., and Hayashi, K. (2007b). Severe form of familial exudative vitreoretinopathy caused by homozygous R417Q mutation in frizzled-4 gene. Ophthalmic Genet *28*, 220-223.

Kumar, P., Henikoff, S., and Ng, P.C. (2009). Predicting the effects of coding non-synonymous variants on protein function using the SIFT algorithm. Nat Protoc *4*, 1073-1081.

Laity, J.H., Lee, B.M., and Wright, P.E. (2001). Zinc finger proteins: new insights into structural and functional diversity. Curr Opin Struct Biol *11*, 39-46.

Lander, E.S., Linton, L.M., Birren, B., Nusbaum, C., Zody, M.C., Baldwin, J., Devon, K., Dewar, K., Doyle, M., FitzHugh, W*., et al.* (2001). Initial sequencing and analysis of the human genome. Nature *409*, 860-921.

Laqua, H. (1980). Familial exudative vitreoretinopathy. Albrecht Von Graefes Arch Klin Exp Ophthalmol *213*, 121-133.

Lemma, V., D'Agostino, M., Caporaso, M.G., Mallardo, M., Oliviero, G., Stornaiuolo, M., and Bonatti, S. (2013). A disorder-to-order structural transition in the COOH-tail of Fz4 determines misfolding of the L501fsX533-Fz4 mutant. Sci Rep *3*, 2659.

Lento, W., Congdon, K., Voermans, C., Kritzik, M., and Reya, T. (2013). Wnt signaling in normal and malignant hematopoiesis. Cold Spring Harb Perspect Biol *5*.

Li, Y., Muller, B., Fuhrmann, C., Van Nouhuys, C.E., Laqua, H., Humphries, P., Schwinger, E., and Gal, A. (1992). The autosomal dominant familial exudative vitreoretinopathy locus maps on 11q and is closely linked to D11S533. Am J Hum Genet *51*, 749-754.

Lim, X., and Nusse, R. (2013). Wnt signaling in skin development, homeostasis, and disease. Cold Spring Harb Perspect Biol *5*.

Lin, S., Cheng, M., Dailey, W., Drenser, K., and Chintala, S. (2009). Norrin attenuates protease-mediated death of transformed retinal ganglion cells. Mol Vis *15*, 26-37.

Logan, C.Y., and Nusse, R. (2004). The Wnt signaling pathway in development and disease. Annu Rev Cell Dev Biol *20*, 781-810.

Luhmann, U.F., Lin, J., Acar, N., Lammel, S., Feil, S., Grimm, C., Seeliger, M.W., Hammes, H.P., and Berger, W. (2005a). Role of the Norrie disease pseudoglioma gene in sprouting angiogenesis during development of the retinal vasculature. Invest Ophthalmol Vis Sci *46*, 3372-3382.

Luhmann, U.F., Meunier, D., Shi, W., Luttges, A., Pfarrer, C., Fundele, R., and Berger, W. (2005b). Fetal loss in homozygous mutant Norrie disease mice: a new role of Norrin in reproduction. Genesis *42*, 253-262.

Luhmann, U.F., Neidhardt, J., Kloeckener-Gruissem, B., Schafer, N.F., Glaus, E., Feil, S., and Berger, W. (2008). Vascular changes in the cerebellum of Norrin /Ndph knockout mice correlate with high expression of Norrin and Frizzled-4. Eur J Neurosci *27*, 2619-2628.

MacDonald, B.T., and He, X. (2012). Frizzled and LRP5/6 receptors for Wnt/beta-catenin signaling. Cold Spring Harb Perspect Biol *4*.

McLeod, D.S., Hasegawa, T., Prow, T., Merges, C., and Lutty, G. (2006). The initial fetal human retinal vasculature develops by vasculogenesis. Dev Dyn *235*, 3336-3347.

Meitinger, T., Meindl, A., Bork, P., Rost, B., Sander, C., Haasemann, M., and Murken, J. (1993). Molecular modelling of the Norrie disease protein predicts a cystine knot growth factor tertiary structure. Nat Genet *5*, 376-380.

Miyakubo, H., Hashimoto, K., and Miyakubo, S. (1984). Retinal vascular pattern in familial exudative vitreoretinopathy. Ophthalmology *91*, 1524-1530.

Miyakubo, H., Inohara, N., and Hashimoto, K. (1982). Retinal involvement in familial exudative vitreoretinopathy. Ophthalmologica *185*, 125-135.

Muller, M., Kusserow, C., Orth, U., Klar-Dissars, U., Laqua, H., and Gal, A. (2008). [Mutations of the frizzled-4 gene. Their impact on medical care of patients with autosomal dominant exudative vitreoretinopathy]. Ophthalmologe *105*, 262-268.

Nallathambi, J., Shukla, D., Rajendran, A., Namperumalsamy, P., Muthulakshmi, R., and Sundaresan, P. (2006). Identification of novel FZD4 mutations in Indian patients with familial exudative vitreoretinopathy. Mol Vis *12*, 1086-1092.

Nikopoulos, K., Gilissen, C., Hoischen, A., Van Nouhuys, C.E., Boonstra, F.N., Blokland, E.A., Arts, P., Wieskamp, N., Strom, T.M., Ayuso, C.*, et al.* (2010a). Next-generation sequencing of a 40 Mb linkage interval reveals TSPAN12 mutations in patients with familial exudative vitreoretinopathy. Am J Hum Genet *86*, 240-247.

Nikopoulos, K., Venselaar, H., Collin, R.W., Riveiro-Alvarez, R., Boonstra, F.N., Hooymans, J.M., Mukhopadhyay, A., Shears, D., van Bers, M., de Wijs, I.J.*, et al.* (2010b). Overview of the mutation spectrum in familial exudative vitreoretinopathy and Norrie disease with identification of 21 novel variants in FZD4, LRP5, and NDP. Hum Mutat *31*, 656-666.

Ober, R.R., Bird, A.C., Hamilton, A.M., and Sehmi, K. (1980). Autosomal dominant exudative vitreoretinopathy. Br J Ophthalmol *64*, 112-120.

Ohlmann, A., Scholz, M., Goldwich, A., Chauhan, B.K., Hudl, K., Ohlmann, A.V., Zrenner, E., Berger, W., Cvekl, A., Seeliger, M.W.*, et al.* (2005). Ectopic norrin induces growth of ocular capillaries and restores normal retinal angiogenesis in Norrie disease mutant mice. J Neurosci *25*, 1701-1710.

Ohlmann, A., Seitz, R., Braunger, B., Seitz, D., Bosl, M.R., and Tamm, E.R. (2010). Norrin promotes vascular regrowth after oxygen-induced retinal vessel loss and suppresses retinopathy in mice. J Neurosci *30*, 183-193.

Ohlmann, A.V., Adamek, E., Ohlmann, A., and Lutjen-Drecoll, E. (2004). Norrie gene product is necessary for regression of hyaloid vessels. Invest Ophthalmol Vis Sci *45*, 2384-2390.

Omoto, S., Hayashi, T., Kitahara, K., Takeuchi, T., and Ueoka, Y. (2004). Autosomal dominant familial exudative vitreoretinopathy in two Japanese families with FZD4 mutations (H69Y and C181R). Ophthalmic Genet *25*, 81-90.

Paes, K.T., Wang, E., Henze, K., Vogel, P., Read, R., Suwanichkul, A., Kirkpatrick, L.L., Potter, D., Newhouse, M.M., and Rice, D.S. (2011). Frizzled 4 is required for retinal angiogenesis and maintenance of the blood-retina barrier. Invest Ophthalmol Vis Sci *52*, 6452-6461.

Pelcastre, E.L., Villanueva-Mendoza, C., and Zenteno, J.C. (2010). Novel and recurrent NDP gene mutations in familial cases of Norrie disease and X-linked exudative vitreoretinopathy. Clin Experiment Ophthalmol *38*, 367-374.

Pendergast, S.D., and Trese, M.T. (1998). Familial exudative vitreoretinopathy. Results of surgical management. Ophthalmology *105*, 1015-1023.

Perez-Vilar, J., and Hill, R.L. (1997). Norrie disease protein (norrin) forms disulfide-linked oligomers associated with the extracellular matrix. J Biol Chem *272*, 33410-33415.

Poulter, J.A., Ali, M., Gilmour, D.F., Rice, A., Kondo, H., Hayashi, K., Mackey, D.A., Kearns, L.S., Ruddle, J.B., Craig, J.E.*, et al.* (2010). Mutations in TSPAN12 cause autosomal-dominant familial exudative vitreoretinopathy. Am J Hum Genet *86*, 248-253.

Poulter, J.A., Davidson, A.E., Ali, M., Gilmour, D.F., Parry, D.A., Mintz-Hittner, H.A., Carr, I.M., Bottomley, H.M., Long, V.W., Downey, L.M.*, et al.* (2012). Recessive mutations in TSPAN12 cause retinal dysplasia and severe familial exudative vitreoretinopathy (FEVR). Invest Ophthalmol Vis Sci *53*, 2873-2879.

Qin, M., Hayashi, H., Oshima, K., Tahira, T., Hayashi, K., and Kondo, H. (2005). Complexity of the genotype-phenotype correlation in familial exudative vitreoretinopathy with mutations in the LRP5 and/or FZD4 genes. Hum Mutat *26*, 104-112.

Qin, M., Kondo, H., Tahira, T., and Hayashi, K. (2008). Moderate reduction of Norrin signaling activity associated with the causative missense mutations identified in patients with familial exudative vitreoretinopathy. Hum Genet *122*, 615-623.

Ranchod, T.M., Ho, L.Y., Drenser, K.A., Capone, A., Jr., and Trese, M.T. (2011). Clinical presentation of familial exudative vitreoretinopathy. Ophthalmology *118*, 2070-2075.

Rehm, H.L., Zhang, D.S., Brown, M.C., Burgess, B., Halpin, C., Berger, W., Morton, C.C., Corey, D.P., and Chen, Z.Y. (2002). Vascular defects and sensorineural deafness in a mouse model of Norrie disease. J Neurosci *22*, 4286-4292.

Richter, M., Gottanka, J., May, C.A., Welge-Lussen, U., Berger, W., and Lutjen-Drecoll, E. (1998). Retinal vasculature changes in Norrie disease mice. Invest Ophthalmol Vis Sci *39*, 2450-2457.

Robitaille, J., MacDonald, M.L., Kaykas, A., Sheldahl, L.C., Zeisler, J., Dube, M.P., Zhang, L.H., Singaraja, R.R., Guernsey, D.L., Zheng, B.*, et al.* (2002). Mutant frizzled-4 disrupts retinal angiogenesis in familial exudative vitreoretinopathy. Nat Genet *32*, 326-330.

Robitaille, J.M., Wallace, K., Zheng, B., Beis, M.J., Samuels, M., Hoskin-Mott, A., and Guernsey, D.L. (2009). Phenotypic overlap of familial exudative vitreoretinopathy (FEVR) with persistent fetal vasculature (PFV) caused by FZD4 mutations in two distinct pedigrees. Ophthalmic Genet *30*, 23-30.

Robitaille, J.M., Zheng, B., Wallace, K., Beis, M.J., Tatlidil, C., Yang, J., Sheidow, T.G., Siebert, L., Levin, A.V., Lam, W.C.*, et al.* (2011). The role of Frizzled-4 mutations in familial exudative vitreoretinopathy and Coats disease. Br J Ophthalmol *95*, 574-579.

Saint-Geniez, M., and D'Amore, P.A. (2004). Development and pathology of the hyaloid, choroidal and retinal vasculature. Int J Dev Biol *48*, 1045-1058.

Sambrook, J., Fritsch, E.F., and Maniatis, T. (1989). Molecular Cloning: A Laboratory Manual (Cold Spring Harbor laboratory Press).

Schafer, N.F., Luhmann, U.F., Feil, S., and Berger, W. (2009). Differential gene expression in Ndph-knockout mice in retinal development. Invest Ophthalmol Vis Sci *50*, 906-916.

Schuback, D.E., Chen, Z.Y., Craig, I.W., Breakefield, X.O., and Sims, K.B. (1995). Mutations in the Norrie disease gene. Hum Mutat *5*, 285-292.

Schulte, G. (2010). International Union of Basic and Clinical Pharmacology. LXXX. The class Frizzled receptors. Pharmacol Rev *62*, 632-667.

Seitz, R., Hackl, S., Seibuchner, T., Tamm, E.R., and Ohlmann, A. (2010). Norrin mediates neuroprotective effects on retinal ganglion cells via activation of the Wnt/beta-catenin signaling pathway and the induction of neuroprotective growth factors in Muller cells. J Neurosci *30*, 5998-6010.

Shastry, B.S. (1998). Identification of a recurrent missense mutation in the Norrie disease gene associated with a simplex case of exudative vitreoretinopathy. Biochem Biophys Res Commun *246*, 35-38.

Shastry, B.S., Hejtmancik, J.F., and Trese, M.T. (1997). Identification of novel missense mutations in the Norrie disease gene associated with one X-linked and four sporadic cases of familial exudative vitreoretinopathy. Hum Mutat *9*, 396-401.

Shukla, D., Singh, J., Sudheer, G., Soman, M., John, R.K., Ramasamy, K., and Perumalsamy, N. (2003). Familial exudative vitreoretinopathy (FEVR). Clinical profile and management. Indian J Ophthalmol *51*, 323-328.

Shukla, S.Y., Kaliki, S., and Shields, C.L. (2012). Asymmetry of familial exudative vitreoretinopathy. J Pediatr Ophthalmol Strabismus *49 Online*, e5-8.

Smallwood, P.M., Williams, J., Xu, Q., Leahy, D.J., and Nathans, J. (2007). Mutational analysis of Norrin-Frizzled4 recognition. J Biol Chem *282*, 4057-4068.

Stahl, A., Connor, K.M., Sapieha, P., Chen, J., Dennison, R.J., Krah, N.M., Seaward, M.R., Willett, K.L., Aderman, C.M., Guerin, K.I.*, et al.* (2010). The mouse retina as an angiogenesis model. Invest Ophthalmol Vis Sci *51*, 2813-2826.

Stone, J., Itin, A., Alon, T., Pe'er, J., Gnessin, H., Chan-Ling, T., and Keshet, E. (1995). Development of retinal vasculature is mediated by hypoxia-induced vascular endothelial growth factor (VEGF) expression by neuroglia. J Neurosci *15*, 4738-4747.

Strauss, O. (2005). The retinal pigment epithelium in visual function. Physiol Rev *85*, 845-881.

Tagami, M., Kusuhara, S., Honda, S., Tsukahara, Y., and Negi, A. (2008). Rapid regression of retinal hemorrhage and neovascularization in a case of familial exudative vitreoretinopathy treated with intravitreal bevacizumab. Graefes Arch Clin Exp Ophthalmol *246*, 1787-1789.

Talks, S.J., Ebenezer, N., Hykin, P., Adams, G., Yang, F., Schulenberg, E., Gregory-Evans, K., and Gregory-Evans, C.Y. (2001). De novo mutations in the 5' regulatory region of the Norrie disease gene in retinopathy of prematurity. J Med Genet *38*, E46.

Tam, S.J., and Watts, R.J. (2010). Connecting vascular and nervous system development: angiogenesis and the blood-brain barrier. Annu Rev Neurosci *33*, 379-408.

Tasman, W., Augsburger, J.J., Shields, J.A., Caputo, A., and Annesley, W.H., Jr. (1981). Familial exudative vitreoretinopathy. Trans Am Ophthalmol Soc *79*, 211-226.

Thompson, J.D., Gibson, T.J., and Higgins, D.G. (2002). Multiple sequence alignment using ClustalW and ClustalX. Curr Protoc Bioinformatics *Chapter 2*, Unit 2 3.

Tokunaga, C.C., Chen, Y.H., Dailey, W., Cheng, M., and Drenser, K.A. (2013). Retinal vascular rescue of oxygen-induced retinopathy in mice by norrin. Invest Ophthalmol Vis Sci *54*, 222-229.

Toomes, C., Bottomley, H.M., Jackson, R.M., Towns, K.V., Scott, S., Mackey, D.A., Craig, J.E., Jiang, L., Yang, Z., Trembath, R.*, et al.* (2004a). Mutations in LRP5 or FZD4 underlie the common familial exudative vitreoretinopathy locus on chromosome 11q. Am J Hum Genet *74*, 721-730.

Toomes, C., Bottomley, H.M., Scott, S., Mackey, D.A., Craig, J.E., Appukuttan, B., Stout, J.T., Flaxel, C.J., Zhang, K., Black, G.C.*, et al.* (2004b). Spectrum and frequency of FZD4 mutations in familial exudative vitreoretinopathy. Invest Ophthalmol Vis Sci *45*, 2083-2090.

Toomes, C., Downey, L.M., Bottomley, H.M., Scott, S., Woodruff, G., Trembath, R.C., and Inglehearn, C.F. (2004c). Identification of a fourth locus (EVR4) for familial exudative vitreoretinopathy (FEVR). Mol Vis *10*, 37-42.

Torrente, I., Mangino, M., Gennarelli, M., Novelli, G., Giannotti, A., Vadala, P., and Dallapiccola, B. (1997). Two new missense mutations (A105T and C110G) in the norrin gene in two Italian families with Norrie disease and familial exudative vitreoretinopathy. Am J Med Genet *72*, 242-244.

Umbhauer, M., Djiane, A., Goisset, C., Penzo-Mendez, A., Riou, J.F., Boucaut, J.C., and Shi, D.L. (2000). The C-terminal cytoplasmic Lys-thr-X-X-X-Trp motif in frizzled receptors mediates Wnt/beta-catenin signalling. EMBO J *19*, 4944-4954.

van Amerongen, R., Mikels, A., and Nusse, R. (2008). Alternative wnt signaling is initiated by distinct receptors. Sci Signal *1*, re9.

Van Nouhuys, C.E. (1981). Congenital retinal fold as a sign of dominant exudative vitreoretinopathy. Albrecht Von Graefes Arch Klin Exp Ophthalmol *217*, 55-67.

Van Nouhuys, C.E. (1991). Signs, complications, and platelet aggregation in familial exudative vitreoretinopathy. Am J Ophthalmol *111*, 34-41.

Wang, Y., Huso, D., Cahill, H., Ryugo, D., and Nathans, J. (2001). Progressive cerebellar, auditory, and esophageal dysfunction caused by targeted disruption of the frizzled-4 gene. J Neurosci *21*, 4761-4771.

Wang, Y., Rattner, A., Zhou, Y., Williams, J., Smallwood, P.M., and Nathans, J. (2012). Norrin/Frizzled4 signaling in retinal vascular development and blood brain barrier plasticity. Cell *151*, 1332-1344.

Warburg, M. (1965). Norrie's disease. Trans Ophthalmol Soc U K *85*, 391-408.

Wu, W.C., Drenser, K., Trese, M., Capone, A., Jr., and Dailey, W. (2007). Retinal phenotype-genotype correlation of pediatric patients expressing mutations in the Norrie disease gene. Arch Ophthalmol *125*, 225-230.

Xia, C.H., Liu, H., Cheung, D., Wang, M., Cheng, C., Du, X., Chang, B., Beutler, B., and Gong, X. (2008). A model for familial exudative vitreoretinopathy caused by LPR5 mutations. Hum Mol Genet *17*, 1605-1612.

Xia, C.H., Yablonka-Reuveni, Z., and Gong, X. (2010). LRP5 is required for vascular development in deeper layers of the retina. PLoS One *5*, e11676.

Xu, Q., Wang, Y., Dabdoub, A., Smallwood, P.M., Williams, J., Woods, C., Kelley, M.W., Jiang, L., Tasman, W., Zhang, K.*, et al.* (2004). Vascular development in the retina and inner ear: control by Norrin and Frizzled-4, a high-affinity ligand-receptor pair. Cell *116*, 883-895.

Yamada, K., Limprasert, P., Ratanasukon, M., Tengtrisorn, S., Yingchareonpukdee, J., Vasiknanonte, P., Kitaoka, T., Ghadami, M., Niikawa, N., and Kishino, T. (2001). Two Thai families with Norrie disease (ND): association of two novel missense mutations with severe ND phenotype, seizures, and a manifesting carrier. Am J Med Genet *100*, 52-55.

Yang, H., Li, S., Xiao, X., Guo, X., and Zhang, Q. (2012a). Screening for NDP mutations in 44 unrelated patients with familial exudative vitreoretinopathy or Norrie disease. Curr Eye Res *37*, 726-729.

Yang, H., Li, S., Xiao, X., Wang, P., Guo, X., and Zhang, Q. (2012b). Identification of FZD4 and LRP5 mutations in 11 of 49 families with familial exudative vitreoretinopathy. Mol Vis *18*, 2438-2446.

Yang, H., Xiao, X., Li, S., Mai, G., and Zhang, Q. (2011). Novel TSPAN12 mutations in patients with familial exudative vitreoretinopathy and their associated phenotypes. Mol Vis *17*, 1128-1135.

Ye, X., Smallwood, P., and Nathans, J. (2011). Expression of the Norrie disease gene (Ndp) in developing and adult mouse eye, ear, and brain. Gene Expr Patterns *11*, 151-155.

Ye, X., Wang, Y., Cahill, H., Yu, M., Badea, T.C., Smallwood, P.M., Peachey, N.S., and Nathans, J. (2009). Norrin, frizzled-4, and Lrp5 signaling in endothelial cells controls a genetic program for retinal vascularization. Cell *139*, 285-298.

Ye, X., Wang, Y., and Nathans, J. (2010). The Norrin/Frizzled4 signaling pathway in retinal vascular development and disease. Trends Mol Med *16*, 417-425.

Yoshida, S., Arita, R., Yoshida, A., Tada, H., Emori, A., Noda, Y., Nakao, S., Fujisawa, K., and Ishibashi, T. (2004). Novel mutation in FZD4 gene in a Japanese pedigree with familial exudative vitreoretinopathy. Am J Ophthalmol *138*, 670-671.

Zeng, X., Tamai, K., Doble, B., Li, S., Huang, H., Habas, R., Okamura, H., Woodgett, J., and He, X. (2005). A dual-kinase mechanism for Wnt co-receptor phosphorylation and activation. Nature *438*, 873-877.

Zhang, K., Harada, Y., Wei, X., Shukla, D., Rajendran, A., Tawansy, K., Bedell, M., Lim, S., Shaw, P.X., He, X.*, et al.* (2011). An essential role of the cysteine-rich domain of FZD4 in Norrin/Wnt signaling and familial exudative vitreoretinopathy. J Biol Chem *286*, 10210-10215.

Zhang, Y., Wang, Y., Li, X., Zhang, J., Mao, J., Li, Z., Zheng, J., Li, L., Harris, S., and Wu, D. (2004). The LRP5 high-bone-mass G171V mutation disrupts LRP5 interaction with Mesd. Mol Cell Biol *24*, 4677-4684.

Table 1. List of the primer sequences used for amplifying the candidate genes

Gene	Location	Primer sequence (5'-3')	Amplicon size	Annealing temperature (°C)	$MgCl_2$ final concentration (mM)
NDP	Exon 1	1F-GCGCCTCACATTTCCGTGGC 1R-TCCTAGGCAAGCCGGCAGC	352	58	1.5
	Exon 2	2F-GGAGGTGAAGCCATTTCCAATT 2R-CTTGCCTGTTTCTGAGGG	499	58	1.5
	Exon 3	3.1F-CCTGGCTAAGGTTGTGGC 3.1R-CACAGCAGCGGGCCTCAG	297	54	1.5
	Exon 3	3.2F-CCAGACTTCCAAGCTGAAGG 3.2R-ACCAAACACTGACAGCCTGA	458	58	1.5
	Exon 3	3.3F-TTGGCTCTCAATGCTGTTTG 3.3R-GCTGTCAAGAGTTCCAGCATC	349	59	1.5
	Exon 3	3.4F-CAGCCAGCGAACTGACATTA 3.4R-TTAGAGAATGATGCCCGTGA	348	58	1.5
	Exon 3	3.5F-GCATGCAAATTAGACAACCAA 3.5R-AGGAGATGCTCAAGCACTAGC	312	58	1.5

Gene	Location	Primer sequence (5'-3')	Amplicon size	Annealing temperature (°C)	$MgCl_2$ final concentration (mM)
FZD4	Exon1	1F-GTGCAAACTGGGGGTGTCTG 1R-TAGCCCGAAGGAGACAGCTC	460	61	1.5
	Exon 2	2.1F-TCAACTCAGCTTTGTGGGAGC 2.1R-GCGGCTGTATAAGCCAGCAT	436	61	1.5
	Exon 2	2.2F-CAGGTGATGAAGAGGTGCCC 2.2R-TCCTTTCCCGGCCTACAGTC	354	61	1.5
	Exon 2	2.3F-GTTTTCCTACCCTGAGCGCC 2.3R-CGGTGAGGGCATCGAGATTT	425	63	1.5
	Exon 2	2.4F-CATCCCCGCAGTGAAAACCA 2.4R-CATGCCTGAAGTGATGCCCA	421	61	1.5
	Exon 2	2.5F-GCAACGTGTGTGATTGCCTG 2.5R-TTTTTGATGCTGGGGTCGGG	440	61	1.5

Gene	Location	Primer sequence (5'-3')	Amplicon size	Annealing temperature (°C)	$MgCl_2$ final concentration (mM)
TSPAN12	Exon 2	2F-ATGTCCCGTGTTCTCTCTCC 2R-CCAGGGGTGGATTTCTTTGT	382	55	1.5
	Exon 3	3F-CAAGATGCAGCAAATGGTAA 3R-TCCAAAAGATCAAGGAAGAGC	306	48	2
	Exon 4	4F-TGAGGCATCATGATTGAAAG 4R-CACTGCTCCCTAATCTTGTGA	341	52	1.5
	Exon 5	5F-AGGGGCTTCATGAAAACTTG 5R-GCGGAGTGAAAATGAACTAACA	285	57	1.5
	Exon 6	6F-GACATTCCGAGTATGCGTGT 6R-GCAGGCCATGAAGTTACCTA	392	60	1.5
	Exon 7	7F-TGTGGTTTCTGAGGCTGACT 7R-TTCTTCTGCTTCTCCCCATA	330	55	1.5
	Exon 8	8.1F-GCTTTCCCTGAGAACCACTG 8.1R-AAGCTGTTTGCCATGGATGT	420	52	2
	Exon 8	8.2F-GGGGACAGACCAAATGATGT 8.2R-TGTCCAGGTGGTGACTTATGA	341	51	1.5
	Exon 8	8.3F-CTTGTTTTACTGGACTTGTGAA 8.3R-ATCAGAAGAATAGATCGCTGAG	428	52	1.5
	Exon 8	8.4F-TGGAGCCATAGTAAAGGTTGAT 8.4R-TGTGTAATATAAGCCCAGGACA	419	55	1.5
	Exon 8	8.5F-ATTTGTCCTGTATAGCATCATT 8.5R-TGATTCTCACAAGCATTTTTC	386	50	1.5
	Exon 8	8.6F-GCTTATCTTTGCCTTCTCCAAA 8.6R-GTGGCATAAGTGCTTGTAATGT	3654	55	1.5

Gene	Location	Primer sequence (5'-3')	Amplicon size	Annealing temperature (°C)	$MgCl_2$ final concentration (mM)
ZNF408	Exon 1	1F- TATCCCCAACCATTTCCGCC 1R- CTGAGGAGAAAGCTGACCACA	532	60	1.5
	Exon 2	2F- CGGTTTCCTCCCACACTTTTC 2R-GCTGTCTAGCAATGTCCAAACC	423	50	1.5
	Exon 3	3F- GGCTTCTAACCTTCCAGGAGT 3R- CCAAGCAGTCTGGGTCCTAA	333	58	1.5
	Exon 4	4F-GAATGTTCCAAAGGCACGGC 4R-AATCAAGCCCCACCCTCCTA	556	60	1.5
	Exon 5	5.1F-CATTGCTCCCTCTAAGGCTCA 5.1R-TGCTTCTTTAGGTGGCACAGC	578	56	1.5
	Exon 5	5.2F-AGTCTGGCTTCCCTACACTCT 5.2R-CAAATGCCCACGCAGGTTG	560	56	1.5
	Exon 5	5.3F-GCTCCATACAGGAGAAAAGCCT 5.3R-TGACCTCAACAACATCCCTGG	566	56	1.5
	Exon 5	5.4F-GTGCCTTCTGCTGCTTCTG 5.4R-AGCTCTACCGGATGTCAATTCAA	469	59	1.5

Primer sequences represented by * were taken from a published report by Meindl *et al*., (1992). Remaining primer sequences were designed by using primer-blast (http://www.ncbi.nlm.nih.gov/tools/primer-blast/).

Extraction of genomic DNA by using Sigma-Aldrich Gen Elute^{TM} blood genomic DNA kit

The principle involved in this method of DNA extraction is as follows: the negatively charged DNA molecules present in a cell lysate are separated while passing through a positively charged silica column. Later, the affinity-bound DNA molecules are eluted by altering the pH of the column with an elution buffer.

The reagents provided along with the kit were:

1. Resuspension solution
2. Lysis solution C
3. Column preparation solution
4. Pre wash solution concentrate
5. Wash solution concentrate
6. Elution solution
7. Proteinase K
8. RNase A solution
9. Binding columns
10. Collection tubes (2 mL capacity)

Pre dilution of reagent concentrates:

1. Dilution of pre wash solution concentrate

To prepare 50 mL of working solution, 22.5 mL of prewash solution concentrate was diluted with 27.5 mL of 95-100% ethanol.

2. Dilution of wash solution concentrate

20 mL of wash solution concentrate was diluted in 80 mL of 95-100% ethanol for the preparation of 100 mL of wash solution.

3. Proteinase K

A stock solution of Proteinase K (20mg/mL) was prepared by dissolving 10 mg powder in 0.5 mL of sterile water and stored at -20 ^{0}C.

Protocol:

a. 200 µL of thawed whole blood sample was transferred to a 1.5 mL centrifuge tube and 200 µL of lysis solution C was added to it. The blood suspension was vortexed thoroughly for 15 seconds to obtain a homogenous mixture.

b. 20 µL of Proteinase K solution was added to the blood suspension and vortexed for thorough mixing of the enzyme. Following this step, the blood sample was incubated at 55^{0} C for 10 minutes.

c. After incubation, 20 µL of RNase A solution was added and incubated for 2 minutes at room temperature.

d. 200 µL of 95-100% ethanol was added to the lysate and mixed thoroughly by vortexing for 5-10 seconds. The lysate was then loaded into a pre-activated silica column.

Column preparation: 500 µL of the column preparation solution was added to each pre-assembled GenElute Miniprep binding column and centrifuged at 12,000g for 1 small minute. After centrifugation, the flow-through liquid was discarded and the column was used for loading blood lysate solution.

e. After loading blood lysate solution, the column was centrifuged at 6,500g for 1 minute and the collection tube containing flow-through liquid was discarded.

f. The column was placed in a new collection tube and 500 µL of the prewash solution was transferred into the column and centrifuged at 6,500g for 1 min.

After centrifugation, the flow-through liquid was discarded and the column was placed in a new collection tube. Washing with pre-wash solution is useful to remove the contaminants associated with the stored blood sample.

g. 500 µL of the wash solution was added into the column and centrifuged at 12,000g for 3 minutes. After discarding the flow-through, to ensure that the column was free from ethanol, it was again centrifuged for a few minutes (3-4 min) at maximum speed.

h. The dried column was placed in a new collection tube and 200 µL of warmed elution buffer was added directly into the center of the column. To elute the DNA the column was centrifuged at 6,500g for 1minute.

i. The obtained eluent containing pure genomic DNA was aliquoted and stored at -20^0 C. Prior to storage, the concentration and purity of the obtained DNA was measured.

Reagents used in DNA extraction

1.1 . 10X phosphate buffered saline (PBS) preparation

8 grams of sodium chloride (NaCl), 0.2 grams of potassium chloride (KCl), 1.44 grams of sodium biphosphate (Na_2HPO4) and 0.24 grams of potassium dihydrogen phosphate (KH_2PO_4; Qualigens Fine Chemicals, Mumbai, India) were added to 800 milliliters (mL) of Mille Q water. The pH of the solution was adjusted to 7.4 with 1M hydrochloric acid. The final volume of the solution was made to 1000 mL with Mille Q water. The prepared solution was autoclaved for 20 min at 15 pounds per square inch (psi) pressure and stored at 4°C temperature.

1.2. Extraction buffer preparation

1 mL of 1M Tris chloride buffer (Tris-Cl) (pH 8.0), 20 mL of 0.5 M ethylene diamine tetra acetate (EDTA;) and 5 mL of 10 % sodium dodecyl sulphate (SDS) were added to 74 mL of autoclaved Mille Q water to make the final volume up to 100 mL.

1.3 . Proteinase K

100 mg of proteinase K (lyophilized powder) was added to 5 ml of autoclaved Mille Q water to make a solution with a concentration of 20 mg/ ml.

1.4. Equilibrated phenol preparation

To 500 mL of melted phenol (Sigma-Aldrich, St Louis, USA) at room temperature, an equal volume (500 mL) of 0.5 M Tris-Cl (pH-8) was added and mixed thoroughly by using a magnetic stirrer for 15 minutes. Then, the solution was allowed to stand still for the separation of two phases. After phase separation, upper aqueous phase of Tris-Cl was removed by gentle aspiration with pipette aid. The same procedure was carried out with 0.1 M Tris-Cl until the phenol reaches to the pH of 8. After equilibration, the final aqueous phase had been removed and 0.1 volume (500 µL) of 0.1 M Tris-Cl containing 0.2% β-mercaptoethanol was added to prevent oxidation of phenol during storage at 4°C.

Preparation of reagents used for agarose gel electrophoresis

1.1 50X TAE (Tris- acetate EDTA)

242 g of Tris-base and 100 ml of 0.5M EDTA were added to 800 mL of autoclaved Mille Q water and allowed to dissolve on a magnetic stirrer. To this, 57.2 ml of glacial acetic acid was added and the volume was made up to 1 liter with Mille Q water. The contents were thoroughly mixed until the entire salt was completely dissolved. The prepared solution was stored at room temperature.

1.2 EtBr (Ethidium Bromide)

1 g of Ethidium Bromide was mixed in 100 ml of autoclaved Mille Q water to obtain 10 mg/ml concentration. The solution was stored in a light tight bottle at room temperature.

1.3 6X loading dye

40 g of sucrose, 0.025 g of Xylene cyanol and 0.025 g of Bromophenol blue were gently mixed in 100 mL of Mille Q water and stored at room temperature.

1.4 30% acrylamide (acrylamide:bisacrylamide, 29:1)

29 g of acrylamide and 1g of N,N-Methylenebisacrylamide was added to Mille Q water to make a stock solution of 100 ml. The solution was stirred continuously until a homogenous mixture was obtained.

Preparation of reagents used for PAGE

1.1 10X TBE (Tris-Borate EDTA)

54 g of Tris-base, 27.5 g of boric acid and 20 ml of 0.5 M EDTA (pH 8) were added to 900 ml of Mille Q water and allowed to dissolve on a magnetic stirrer. The final volume of the solution was made up to 1 liter with Mille Q water.

1.2 0.5 M EDTA

186.1 g of ethylene diamine tetra acetate (EDTA) was added to 800 ml of double distilled water and stirred vigorously on a magnetic stirrer. The pH was adjusted to 8.0 with sodium hydroxide NaOH pellets (approximately 20 g of pellets). The solution was sterilized by autoclaving and stored at room temperature.

1.3 10% APS (Ammonium per sulphate)

0.1 g of APS was added to 1 ml of Mille Q water in a 1.5 ml centrifuge tube and mixed thoroughly by vortexing the tube. The tube was wrapped with aluminum foil and stored at 4˚C.

Protocol for PCR product purification by using Nucleospin extract II columns

a. The PCR amplicons were diluted with sterile deionized water to a total volume of 100 µL.

b. 200 µL of binding buffer was mixed with the PCR amplicons and transferred to the centre of a nucleic acid binding column placed in a 2 mL collection tube.

c. The tubes were centrifuged for 1 minute at a speed of 11,000 x g. The flow-through was discarded and the column was again placed in the collection tube.

d. The columns were then washed twice with 700 µL of 1x wash buffer followed by centrifugation at 11,000 x g for 1 min.

e. After washing, the columns were dried by further centrifugation at 11,000 x g for 2 minutes.

f. Avoiding contact with the flow-through liquid, the columns were transferred to a new 1.5 mL microfuge tube and 15-30 µL of deionized water was added at the centre of the column for elution of the PCR amplicons.

g. To collect the eluent, the microfuge tubes were centrifuged at 11,000 x g for 1 min. The eluent was checked for purity using agarose gel electrophoresis as described previously.

Protocol for precipitation of sequencing PCR product

a. The 96-well PCR plate in which the sequencing PCR had carried out was briefly centrifuged at 100g for one minute.

b. 1 µL of 125 mM EDTA (pH 8.0) was added to each well, briefly mixed on a shaker and centrifuged at 100 g for one minute.

c. 1 µL of 3M sodium acetate (pH 4.6) was mixed in each well, followed by 25 µL of 100% ethanol. The plate was sealed with aluminum foil to prevent the ethanol evaporation and gently mixed on a shaker for 5 min.

d. After a gentle mixing, the plates were incubated on ice for 15 minutes for complete precipitation. After incubation, the plates were centrifuged at 3000 g for 30 minutes at 4°C.

e. Following centrifugation, the plate was gently inverted onto tissue paper and a pop spin was given at 185 g for 1 min to remove the leftover supernatant at the bottom of the plate.

f. The precipitated DNA was washed with 35 µL of 70% ethanol by centrifugation at 3000 g for 15 minutes.

g. Following centrifugation, the supernatant was decanted by inverting the plate on a tissue towel and a pop spin was given at 185 g for 1 min.

h. To remove the ethanol remnants, the plate was air dried for 5-10 minutes.

Protocol for Restriction digestion

a. Suitable restriction enzymes with 4-8 bp length recognition sites and specificity for the variation containing nucleotide sequence were selected using online Neb cutter 2 program (http://tools.neb.com/NEBcutter2/, Vincze *et al*., 2003).

b. A 10 µL reaction mixture was prepared in a 0.2 mL microfuge tube using 3-4 µL of PCR product, 2-3 units of the enzyme and 1X enzyme compatible buffer. The final volume was made up to 10 µL with autoclaved Mille Q water.

c. The tubes were incubated for an appropriate time at optimum temperature as recommended by the enzyme manufacturer. The reaction mixture was intermittently vortexed during incubation to achieve a complete digestion.

d. After incubation the reaction mixtures were analyzed using polyacrylamide gel electrophoresis. The details of the restriction enzymes used are listed in table 1.

Table 1: Restriction enzymes used to analyze genetic variants

Restriction enzyme (units/µl)	Cutting site	Optimum temperature and time for digestion	Product manufacture
Mn1I (10 U/ µL)	CCTC/	37°C, 16hrs	Fermentas

INFORMED CONSENT FOR COLLECTION OF BLOOD SAMPLES FOR RESEARCH

I hereby consent to the collection of the blood sample of myself/my child or ward, by staff of the L.V. Prasad Eye Institute on the understanding that:

This sample is being collected solely for the purpose of research. The research pertains to eye diseases that are known to or might potentially run in families. The procedure for sample collection involves withdrawal of a few ml. of blood. This type of study generally involves a few or more families in which individuals have the same ailment. No harm shall come to me (my child/ward) by providing the sample. The results of the study will not be of immediate benefit to the patient. Complete confidentiality will be maintained in the handling and processing of samples. The above statement has been read out or explained to me and having understood the same. I put my signature or thumb impression.

Patient's name:

MR no:

Date:

Signature/Left hand thumb impression of patient/Guardian

Name (capitals):

Relationship (if guardian):

Witness 1: Signature

Name (capitals):

Designation

1. **Ganeswara Rao Musada**, Subhadra Jalali, Anjli Hussain, Anupama Reddy Chururu, Pramod Reddy Gaddam, Subhabrata Chakrabarti, Inderjeet Kaur. *Mutation spectrum of the Norrie disease pseudoglioma (NDP) gene in a large cohort of Indian retinopathy of prematurity and familial exudative vitreo retinopathy patients* (submitted to Molecular Vision journal and it is under revision)

2. **Ganeswara Rao Musada**, Syed Hameed, Subhadra Jalali, Subhabrata Chakrabarti, Inderjeet Kaur. *Mutations in the ZNF408 gene are involved in Indian familial exudative vitreoretinopathy patients* (submitted as a brief report in the journal of Medical Genetics)

3. **Ganeswara Rao Musada**, Subhadra Jalali, Subhabrata Chakrabarti, Inderjeet Kaur. *Mutation spectrum of Frizzled-4 (FZD4) and TSPAN12 genes in Indian familial exudative vitreoretinopathy patients.* (in the process of submission to Investigative ophthalmology & visual science journal)

1. **Ganeswara R. Musada**, Subhadra Jalali, Padmaja K. Rani, Anupama R. Chururu, Pramod R. Gaddam, Subhabrata Chakrabarti and Inderjeet Kaur. *Molecular genetic analysis of Norrie Disease Pseudoglioma (NDP) gene in Indian Familial Exudative Vitreoretinopathy (FEVR) and Retinopathy of Prematurity (ROP) patients* (Invest Ophthalmol Vis Sci 2012; 53: E-Abstract 1580).

2. Sonika rathi, Subhabrata Chakrabarti, **Ganeswara R. Musada**, Subhadra Jalali, Ramesh Kekunnaya and Inderjeet Kaur. Quantitative Analysis of Vitreous Humor Reveals Distinct Protein Profiles in Patients with Retinopathy of Prematurity (Invest Ophthalmol Vis Sci 2013; 54: E-Abstract 587).

3. Inderjeet Kaur, Sonika rathi, **Ganeswara R. Musada**, Subhadra Jalali, Ramesh Kekunnaya and Subhabrata Chakrabarti. Genetic Screening of *TSPAN12, NDP* and *FZD4* Genes in Indian Patients with Retinopathy of Prematurity (Invest Ophthalmol Vis Sci 2013; 54: E-Abstract 6204)

4. Inderjeet Kaur, Sonika Rathi, **Ganeswara R. Musada**, Subhadra Jalali, Ramesha Kekunnaya, Padmaja K. Rani and Subhabrata Chakrabarti. Molecular Genetic and Functional Analysis in a Large Cohort Indicate Novel Genes in Retinopathy of Prematurity (Invest Ophthalmol Vis Sci 2011;52: E-Abstract 3996).

1. Presented a poster at Indian Eye Research Group – ARVO - India Chapter annual meeting (Hyderabad, India) on '*Molecular genetic analysis of Zinc Finger Protein - 408 (ZNF408) gene in Indian Familial Exudative Vitreoretinopathy (FEVR) patients*' held on July, 2014.

2. Presented a paper at ASIA-ARVO-2013 conference (Delhi, India) on '*Molecular Genetic Analysis of Norrie Disease Pseudoglioma (NDP), Frizzled-4 (FZD4) and Tetraspanin-12 (TSPAN12) Genes in Indian Familial Exudative Vitreoretinopathy (FEVR) Patients*.

3. Presented a poster at the annual meeting of The Association for Research in Vision and Ophthalmology (ARVO-2012) held at Fort Lauderdale, (Florida, USA) on *'Molecular genetic analysis of Norrie Disease Pseudoglioma (NDP) gene in Indian Familial Exudative Vitreoretinopathy (FEVR) and Retinopathy of Prematurity (ROP) patients* (Invest Ophthalmol Vis Sci 2012; 53: E-Abstract 1580).

4. Presented a poster at Indian Eye Research Group annual meeting (Hyderabad, India) on '*Molecular genetic analysis of Norrie Disease Pseudoglioma (NDP) and Tetraspanin 12 (TSPAN12) gene in Indian Familial Exudative Vitreoretinopathy (FEVR) patients*' held on July, 2011.

5. Presented a poster at Indian Eye Research Group annual meeting (Hyderabad, India) on '*Molecular genetic analysis of Norrie Disease Pseudoglioma (NDP) gene in Familial Exudative Vitreoretinopathy (FEVR) patients and Indian Retinopathy of Prematurity (ROP) babies*' held on July, 2010.

Investigative Ophthalmology & Visual Science

Invest Ophthalmol Vis Sci 2012;53: E-Abstract 1580.

1580—D801

Molecular Genetic Analysis of Norrie Disease Pseudoglioma (*NDP*) Gene in Indian Familial Exudative Vitreo Retinopathy (FEVR) and Retinopathy of Prematurity (ROP) Patients

Ganeswara R. Musada[1A], Subhadra Jalali[1B], Padmaja K. Rani[1B], Anupama R. Chururu[2], Pramod R. Gaddam[2], Subhabrata Chakrabarti[1A], Inderjeet Kaur[1A].

[A]Kallam Anji Reddy Molecular Genetics Laboratory, [B]Smt Kanuri Santhamma Retina Vitreous Centre, [1]LV Prasad Eye Institute, Hyderabad, India; [2]Department of Pediatrics, Fernandez Hospital, Hyderabad, India.

Purpose:

Norrin β-catenin signaling pathway defects are known for their involvement in the pathogenesis of FEVR; however, its role in ROP is unclear. Norrin protein encoded by Norrie disease pseudoglioma (*NDP*) gene is responsible for the activation of β-catenin signaling in the retina. The present study aimed to understand the involvement of *NDP* gene in FEVR and ROP patients from South India using genetic and bioinformatics tools.

Methods:

188 unrelated patients with FEVR (110) and ROP (78) and 192 controls were screened for mutations/variations in the entire coding and untranslated (UTR) regions of *NDP* gene by PCR based direct sequencing. The missense variants were further analyzed by generating 3D structure models for wild and mutant Norrin proteins using the I-TASSER server.

Results:

A total of 10 mutations were identified in 12 FEVR patients, of which 6 were novel, including 3 missense, 2 frameshift, and one UTR mutation. Three variants in the UTR region of gene including a 14bp deletion, an intronic variation and a novel SNP were identified in four different ROP patients. The missense mutations identified were predicted to be pathogenic as they replaced evolutionarily highly conserved amino acids with a SIFT score < 0.005 and possibly changes in the local conformation and multimerization of norrin protein.

Conclusions:

NDP gene variants were identified in 12% and 5% of the FEVR and ROP cases respectively, indicating its potential role in FEVR and ROP pathogenesis in the Indian patients.

Molecular Genetic Analysis of Zinc Finger Protein–408 *(ZNF408)* Gene in Indian Familial Exudative Vitreoretinopathy (FEVR) Patients

Ganeswara Rao Musada[1], Syed Hameed[1], Subhadra Jalali[2], Subhabrata Chakrabarti[1], Inderjeet Kaur[1]

[1]Kallam Anji Reddy Molecular Genetics Laboratory, Champalimaud Translational Centre for Eye Research, Brien Holden Eye Research Centre, [2]Smt Kanuri Santhamma Centre for Vitreo Retinal Diseases, L V Prasad Eye Institute, Hyderabad, India.

Purpose:

Familial exudative vitreoretinopathy (FEVR, MIM # 133780) is a vasoproliferative disorder of the retina characterized by non-formation of peripheral retinal vasculature. *ZNF408* is a recently identified candidate gene for FEVR. The ZNF408 protein is predicted to contain single SET (Su(var)3-9, Enhancer of zeste and Trithorax) and ten zinc finger domains based on its conserved amino acid sequence. This protein functions as a transcription factor. The present study aimed at understanding the role of this gene in FEVR patients from India.

Methods:

The DNA of 110 unrelated FEVR patients and 115 unaffected controls were screened for variations in the entire coding and untranslated region (UTR) of *ZNF408* gene by resequencing. Segregation of the disease-associated variants was assessed in the family members of the probands. The effect of observed missense changes were further analyzed by SIFT and PolyPhen-2 analysis.

Results:

The screening of *ZNF408* gene revealed 4 novel missense mutations (P44S, M232V, T617N and E715D) and two 5' UTR mutations in seven different FEVR probands. Additionally, 2 synonymous changes and 3 reported polymorphisms were detected. The T617N mutation was located in the tenth zinc finger domain of the protein and may interfere with its DNA binding domain activity. The remaining variations were not predicted to be located in functionally important domains of the ZNF408.

Conclusions:

The study identified *ZNF408* mutations in 3.6% (4/110) of the FEVR patients, indicating its potential role in FEVR pathogenesis. Thus, the study validates the involvement of *ZNF408* gene in FEVR development.

Molecular Genetic Analysis of Norrie Disease Pseudoglioma (*NDP),* Frizzled-4 *(FZD4)* and Tetraspanin-12 (*TSPAN12*) Genes in Indian Familial Exudative Vitreo Retinopathy (FEVR) Patients

Ganeswara Rao Musada[1], Subhadra Jalali[2], Subhabrata Chakrabarti[1,] Inderjeet Kaur[1]

[1]Kallam Anji Reddy Molecular Genetics Laboratory, [2]Smt Kanuri Santhamma Centre for Vitreo Retinal Diseases, L V Prasad Eye Institute, Hyderabad, India.

Purpose:

Familial exudative vitreoretinopathy (FEVR, MIM # 133780) is a vasoproliferative disorder of the retina resulting from ischemia due to non-formation of peripheral retinal vasculature. The defects in candidate genes, which encode for a ligand (*NDP*) and receptor complex (*FZD4, LRP5 and TSPAN12*) involved in the Norrin β-catenin signaling pathway, have been associated with the disease pathogenesis. The present study aimed at understanding the role of these genes in FEVR patients from India.

Methods:

The DNA of 110 unrelated FEVR patients and 115 unaffected controls were screened for variations in the entire coding and untranslated (UTR) regions of *NDP, FZD4,* and *TSPAN12* genes by resequencing. Segregation of the disease-associated variants was assessed in the family members of the probands. The effect of observed missense changes were further analyzed by generating a 3D structure model for the wild type and mutant proteins using the I-TASSER server.

Results:

The screening of *NDP, FZD4* and *TSPAN12* genes revealed 24 different mutations in 27 /110 FEVR families (24%). Additionally 3 novel and 6 reported single nucleotide polymorphisms (SNP) were detected. Among the observed mutations, 16 mutations were novel, including missense (n=8), frame shift (n=4) and 3' UTR (n=4) changes. The missense mutations were mainly located in the domains, which are functionally crucial in formation of the ligand-receptor complex and they also replaced the highly conserved amino acids (SIFT score < 0.005) and were predicted to be pathogenic.

Conclusions:

The *NDP, FZD4* and *TSPAN12* gene mutations were identified in 10%, 8% and 7% of the patients, respectively, indicating their potential role in FEVR pathogenesis. The observed mutations segregated with the disease phenotype with variable expressivity. The *FZD4* and *TSPAN12* mutations exhibited autosomal dominant and autosomal recessive modes of inheritance, respectively.

Molecular Genetic Analysis of Norrie Disease Pseudoglioma (*Ndp)* Gene and Tetraspanin 12 (*TSPAN12*) Gene in Indian Familial Exudative Vitreo Retinopathy (FEVR) Patients

Ganeswara Rao Musada[1], Subhadra Jalali[2], Padmaja K Rani[2], Subhabrata Chakrabarti[1,] Inderjeet Kaur[1]

[1]Kallam Anji Reddy Molecular Genetics Laboratory, Champalimaud Translational Centre for Eye Research, Prof Brien Holden Eye Research Centre, Hyderabad Eye Research Foundation, [2]Smt Kanuri Santhamma Retina Vitreous Centre, L V Prasad Eye Institute, Kallam Anji Reddy Campus, Hyderabad, India.

Purpose:

Familial exudative vitreo-retinopathy (FEVR) is a genetically heterogenous disorder characterized by impaired development of retinal vasculature. Norrin β-catenin signaling is the recognized pathway responsible for the disease phenotype. The present study explored the relative role of Norrie disease pseudoglioma (*NDP*) and Tetraspanin 12 (*TSPAN*12) genes, which encode for ligand, norrin and a ligand-frizzled4 receptor complex facilitator protein, TSPAN12 respectively, in Indian FEVR patients.

Methods:

A total of 110 unrelated clinically well characterized FEVR cases (61 familial and 49 sporadic) with different stages of FEVR, their available family members and 100 normal controls were enrolled in the study with a prior informed written consent. Genomic DNA was isolated from peripheral leukocytes. The entire coding region and 5' and 3' untranslated regions of *NDP* and *TSPAN*12 genes were analyzed by polymerase chain reaction based direct sequencing. The variations identified were further assessed for segregation patterns and genotype-phenotype correlation.

Results:

Taken together 16 different mutations were identified in *NDP* and *TSPAN12* genes in 21 different families, of which 13 were novel. The novel changes included 6 missense, 3 frame shift, 3 intronic and one UTR mutation. The six novel missense mutations were predicted to be pathogenic as they replaced highly conserved amino acids in the functional domains of the proteins with a SIFT score < 0.005. Variable expressivity of mutations was observed in some of the families.

Conclusions:

NDP and *TSPAN12* gene mutations were identified in 12% and 7% of the FEVR cases respectively indicating their potential role in FEVR pathogenesis in the Indian patients.

Molecular Genetic Analysis of Norrie Disease Pseudoglioma (*NDP)* Gene in Familial Exudative Vitreo Retinopathy (FEVR) Patients and Indian Retinopathy of Prematurity (ROP) Babies

Ganeswara Rao Musada[1], Inderjeet Kaur[1], Subhadra Jalali[2], Padmaja K Rani[2] Anupama Reddy Chururu[3], Pramod Reddy Gaddam[3]

[1]Kallam Anji Reddy Molecular Genetics Laboratory, [2]Smt Kanuri Santhamma Retina Vitreous Centre, LV Prasad Eye Institute, Hyderabad, India; [3]Department of Pediatrics, Fernandez Hospital, Hyderabad, India.

Purpose:

The study aims to screen the *NDP* gene in Indian patients with ROP and FEVR, to understand its role in disease pathogenesis and susceptibility.

Methods:

A total of 78 premature babies with different stages of ROP and 80 babies with No-ROP (gestational age $\leq$ 35 weeks and birth weight $\leq$ 1700 gms), 70 FEVR patients and 40 full term controls were included in the study. Genomic DNA was isolated from blood samples and polymerase chain reaction was performed for the entire coding region of *NDP.* Amplicons were screened for the detection of variations by direct sequencing.

Result:

Overall, six *NDP* variations including a reported mutation (R121Q), SNP (rs45501198), novel single nucleotide deletion (c.477delC) and a substitution (c.556C>G) were observed in seven families of FEVR. The observed deletion led to formation truncated protein instead wild type protein. The C>G substitution led to H50D amino acid change in the protein. In case of ROP a 14bp deletion in CT repeat region of 5**'** untranslated region (UTR) and a nucleotide substitution (c.1332G>A) in 3' UTR were observed in two babies. The same variations were observed in two FEVR families also.

Conclusions:

The mutations observed in FEVR cases were predominantly confined to the coding region of *NDP,* whereas in ROP variations were observed in the UTR. Thereby, this result supports the previous findings that the structural changes observed in norrin may lead to FEVR and changes occurred in norrin expression along with premature birth predisposes the babies to ROP

1. Awarded Association for Research in Vision and Ophthalmology (ARVO) International Travel Grant for attending ARVO annual meeting-2012, at Fort Lauderdale, Florida, USA.

2. Won the best poster award at Indian Eye Research Group (IERG) annual meeting held in Hyderabad, India, 2011.

3. Recipient of Graduate Aptitude Test in Engineering (GATE) fellowship (AICTE), 2005.

BRIEF BIOGRAPHY OF THE CANDIDATE

Ganeswara Rao Musada has been working at Kallam Anji Reddy Molecular Genetics Laboratory at LV Prasad Eye Institute for past seven years. He joined this institute after his academic training (M.Tech., Medical Biotechnology) at University of Hyderabad, Hyderabad, India.

After joining LVPEI, he was involved in research related to 'Molecular Genetic Analysis of Familial Exudative Vitreoretinopathy in Indian patients'. He was also involved in teaching the graduate students at the Bausch and Lomb School of Optometry, L V Prasad eye institute.

His PhD work has been presented at various International, National conferences, and under the process of publication in peer reviewed journals. He presented his work at the Association for Research in Vision and Ophthalmology (ARVO)-2012 annual meeting held at Fort Lauderdale, Florida, USA and was awarded with the travel fellowship by ARVO. His work was selected for the best poster award in Indian Eye Research Group-ARVO India Chapter-2011 annual meeting held at Hyderabad, India.

BRIEF BIOGRAPHY OF THE SUPERVISOR

PERSONAL DATA

Name	**Dr. INDERJEET KAUR**
Sex	Female
Permanent Address	15/8, Raj Krishna Pal Lane, Kolkata - 700075, India Ph- +91-33-24183164
Address for Correspondence	Brien Holden Eye Research Centre L.V. Prasad Eye Institute Road No. 2, Banjara Hills Hyderabad – 500034, India Phone: +91-40-30612524 Fax: +91-40-23548271 E-Mail: inderjeet@lvpei.org Web: http://www.lvpei.org
Present Position	Research Scientist L.V. Prasad Eye Institute Hyderabad, India
Date of Birth	19th May, 1973
Marital Status	Married to Dr. Subhabrata Chakrabarti, Scientist, L.V. Prasad Eye Institute, Hyderabad

ACADEMIC DATA

INSTITUTION AND LOCATION	DEGREE		FIELD OF STUDY
Punjab University, Chandigarh, India	B.Sc.	1993	Life Sciences
Punjabi University, Patiala, India	M.Sc.	1995	Forensic Sciences
Guru Nanak Dev University, Amritsar, India	Ph.D.	2003	Human Genetics
HERF, LVPEI, India	PDF	2005	Human Genetics

A. Research Positions

a) **1996-2000** **Research Fellow**, Centre for Genetic Disorders, GNDU, Amritsar, India

b) **2000-2005** **Lecturer** (Biochemical and Molecular genetics), Dept of Human Genetics GNDU Amritsar

c) **2003 -2005** **Post doctoral Research Associate**, LVPEI, India

d) **2005-Till date** **Staff Scientist** (HERF), LVPEI, India

B. HONORS, FELLOWSHIPS AND AWARDS *(Chronological order)*

1. **1995** **First Prize** in the Quiz contest on Radiation Physics organized by Indian Society for Radiation Physics, Patiala.
2. **1996** **UGC Junior Lectureship**, India
3. **2003** **DBT Postdoctoral Research Fellowship** India
4. **2004** **JSPS-DST Travel fellowship** under Indo-Japan Cooperative science program
5. **2005** **AMJAD RAHI PRIZE** for best paper presentation. 14th Annual meeting of Indian Eye Research Group, Hyderabad
6. **2006** **Visiting Scientist**, National Eye Institute, NIH, Bethesda, MD, USA February - April 2006
7. **2007** **Young Investigator Award (MERIT) in Basic Sciences**, ASIA-ARVO meeting on Research in Vision and Ophthalmology, Singapore March 2007
8. **2007** **ARVO International Travel fellowship grant** for attending ASIA-ARVO meeting on Research in Vision and Ophthalmology, Singapore March 2007
9. **2007** **Visiting Scientist**, Laboratory of Cellular & Molecular Biology, National Institute of Sensory Organs, Tokyo, JAPAN under Indo-Japan Collaborative Research program on AMD
10. **200**9 **DST International travel Grant** for attending the ARVO meeting May 2-7, 2009.
11. **2010 International Society for Eye Research (ISER) Travel fellowship** (USA), for attending the International Congress on Eye Research at Montreal, Canada July 2010.
12. **2011 DBT Crest Award (Cutting Edge Research Enhancement and Scientific Training Award)** for advanced training in Proteomics and Transcriptomics at Mass Eye and Ear Infirmary, Harvard University, Boston, USA from October 2011-March 2012
13. **2011 B M Birla Science Medal (Biological Sciences)**
14. **2013 Member, Editorial Board for Journal of Genetics, Indian academy of Sciences**

A. PROJECTS Undertaken as Principal Investigator

1. Bilateral Indo-Australian project on "Establishing a risk assessment chip for the eye disease age-related macular degeneration"
2. Identification of biomarkers for risk prediction and disease progression in Retinopathy of prematurity (ROP)
3. Genetics of Retinopathy of Prematurity
4. Genetic evaluation of Factor B and complement component C2 in the susceptibility to Age-related Macular Degeneration
5. Understanding the genetic signatures in Uveal melanoma by Next Gen Sequencing
6. *Understanding the molecular pathology of Corneal Congenital Anesthesia*
7*. Developing a robust cost effective test for the identification of Fungal infection by using Real time HRM analysis*
8. AMD Transcriptomics (in collaboration with Prof Ambati, University of Kentucky, USA
(Italicized are the newly started projects)

B. PROJECTS AS Co-Investigator

1. German collaborative project on **"Genetic dissection of POAG and AMD in a population cohort from Central India: The Nagpur-CIEMS Study".**
2. **Vision Cooperative Research Centre** Australia Strategic researches grant on "**Genetics of Myopia**"
3. **DST** Project on **Loop mediated isothermal amplification (LAMP) method for the diagnosis of Viral Retinitis caused by Herpes Simplex, Varicella Zoster and Cytomegalo Viruses 2008-2010**.
4. Program support on Glaucoma :Translational Research on Eye Diseases"

C. GRANTS

a) International Grants

1) **Indo-Australian grant**, Department of Biotechnology, Government of India 1/4/2007 to 31/3/2010 **[Amount: Rs. 73.26 lakhs] (PI)**
This project is aimed to identify and assess the role of major candidate genes in AMD and devise means of predictive testing
2) German grant; Univ. of Heidelberg, Germany 1/1/09 to 31/12/2014 **[Amount: Rs. 45 lakhs** (Received in First year**) {Co-Investigator}**
3) German collaborative project on **"Genetic dissection of POAG and AMD in a population cohort from Central India: The Nagpur-CIEMS Study".**
4).Vision Cooperative Research Centre (Australia) **7/1/2004 to 7/1/2011** Strategic researches grant on "**Genetics of Myopia**" **(USD125,000)**

b) National Grants

1) **Department of Biotechnology, Government of India** 1/4/2012 to 31/3/2015 [**Amount: Rs. 109.50 lakhs**] **(Coordinator & PI)**
2) Program Support, Department of Biotechnology, Government of India 24/9/2007 to 23/8/2012 **[Amount: Rs. 55.20 lakhs] ----- (PI)**
3) DST SERC Fast Track Scheme grant on AMD **August 2007- 2010** [Amount: **Rs. 12 lakhs**
4) DST grant under Indo-Japan Collaborative research program on "Molecular genetics and Proteome analysis of AMD patients" from **2003-2008 (**Amount: **5 lakhs + travel fellowships)**

AS Co-Investigator

1. **DST** Project on **Loop mediated isothermal amplification (LAMP) method for the diagnosis of Viral Retinitis caused by Herpes Simplex, Varicella Zoster and Cytomegalo Viruses 2008-2010**. (**12 lakhs**)

E. PEER-REVIEWED PUBLICATIONS *(in chronological order)*

1. Ramappa M, Chaurasia Sunita, Chakrabarti S, **Kaur I**, Sangwan VS. Clinical spectrum of congenital corneal anesthesia in Southern India. ***J AAPOS*** 2014; [IN PRESS].
2. Garland DL, Fernandez-Godino R, ***Kaur I,*** Speicher KD, Harnly JM, Lambris JD, Speicher DW, Pierce EA Mouse genetics and proteomic analyses demonstrate a critical role for complement in a model of DHRD/ML, an inherited macular degeneration.***Hum Mol Genet***. 2014 Jan 1;23(1):52-68. doi: 10.1093/hmg/ddt395. Epub 2013 Aug 13.

3. **Kaur I**, Cantsilieris S, Katta S, Richardson AJ, Schache M, Pappuru RR, Narayanan R, Mathai A, Majji AB, Tindill N, Guymer RH, Chakrabarti S*****, Baird PN. Association of the del443ins54 at the *ARMS2* locus in Indian and Australian cohorts with Age-Related Macular Degeneration. ***Mol Vis*** 2013; 19: 820-826.
4. Bhattacharya S K, Lee R K,. Grus F H, The Seventh ARVO/Pfizer Ophthalmics Research Institute Conference Working Group (includes Kaur I). Molecular Biomarkers in Glaucoma ***IOVS***, 2013:54(1) 121-131.
5. Chakrabarti S*****, Ramappa M, Chaurasia S, **Kaur I**, Mandal AK. *FOXC1*-associated phenotypes in humans may not always exhibit corneal neovascularization. ***Proc Natl Acad Sci, USA*** 2012: 109: E1509. [1]
6. Thakkinstian A, McEvoy M, Chakravarthy U, Chakrabarti S, McKay GJ, Ryu E, Silvestri G, **Kaur I**, Francis P, Iwata T, Akahori M, Arning A, Edwards A, Seddon J, Attia J. The Association between Complement Component 2/Complement Factor B Polymorphisms and Age-Related Macular Degeneration: A HuGE Review and Meta-Analysis. ***Am J Epidemiol*** 2012; 176: 361-372. [1]
7. Thakkinstian A, McKay GJ, McEvoy M, Chakravarthy U, Chakrabarti S, Silvestri G, **Kaur I**, Li X, Attia J. Systematic review and meta analysis of the association between complement component 3 and age-related macular degeneration: A HUGE review and meta analysis. ***Am J Epidemiol*** 2011; 173: 1365-1379. ***[10]***
8. Chakrabarti S*****, Ghanekar Y, Kaur K, **Kaur I**, Mandal A, Rao KN, Parikh RS, Thomas R, Majumder PP. A polymorphism in the *CYP1B1* promoter is functionally associated with primary congenital glaucoma. ***Hum Mol Genet*** 2010; 19: 4083-4090
9. **Kaur I**, Rathi S, Chakrabarti S*****. Variations in *TIMP3* are associated with age-related macular degeneration. ***Proc Natl Acad Sci, USA*** 2010; 107: E112-113. [5]
10. Rao KN, Kaur I, Parikh R, Mandal A, Chandrasekhar G, Thomas R, Chakrabarti S*. Variations in NTF4, VAV2 and VAV3 genes are not involved with primary open angle and primary angle closure glaucomas in an Indian population. ***Invest Ophthalmol Vis Sci*** 2010; 51: 4937-4941. [10]
11. **Kaur I**, Katta S, Reddy RK, Narayanan R, Mathai A, Majji AB, Chakrabarti S*****. The Involvement of Complement Factor B and Complement Component C2 in an Indian Cohort with Age-Related Macular Degeneration. ***Invest Ophthalmol Vis Sci*** 2010; 51:59-63. [14]
12. **Kaur I***, Hussain Avid, Naik M, Murthy R, Honavar SH. Mutational Analysis of Fork-Head Transcriptional Factor Gene FOXL2 in Indian Familial Cases of Blepharophimosis Ptosis Epicanthus Inversus Syndrome. ***BJO*** 2011; 95(6):881-6. [2]
13. Reddy AK, Garg P, **Kaur I**. Spectrum and Clinico-microbiological profile of Keratitis Caused by Rare Species of Nocardia identified by 16S rRNA gene sequencing. **Eye** December 2010; 24:1259-62. [4]
14. Reddy AK, Balne P, Reddy RK, Mathai A, **Kaur I**. Development and Evaluation of Loop Mediated Isothermal Amplification (LAMP) Assay for the Rapid and Inexpensive Detection of Cytomegalovirus DNA in Vitreous Specimens from Suspected Cases of Viral Retinitis. **Journal of Clinical Microbiology**: 2010; 48:2050-2 [5]
15. Reddy AK, Balne P, Reddy RK, Mathai A, **Kaur I**. Loop Mediated Isothermal Amplification (LAMP) Assay for the Diagnosis of Retinitis Caused by Herpes Simplex Virus-1. **Clinical Microbiology and Infection**: 2010; 17:210-3.

16. Katta S, Chakrabarti S, Kaur I. The molecular genetic basis of Age-related macular degeneration: An Overview. **J Genet** 2009; 88: 425-449. [41]
17. Rao KN, **Kaur I**, Chakrabarti S. Lack of association of three POAG susceptible loci with primary glaucomas in an Indian population. ***Proc Natl Acad Sci, USA*** 2009: 106: E125-126. [9]
18. Reddy AK, Garg P, **Kaur I**. Speciation and Susceptibility of Nocardia Isolated from Ocular Infections. ***Clinical Microbiology and Infection***: 2010;16:1168-71 [
19. Chakrabarti S, Kaur K, Rao KN, Mandal AK, **Kaur I**, Parikh RS, Thomas R. The transcription factor gene *FOXC1* exhibits a limited role in primary congenital glaucoma. ***Invest Ophthalmol Vis Sci*** 2009; 50: 75-83. [**20**]
20. Rao KN, Ritch R, Dorairaj SK, **Kaur I**, Liebmann J, Thomas R, Chakrabarti S. Exfoliation syndrome and exfoliation glaucoma-associated *LOXL1* variations are not involved in pigment dispersion syndrome and pigmentary glaucoma. ***Mol Vis*** 2008; 14: 1254-1262. [**10**]
21. Chakrabarti S, Rao KN, **Kaur I**, Parikh RS, Mandal AK, Chandrasekhar G, Thomas R. The *LOXL1* Gene Variations are not associated with primary open angle and primary angle closure glaucomas. ***Invest Ophthalmol Vis Sci*** 2008; 49: 2343-2347. [**17**]
22. **Kaur I**, Katta S, Hussain A, Hussain N, Mathai A, Narayanan R, Hussain A, Reddy R, Majji AB, Das TP, Chakrabarti S. Variants in the 10q26 gene cluster (*LOC387715* and *HTRA1*) exhibit enhanced risk of age-related macular degeneration along with *CFH* in Indian patients. ***Invest Ophthalmol Vis Sci*** 2008; 49: 1771-1776. [3**7**]
23. **Kaur I**, Ghanekar Y, Chakrabarti S. Understanding the genetics of age-related macular degeneration: some insights into the disease pathogenesis. ***Int J Hum Genet*** 2008: 8: 161-169.[3]
24. Hussain N, Ghanekar Y, **Kaur I**. The Future Implications and Indications of AntiVEGF Therapy in Ophthalmic Practice. ***Indian J Ophthalmol*** 2007;55: 445-50.[11]
25. **Kaur I**, Hussain A, Hussain N, Das TP, Pathangay A, Mathai A, Hussain A, Nutheti R, Nirmalan PK, Chakrabarti S. Analysis of *CFH*, *TLR4* and *APOE* polymorphisms in India suggests the Tyr402His variant of *CFH* to be a global marker for age-related macular degeneration. ***Invest Ophthalmol Vis Sci*** 2006; 47: 3729-3735. [**61**] **†**
26. Chakrabarti S, Kaur K, **Kaur I**, Mandal AK, Parikh R, Thomas R, Majumder PP. Globally, *CYP1B1* mutations in primary congenital glaucoma are strongly structured by geographic and haplotype backgrounds. ***Invest Ophthalmol Vis Sci*** 2006; 47: 43-47. [**18**]
27. **Kaur I**, Roy S, Chakrabarti S, Sarhadi VK, Majumder PP, Bhanwer AJS, Singh JR.Genomic diversities and affinities among four endogamous groups of Punjab (India)using insertion/deletion and mitochondrial DNA polymorphisms. ***Hum Biol*** 2002; 74:819-836. [**2**] **(IF=0.8)**

Book Chapters

1. Chakrabarti S*****, **Kaur I**, Baird PN. Genetics of Age Related Macular Degeneration. In ***Encyclopedia of Life Sciences***; John Wiley and Sons Ltd, UK 2012 [IN PRESS].
2. Sikka R, Babu IR, **Kaur I**, Rani PK, Bhanwer AJS, Chakrabarti S*. Some insights on the genomics of diabetic retinopathy. ***Proceedings of the Indian Society of Human Genetics***. Punjab University Press, Chandigarh, India; 2012 [IN PRESS]
3. Katta S, Chakrabarti S, Kaur I, Hussain N. Genetics of Age Related Macular Degeneration. In Natarajan S and Hussain N (eds.) ***Textbook of Vitreoretinal Diseases and Surgery***; Jaypee Brothers Medical Publishers (P) Ltd, New Delhi, India; 2009: 1-13.
4. **Kaur I,** Komatireddy S, Devi KR, Chakrabarti S. Genetics of diabetes and diabetic eye diseases. In Das TP and Rani A (eds.) ***Diabetic Eye diseases***; JayPee Brothers Medical Publishers (P) Ltd, New Delhi, India; 2006: 31-41.

Manuscript under submission:

Garland D, Godino RF, Kaur I, Speicher K, Harnly JM, Lambris,JD Speicher D, Pierce EA. Proteomic and Genetic analyses demonstrate a critical role for the Complement System in Basal Deposit Formation in a Mouse Model of Inherited Macular Dystophy (under submission)

PUBLISHED ABSTRACTS (2010-2012)

1) Chakrabarti S, Rao KN, Siddiqui S, Senthil S, Chandrasekhar G, Mandal AK, Rao HB, Ramappa M, Sangwan VS, **Kaur I**. Functional analysis of fibulin 5 (*FBLN5*) gene in primary open angle glaucoma. ***Invest Ophthalmol Vis Sci***. 2012; 53: E-Abstract 4502.
2) Musada GR, Jalali S, Rani PK, Chururu AR, Gaddam PR, Chakrabarti S, **Kaur I**. Molecular genetic analysis of Norrie Disease Pseudoglioma (NDP) gene in Indian familial exudative vitreoretinopathy (FEVR) and retinopathy of prematurity (ROP) patients. ***Invest Ophthalmol Vis Sci***. 2012; 53: E-Abstract 1580.
3) **Kaur I**, Katta S, Siddiqui S, Pappuru RK, Narayanan R, Majji AB, Mathai A, Chakrabarti S. Plasma protein profiles of patients with age-Related Macular Degeneration. ***Invest Ophthalmol Vis Sci***. 2012; 53: E-Abstract 2479.
4) Chakrabarti S, Nagireddy S, Rao KN, Senthil S, Rao HB, Mandal AK, Chandrasekhar G, **Kaur I**. Whole genome expression and candidate gene analysis reveals the involvement of novel genes in primary open angle glaucoma. ***Invest Ophthalmol Vis Sci***. 2011; 52: E-Abstract 4599.
5) **Kaur I**, Rathi S, Musada GR, Jalali S, Kekunnaya R, Rani PK, Chakrabarti S. Molecular genetic and functional analysis in a large cohort indicate novel genes in retinopathy of prematurity. ***Invest Ophthalmol Vis Sci***. 2011; 52: E-Abstract 3996.
6) Chakrabarti S, Reddy R, Narayanan R, Mathai A, Majji AB, **Kaur I**. The Susceptibility of Extracellular Matrix-Related Gene Variants in Age-Related Macular Degeneration. ***Invest Ophthalmol Vis Sci***. 2010; 51: E-Abstract 2479.
7) Kollu NR, **Kaur I**, Parikh RS, Mandal AK, Thomas R, Chakrabarti S. Evaluation of *NTF4, VAV2 a*nd *VAV3* Genes in Primary Open Angle and Primary Angle Closure Glaucomas in an Indian Population. ***Invest Ophthalmol Vis Sci***. 2010; 51: E-Abstract 6436.
8) Katta S, **Kaur I**, Reddy R, Narayanan R, Mathai A, Majji AB, Chakrabarti S. The del443ins54 Polymorphism in ARMS2 is Strongly Associated With Age-Related Macular Degeneration in an Indian Cohort. ***Invest Ophthalmol Vis Sci***. 2010; 51: E-Abstract 1260.

F. INVITED LECTURES/ PAPER PRESENTATIONS

International meetings:

1. **Invited talk** on "**Glaucoma genetics: Differences in ethnic groups?"** Presented at the Seventh **Annual ARVO/Pfizer Ophthalmic Research Institute** on "Molecular Biomarkers in Glaucoma" Fort Lauderdale, Florida April 29-30, 2011
2. **Invited talk** on "**Genetics of Retinopathy of Prematurity**: a potentially blinding disorder in pre-term babies." Presented at the International Society of Genetic Eye Diseases Meeting, Bangalore, India Jan14-15, 2011.
3. **Invited talk** on "**Genetics of Retinopathy of Prematurity**: a potentially blinding disorder in pre-term babies." Presented at the TWAS 21st General Meeting, Hyderabad, India October18th-22nd, 2010.

4. **Invited talk** on “A Molecular genetic study of retinopathy of prematurity.” Presented at the Centre for Eye Research, University of Melbourne, Melbourne, Australia. October 8th, 2010
5. **Invited talk** on “**Biomarker identification in POAG: A preliminary experience from an Indian cohort”** at the session entitled "Proteomic and Lipidomic approaches in Glaucoma" at the XIX annual meeting of **International Society for Eye research (ISER)** held at Montreal, Canada from July18-23, 2010.
6. **Invited talk** on "Mutation Spectrum of Norrie Disease Pseudoglioma (NDP) gene in Indian ROP and FEVR Patients" at the **World ROP meeting** 2009 held at New Delhi, India Nov 20-23, 2009.
7. **Invited talk** on “Genetics of Age-related Macular Degeneration: an update from India” at AMD symposium in **ASIA ARVO** meeting at HICC, Hyderabad, India from Jan 15-18th, 2009.
8. **Moderator** for Myopia: Nature vs. Nurture session in **ASIA ARVO** meeting at HICC, Hyderabad, India from Jan 15-18th, 2009.
9. Paper Presentation on "Contributions of the *ARMS2* (LOC387715) and *HTRA1* gene variants in the risk of Age related macular degeneration among Indian patients" at **Human Genome Meeting (HUGO)** 2008 held at HICC, Hyderabad, India from Sept 27-30th, 2008.
10. **Invited talk** on “AMD Genetics: an Update from India” at **Centre for Eye Research, Melbourne, Australia** August 4th 2008
11. Paper presentation at **Asia ARVO Meeting** on Research in Vision and Ophthalmology, Singapore (2007)
12. **Invited talk** on “Molecular genetics of Age-related macular degeneration in India” at **National institute of Sensory Organs**, National Tokyo medical Centre, Tokyo (March 2007)
13. **Invited** talk on “Molecular genetics of inherited eye diseases in India” at **National Eye Institute**, NIH, Bethesda, MD, USA, 2006.

National meetings:

14. **Invited talk** at **Evidence 2012** meeting on “Innate Immunity in Glaucoma: Recent updates.” Hyderabad, India August 2012.
15. **Invited talk** on "Molecular mechanisms and risk assessment in a complex age-related eye disease" at the **SAP meeting** held at **Guru Nanak Dev University**, Amritsar March 16, 2011.
16. Invited talk on “Pharmacogenomics” at the **Thadikonda Seminar in Pharmaceutical Sciences**" on August 22, 2011, Hyderabad.
17. Chaired a session on “Genetics of Complex Eye diseases” at symposium Eye 2011, Bhubaneswar, Orissa, January 16, 2011.
18. **Invited talk** on “Genetics of age related macular degeneration-An update”. Presented at the “Recent Advances in Ocular Genetics and Gene Therapy”, **Narayana Nethralaya**, Bangalore 2010.
19. **Invited talk** on “Genetics of age related macular degeneration”. Presented at MGNIRSA, Institute of Genetics, Hyderabad 2010.
20. Visited Padmavati Mahila University, Tirupati as **Guest faculty** and gave **3** talks for the M.Sc. Biotechnology and M.Tech. Genetic engineering students on Pharmacogenomics, Genetic testing and Advances in Proteomics and a public lecture on the research work and activities of LVPEI, December15-17th , 2008

21. Paper presentation on " Molecular genetic study of Blepharophimosis Ptosis Epicanthus Inversus Syndrome" at **Indian society of Human Genetics** meeting Vishakhapatnam February, 2008
22. Paper presentation on "The *LOC387715* and *HTRA1* Gene Variants Exhibit Enhanced Risk of AMD Along With *CFH* in Indian Patients" at XVI **Annual Conference of Vitro-Retinal Society of India**, Missouri. September 2007
23. **Invited talk** on "Genetics and Biomarkers for AMD" at 1st **Indian AMD congress**, Agra. October 2006
24. **Invited talk** on "Biomarkers for AMD" at 2nd **Macula workshop** LVPEI-Novartis Macula Centre, Hyderabad December 2006
25. Presented a research paper on "Global Implication of CFH polymorphism in AMD" at XIV **Annual Conference of Vitro-Retinal Society of India**, Khajuraho. December 2005.
26. Paper presentation on "The Y402H polymorphism in the Complement Factor H gene is associated with susceptibility to Age Related Macular Degeneration in Indian patients." 14th **Annual meeting of Indian Eye Research Group**, Hyderabad (2005)
27. Paper presentation on "A study of genetic diversity and affinities among four ethnic groups of Punjab using mitochondrial DNA polymorphisms." 28th **Annual conference of the Indian society of Human Genetics**, Jammu (2003)
28. Paper presentation on "A genetic diversity study of Punjabi populations using three microsatellite markers." 27th **Annual conference of the Indian society of Human Genetics**, Thiruvanthapurum (2002)

G. SCIENTIFIC ORGANIZER

i) Organizing secretary, **Indian Eye Research Group-ARVO India Chapter meeting 2012** at Hyderabad, July29-31, 2012
ii) Organized the "**Thadikonda Seminar in Pharmaceutical Sciences**" on August 22, 2011, at Hyderabad.
iii) Organizing secretary, **Indian Eye Research Group meeting 2011** at Hyderabad, July3031, 2011.
iv) Organized **LVPEI-Novartis symposium on "Recent advances in the understanding of the biology of diseases**" at Hyderabad July 29, 2011
v) Chaired a session on "Genetics of Complex Eye diseases" at symposium Eye 2011, Bhubaneswar, Orissa, January 16, 2011.
vi) Member, Local organizing Committee, **TWAS 2010**
vii) Organizing secretary, **Indian Eye Research Group meeting 2010** at Hyderabad, July31-August 1st, 2010.
viii) Organizer, Special Interest group meeting on **Technological advances in proteomics for ocular diseases: How far we have come**, **Asia ARVO Hyderabad India 2009**

H. OTHER ACADEMIC ASSIGNMENTS

1)Editorial Board: Journal of Genetics(since December 2012)

2)Reviewer = 8 Journals

i) BMC Ophthalmology
ii) IOVS
iii) European Journal of Clinical Nutrition
iv) Plos Genetics
v) Molecular Vision
vi) Journal of Genetics
vii) Indian Journal of Ophthalmology
viii) Indian Journal of Human Genetics
ix) Journal of Biosciences

2) Ph.D. thesis being guided = 5

a) Saritha Katta (CSIR Senior Research fellow) [2006 – 2011] (BITS Pilani)
b) Ganeswara Rao (Senior Research fellow) [2007 – till date] (BITS Pilani)
c) Srujana Sahebjada (Junior research fellow) [2009-till date] (University of Melbourne, Australia)
d) Sonika Rathi (Junior Research fellow) [2010-till date] (BITS Pilani)
e) Saika Siddiqui (Junior Research fellow) [2011-2012] (Hyderabad central University)

4) Summer Project student guided: **6**

5) Research technician trained: **9**

- Avid Hussain (2005-07): Molecular Genetics
- Srinivas sripathi(April-July,2009): Molecular Genetics
- Praveen Balne(2008-09): LAMP and other molecular biological techniques for the identification of microbial species
- Purushottam (2009-10): Molecular Genetics
- Indushree Rajanbabu (2010-2011) : Molecular genetics
- Farheen Fatima (2011-till date) : Molecular genetics
- Hameed (2011-till date) : Molecular genetics
- Shahana (2012-till date) : Molecular genetics
- Ramadevi (2012-till date) : Molecular genetics
-

Ph.D. Supervisor
a) Birla Institute of Technology and Sciences (BITS), Pilani, Rajasthan, India
b) School of Life Sciences, University of Hyderabad, Hyderabad, India
c) University of Melbourne, Melbourne, Australia
d) University of New South Wales (UNSW) Sydney Australia

I. OTHER ACTIVITIES (Non-Medical)
NABH Internal Auditor for Eye bank and Purchase dept of LVPEI.